

JPL Publication 91-31

# Proceedings of the Fifteenth NASA Propagation Experimenters Meeting (NAPEX XV) and the Advanced Communications Technology Satellite (ACTS) Propagation Studies Miniworkshop

Held in London, Ontario, Canada, June 28-29, 1991

Faramaz Davarian  
Editor

(NASA-CR-194539) PROCEEDINGS OF  
THE FIFTEENTH NASA PROPAGATION  
EXPERIMENTERS MEETING (NAPEX 15)  
AND THE ADVANCED COMMUNICATIONS  
TECHNOLOGY SATELLITE (ACTS)  
PROPAGATION STUDIES MINIWORKSHOP  
(JPL) 275 p

N94-16035  
--THRU--  
N94-16051  
Unclass

G3/32 0189029

July 1, 1991



National Aeronautics and  
Space Administration

Jet Propulsion Laboratory  
California Institute of Technology  
Pasadena, California



JPL Publication 91-31

Proceedings of the Fifteenth NASA  
Propagation Experimenters Meeting  
(NAPEX XV) and the Advanced  
Communications Technology Satellite  
(ACTS) Propagation Studies  
Miniworkshop

Held in London, Ontario, Canada, June 28–29, 1991

Faramaz Davarian  
Editor

July 1, 1991

**NASA**

National Aeronautics and  
Space Administration

Jet Propulsion Laboratory  
California Institute of Technology  
Pasadena, California

This publication was prepared by the Jet Propulsion Laboratory, California Institute of Technology, under a contract with the National Aeronautics and Space Administration.



## PREFACE

The NASA Propagation Experimenters Meeting (NAPEX) is a forum convened to discuss the studies supported by the NASA Propagation Program. The reports delivered at this meeting by the management and the investigators of the program summarize the recent activities, as well as plans for the future. Representatives from domestic and international organizations who conduct radio wave propagation studies are invited to NAPEX for discussion and exchange of information. This Proceedings records the content of NAPEX XV and the Advanced Communications Technology Satellite (ACTS) Miniworkshop that followed it.

NAPEX XV, which took place in the Sheraton Armouries Hotel, London, Ontario, Canada, on June 28, 1991, started on a solemn note because of the unfortunate failure of the Olympus satellite. However, spirits rose as soon as Dr. Bertram Arbesser-Rastburg of the European Space Agency (ESA) announced the possibility of recovering Olympus in an early course of time, and the meeting proceeded with due enthusiasm. There were three sessions. The morning session, chaired by Mr. John Kiebler in place of Mr. Dean Olmstead, who was unable to attend the meeting, was dedicated to Olympus and ACTS studies and measurements. Following the opening remarks by Dr. Faramaz Davarian, the morning session covered eight technical papers. There were two sessions in the afternoon. In the first one, Mr. John Kiebler led the topics in propagation studies and measurements and covered seven technical papers. The last session in the afternoon, chaired by Dr. Faramaz Davarian, was dedicated to a computer-based propagation model development plan and included two formal technical papers and a number of informal presentations.

Finally, the meeting was adjourned with closing remarks by Dr. David V. Rogers.

Sincere thanks are due to Dr. Ernie K. Smith and Heidi Vice for organizing and executing the logistics of the meeting flawlessly. Thanks are also due to Dr. Jack Chakraborty for his assistance in preparing this Proceedings and organizing the ACTS Miniworkshop, and Erin Kan for editing this publication.

NAPEX XVI is scheduled for late May 1992.

Faramaz Davarian

## ABSTRACT

The NASA Propagation Experimenters Meeting (NAPEX), supported by the NASA Propagation Program, is convened annually to discuss studies made on radio wave propagation by investigators from domestic and international organizations. NAPEX XV was held on June 28, 1991, in the Sheraton Armouries Hotel, London, Ontario, Canada. Participants included representatives from Canada, Japan, Germany, the Netherlands, and the United States, including researchers from universities, government agencies, and private industries. The meeting was organized into three technical sessions. The first session was dedicated to Olympus and ACTS studies and experiments, the second session was focused on the propagation studies and measurements, and the third session covered computer-based propagation model development. In total, sixteen technical papers and some informal contributions were presented.

Following NAPEX XV, the Advanced Communications Technology Satellite (ACTS) Miniworkshop was held on June 29, 1991 to review ACTS propagation activities with emphasis on ACTS hardware development and experiment planning. Five technical papers were presented by contributors from government agencies, private industry, and university research establishments.

## FOREWORD

The NASA Propagation Information Center is located in the Electrical and Computer Engineering Department at the University of Colorado at Boulder. The Center has two main objectives: to assist the management of the NASA Propagation Program by serving as an information resource to those within and outside the propagation community, and to provide graduate instruction and thesis supervision in radio wave propagation. The Center, funded by NASA, was founded in July 1988. It is staffed by Professor Emeritus Warren L. Flock and Professor Adjunct Ernest K. Smith, co-directors; Heidi Vice, student assistant; and Zeng-jun Zhang, Senior Professional Research Assistant (until August 31, 1991).

Professors W.L. Flock and E.K. Smith are involved in several on-going activities that allow the Center to attain its goals. Flock is the Editor of the NASA Earth-Space Propagation Newsletter, and Smith is Associate Editor for Propagation for the IEEE Antennas and Propagation Magazine. Both publications reach the propagation community world-wide. Smith is also co-chairman of the URSI Working Group on Natural Noise.

The Center organizes monthly Telecommunications Policy Luncheons and Flock and Smith are actively involved in many propagation groups and workshops: CCIR SG 5/6; URSI Commissions E,F,G; IEEE Wave Propagation Standards Committee; IEEE APS and NAPEX (NASA Propagation Experimenters).

Smith serves on several thesis committees, both at the master's and the Ph.D. level. He teaches a course in the spring semester on "Earth-Space Propagation" in collaboration with Dr. David C. Hogg. This is a course pioneered by Professor Flock. In the fall of 1989 he offered "Fundamentals of Propagation," taught jointly with Dr. Kenneth Davies.

The Center also produces and reviews propagation handbooks and maintains a list of many journal articles and reports that the NASA Propagation Experimenters have produced documenting the results of their investigations. Anyone interested in these materials should call Ernie Smith or Warren Flock at the Center.

Phone: (303) 492-7123 E.K. Smith  
(303) 492-7012 W.L. Flock  
(303) 492-4614 H.Vice  
FAX: (303) 492-2758



CONTENTS

NAPEX XV MEETING

NAPEX XV SUMMARY . . . . . 1  
F. Davarian and E. K. Smith

OPENING REMARKS . . . . . 6  
F. Davarian

    SESSION 1: OLYMPUS AND ACTS STUDIES AND EXPERIMENTS  
                Chairman: J. Kiebler, NASA Consultant

INTRODUCTORY REMARKS FOR NAPEX XV . . . . . 11  
J. Kiebler, NASA Consultant

A REVIEW OF OPEX ACTIVITIES AND MEASUREMENT RESULTS . . . . . 12  
B. Arbesser-Rastburg, ESA-ESTEC

OLYMPUS PROPAGATION MEASUREMENT RESULTS AT VIRGINIA TECH . . . . . 20  
W. Stutzman, Virginia Tech

DATA ACQUISITION, PREPROCESSING AND ANALYSIS FOR THE  
VIRGINIA TECH OLYMPUS EXPERIMENT . . . . . 28  
P. W. Remaklus, Virginia Tech

EARTH-SPACE PROPAGATION RESEARCH AT CRC . . . . . 36  
R. L. Olsen, CRC, Canada

THE ACTS PROPAGATION PROGRAM . . . . . 50  
D. Chakraborty and F. Davarian, JPL

PROPAGATION MEASUREMENTS IN ALASKA USING ACTS BEACONS . . . . . 55  
C. E. Mayer, U. of Alaska

PLANNED LMSS PROPAGATION EXPERIMENT USING ACTS: PRELIMINARY  
ANTENNA POINTING RESULTS DURING MOBILE OPERATIONS . . . . . 61  
J. R. Rowland and J. Goldhirsh, APL; W. J. Vogel and  
G. W. Torrence, U. of Texas

PROPAGATION-RELATED AMT DESIGN ASPECTS AND SUPPORTING  
EXPERIMENTS . . . . . 73  
K. Dessouky and P. Estabrook, JPL

    SESSION 2: TOPICS IN PROPAGATION STUDIES AND  
                MEASUREMENTS  
                Chairman: J. Kiebler, NASA Consultant

WHAT IS HAPPENING AT CCIR STUDY GROUP 5? . . . . . 83  
D. V. Rogers, CRC, Canada

PROPAGATION RESEARCH IN JAPAN . . . . .	88
H. Wakana, CRL, Kashima, Japan	
A COMPARISON OF CLOUD ATTENUATION MODELS USING MEASURED CLOUD DATA . . . . .	95
G. C. Gerace and E. K. Smith, U. of Colorado; E. R. Westwater, WPL/NOAA	
MEASUREMENTS OF ATMOSPHERIC EMISSION AND ABSORPTION:	
BRIGHTNESS TEMPERATURE AND ATTENUATION STATISTICS AT 20.6 AND 31.65 GHZ . . . . .	107
E. R. Westwater and M. J. Falls, NOAA/ERL/WPL	
COMPARISON OF OLYMPUS BEACON AND RADIOMETRIC ATTENUATION MEASUREMENTS AT BLACKSBURG, VIRGINIA . . .	116
J. B. Snider, M. D. Jacobson, R. H. Beeler, and D. A. Hazen, NOAA/ERL/WPL	
SATELLITE SOUND BROADCAST PROPAGATION MEASUREMENTS . . . .	123
W. J. Vogel and G. W. Torrence, U. of Texas	
AN OVERVIEW OF THE TEXT "PROPAGATION EFFECTS FOR LAND-MOBILE-SATELLITE SYSTEMS: EXPERIMENTAL AND MODELING RESULTS" . . . . .	132
J. Goldhirsh, APL; W. J. Vogel, U. of Texas	
HANDBOOKS OF THE NASA PROPAGATION PROGRAM, PAST HISTORY AND THOUGHTS TO THE FUTURE . . . . .	140
E. K. Smith, U. of Colorado	
SESSION 3: COMPUTER-BASED PROPAGATION MODEL Chairman: F. Davarian, JPL	
INFORMAL PRESENTATION OF CONTRIBUTIONS AND DISCUSSIONS:	
DATABASE FOR PROPAGATION MODELS . . . . .	147
A. V. Kantak, JPL	
A CCIR-BASED PREDICTION MODEL FOR EARTH-SPACE PROPAGATION . . . . .	159
Z. Zhang and E. K. Smith, U. of Colorado	
SOFTWARE FOR PROPAGATION . . . . .	173
W. Vogel, U. of Texas	
A STUDY OF LAND MOBILE SATELLITE SERVICE MULTIPATH EFFECTS USING SATLAB SOFTWARE . . . . .	176
R. L. Campbell, Michigan Tech	
CLOSING REMARKS ON THE NASA PROPAGATION PROGRAM . . . . .	187
D. V. Rogers, Propagation Advisory Committee Representative, CRC, Canada	

# ACTS PROPAGATION STUDIES MINIWORKSHOP

Chairman: D. (Jack) Chakraborty

INTRODUCTORY REMARKS FOR ACTS MINIWORKSHOP . . . . .	191
J. Kiebler, NASA Consultant	
ADVANCED COMMUNICATIONS TECHNOLOGY SATELLITE (ACTS) PROGRAM . . . . .	192
R. Bauer, LeRC	
20-GHz ACTS BEACON SPECTRAL ANALYSIS . . . . .	220
D. Chakraborty and J. Gevargiz, JPL	
ACTS BEACONS MEASUREMENTS DATA . . . . .	238
F. Gargione, GE	
ACTS PROTOTYPE PROPAGATION TERMINAL UPDATE . . . . .	263
W. Stutzman, Virginia Tech	





## NAPEX XV ATTENDEES

Mr. Bertram Arbesser-Rastburg  
ESA-ESTEC, Mailcode XEP  
Keplerlaan 1  
NL 2200 AG Noordwick  
The Netherlands  
Phone: +31-1719-84541  
FAX: +31-1719-84999

Dr. Anna Benarroch  
ETSI Telecomacion, UPM  
28040 Madrid, Spain

Mr. Robert Bauer  
NASA Lewis Research Center, MS 54-6  
21000 Brookpark  
Cleveland, OH 44135  
Phone: 216-433-3431  
FAX: 216-433-6371

Dr. Richard Campbell  
Dept. of Electrical Engineering  
Michigan Tech. University  
Houghton, MI 49931  
Phone: 906-487-2848  
FAX: 906-487-2949

Dr. Dayamoy "Jack" Chakraborty  
Jet Propulsion Laboratory, MS 161-228  
4800 Oak Grove Drive  
Pasadena, CA 91109  
Phone: 818-354-1877  
FAX: 818-393-4643

Dr. Faramaz Davarian  
Jet Propulsion Laboratory, MS 161-228  
4800 Oak Grove Drive  
Pasadena, CA 91109  
Phone: 818-354-4820  
FAX: 818-393-4643

Mr. Robert DeBolt  
1354 Toedtli Drive  
Boulder, CO 80303  
Phone: 303-497-5324  
FAX: 303-497-5993

Dr. Khaled Dessouky  
Jet Propulsion Laboratory, MS 161-228  
4800 Oak Grove Drive  
Pasadena, CA 91109  
Phone: 818-354-0412  
FAX: 818-393-4643

Dr. Asoka Dissanayake  
COMSAT Laboratories  
22300 Comsat Drive  
Clarksburg, MD 20871  
Phone: 301-428-4411  
FAX: 301-428-3686

Dr. Paul Duvoisin  
Dept. of Electrical Engineering  
Tulane University  
204 Stanley Thomas Hall  
New Orleans, LA 70118  
Phone: 504-865-5785  
FAX: 504-865-5526

Mr. Jakob Dyk  
EH 11-03  
Eindhoven University of Technology  
P.O. Box 513  
5600 MB, Eindhoven  
The Netherlands  
Phone: 040-473417  
FAX: 040-455197

Mr. Leonard Fedor  
NOAA/ERL/WPL, R45x5  
325 Broadway  
Boulder, CO 80303

Mr. Gerald Gerace  
4355 Brookfield Drive  
Boulder, CO 80303  
Phone: 303-499-4078

Dr. Julius Goldhirsh  
Johns Hopkins University  
Applied Physics Laboratory  
Johns Hopkins Road  
Laurel, MD 20723-6099  
Phone: 301-953-5042  
FAX: 301-953-1093

Mr. George Hagn  
SRI International  
1611 N. Kent Street  
Arlington, VA 22209  
Phone: 703-247-8470  
FAX: 703-247-8569

Mr. Richard Horttor  
Jet Propulsion Laboratory, MS 161-228  
4800 Oak Grove Drive  
Pasadena, CA 91109  
Phone: 818-354-6169  
FAX: 818-393-4643

Dr. Anil Kantak  
Jet Propulsion Laboratory, MS 161-228  
4800 Oak Grove Drive  
Pasadena, CA 91109  
Phone: 818-354-1825  
FAX: 818-393-4643

Mr. John Kiebler  
NASA Office of Commercial Programs  
Code C, Crystal City, Gateway 4  
1213 Jefferson Davis Highway  
Crystal City, VA 22202  
Phone: 703-557-5316  
FAX: 703-557-9060

Dr. Peter Kinman  
Jet Propulsion Laboratory, MS 161-228  
4800 Oak Grove Drive  
Pasadena, CA 91109  
Phone: 818-354-8888  
FAX: 818-393-4643

Dr. Hans Liebe  
NOAA/ITS  
325 Broadway  
Boulder, CO 80303  
Phone: 303-497-3310

Dr. Antonio Martellucci  
Fondazione Ugo Bordini  
Via B. Castiglione 59  
00142 Roma  
Phone: +39-6-5480-2116  
FAX: +39-6-5480-4402

Dr. Charlie Mayer  
University of Alaska  
Dept. of Electrical Engineering  
539 Duckering Bldg.  
Fairbanks, AK 99775-0660  
Phone: 907-474-6091  
FAX: 907-474-6087

Dr. Roderic Olsen  
Communications Research Centre  
P.O. Box 11490 Station H  
Ottawa, Ontario  
Canada K2H 8S2  
Phone: 613-998-2564  
FAX: 613-990-7987

Mr. Gerd Ortgies  
Forschungsinstitut der Deutschen Bundespost  
Telekom, Am Karalleriesand 3  
D-6100 Darmstadt  
Fed. Rep. Germany  
Phone: 06151-83-2545  
FAX: 83-4791

Mr. Peter Papazian  
Dept. of Commerce  
ITS.S1 Rm. 3403B  
325 Broadway  
Boulder, CO 80303  
Phone: 303-497-5369  
FAX: 303-497-5993

Dr. Tim Pratt  
Virginia Tech.  
Bradley Dept. of Electrical Engineering  
340 Whittemore Hall  
Blacksburg, VA 24061-0111  
Phone: 703-231-6681  
FAX: 703-231-3355

Mr. Johannes Raczek  
Forschungsinstitut der Deutschen Bundespost  
Telekom, Am Karalleriesand 3  
Fed. Rep. Germany  
Phone: (06151) 83-2545  
FAX: 83-4791

Mr. Will Remaklus  
Virginia Tech.  
Bradley Dept. of Electrical Engineering  
340 Whittemore Hall  
Blacksburg, VA 24061-0111  
Phone: 703-231-6834  
FAX: 703-231-3355

Mr. Friedrich Ruecker  
Forschungsinstitut der Deutschen Bundespost  
Telekom, Am Karalleriesand 3  
Fed. Rep. Germany  
Phone: 06151-83-2545  
FAX: 83-4791

Mr. Erkki Salonen  
Helsinki University of Technology  
Radio Laboratory, Otakarri 5A  
02150 Espoo 15  
Finland  
Phone: 358-0-4512249  
FAX: 358-0-460224

Dr. Ernest K. Smith  
NASA Propagation Information Center  
Electrical and Computer Engineering  
Campus Box 425  
University of Colorado  
Boulder, CO 80309-0425  
Phone: 303-492-7123  
FAX: 303-492-2578

Dr. Warren L. Stutzman  
Virginia Tech.  
Bradley Dept. of Electrical Engineering  
340 Whittemore Hall  
Blacksburg, VA 24061-0111  
Phone: 703-231-6834  
FAX: 703-231-3355

Mr. Dennis Sweeney  
Virginia Tech.  
Bradley Dept. of Electrical Engineering  
340 Whittemore Hall  
Blacksburg, VA 24061-0111  
Phone: 703-231-6834  
FAX: 703-231-3355

Mr. Noulie Theofylaktos  
NASA Lewis Research Center, MS 55-1  
21000 Brookpark Road  
Cleveland, OH 44135  
Phone: 216-433-2702  
FAX: 216-433-8705

Mr. Arvydas Vaisnys  
Jet Propulsion Laboratory, MS 161-228  
4800 Oak Grove Drive  
Pasadena, CA 91109  
Phone: 818-354-6219  
FAX: 818-393-4643

Dr. Wolfhard Vogel  
EERL/University of Texas  
10100 Burnet Road  
Austin, TX 78758  
Phone: 512-471-8608  
FAX: 512-471-8609

Dr. Hiromitsu Wakana  
Kashima Space Research Center, CRL  
893-1 Hirai, Kashima  
Ibaraki 314  
Japan  
Phone: +81-299-84-4119  
FAX: +81-299-83-5728

Dr. Alan Webster  
Faculty of Engineering  
University of Western Ontario  
Ontario, Canada N6A 5B9

Dr. Edgeworth Westwater  
NOAA/ERL/WPL, R/E/WPS  
325 Broadway  
Boulder, CO 80303  
Phone: 303-497-6527  
FAX: 303-497-6978



## NAPEX XV Summary

Faramaz Davarian  
Jet Propulsion Laboratory, MS 161-228  
4800 Oak Grove Drive  
Pasadena, CA 91109

Ernest K. Smith  
NASA Propagation Information Center  
University of Colorado  
Boulder, CO 80309-0425

The NASA Propagation Experimenters Meeting (NAPEX XV) was held at the Sheraton Armouries Hotel in London, Ontario, on June 28, 1991, in conjunction with the North American Radio Science Meeting at the University of Western Ontario, June 24-28. There were 39 registrants in NAPEX XV, representing institutions in Europe, Japan, and the USA. Opening remarks were made by Faramaz Davarian. The first session, "Olympus and ACTS Studies and Experiments," was chaired by John Kiebler in the absence of Dean Olmstead, who had to cancel at the last minute. In his review of Olympus Propagation Experimenters (OPEX) activities and measurements, Bertram Arbesser-Rastburg of ESA/ESTEC reviewed the sequence of events surrounding the loss of the Olympus satellite. He estimated the chances of the satellite's resuming full operation at 50%, a better probability than most of the experimenters had believed possible. Olympus propagation work at Virginia Tech was then described by Warren Stutzman and Will Remaklus. Following the coffee break, Rod Olsen described Earth-space propagation work at the Communications Research Center (CRC) in Ottawa. Charlie Mayer described the needs, facilities, and plans for propagation measurements in Canada. Julius Goldhirsh described the work at Johns Hopkins University's Applied Physics Laboratory (APL), including an antenna-pointing experiment for Land-Mobile Satellite Service (LMSS). The morning session concluded with a presentation by Khaled Dessouky of JPL on proposed mobile experiments with the Advanced Communications Technology Satellite (ACTS). The conferencers stirred with anticipation at the lunch break when Dick Horttor announced a 6.0 earthquake in Sierra Madre, a town near JPL in southern California.

Session II, "Topics in Propagation Studies and Measurements," was also chaired by John Kiebler. David Rogers led with a description of the rapidly changing state of affairs at the International Radio Consultative Committee (CCIR). Next was Hiromitsu Wakana, from the Communications Research Laboratories in Japan, describing recent work there, particularly with regard to the multi-path in the aeronautical mobile service. He was followed by Gerald Gerace, an Air Force captain and Ph.D. candidate at the University of Colorado, who compared cloud models with measurements from Wave Propagation Laboratory (WPL)/NOAA. Ed Westwater then described the current radiometry program supported by NASA at WPL/NOAA. Wolf Vogel, from the University of Texas at Austin, described measurements made near L-band in support of direct sound broadcasting. These involved transmissions from a telescoping, van-mounted tower to a receiver inside various types of buildings.

The recent draft handbook on Land-Mobile satellite systems was first presented by Julius Goldhirsh and then critiqued by Ernie Smith. Ernie reported on a meeting on the previous day on handbooks whose general conclusions were to call the LMSS text something else and to aim future handbooks towards the systems engineer.

Session III, the final session of NAPEX XV, was to be an informal presentation of computer models of propagation methods and was chaired by Faramaz Davarian, the JPL program manager of the NASA Propagation Program. There were two formal presentations, Anil Kantak of JPL presented a proposal for a code covering a comprehensive collection of different models. Ernie Smith, from the University of Colorado and the NASA Propagation Information Center,

presented a paper for Zhang Zengjun, a Chinese visiting scholar working with him, who had programmed the current CCIR methods as incorporated in Report 564 (1990 version).

The NAPEX reception and banquet was also held at the Sheraton Armouries and was attended by 45 people. An added attraction was an after-dinner presentation by Dick Horttor of JPL who showed the Magellan tapes which had been the highlight of the International Radio Science Union/Antenna Propagation Society (URSI/APS) Plenary Session on Wednesday morning. Honored guests at the banquet were Prof. Alan Webster and his wife Erma, from the University of Western Ontario, and Rod Olsen, from the CRC, Ottawa.

The ACTS Propagation Mini-Workshop, Saturday morning, June 29, was chaired by Jack Chakroborty of JPL. There were 34 registrants. John Kiebler and Faramaz Davarian gave introductory comments. John Gevargiz of JPL followed with a presentation of a spectral analysis study of the ACTS 20-GHz beacon signals. This, in turn, was followed by Frank Gargione of GE, speaking on the measured characteristics of the ACTS beacons. After the coffee break, Warren Stutzman took the floor to update the group on the ACTS propagation prototype terminals.

## AGENDA

### NAPEX XV NASA PROPAGATION EXPERIMENTERS MEETING AND ACTS PROPAGATION STUDIES MINIWORKSHOP THE SHERATON ARMOURIES HOTEL LONDON, ONTARIO, CANADA JUNE 28/29, 1991

June 28, 1991

8:30 AM OPENING REMARKS  
F. Davarian, JPL

#### **SESSION 1. Olympus and ACTS Studies and Experiments**

Chairman: J. Kiebler, NASA Consultant

- 8:45 AM 1) Introductory Remarks for NAPEX XV  
J. Kiebler, NASA Consultant
- 8:50 AM 2) A Review of OPEX Activities and Measurements Results  
B. Arbesser-Rastburg, ESA-ESTEC
- 9:10 AM 3) Olympus Propagation Measurement Results at Virginia Tech  
W. Stutzman, Virginia Tech
- 9:30 AM 4) Data Acquisition, Preprocessing and Analysis for the  
Virginia Tech Olympus Experiment  
P. W. Remaklus, Virginia Tech
- 9:50 AM COFFEE/TEA BREAK
- 10:05 AM 5) Earth-Space Propagation Research at CRC  
R. L. Olsen, CRC, Canada
- 10:25 AM 6) The ACTS Propagation Program  
D. Chakraborty and F. Davarian, JPL
- 10:45 AM 7) Propagation Measurements in Alaska Using ACTS Beacons  
C. E. Mayer, U. of Alaska
- 11:05 AM 8) Planned LMSS Propagation Experiment Using: Preliminary  
Antenna Pointing Results During Mobile Operations  
J. R. Rowland and J. Goldhirsh, APL; W. J. Vogel and  
G. W. Torrence, U. of Texas

11:25 AM 9) Propagation-Related AMT Design Aspects and Supporting Experiments  
K. Dessouky and P. Estabrook, JPL

11:45 AM LUNCH BREAK

## **SESSION 2. Topics in Propagation Studies and Measurements**

**Chairman:** J. Kiebler, NASA Consultant

1:15 PM 1) What Is Happening at CCIR Study Group 5?  
D. V. Rogers, CRC, Canada

1:35 PM 2) Propagation Research in Japan  
H. Wakana, CRL, Kashima, Japan

1:55 PM 3) A Comparison of Cloud Models Using Measured Cloud Data Attenuation  
G. C. Gerace and E. K. Smith, U. of Colorado; E. R. Westwater, WPL/NOAA

2:10 PM 4) Measurements of Atmospheric Emission and Absorption  
E. Westwater and J. Snider, WPL/NOAA

2:30 PM 5) Satellite Sound Broadcast Propagation Measurements  
W. J. Vogel and G. W. Torrence, U. of Texas

2:50 PM 6) An Overview of the Text "Propagation Effects for Land-Mobile-Satellite Systems: Experimental and Modeling Results"  
J. Goldhirsh, APL; W. J. Vogel, U. of Texas

3:10 PM 7) Handbooks of the NASA Propagation Program, Past History and Thoughts to the Future  
E. K. Smith, U. of Colorado

3:25 PM COFFEE/TEA BREAK

## **SESSION 3. Computer-Based Propagation Model**

**Chairman:** F. Davarian, JPL

3:40 PM INFORMAL PRESENTATION OF CONTRIBUTIONS AND DISCUSSIONS

5:20 PM CLOSING REMARKS ON THE NASA PROPAGATION PROGRAM  
D. V. Rogers, Propagation Advisory Committee Representative, CRC, Canada

6:30 PM RECEPTION

7:30 PM BANQUET



## **AGENDA ACTS MINIWORKSHOP**

**D. "Jack" Chakraborty, Chairman**

**June 29, 1991**

- |          |    |   |
|----------|----|---|
| 8:30 AM  | 1) | Introductory Remarks for ACTS Miniworkshop<br>J. Kiebler, NASA Consultant     |
| 8:50 AM  | 2) | Advanced Communications Technology Satellite (ACTS) Program<br>R. Bauer, LeRC |
| 9:10 AM  | 3) | 20-GHz ACTS Beacon Spectral Analysis<br>D. Chakraborty and J. Gevorgiz, JPL   |
| 9:30 AM  | 4) | ACTS Beacons Measurements Data<br>F. Gargione, GE                             |
| 9:50 AM  |    | COFFEE/TEA BREAK  |
| 10:05 AM | 5) | ACTS Prototype Propagation Terminal Update<br>W. Stutzman, Virginia Tech      |
| 10:40 AM |    | OPEN DISCUSSION   |
| 11:45 AM |    | ADJOURN   |

## **OPENING REMARKS**

**Faramaz Davarian**  
Jet Propulsion Laboratory  
California Institute of Technology  
4800 Oak Grove Drive  
Pasadena, CA 91109

### **1. TASKS AND ACCOMPLISHMENTS DURING THE LAST YEAR**

Let us begin by reviewing our past year's major tasks and accomplishments. The tasks have been:

- Olympus data collection and processing
- The ACTS Propagation Program
- Satellite Sound Broadcast measurements and analysis
- LMSS Propagation Effects Handbook
- Radiometric techniques
- Information dissemination and program review

During the last year, we completed construction of the Olympus propagation terminals and began collecting data as of mid-August 1990. Our investigators at Virginia Tech have completed the preprocessing software and have successfully processed nine months of data. The data analysis software is almost completed and the results of the measurement analysis will be published soon. As you are probably aware, the Olympus Propagation Experimenters (OPEX) group suffered a setback due to the loss of the satellite in late May 1991. We are saddened by this loss and are trying to find ways to minimize the impact of this unhappy accident.

The Second ACTS Propagation Studies Workshop (APSW-II) was held in Santa Monica in late November 1990. The recommendations resulting from that workshop were used to draft a plan for the ACTS Propagation Program that will be discussed later today. Funds will be available for experimenters who wish to participate in the ACTS Propagation Measurement Program. A NASA notice of research announcement (NRA) has been drafted and will be released in early fall.

During the last year, our effort to characterize Satellite Sound Broadcast channels was very fruitful, and our investigator, Wolf Vogel, was able to provide NASA with useful propagation data in time to possibly influence WARC 92 decisions.

Propagation handbooks are perhaps our most celebrated products. The preliminary version of the LMSS Propagation Effects Handbook, that describes propagation effects in Land-Mobile satellite links, is now available, and the authors are collecting comments.

In the last three years, we have learned that ground-based radiometers are a very practical and cost-effective means of collecting propagation data. The NOAA radiometers have been busy

collecting propagation data and our investigators at the Wave Propagation Laboratory have analyzed the measurements, as you will hear later today.

We remain committed to providing our users with our study results in a timely fashion. The University of Colorado has published four newsletters and helped us with information dissemination. Our review committee, consisting of Prof. Gert Brussaard and Dr. David Rogers, has continued providing us with enlightening advice.

Regarding international activities, I attended the Olympus Propagation Experimenters workshop and meeting last April in the Netherlands. I also attended an AGARD meeting in Greece last October. Participation in international meetings enhances the atmosphere for cooperation and scientific exchange between the NASA Propagation Program and the international propagation community.

## **2. PLANS FOR 1991-92**

The program will focus on the following areas during the next year:

- OPEX activities
- The ACTS Propagation Program
- Satellite Sound Broadcast experiments and studies
- Radiometric techniques
- Software propagation models
- Review and revision of the NASA Propagation Handbooks
- Fade detection and compensation
- CCIR activities
- Information dissemination and program review

The loss of the Olympus spacecraft has placed OPEX in a peculiar position. Cooperation among the OPEX members is needed to lessen the damage resulting from the loss of the satellite. Some OPEX members have collected over one year of data; some, like us in the U.S., have collected less than one year of data; and others were about to start their measurements. Since no more data will be collected, we need to share our limited data banks generously. We also need to exchange ideas about minimizing the impact of the satellite loss. In short, OPEX has suffered a loss, but it is not dead.

The ACTS propagation campaign will gain full momentum during the next year or two. The propagation terminal prototype will be completed, parts for the experiment terminals will be ordered, and experimenters will be selected. A NASA NRA will be released in early fall 1991, and experimenters will be selected about nine months later. The mobile propagation terminal will be completed and tested, and the ACTS Propagation Program plan will be finalized. Our objectives also call for the participation of the propagation community in the ACTS conference in August, in San Jose, California. Later this year or early next year, we will have a full two-day workshop (APSW-III).

Regarding our Satellite Sound Broadcast efforts, we are planning to supplement our studies with field measurements using satellite beacons. Our cooperation with the Satellite Sound Broadcast task at JPL will proceed. Also, we will maintain our support of the national and international efforts to enable the Satellite Sound Broadcast service.

We will continue increasing our propagation database at 20, 30, and 90 GHz, using NOAA's ground-based radiometers. A more active role for NOAA investigators to support the ACTS effort is envisaged.

A new effort next year will be the creation of a software package incorporating the propagation models that can be found in the NASA Propagation Handbooks and elsewhere. The aim is to facilitate the use of propagation models by system engineers and other users of propagation data. After completion, the software package will be distributed to the user community free of charge. As you may have noticed, today's agenda includes a session to discuss the approach for developing the software.

Towards the end of the year, the LMSS Propagation Effects document will be published with the title "Propagation Effects for Land-Mobile Satellite Systems: Experimental and Modeling Results." We are also planning to revise our existing two handbooks, and discussion is now in progress as to whether a consolidation of the handbooks for above and below 10 GHz is warranted.

Fade compensation is crucial for the successful operation of low-margin terminals, especially when operated in the Ka-band. We addressed this problem in the past year as part of our Olympus effort. The importance of this subject warrants the examination of it from a different angle, namely, the control and signal processing viewpoint. We hope to interest a research group with a strong background in signal processing and controls to have a fresh look at the problem of fade detection and mitigation.

Little CCIR activity occurred during the past year, except for Robert Crane's attendance at an IWP-5/3 meeting last December. However, now that we understand the new CCIR organization, our CCIR activities will increase.

The NASA information center at the University of Colorado will continue its cooperation with the NASA Propagation Program.

**NAPEX XV**

**Session 1**

**OLYMPUS AND ACTS  
STUDIES AND EXPERIMENTS**

Chairman:

John Kiebler  
NASA Consultant



INTRODUCTORY REMARKS FOR NAPEX XV  
JOHN W. KIEBLER

0 WELCOME TO NAPEX XV

0 ORGANIZATION CHANGES AT NASA HEADQUARTERS

- COMMUNICATIONS AND INFORMATION SYSTEMS DIVISION IN THE OFFICE OF SPACE SCIENCE AND APPLICATIONS (OSSA) HAS BEEN DISBANDED
- INFORMATION SYSTEMS RELOCATED TO FLIGHT SYSTEMS DIVISION IN OSSA
- TECHNOLOGY DEVELOPMENT MOVED TO INFORMATION SCIENCES AND HUMAN FACTORS DIVISION IN OFFICE OF AERONAUTICS, EXPLORATION AND TECHNOLOGY (OAET)
- ACTS SPACECRAFT DEVELOPMENT THROUGH LAUNCH RELOCATED TO EARTH SCIENCE AND APPLICATIONS DIVISION IN OSSA
- ACTS EXPERIMENTS PROGRAM MOVED TO OFFICE OF COMMERCIAL PROGRAMS (OCP)
- RADIO SCIENCE AND SUPPORT STUDIES WHICH INCLUDES THE PROPAGATION PROGRAM MOVED TO OCP
- CENTER FOR THE COMMERCIAL DEVELOPMENT OF SPACE (COMMUNICATIONS) BEING ESTABLISHED IN OCP
- RAY ARNOLD, FORMERLY DIRECTOR OF THE COMMUNICATIONS AND INFORMATION SYSTEMS DIVISION IS NOW DEPUTY ASSISTANT ADMINISTRATOR FOR COMMERCIAL PROGRAMS
- DEAN OLMSTEAD IS NOW THE ACTS EXPERIMENTS PROGRAM MANAGER IN OCP

0 NON-U.S. PARTICIPATION IN THE ACTS PROGRAM

- POLICY STILL UNDER REVIEW WITH OBJECTIVE OF ALLOWING SOME PARTICIPATION
- VERY ENCOURAGING THAT CHANGES WILL BE MADE TO CURRENT POLICY
- PARTICIPATION IN ACTS PROPAGATION PROGRAM VIRTUALLY ASSURED
- OUR NON-U.S. COLLEAGUES ARE INVITED TO PARTICIPATE IN THE ACTS MINI-WORKSHOP TOMORROW MORNING

## A REVIEW OF OPEX ACTIVITIES AND MEASUREMENT RESULTS

B. Arbesser-Rastburg

ESA-ESTEC, Noordwijk, The Netherlands

### Abstract

A summary is given of the measurements carried out in the framework of OPEX (OLYMPUS Propagation Experimenters Group). In particular, the progress since mid 1990 is presented. In this period two OPEX meetings were held, OPEX XIV (October 1990) and OPEX XV (April 1991) and the First OPEX Workshop was held at ESTEC on 23-24 April 1991.

### 1. Introduction

The OLYMPUS Propagation Experimenters were well prepared when ESA's large communications satellite OLYMPUS was launched in summer of 1989. All important aspects of the measurement programme had been jointly defined and as far as possible standardized. Handbooks had been produced to define the requirements for the measurement hardware and the data processing software. However, only a handful of measurement sites were actually ready to operate - delays in funding and/or hardware delivery had delayed the start-up of the majority of stations. This was not considered a dramatic drawback since the satellite was designed for an operational lifetime of at least five years and a measurement over three years was generally considered sufficient.

In the time since the launch several new stations became operational and an even larger number were just about to be completed when a major anomaly in the spacecraft's attitude control caused a disruption of all OLYMPUS experiments on 29 May 1991 at 03:21 UTC.

### 2. Rain Attenuation Measurements

Several intensive rainstorms with one-minute rainfall rates exceeding 30 mm/h were observed during the first 1.5 years of operation. British Telecom Research Labs operated their 20/30 GHz beacon receivers with a 6.1 meter steerable antenna which gave a good dynamic range. Figure 1 shows an example of a time series recorded during a storm on 15 August 1990 [1].

An interesting aspect of multi-frequency beacon measurements is the instantaneous frequency scaling which is required for open-loop up-link power control systems. Although the long-term average of rain-attenuation scaling is fairly constant, the instantaneous ratio is not. Figure 2 shows a scatterplot of instantaneous 30 GHz versus 20 GHz copolar attenuation values measured at Darmstadt, Germany on 26 August 1990 [2]. Each point represents a 30-second average value - the averaging was used to remove scintillations. The pronounced hysteresis effect visible on the plot (increasing slope lower than decreasing slope, counterclockwise progression) comes from the fact that the drop-size distribution changes during the event.

At the combined experiment of the Dutch PTT and Delft University, the site diversity performance of 2 stations situated 10 km apart was investigated [3]. For high availability services at Ka-band (e.g. HDTV feeder links) site-diversity may be the only fade restoration method that produces enough margin. Several events of the summer of 1990 were analyzed. In most cases of convective storm the diversity performance was adequate (Figure 3). However, there was also an event with extreme high rainrates observed where both sites were affected at the same time (Figure 4). This means that the site distance was insufficient to produce the required time-lag between the rain attenuations occurring on the links.



### 3. Cloud attenuation and scintillation measurements

For very small Ka-band terminals which are designed for low availability systems with hardly any propagation margin not only rain but also clouds can constitute a problem. Rain occurs in most places for less than 5 percent of the time but clouds occur for more than 50 percent of the time in temperate climate regions. It is therefore necessary to investigate the occurrence of clouds and the related fade in the same way as has been done with rain in the past. Several experimenters have embarked on such investigations, but results have not been analyzed yet.

A theoretical assessment of the propagation phenomena relevant to low-availability systems has been completed in spring of 1990 [4].

Tropospheric scintillations which are rapid signal fluctuations caused by air turbulence also affect the link budget and can be problematic for dynamic fade restoration techniques. In previous experiments using Ku-band beacons, it had been established that scintillations are more intensive at low elevation angles (longer path) and at higher temperatures (more turbulence). At the University of Louvain-la-Neuve (Belgium) one of the two receiving stations is equipped with a special 30 Hz acquisition mode for measuring the scintillations at 12 and 30 GHz [5]. Figure 5 shows the measured spectral density of the 30 GHz beacon signal. The well known "-8/3" law of propagation through turbulent layers is also plotted; it shows that the measured spectrum is in good agreement with theory.

### 4. Depolarization Measurements

Depolarization by oblate raindrops and by ice-needles may cause severe interference problems with frequency re-use systems. Most experimenters in the OPEX group are therefore undertaking measurements of the crosspolar beacon levels. A special working group has been set up to study the proper bias removal procedures [6].

In several stations specialized switching receivers make use of a special feature of the OLYMPUS 20 GHz beacon: The transmitted polarization plane alternates between two orthogonal orientations at a rate of 933 Hz. Since this switching rate is much higher than the de-correlation time, the received signals (2 co- and 2 crosspolar levels) allow for a quasi-simultaneous retrieval of the full transmission matrix.

Event analysis was performed and reported by the DBP-Telekom group [7] and by the Technical University of Eindhoven [8]. Some limited statistics (Figure 6) were presented by Telecom Denmark at the OPEX 14 meeting [9].

An important conclusion from these measurements is the observation that the XPD prediction of the CCIR [10] heavily under-estimates the ice-depolarization at low attenuation values.

### 5. Radiometric Measurements

All major stations in the OPEX program are equipped with one or more radiometers. Measuring the sky noise temperature at one frequency within the water vapour absorption line (22 GHz) and another one well outside this line (e.g. 30 GHz) allows to retrieve the vapour and liquid water content of atmosphere along the beacon reception path. [11] This information is used for calculating the clear air ("0 dB") reference level for the beacon measurements and to investigate cloud attenuation. Special cloud studies with a scanning radiometer are undertaken by the Fondazione Ugo Bordoni in Rome, whose staff is also in charge of the network of 20 GHz receivers in Italy (25 sites).

Another specialized application of ground based radiometry is the simultaneous measurement of the 19 GHz sky-noise temperature at two orthogonal polarizations, as reported by DLR [12]. An example for the observed differential sky noise temperature ( $T_h - T_v$ ) is given in Figure 7.

The OPEX working group on radiometry (which is also in charge of auxiliary measurements) has very active participation in the field of comparing and improving retrieval algorithms. A handbook will be published summarizing all major findings.

## 6. Radar Measurements

Several sites are equipped with specific meteorological radars operating at S-, C- or X-band. These radars are used to establish the drop size distribution of a rain-cell, the horizontal and vertical structure of the precipitation event, the existence and extent of a melting layer. Radars with doppler processing are also capable of measuring the air turbulence.

In order to better coordinate their measurements and analyses, the experimenters have formed a Radar Working Group within OPEX. Of particular interest are the backscatter (at radar frequency) and forward-scatter (at beacon-frequency) programmes used for raindrops and ice/water mixtures. An anisotropic melting layer model is also being studied and developed. It is envisaged that all the achievements of this working group will be published in a handbook. Since the processing of radar data is known to be time-consuming, analyzed results of joint radar and beacon measurements have not been available until now but are expected to be presented at the OPEX 16 meeting in Aveiro, in October 1991.

## 7. The Standardized DAPPER Software

The Data Preprocessing and Analysis Software was completed and distributed by ESA to all signatories of the OPEX agreement. The general distribution was preceded by a half-year beta-testing phase in which some experimenters had volunteered to participate. Currently, a conversion of the UNIX-based software to HP-UX is underway which will make the software available to experimenters using HP-9000 workstations rather than 386- or 486 based PCs.

## 8. Implications of the OLYMPUS Failure.

On 29 May 1991 at 03:21 UTC the spacecraft went into the "Emergency Sun Acquisition"-mode which is the pre-programmed position for coping with any sort of potentially dangerous malfunctions. Attempts to repoint the spacecraft back to the nominal position failed and left the spacecraft in a spinning condition with depleted batteries. The cause for the problem is under investigation by a special inquiry board.

With the sun getting into a more favourable angle towards the solar panel new attempts were made to command the satellite. The recovery of the spacecraft has begun by successfully executing telecommands on 19 June. However, at this point it is still unclear whether the spacecraft operation can be completely re-established.

If the recovery is successful, the remaining lifetime of the satellite will be reduced since some of the fuel needed for station keeping will have been spent in the recovery procedures. But any period of more than one year continuous operation can be considered worthwhile to continue the interrupted experiments and to start those measurements that were just about to begin when the failure occurred.

If, on the other hand, the nominal operation of the propagation beacons under nominal attitude control conditions cannot be restored, the OPEX group will have to turn to alternate beacon sources in order to achieve the goal of establishing better propagation prediction tools for satellite services using frequencies above 10 GHz. After all, the cost of the ground equipment exceeds US\$ 20 million and a decision to discontinue this research activity would mean that this investment is lost.

Unfortunately, there is no exact replacement of the OLYMPUS beacon payload in orbit, which means that experimenters will have to convert their stations to receive beacon signals from other spacecraft. Of course, the possibility of re-flying the OLYMPUS beacon payload that was built for flight model 2 exists but even if the technical, contractual and financial questions can be solved, a time frame of at least 2 years is expected for getting this payload into orbit.

In order to co-ordinate the conversion activities and establish the new mode of co-operation in the OPEX group, a special OPEX meeting has been set up for 3 July 1991 at ESTEC.

## 9. Conclusion

The OPEX group has been very active during the last year and the First OPEX Workshop gave ample evidence of this point. First results have been obtained and links have been established to other propagation experimenters groups such as the INTERKOSMOS experimenters in Eastern Europe. Now, many groups are using the break in the measurements to analyze the data collected so far. Everyone of course hopes that OLYMPUS can be fully restored to the good performance displayed so far. However, even if this cannot be accomplished, the co-operative spirit of the group will continue to ensure scientific results at the highest level to the benefit of the sponsors and, through the submission to the CCIR, the whole satellite communications industry.

## References

1. J. Harris, "BTRL OLYMPUS Experiment - Status & Results", Proc. OPEX XIV Meeting, Felixtowe, 15-17 Oct 1990.
2. F. Rücker, G. Ortgies & F. Dintelmann, "Aspects of Attenuation Frequency Scaling" Proc. OPEX Workshop ESTEC, 23-24 April 1991, Paper Nr 3.3
3. G.J.C. Verhoef, "Event Analysis of the Site-Diversity Experiment in the Netherlands" Proc. OPEX Workshop ESTEC, 23-24 April 1991, Paper Nr 2.1
4. E. Salonen, S. Karhu S & S. Uppala, "Study of Propagation Phenomena for Low Availabilities" ESA-ESTEC Final Report Contract # 8025/88/NL/PR, 1990.
5. D. Vanhoenacker, J. Matagne, H. Vasseur & A. Vander Vorst, "First Analysis of the Effects of Atmospheric Fluctuations on the 12.5, 20 and 30 GHz OLYMPUS Beacons." Proc. OPEX Workshop ESTEC, 23-24 April 1991, Paper Nr 4.2
6. F. Dintelmann "A note on X-polar bias removal", Private communication, February 1991.
7. F. Rücker, F. Dintelmann & G. Ortgies, " Analysis of 20 GHz Crosspolar Events" Proc. OPEX Workshop ESTEC, 23-24 April 1991, Paper Nr 2.3
8. R.A. Hogers, M. Herben, G. Brussaard (EUT): "Depolarization Analysis of the 12.5 and 30 GHz OLYMPUS Beacon Signals" Proc. OPEX Workshop ESTEC, 23-24 April 1991, Paper Nr 2.4
9. J R Larsen, "Separation of XPD data due to rain and ice depolarisation", Proc. OPEX XIV, Felixtowe October 1990, pp 83-85.
10. CCIR SG5, "Propagation Data & Prediction Methods Required for Earth Space Telecommunication Systems", Report 564-3 (MOD F), XVIIth General Assembly Düsseldorf 1990.
11. J. Lavergnat & C. Mallet, "Zero Level Retrieval by Means of a Multifrequency Radiometer" Proc. OPEX Workshop ESTEC, 23-24 April 1991, Paper Nr 1.3
12. A. Hornbostel, "DLR Status Report", Proc. OPEX XIV, Felixtowe 15-17 Oct 1990, pp 63-66.

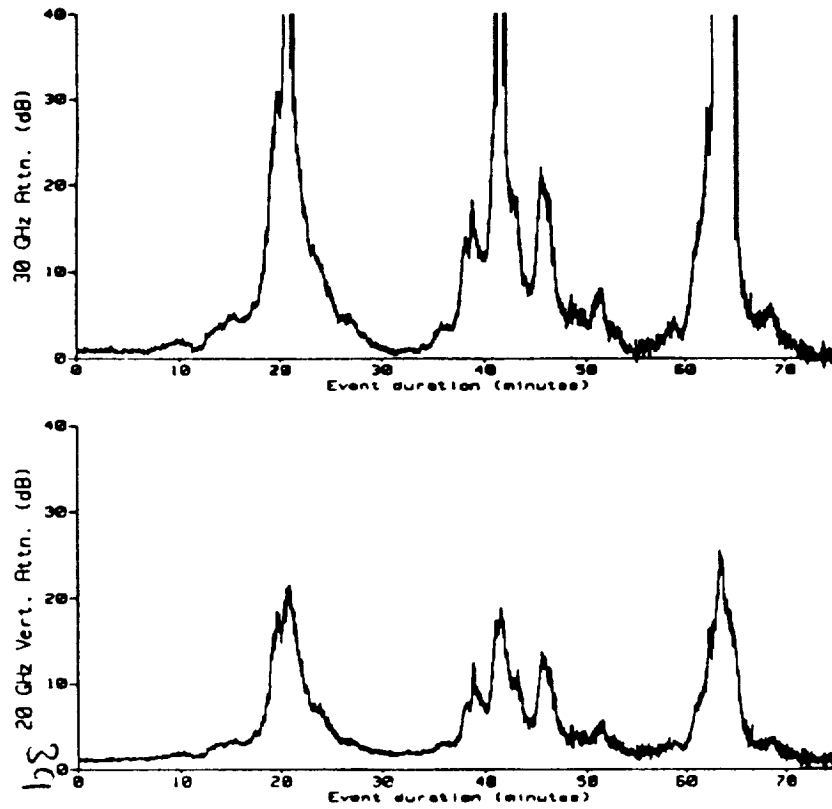


Figure 1: Co-polar attenuation of OLYMPUS 20 & 30 GHz beacons measured at BTRL Martlesham on 15 August 1990 from 16:50 UTC to 18:05 UTC. (Elevation: 27.5 deg)

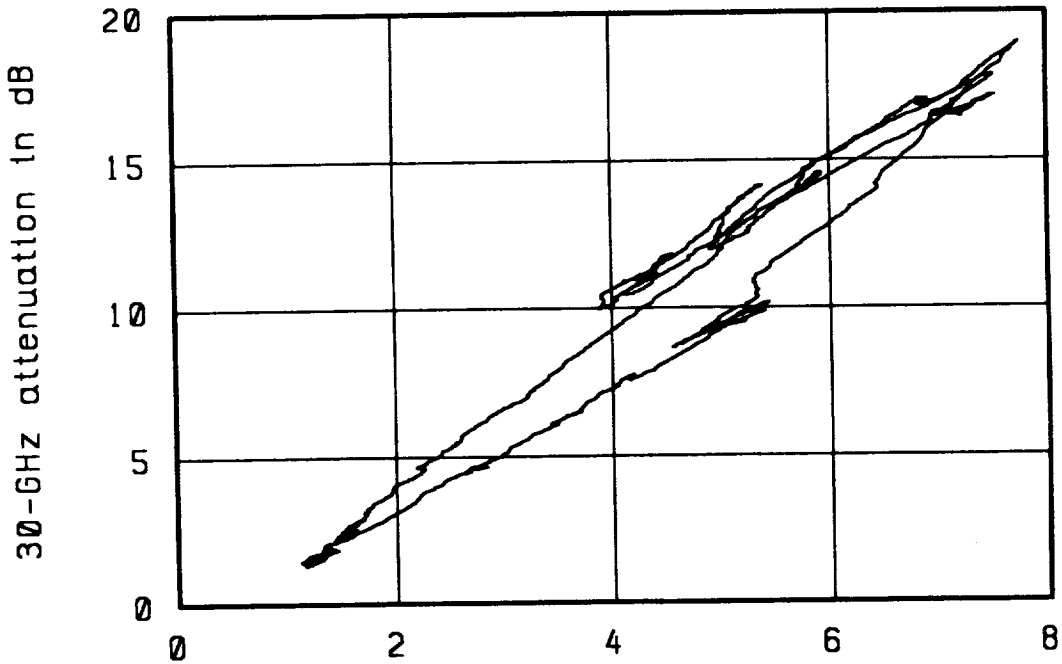


Figure 2: Scatterplot of instantaneous 30 GHz versus 20 GHz copolar attenuation measured at Darmstadt, Germany on 26 August 1990 from 14:00 to 15:00 UTC (data averaging: 30 seconds)

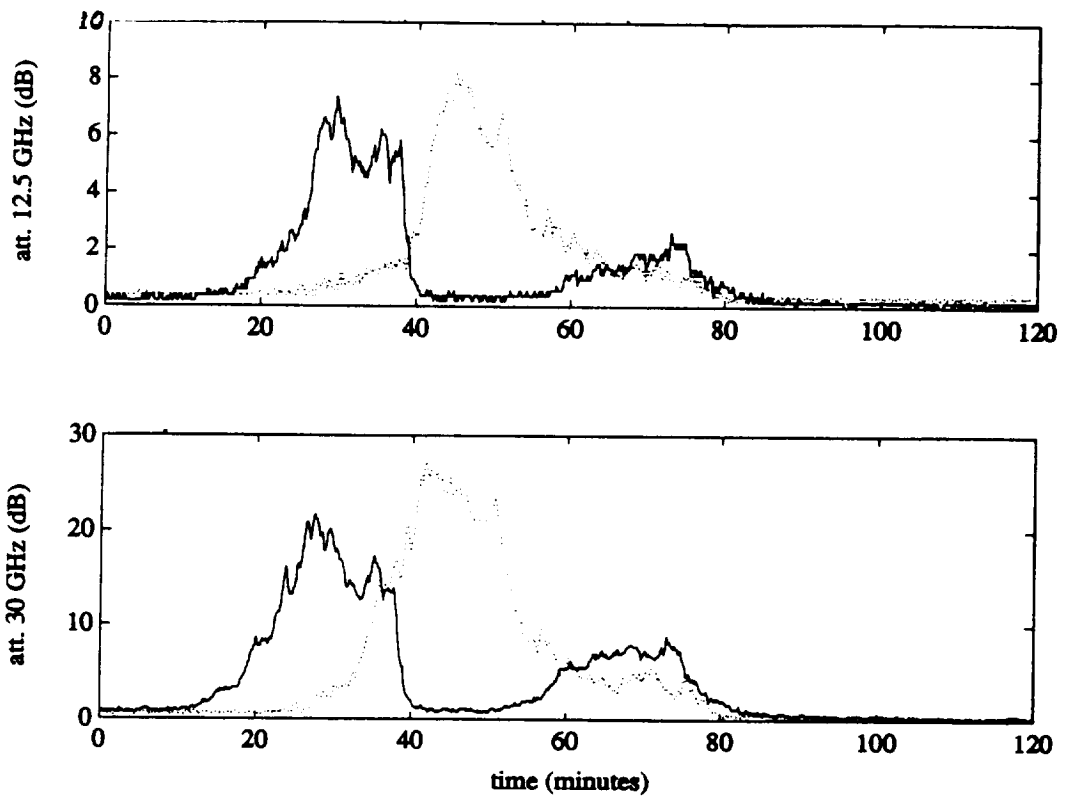


Figure 3: Site diversity observation in Delft (solid line) and Leidschendam (dotted line) on 27 June 1990 from 20:00 to 22:00 UTC. Here the 10 km site distance is sufficient.

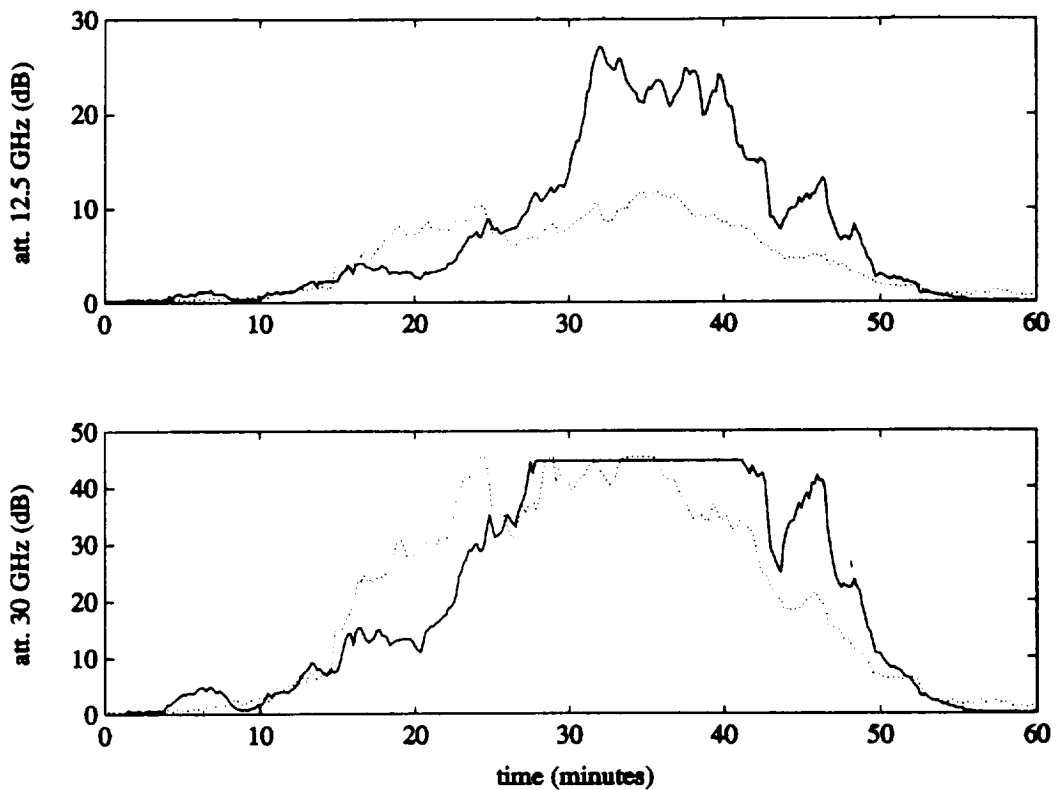


Figure 4: Site diversity observation in Delft (solid line) and Leidschendam (dotted line) on 30 June 1990 from 14:00 to 15:00 UTC. Here the 10 km site distance is in-sufficient.

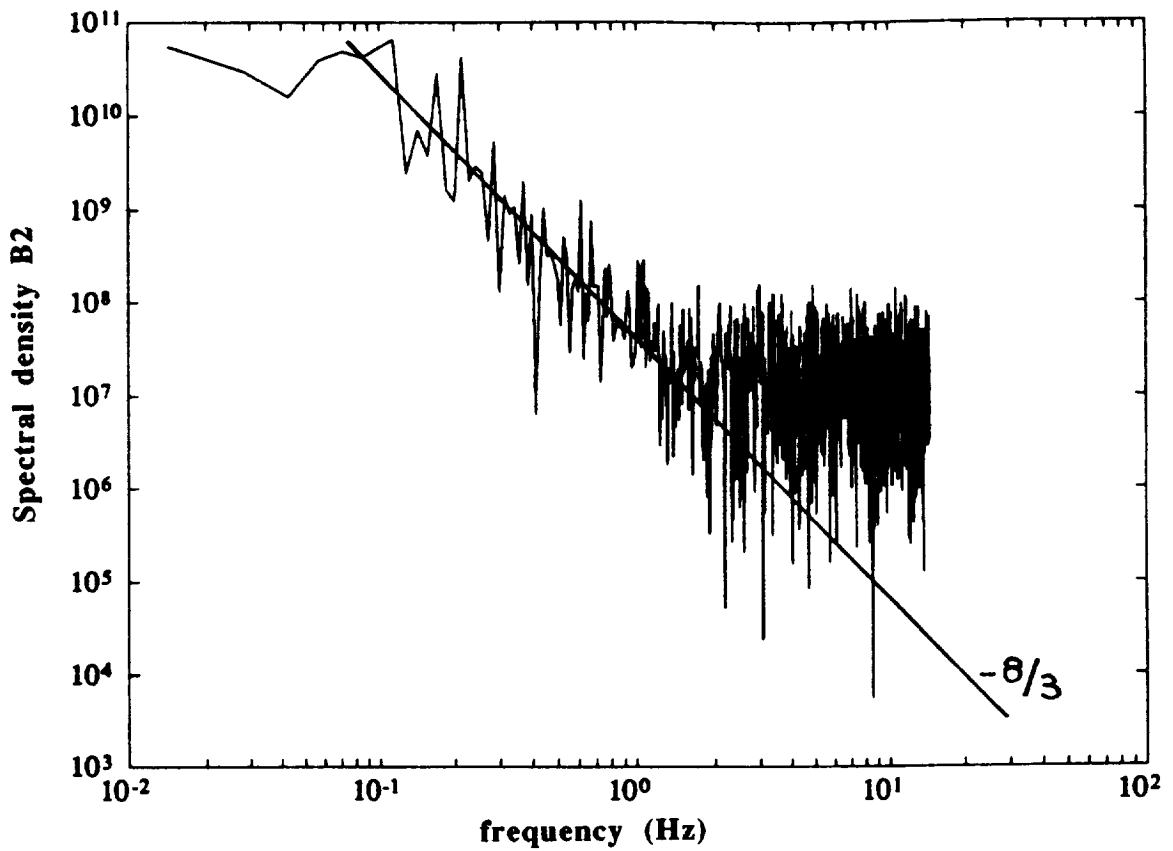


Figure 5: Spectral density of scintillations at 30 GHz measured at Louvain.

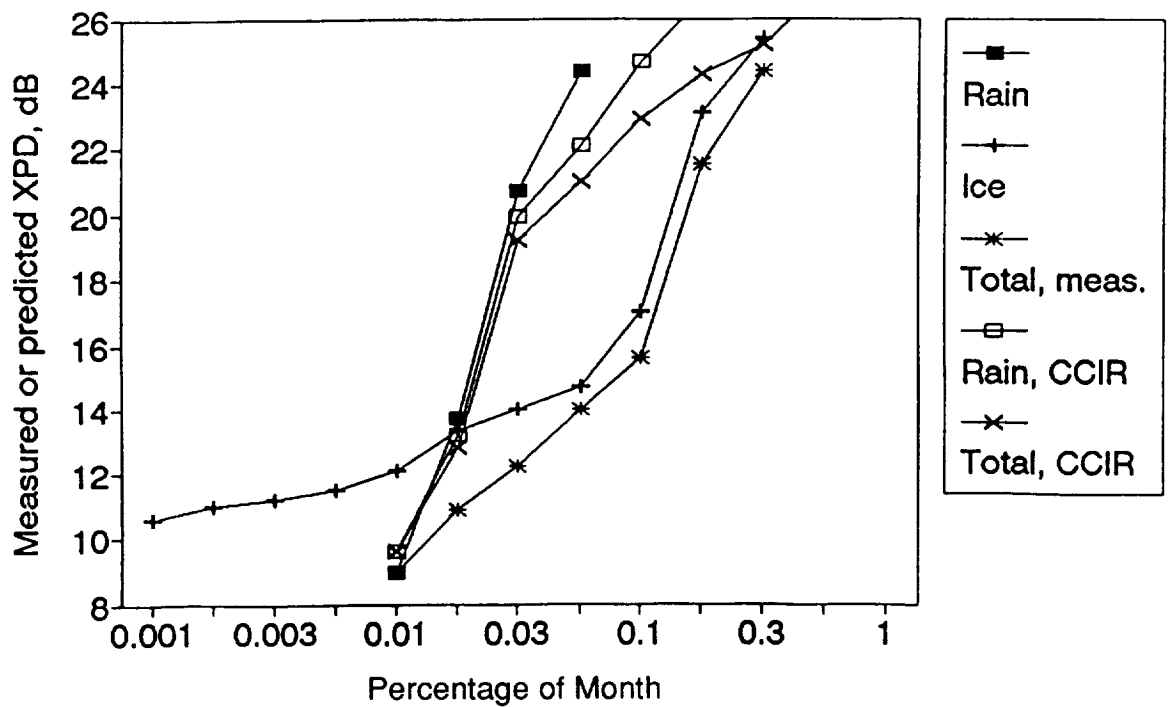


Figure 6: Cumulative statistics of 30 GHz XPD measured in Albertslund and compared with the CCIR predictions. (Preliminary analysis based on 11 days in June 1990)

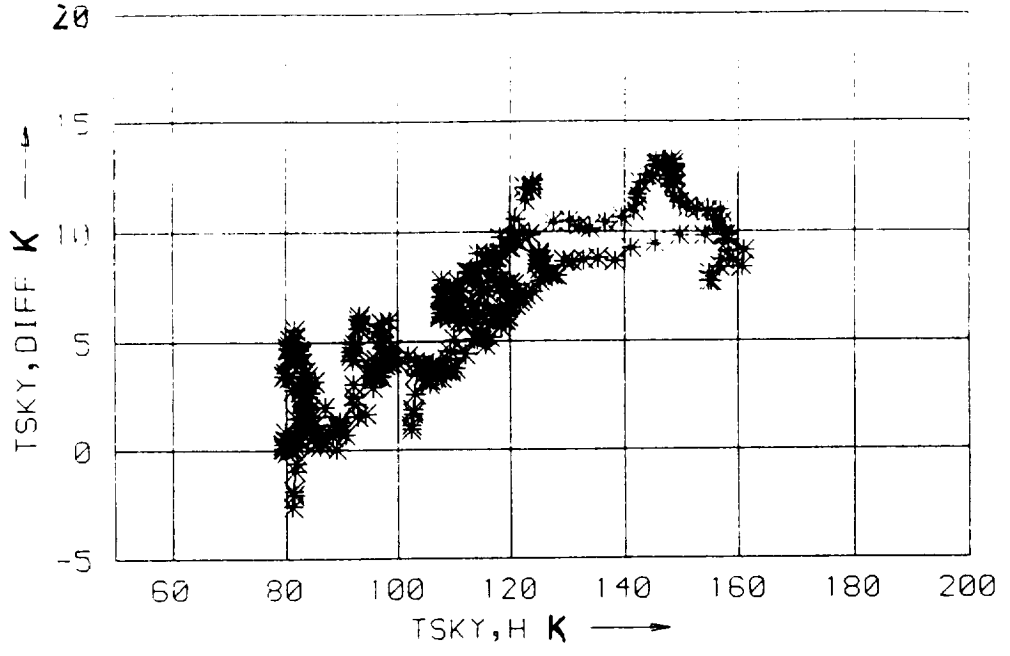


Figure 7: Differential 19 GHz sky noise temperature ( $T_h - T_v$ ) versus  $T_h$  observed at DLR (Oberpfaffenhofen) on 5 Sept 1990 from 01:30 to 02:00 UTC.

**OLYMPUS PROPAGATION MEASUREMENT RESULTS  
AT VIRGINIA TECH**

Warren Stutzman

for the

Satellite Communications Group  
Bradley Department of Electrical Engineering  
Virginia Polytechnic Institute & State University  
Blacksburg, Virginia 24061-0111

**Abstract** - Virginia Tech is performing a comprehensive set of propagation measurements using the OLYMPUS satellite beacons at 12.5, 20, and 30 GHz. A second 20 GHz diversity terminal is portable and is moved to various spacings up to 50 m away from the fixed 20 GHz terminal. Total power radiometers are included in each terminal also. Radiometer data are used both to set the absolute level of the beacon data and to predict path attenuation. This paper presents initial results from the experiment set.

## 1. Introduction

The European Space Agency launched the OLYMPUS satellite in July 1989. In addition to communications experiment packages in Ku- and Ka-bands, OLYMPUS has frequency coherent propagation beacons at 12.5, 19.77 and 29.66 GHz. These beacons are visible from Blacksburg at an elevation angle of 14°. Virginia Tech has four receivers, one at each frequency plus a second portable terminal at 20 GHz for short-baseline diversity measurements.

The receiving system was constructed to take advantage of the frequency coherent beacons. A frequency locked loop derives frequency tracking information from the 12 GHz receiver which experiences smaller fading than that at 20 and 30 GHz. This permits accurate fade measurements of the relatively frequently occurring deep rain fades (25 dB or more) on 20 and 30 GHz. The 12 GHz derived FLL also permits rapid reacquisition after loss of lock.

Measurements at Virginia Tech began in August 1990. Statistical results are currently being processed. These include; fade, fade rate, and fade duration for rain and scintillation events. Frequency scaling results are especially valuable due to the common elevation angle and location of the receivers. Initial results confirm the somewhat less than frequency squared scaling law. For a diversity separation of 50 m for the two 20 GHz receivers, no improvement during rain fading is experienced, while decorrelation for scintillation events is common.

Unfortunately, the OLYMPUS spacecraft lost altitude control on May 29 and has been nonfunctional since. Meanwhile, radiometer measurements continue at Virginia Tech.



These data will be used to characterize propagation conditions on VSAT-type networks for next generation small aperture Ka-band systems.

## 2. The Measurement System

The propagation experiment system at Virginia Tech continuously records the 12.5, 20, and 30 GHz OLYMPUS beacons using receiving antennas 12, 5, and 4 feet in diameter, respectively. A block diagram of the measurement system is shown in Figure 1.

A unique feature of the OLYMPUS beacon package is that the three spacecraft beacons are coherent since they are derived from a common oscillator. The Virginia Tech OLYMPUS receivers take advantage of their coherence by deriving frequency locking information from the 12.5 receiver. This information is used to maintain lock for all four receivers. In effect, this widens the dynamic range of the 20 and 30 GHz receivers, which experience more fading during a rain event than does the 12.5 GHz receiver.

The receivers at all three frequencies are very similar. Each receiver has a low noise amplifier followed by a mixer-preamp whose output IF frequency is 1120 MHz. A motorized attenuator is included in the RF section to aid in system calibration. The 1120 MHz IF is subsequently mixed down to produce lower IF frequencies of 70 MHz and 10 kHz. The 10 kHz signal is then used in detection and tracking.

A hybrid analog/digital receiver is used in the detection scheme for the 12.5 GHz system. The analog portion of the receiver tracks the carrier frequency and maintains the signal within a 3 Hz window. Simultaneously, the 10 kHz carrier is sampled at a 1 kHz rate by a 12 bit A/D converter. Each sample is then filtered by a digital FIR filter and the resulting 16 bit I and Q values are recorded by the data acquisition system.

Clouds and scintillation can produce up to 3 dB of attenuation at 30 GHz on a 14° elevation-angle path and may be present for a large percentage of the time. Therefore, it is important in a slant-path propagation experiment to be able to set the clear air reference level accurately. Radiometers operate at each beacon frequency in our receiving system to aid in setting this clear air reference level. The radiometers are of the total power design; the RF and IF sections are housed in a temperature controlled environment to keep gain constant. The radiometer design is unique in that it uses the same RF chain as the beacon receiver.

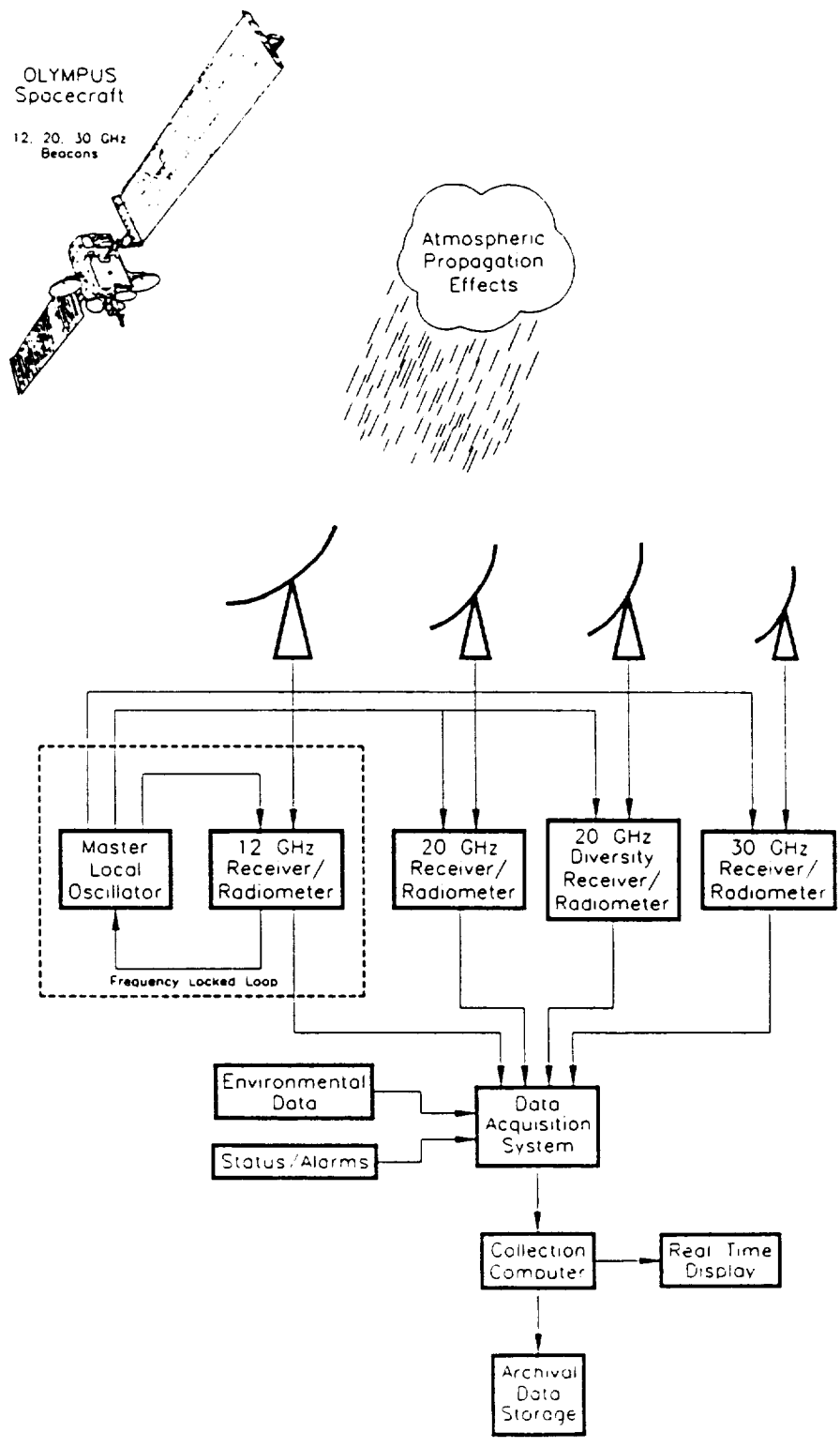


Figure 1. The OLYMPUS measurement system at Blacksburg, VA.

The output of the receivers and radiometers are continuously monitored by a PC-based data acquisition system (DAS). Analysis is performed on a large PC.

### 3. The Experiment Program

The experiment produces a number of primary and secondary attenuation statistics. Beacon attenuation cumulative distributions referenced both to free space and to clear air are produced. Frequency scaling between frequencies is determined. Secondary statistics such as fade slope, fade duration, and fade interval are also generated.

Radiometer predictions of attenuation are also produced. Small scale diversity as a function of the spacings (and vertical height differences) of the two 20 GHz terminals is examined.

Uplink power control applications are considered as well. Here it is hoped that on a 20/30 link with rain fading on the uplink at 30 GHz the control of the uplink power level (alternatively, coding rate) can be based on beacon measurements at 20 or 30 GHz.

### 4. Results

Attenuation statistics are being analyzed. Figure 2 shows an example of cumulative distributions for January.

Radiometer data must be accurate to set the beacon reference level, so we examine it first. Radiometer data also take on new significance now that the OLYMPUS beacons are unavailable. Radiometer data have been reduced for the month of January 1991. Radiometer predicted attenuation has an rms deviation of 0.025 dB from directly measured beacon attenuation. This included events with fades as high as 10 dB. Figure 3 shows a scatter plot of radiometric attenuation versus beacon attenuation referenced to free space.

Scintillation events have been analyzed. Preliminary findings show that the spectrum at all frequencies obeys the popular - 8/3 power law. The diversity site (up to 50 m separation) does offer improvement for scintillation events, but not for rain events.

A major use for our data is in uplink power control studies on narrow margin communication links as for Ka-band VSAT application.

We have found that simple scaling laws work very well. They apply to both attenuation and to unnormalized signal levels as would be encountered in practice. For example, predicted attenuation at 30 GHz follows from measured 20 GHz attenuation as

$$A_{30} = a + b A_{20} \quad (1)$$

$$\log A_{30} = c + d \log A_{20} \quad (2)$$

ARD and AFS  
20 GHz: 05-JAN-91 through 31-JAN-91

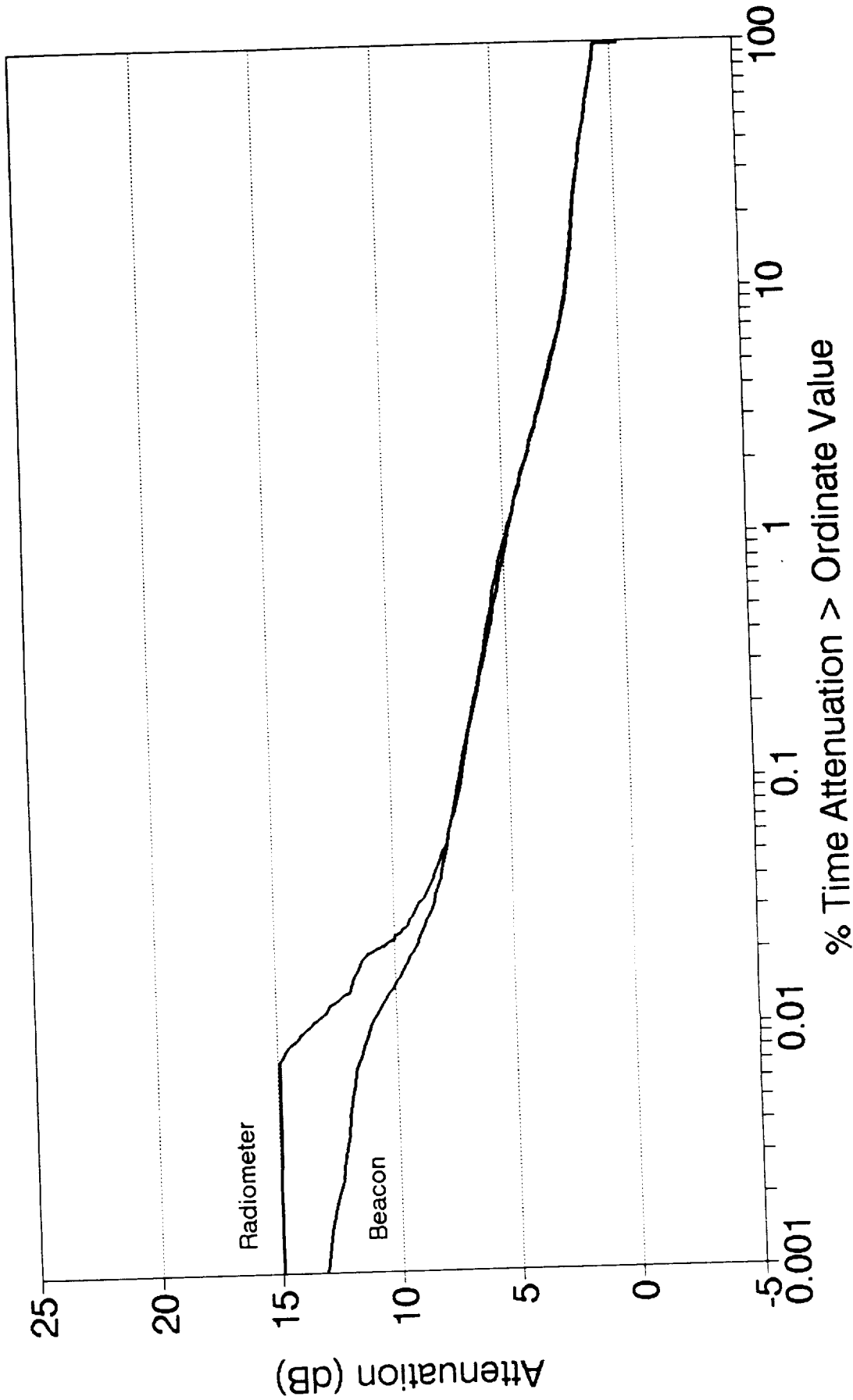


Figure 2. Measured cumulative distributions for January 1991 of beacon attenuation referenced to free space and attenuation predicted from radiometer measurements.

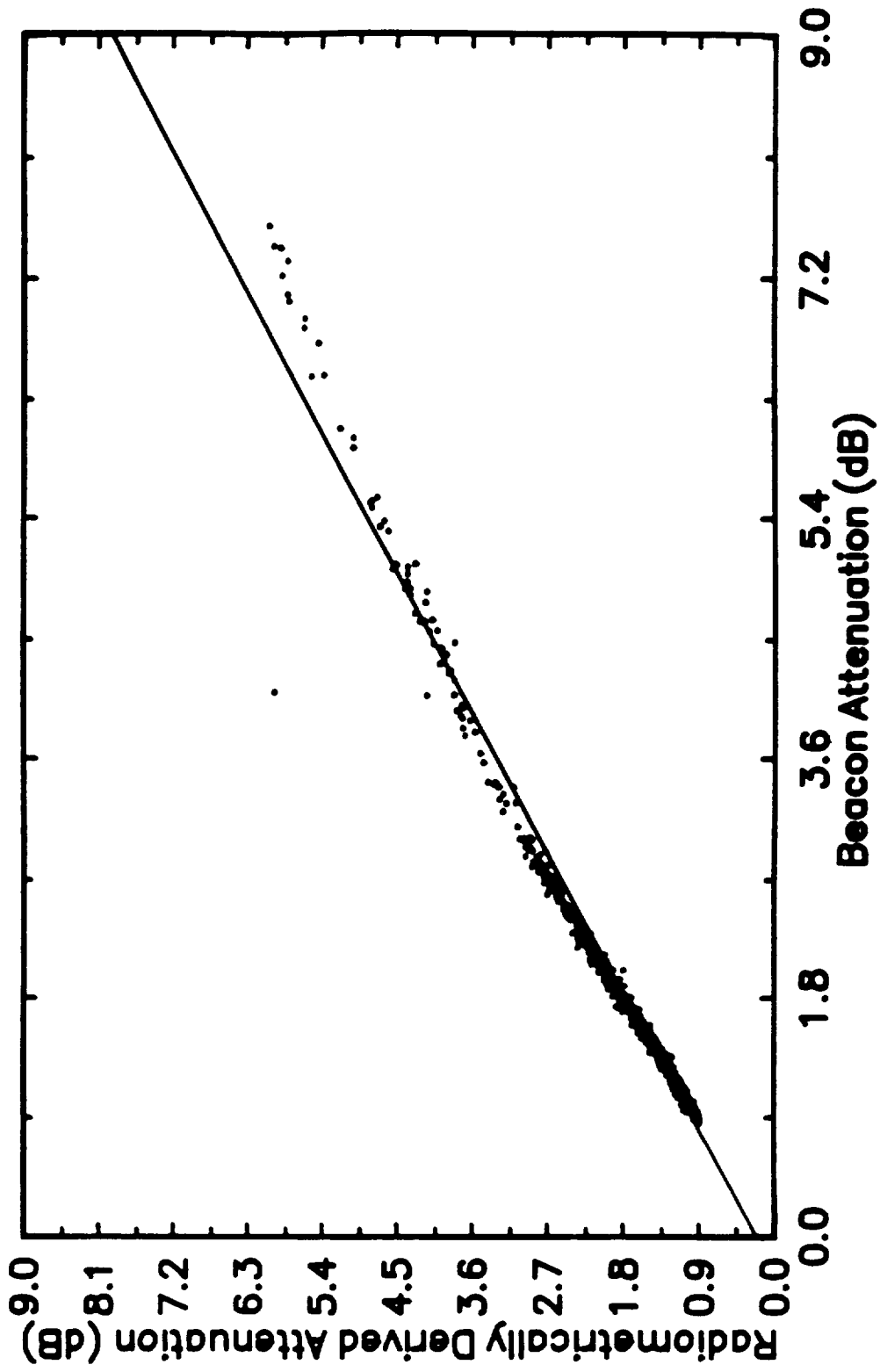


Figure 3. Scatter plot of attenuation predicted from radiometer measurements versus beacon measured attenuation referenced to free space for an event on January 20, 1991 lasting a few hours.

for attenuation in dB. In practice,  $A_{20}$  could be measured from a beacon or even a radiometer. Predictions can also be made from delayed 30 GHz attenuation as

$$A_{30}(t) = e + f A_{30}(t - t_0) \quad (3)$$

Figure 4 shows the rms error for this last prediction method.

## 5. Conclusions

The experiment program at Virginia Tech has several unique opportunities. The collection of simultaneous data at three frequencies spanning the 12 to 30 GHz region is extremely useful in frequency scaling studies. This is possible because all links have the same path (14° elevation, 105° azimuth). The 14° elevation angle is relatively low and data in this region are also very useful because this is at the lower limit for CONUS coverage with domestic satellites. Our experiment records low-fade events accurately. This is valuable in amassing a database for low margin operational satellite links such as VSAT systems. Another feature of our OLYMPUS program is that it provides a test bed for ACTS due to the similarity of frequencies (ACTS beacons are at 20.2 and 27.5 GHz).

Initial results show that radiometer prediction attenuation agrees with beacon measured attenuation to the fractional dB level for fading up to 10 dB. Small baseline diversity, as expected, offers no improvement to rain fading, but does for scintillation events.

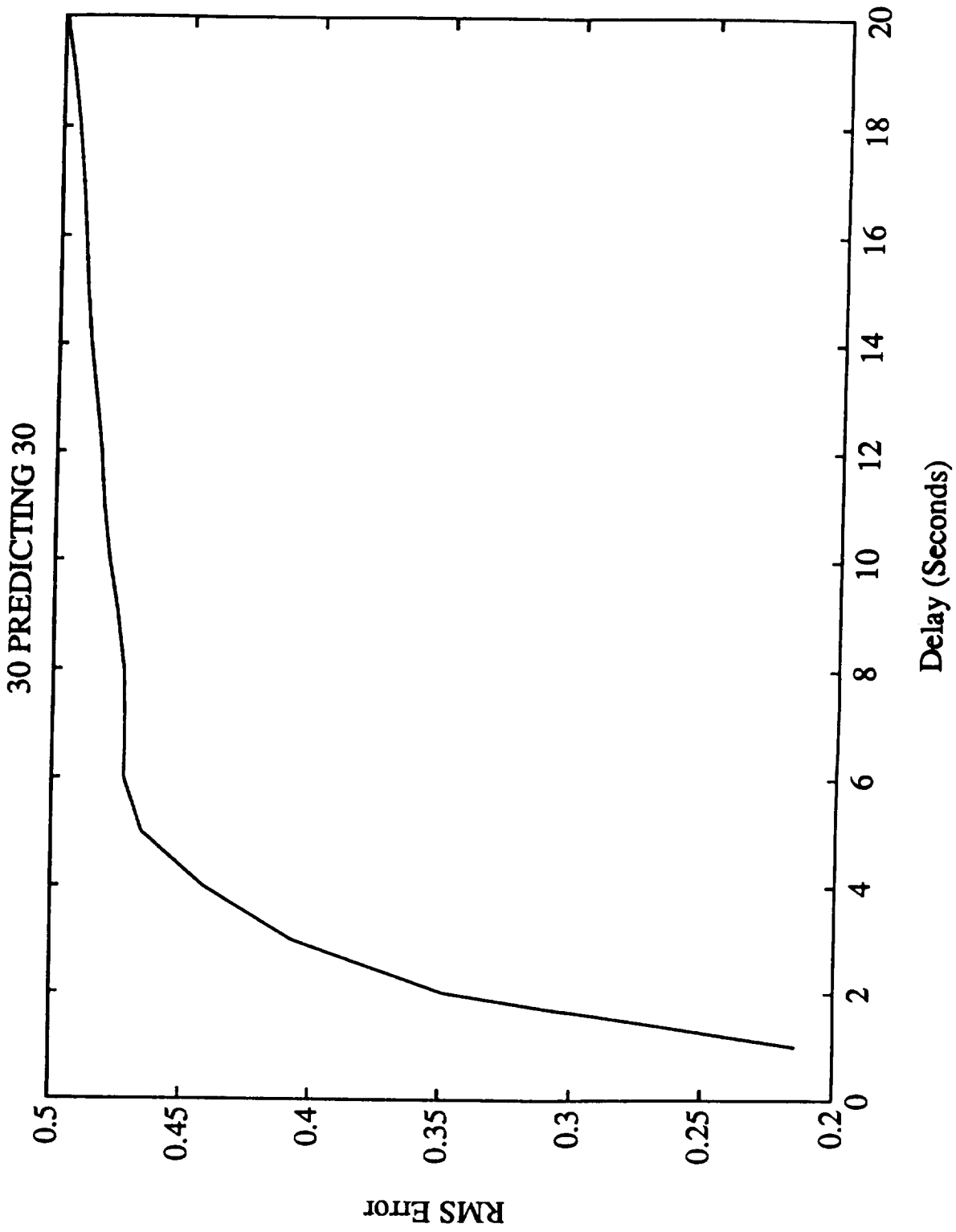


Figure 4. RMS error of predicting 30 GHz attenuation from an earlier 30 GHz attenuation level for an event of January 7, 1991.

# Data Acquisition, Preprocessing and Analysis for the Virginia Tech OLYMPUS Experiment

P. W. Remaklus

for the

Satellite Communications Group  
Bradley Department of Electrical Engineering  
Virginia Polytechnic Institute and State University  
Blacksburg, Virginia 24061

## Abstract

Virginia Tech is conducting a slant path propagation experiment using the 12, 20 and 30 GHz OLYMPUS beacons. Beacon signal measurements are made using separate terminals for each frequency. In addition, short baseline diversity measurements are collected through a mobile 20 GHz terminal. Data collection is performed with a custom data acquisition and control system. Raw data are preprocessed to remove equipment biases and discontinuities prior to analysis. Preprocessed data are then statistically analyzed to investigate parameters such as frequency scaling, fade slope and duration, and scintillation intensity.

## The OLYMPUS Experiment

The Virginia Tech experiment equipment consists of four terminals, each of which contains a beacon receiver and a radiometer. As shown in Figure 1, each terminal utilizes a separate antenna and all are frequency locked to the 12 GHz beacon. Locking to the less fade prone 12 GHz beacon allows measurement of 20 and 30 GHz fades to the noise floor. Sky noise measurements via radiometers provide a means to measure gaseous attenuation and hence the clear sky attenuation. Clear sky attenuation is then added to the measured beacon attenuation to obtain attenuation referenced to free space. System status and environmental data are collected to monitor system performance and examine correlations between propagation measurements and weather conditions.

## Data Collection

Data collection and system control is performed by a standalone data acquisition and control system (DACS). Figure 2 is a block diagram of the major DACS components. The DACS is 80286 microprocessor based and is connected to the PS/2 Model 60 collection computer through a parallel data interface. I and Q detector cards each accept two 10 kHz IF signals from the receivers and output in-phase and quadrature power measurements for the two channels at a 10 Hz rate. Status signals and alarms, such as loss of lock, are input to the digital input card. Similarly, analog signals such as temperature, wind speed, barometric pressure... are recorded via the analog input card. The radiometer input card counts the pulse train from each of the radiometers while the digital output card controls the waveguide switches and noise diodes that are used for radiometer calibrations. Data from the DACS



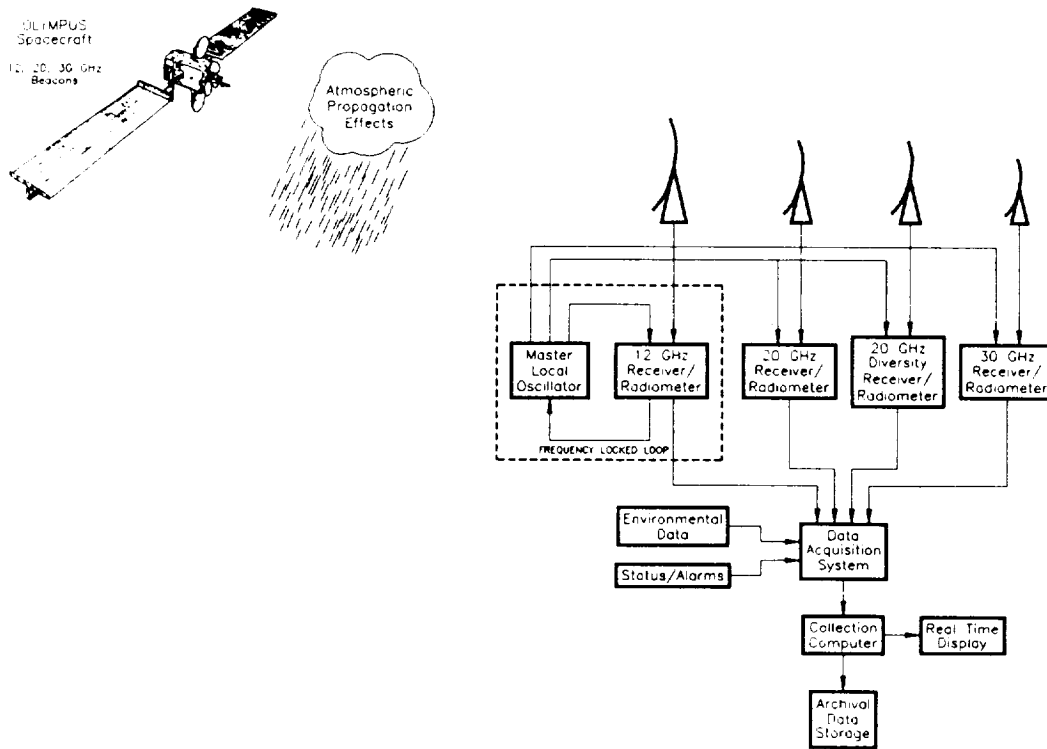


Figure 1: Virginia Tech OLYMPUS system hardware overview.

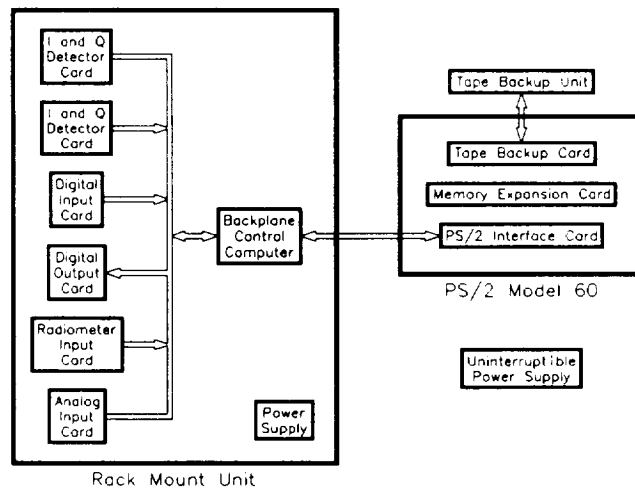


Figure 2: Data acquisition and control system overview.

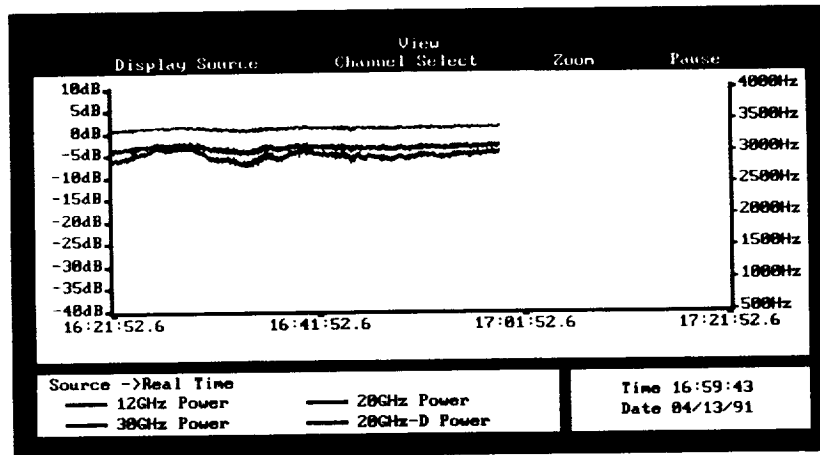


Figure 3: Real time display screen.

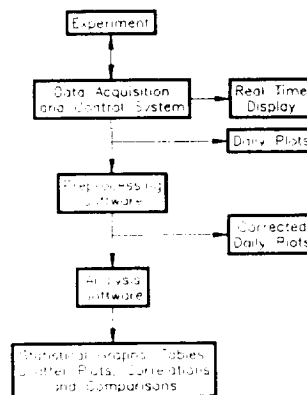


Figure 4: OLYMPUS experiment data flow.

are output to the Model 60 personal computer for storage to hard disk and realtime display. An example of a realtime display screen is presented in Figure 3. Once a day, the collected data are copied to tape for archival storage and input to preprocessing. Data flow within the experiment is shown in Figure 4.

## Preprocessing

Raw data is generally not suitable for input to analysis. For example, discontinuities during system maintenance and random glitches in the data must be removed prior to statistical processing. Furthermore, collected radiometer data require the application of periodic calibration information to obtain sky temperature. Preprocessing at Virginia Tech consists of several computer programs. These programs are:

- **DP:** Generates daily plots using raw data.
- **EXAMINE:** Automatic location of data discontinuities and extraction of radiometer calibration information.

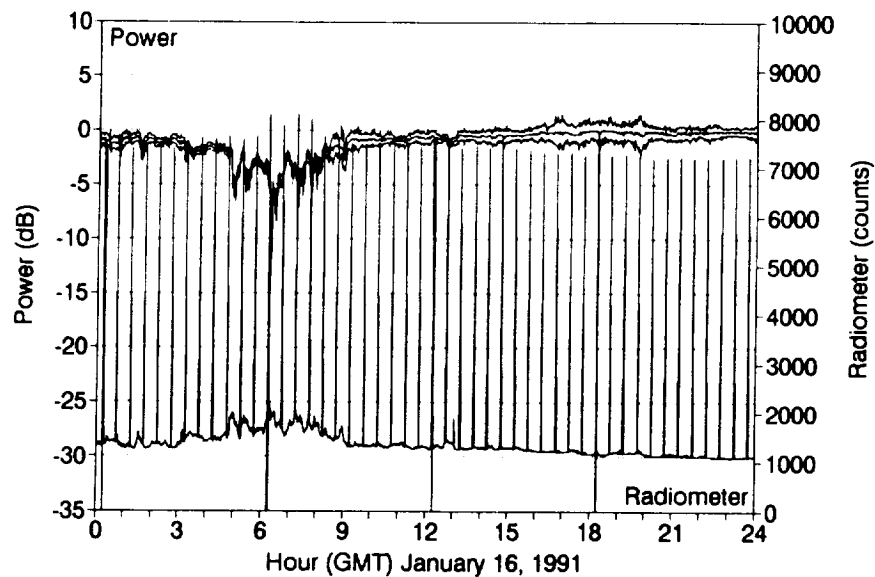


Figure 5: Daily plot of raw beacon and radiometer data.

- **EDIT**: Allows operator classification of data.
- **RPRECAL**: Calculates radiometer calibration parameters.
- **RCAL**: Converts collected radiometer data into sky temperature.
- **FILTER**: Low pass filters the radiometer data to improve resolution.
- **DIURNAL**: Removes the effect of spacecraft motion.
- **CDP**: Generates calibrated daily plots.

Within several days of collection, raw data is processed by **DP** to obtain daily plots for each of the four terminals. Figure 5 is a daily plot for the 20 GHz system on January 16, 1991. The upper three curves are one minute maximum, average and minimum levels of the received beacon signal. The separation between maximum and minimum curves provides an indication of scintillation activity. The large spikes in the radiometer data are periodic noise diode calibrations while the beacon dropouts correspond to radiometer ambient load calibrations. These plots along with written log information are invaluable to the operator when **EDIT** is executed. Prior to **EDIT**, the data is analyzed by **EXAMINE**.

**EXAMINE** attempts to autonomously find and classify discontinuities in the data and extract radiometric calibration information. Noise diode and ambient load calibration levels are easily removed since these events occur at known times during the day. However, data discontinuities are more difficult to locate. Three types of discontinuities are most prevalent in the data:

- DACS downtime
- Alarms
- Questionable data

DACS downtime is easily located because there is no collected data for the duration of the outage. Phase locked oscillator blocks and the 12 GHz frequency locked loop output alarms

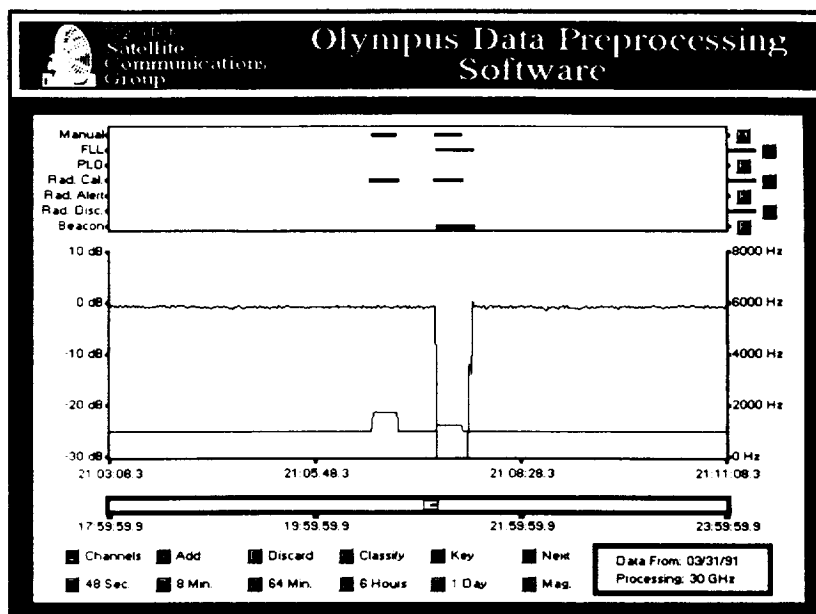


Figure 6: EDIT display screen in 8 minute mode.

are stored in the collected data. When an alarm condition is detected, all data channels that could be affected by the alarm condition are marked as discontinuous for the duration of the alarm. Questionable data are located by comparing the rate of change of a data channel with a limiting condition. Presently, beacon data are marked discontinuous for signal changes of greater than 1 dB/sec or phase differences of more than 15° between samples. Most beacon data with these characteristics are valid; however locating false discontinuities is preferable to missing actual discontinuities. The next phase of preprocessing, **EDIT**, allows the operator to add, modify or remove discontinuities located by **EXAMINE**.

**EDIT** is a mouse driven, graphical program which allows the operator to view data from one day and confirm, modify or add discontinuity classification information to the output from **EXAMINE**. Data can be marked as category:

- 0 Normal operation
- 1 Clear air downtime
- 2 Event downtime
- 3 Calibration downtime

Figure 6 is an example of the EDIT display screen in eight minute display mode. The top of the display uses color bars to indicate the classification of the data directly below. This display shows that an operator manually performed a noise diode calibration and then an ambient load calibration on the 30 GHz system. The buttons on the bottom portion of the screen allow the operator to select the channel for display, time period for display, and to classify data as desired.

After using **EDIT** to remove all data problems, **RPRECAL** and **RCAL** are executed to convert the radiometer data into sky temperature. **RPRECAL** processes calibration information from **EXAMINE** and **EDIT** for the previous, current and next day to obtain

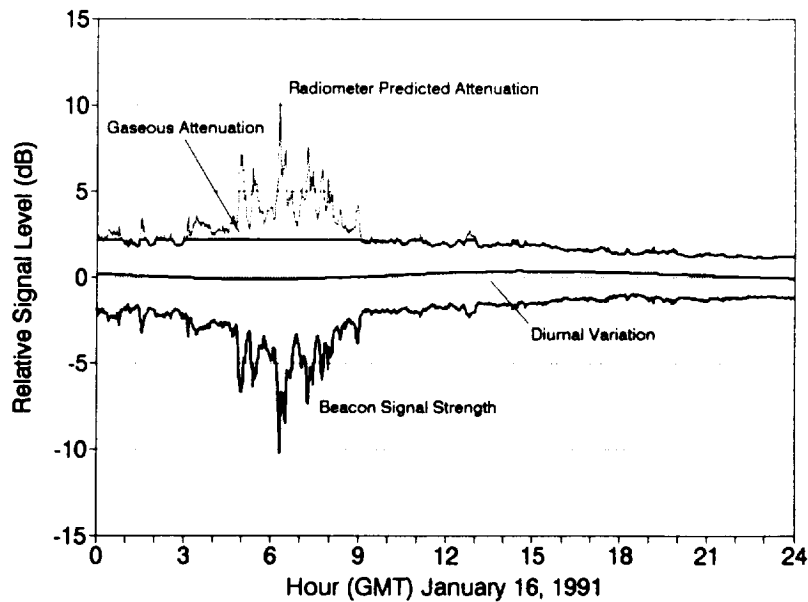


Figure 7: Diurnal bias removal.

the calibration parameters necessary to convert raw radiometer data into sky temperature. **RCAL** then applies these calibrations to the data. **FILTER** then applies a 10 second moving average filter to the radiometer data. This improves the resolution of the radiometer data to about 0.1 K.

The final stage of preprocessing is the removal of diurnal biases and calibration of the beacon data to attenuation relative to free space. Because Blacksburg is located far off the boresight of the OLYMPUS beacons, diurnal variations of several dB are commonly present. Removal of this bias can only be performed after the gaseous attenuation has been removed from the beacon signal thus leaving only the diurnal variation. Figure 7 illustrates the bias removal procedure for the 20 GHz system during a rain event on January 16, 1991. Each of the curves on the plot was obtained from six minute average data. Averaging is necessary to remove scintillations from the beacon signal and maintain a uniform number of points for each of the curves. The upper curve on the plot is the radiometer predicted attenuation in absolute dB. Note that the radiometer measures beacon attenuation quite accurately to about 3–4 dB. The lower curve on the plot is the beacon level during the day relative to an arbitrary 0 dB baseline. The middle curve is obtained from a sixth order curve fit of selected portions of the upper and lower curves added on a point by point basis. This curve fit information along with thresholded radiometer predicted attenuation is then applied to the raw beacon data to obtain attenuation referenced to free space. As shown in Figure 7, radiometer data is thresholded at 90 K for 12 GHz and 110 K for 20 and 30 GHz. Attenuation beyond this point is measured more accurately through beacon measurements. A plot of calibrated beacon and radiometer data is shown in Figure 8. If this plot showed any discontinuities or appeared incorrect, the operator would return to **EDIT** and remove any problematic data or modify radiometric calibration parameters. Once satisfied with the quality of the data it is input to the analysis software.

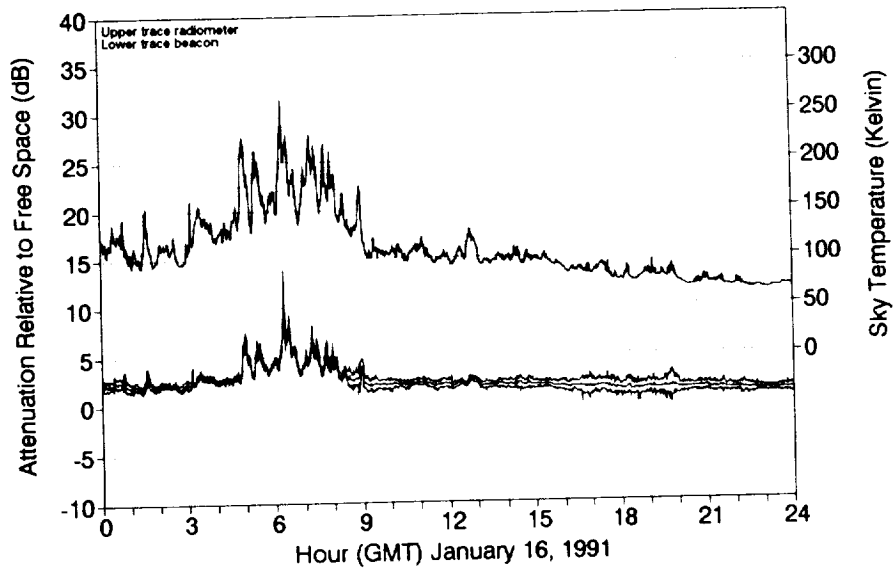


Figure 8: Calibrated daily plot.

## Analysis

Presently, the analysis software is under development. Analysis requires the following data from each of the four terminals:

- Attenuation with respect to free space
- Attenuation with respect to clear air
- Sky temperature
- Rain gauge tip times

Output table and graphs include:

- Cumulative rain rate distributions
- Beacon attenuation with respect to free space
- Beacon attenuation with respect to clear air
- Scintillation index
- Fade slope
- Non-fade duration
- Ultimate fade depth versus fade slope
- Diversity gain
- Frequency scaling

Figure 9 is an exceedance plot of attenuation referenced to clear air for January 1991. Note that frequency scaling of attenuation is clearly present and that some scintillation activity is indicated by negative attenuation in the 99–100% region.

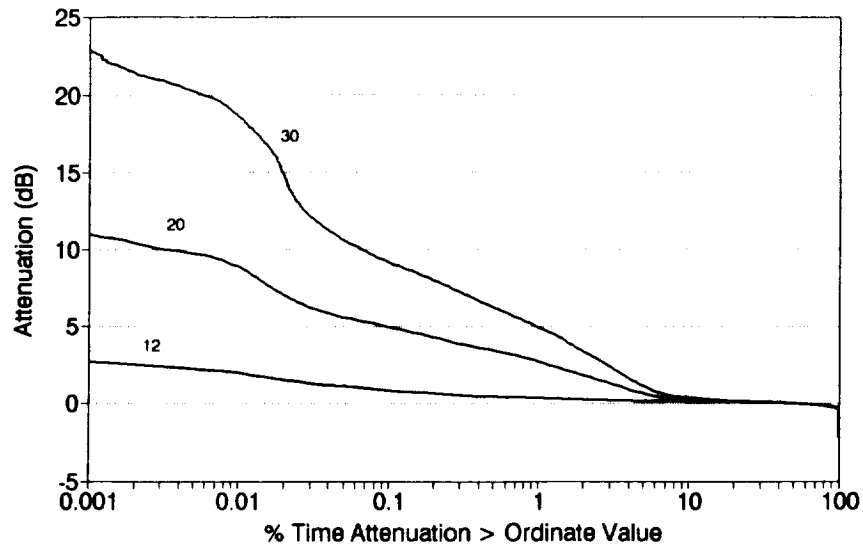


Figure 9: Exceedance plot of 20 GHz attenuation referenced to clear air for January 1991.

## Conclusions

Virginia Tech has constructed and is operating a propagation measurement system for the OLYMPUS experiments. Procedures and methods for data collection, preprocessing and analysis have been selected and utilized successfully. Presently, data analysis software for primary statistics; rain rate, attenuation referenced to free space... is complete. Secondary statistical analysis; fade rate, fade duration... software is under development and should be completed in the near future.

# **EARTH-SPACE PROPAGATION RESEARCH AT CRC**

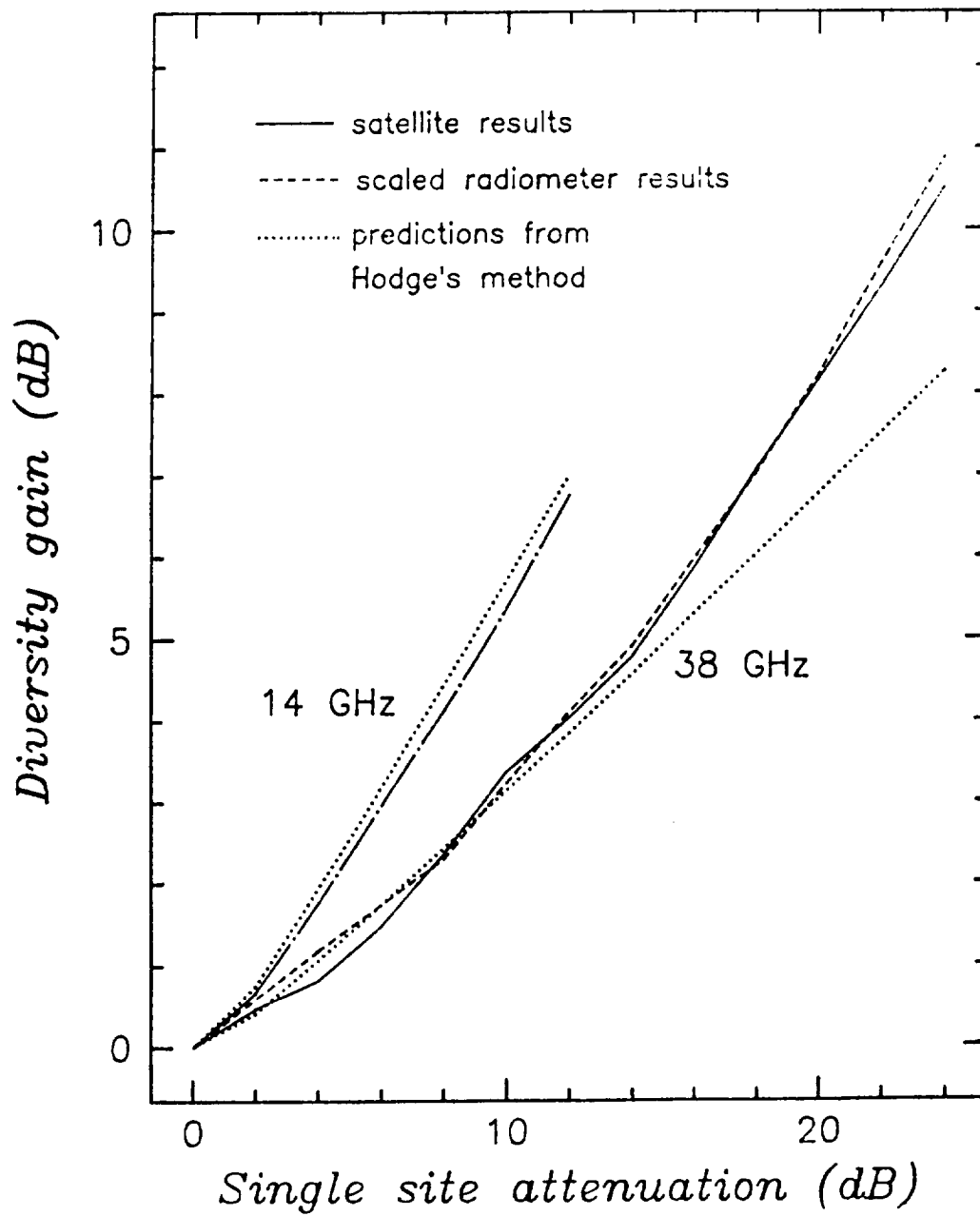
Roderic L. Olsen  
Communications Research Centre  
Department of Communications  
Ottawa, Canada

## **OUTLINE:**

- **14/38 GHz site-diversity measurements (LES-8 satellite)**
  - **Intercontinental rain attenuation studies for INTELSAT**
  - **Low-angle fading project**
  - **Rain attenuation measurements in SE Asia**
  - **Studies of propagation mitigation at EHF**
  - **Interference studies**
- } **Recent Past**



# SITE DIVERSITY RESULTS USING 38 GHz LES-8 SATELLITE AND 14 GHz RADIOMETER



(Lam and Olsen, 1988)

# **ASSESSMENT OF JOINT ATTENUATION ON LOW-FADE-MARGIN INTERNATIONAL SATELLITE SERVICES** (Segal and Allnutt, 1991a,b)

- **INTELSAT International Business Service:**

Uplink	14 GHz
Downlink	11/12 GHz
Rain fade margin	2.5 dB

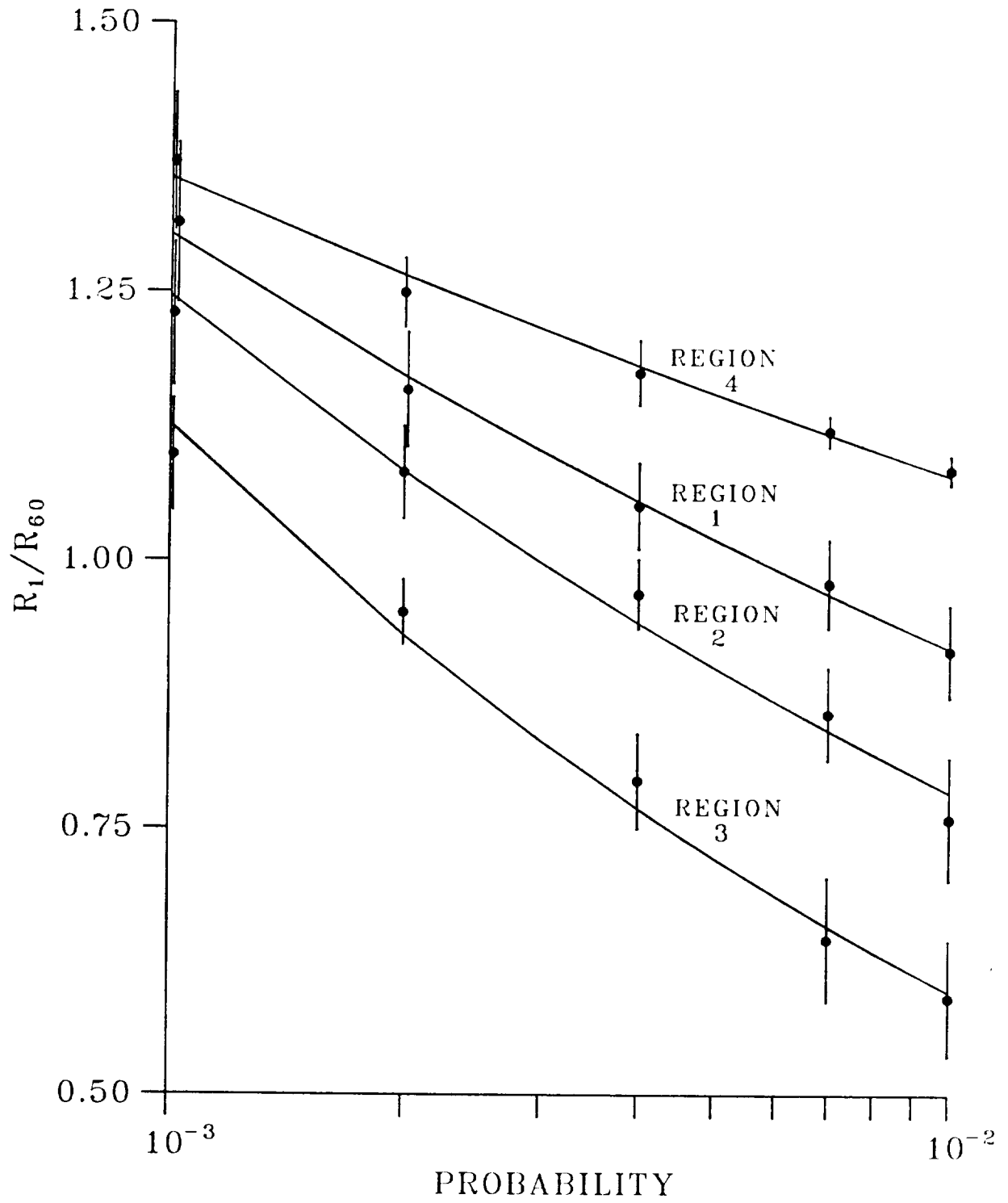
- **Study of possible detrimental effects due to correlation in rain attenuation between uplink and downlink during business hours (use of prediction approach based on rainrate statistics):**

**N.A. ↔ EUROPE ; N.A. ↔ PACIFIC**

## **Main Conclusions**

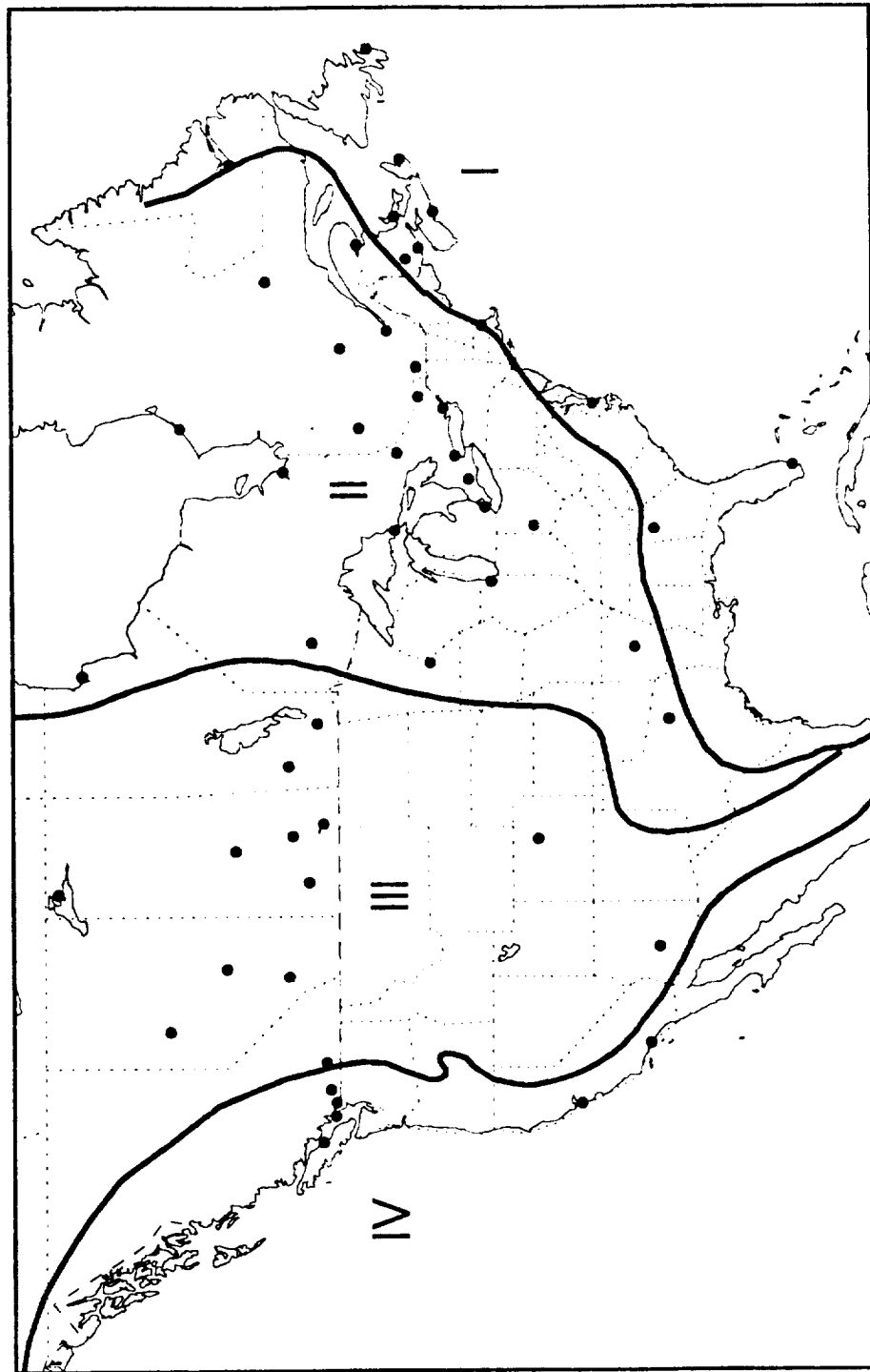
- **Max. diurnal enhancement approx. equal to max. seasonal enhancement**
- **Effect of large diurnal variations in continental climate swamped by much larger fade probabilities (with smaller variability) in maritime climate**
- **Side-benefit: Development of technique for predicting rainrate one-minute statistics from one-hour statistics**

# ONE HOUR TO ONE MINUTE CONVERSION FACTOR CURVES



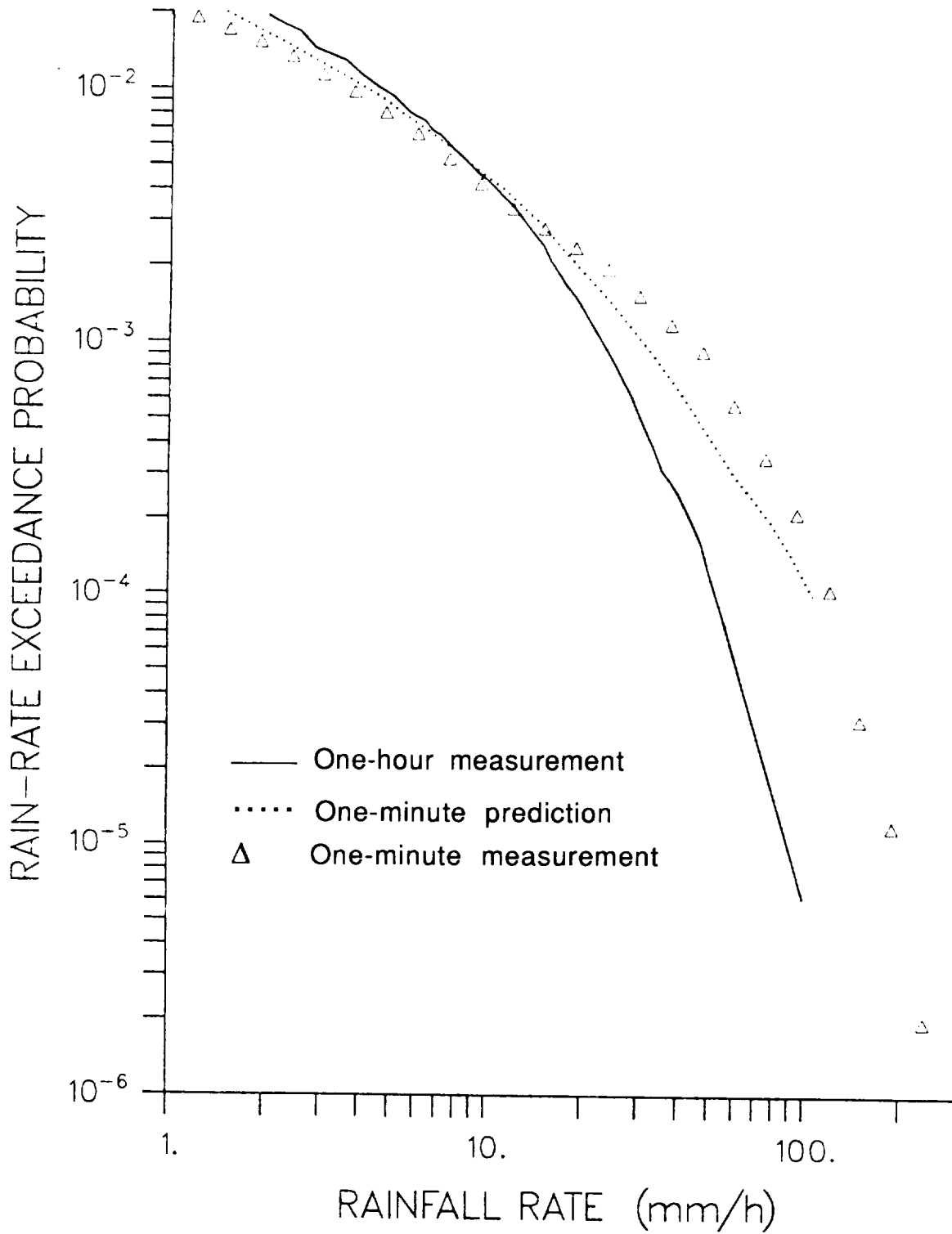
(Segal and Allnutt, 1991b)

# NORTH AMERICAN RAIN ZONES FOR HIGH-PROBABILITY REGIME



(Segal and Allnutt, 1991b)

# CUMULATIVE RAIN-RATE DISTRIBUTIONS FOR MIAMI



(Segal and Allnutt, 1991b)

# **LOW-ANGLE FADING PROJECT**

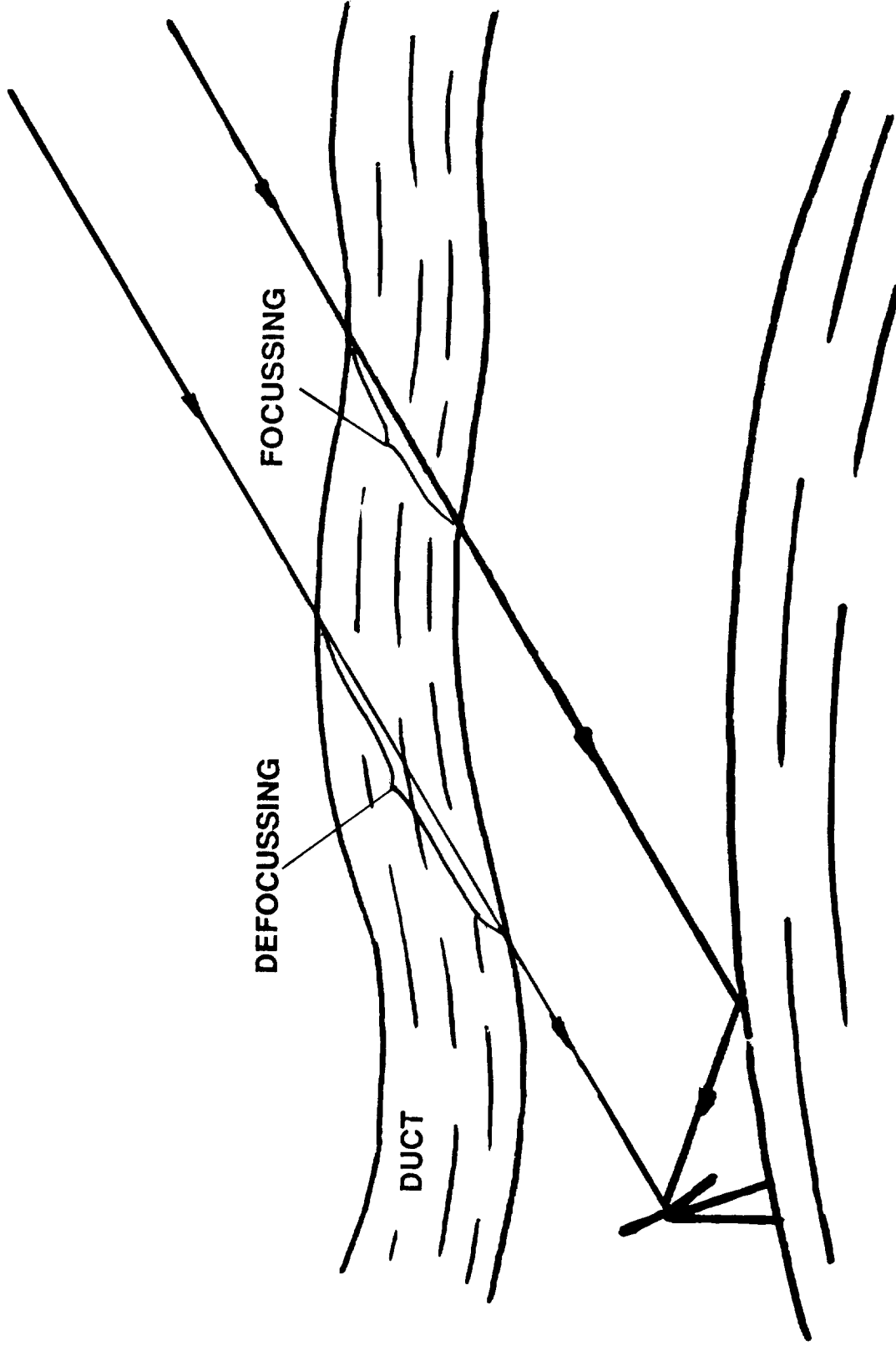
**OBJECTIVE:** To develop a climatological model for fading at elevation angles less than about  $4^\circ$

## **BACKGROUND:**

- **CRC has largest low-angle fading data base in the world (4, 6, 7, 30, 38 GHz; Ottawa, St. Johns', Resolute, Eureka, Alert) (e.g., see Lam, 1987)**
- **CRC has developed model for frequency and percentage-of-time scaling of low-angle fading data ( $< 4^\circ$  elevation angles) (CCIR, 1989)**
- **CRC has new physical explanation of fading at the very lowest angles (Olsen *et al.*, 1987)**
- **CRC has developed climatological model for multipath fading statistics on terrestrial links (Worldwide version adopted by CCIR)**
- **CRC/University of Western Ontario conducting terrestrial experiment to compare refractivity profile and acoustic sounder measurements, etc. with phased array radio measurements**

**POSSIBLE APPROACHES:** (a) Tie existing and new data to refractivity gradient statistics, (b) Ray tracing studies to determine beamwidth and elevation-angle dependence

# PHYSICS OF VERY-LOW-ANGLE FADING



## **RAIN ATTENUATION MEASUREMENTS IN ASEAN COUNTRIES OF SE ASIA**

- **Project funded by Canadian International Development Agency**
- **12 GHz radiometric measurements of rain attenuation statistics along paths to future INTELSAT satellite**
  - 2 radiometers in Thailand (site-diversity configuration)
  - 1 radiometer in Singapore
  - 2 radiometers in Indonesia
- **Initial measurements in fall of 1991**
- **Aim is to have ASEAN researchers doing the analysis with CRC scientists as consultants**



# **CHANNEL IMPAIRMENT MITIGATION AND NETWORKING TECHNIQUES FOR EHF PERSONAL SATELLITE COMMUNICATIONS**

- **Joint project with the University of Ottawa and Telesat Canada** - funding of 4 graduate students, 2 post-doctoral fellows over 3 years (Yongaçoğlu *et al.* , 1991)
- **Use of existing EHF data and data from Olympus experiment** (see Olsen *et al.*, 1990)

## **OBJECTIVES:**

- **Evaluate impairment mitigation techniques for both slowly and rapidly changing channel conditions**
- **Jointly optimize candidate techniques using software/hardware simulations**
- **Develop practical mitigation techniques using digital processing based hardware**
- **Test prototype hardware over satellite link**
- **Investigate new networking strategies**

# INTERFERENCE STUDIES

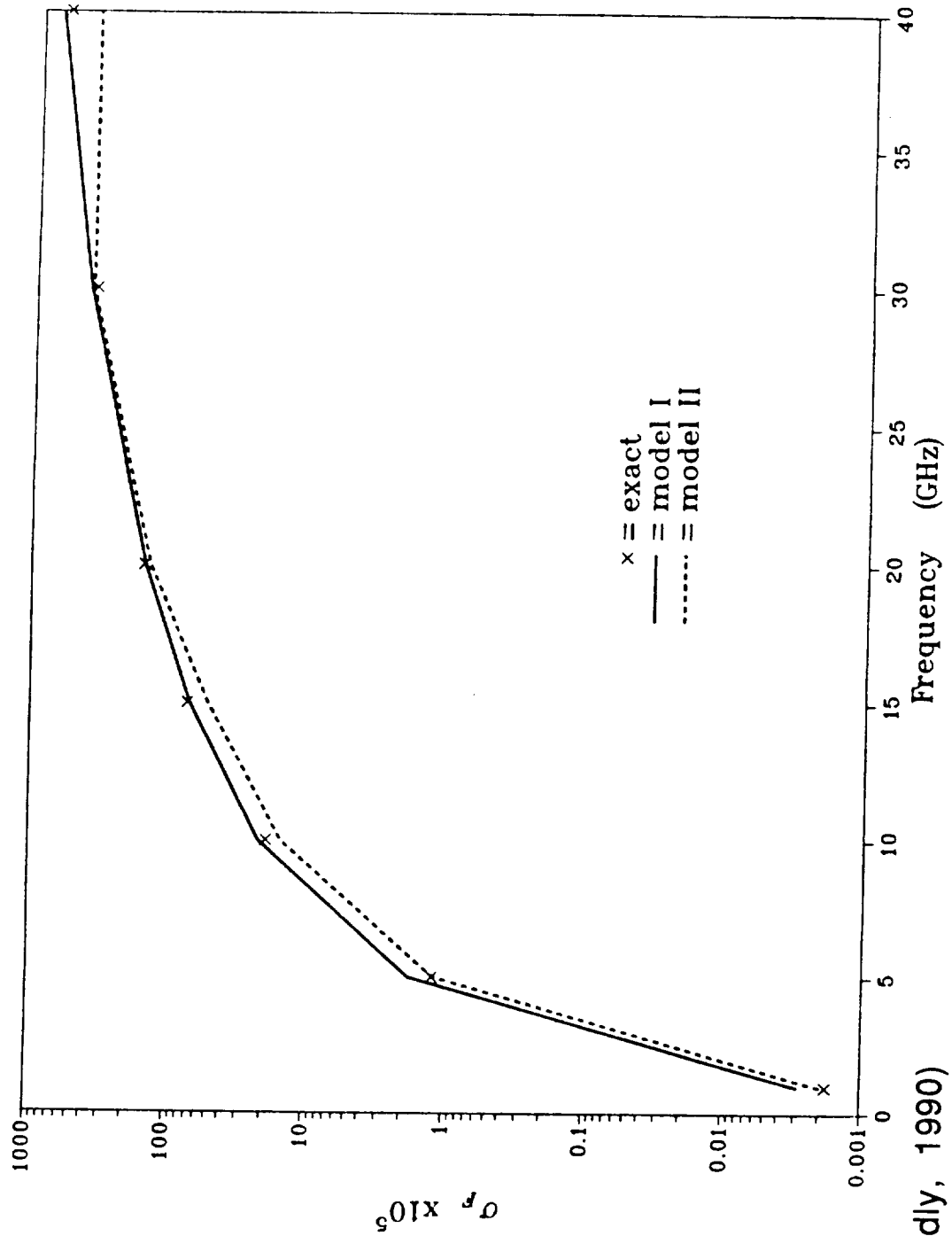
## 1. DUCT PROPAGATION

- **Experimental investigation of negative correlation between transhorizon interfering signal from earth-station and fading signal at terrestrial receiver** (Olsen and Bilodeau, 1991; Bilodeau and Olsen, 1991)

## 2. HYDROMETEOR SCATTER

- **Development of model for scattering cross-section of melting snow** (contracts to University of British Columbia, sub-contracts to University of Mississippi, earlier rain cross sections from Dartmouth College, see Kharadly, 1990,1991)
- **Comparison of relative importance of rain scatter and melting snow scatter** (contract to University of British Columbia)
- **Calculation of new radar reflectivity profiles from polarimetric radar data** (contract to Alberta Research Council, see Kochtubajda *et al.*, 1991)

Forward-Scattering Cross Section  
of Melting Snow ( $\text{m}^2/\text{m}^3$ )  
 $R = 12.5\text{mm/h}$   $T = 0^\circ\text{C}$   $S = 0.1$

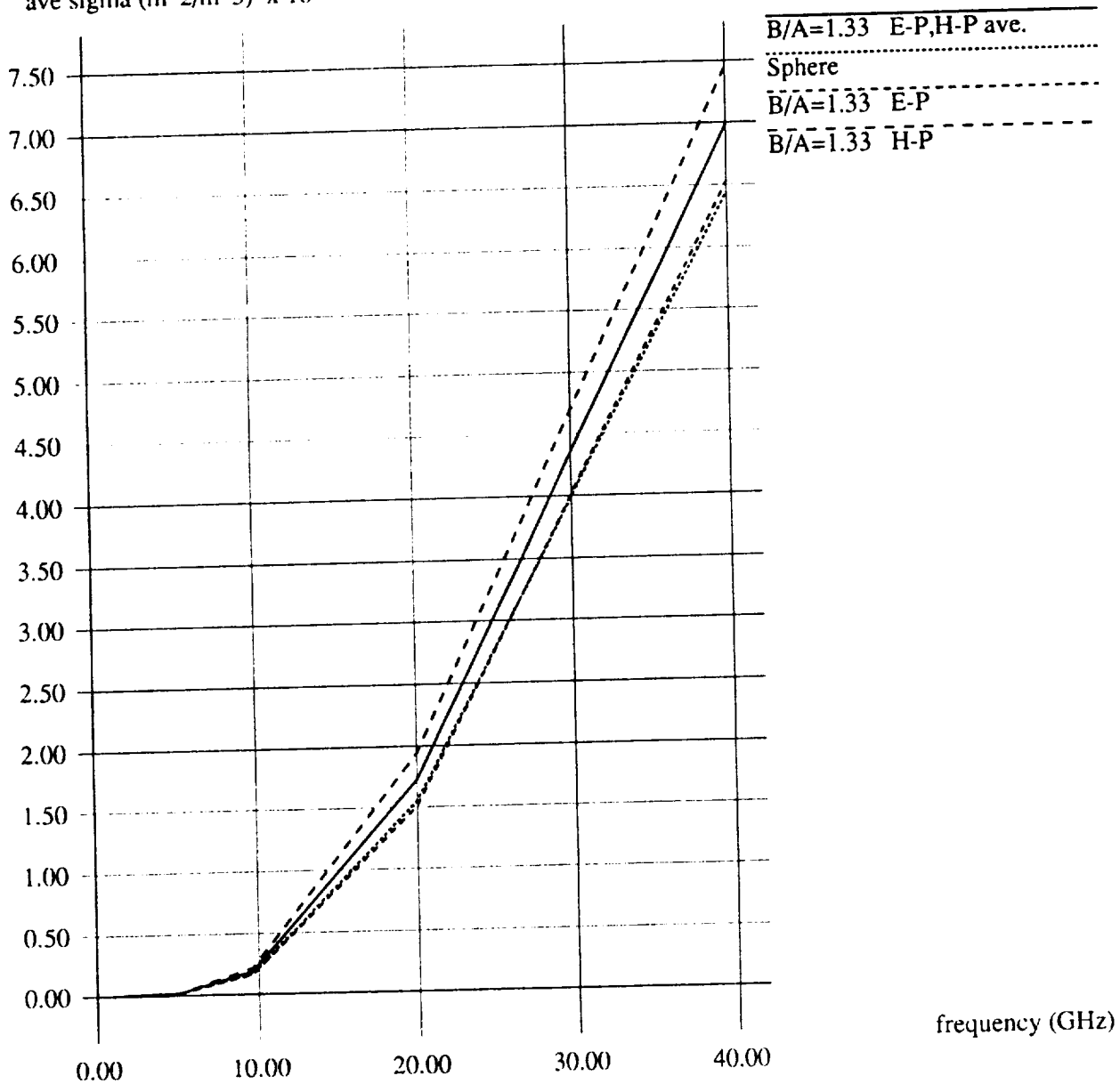


(Kharadly, 1990)

# COMPARISON OF SPHERICAL AND OBLATE SPHEROIDAL MODELS OF MELTING SNOW PARTICLES

**R=12.5 S=0.10 Uniform distribution**

ave sigma (m<sup>2</sup>/m<sup>3</sup>) x 10<sup>-3</sup>



(Kharadly, 1991)

## References

- Bilodeau, C. and R.L. Olsen (July 1991), "Observed signals on transhorizon path and line-of-sight paths: A case of negative correlation," in *Proc. SBMO Int. Microwave Symp.*, Rio de Janeiro, Brazil.
- CCIR Doc. 5/126 (25 March 1988) [Canada], "Measurements of very low angle fading on satellite-earth paths," CCIR Secretariat, International Telecommunication Union, Geneva, Switzerland.
- Kharadly, M. (1990), "A model for evaluating the bistatic scattering cross sections of melting snow," Phase III Report on Research Contract CRC 36100-9-0247-/01-ST, Department of Electrical Engineering, University of British Columbia, Vancouver, Canada.
- Kharadly, M.(1991), "A model for evaluating the bistatic scattering cross sections of melting snow," Phase IV Report on Research Contract CRC 36001-0-6572, Department of Electrical Engineering, University of British Columbia, Vancouver, Canada.
- Kochtubajda, B.D. (1991), "Feasibility study for the extraction of melting layer statistics from archived ARC S-band weather radar observations," Final Report on CRC Research Contract, Alberta Research Council, Edmonton, Canada.
- Lam, W.I. (1987), "Low angle signal fading at 38 GHz in the high arctic," *IEEE Trans. Antennas Propagat.*, Vol. AP-35, pp. 1495-1499.
- Lam, W.I. and R.L. Olsen (1988), "Measurements of site diversity performance at EHF," in *Proc. Int. Symp. on Radio Propagation*, Beijing, China.
- Olsen, R.L., L. Martin and T. Tjelta (1987), "A review of the role of surface reflection in multipath propagation over terrestrial microwave links," in *NATO/AGARD Conf. Proc. No. 407*, pp. 2/1-23, North Atlantic Treaty Organization, Paris, France.
- Olsen, R.L., D. Makrakis, D.V. Rogers, R.C. Bérubé, Y.M.M. Antar, J. Albert, W.I. Lam, J.I. Strickland, S.Y.K. Tam, S.L. Foo, L.E. Allan and A. Hendry (1990), "The Canadian Olympus propagation experiment," in *Proc. IEEE Global Telecommunications Conference*, San Diego, USA.
- Olsen, R.L. and C. Bilodeau (1991), "Observed negative correlation between an interfering signal on a transhorizon path and wanted signals on terrestrial line-of-sight paths," *Electron. Lett.*, Vol. 27, No 4, pp. 332-334.
- Segal, B. and J.E. Allnutt (1991a), "Assessment of joint attenuation distributions in the 14/11 and 14/12 GHz bands on low-margin international satellite services," in *Proc. Int'l Conf. on Antennas and Propagation*, in *IEE Conf. Publication CP 333*, Vol. 2, pp. 370-373.
- Segal, B. and J.E. Allnutt (1991b), "On the use of long sampling-time rainfall observations for predicting high-probability attenuation on earth-space paths," in *IEE Conf. Publication CP 333*, Vol. 2, pp. 754-757.
- Yongaçoğlu, A., J.-Y. Chouinard, R. Olsen, D. Rogers, D. Makrakis and K.M.S. Murthy (April 1991), "Impairment mitigation techniques for EHF personal satellite communications," in *Proc. OPEX Workshop*, ESTEC, European Space Agency, Noordwijk, Netherlands.

**THE ACTS PROPAGATION PROGRAM**

D. Chakraborty and F. Davarian  
Jet Propulsion Laboratory  
California Institute of Technology  
Pasadena, California

**Introduction**

The purpose of the Advanced Communications Technology Satellite (ACTS) is to demonstrate the feasibility of the Ka-band (20 and 30 GHz) spectrum for satellite communications, as well as to help maintain U.S. leadership in satellite communications. ACTS incorporates such innovative schemes as time division multiple access (TDMA), microwave and baseband switching, onboard regeneration, and adaptive application of coding during rain-fade conditions.

The success or failure of the ACTS experiment will depend on how accurately the rain-fade statistics and fade dynamics can be predicted in order to derive an appropriate algorithm that will combat weather vagaries, specifically for links with small terminals, such as very small aperture terminals (VSATs) where the power margin is a premium.

This article describes the planning process and hardware development program that will comply with the recommendations of the ACTS propagation study groups.

**ACTS Propagation Terminal Development Plan**

A plan for the ACTS propagation terminal was initiated at the first ACTS Propagation Studies Workshop, November 28-29, 1989. The workshop's goal was to develop the ACTS Propagation Studies Program. During this workshop, participants delivered a set of recommendations regarding propagation studies and experiments that would use ACTS. In their recommendations, the group addressed a number of topics, including the need for propagation data and the configuration and number of propagation terminals needed.

The participants also provided guidelines regarding measurement parameters and requirements. These guidelines specify how the terminal should be configured so that it can record the following propagation and meteorological parameters:

- 20-GHz beacon receive signal level
- 27-GHz beacon receive signal level
- 20-GHz radiometric sky noise temperature
- 27-GHz radiometric sky noise temperature
- Point rain rate near the terminal

- Atmospheric temperature at the Earth's surface
- Atmospheric humidity at the Earth's surface

In response to the recommendations concerning propagation terminals, a two-phase plan has been devised. In phase 1, a terminal prototype is being developed, and in phase 2, six to eight terminals will be manufactured for distribution to ACTS propagation experimenters.

#### Prototype Receive Terminal Development

A NASA research grant was awarded to Virginia Polytechnic Institute in early 1991 for the Prototype development. The Prototype ACTS propagation receiver terminal will consist of a common antenna, a dual-channel digital receiver, a dual-channel analog radiometer, and a data acquisition system. The terminal will also be equipped with meteorological recorders for measuring the point rain rate and the atmospheric temperature and humidity.

A simplified block diagram of the receiver terminal is shown in Fig. 1. The salient features of the terminal are as follows:

- 1.2-m common antenna
- Ortho-Mode Transducer (OMT) to split 20-GHz V- and H-Pol (if used)
- 20-/30-GHz diplexer to split 20- and 30- GHz V-Pol signal
- Cost-effective low-noise amplifiers followed by single downconversion to 70-MHz intermediate frequency (IF)
- Total power radiometer with detectable sensitivity of  $\pm 1$  K
- Data collection - PC/AT-based

The design will be based upon modular form for easier integration and testing.

Worst-case ACTS link budget is shown in Table 1.

Table 1. ACTS Link Calculations

Beacon frequency band (GHz)	27.5	20
Common antenna size (m)	1.2	1.2
Antenna gain (dB)	49	46.4
Nominal CONUS EIRP (dBW)	16	16
Transmission loss (dB)	2.0	1.8
Modulation loss (dB)	-	3.2
Path loss at 30-deg elevation (dB)	215	212
Total loss (dB)	217	217
Low-noise-amplifier noise figure (dB)	7	7
Receive G/T (dB/K)	17.6	15.1
Carrier-to-noise density (C/N), (dB-Hz)	45.2	42.7
C/N over 15 Hz (dB)	33.4	30.9

The above table shows the worst-case C/N within the CONUS coverage. For an experimental site in Alaska, the reduced EIRP as seen from Alaska can be compensated by a 2-m antenna.

#### Schedule

The tentative schedule summary for ACTS Propagation Studies is shown below:

Completion of Prototype Terminal	Feb. '92
Selection of Experimenters	Aug. '92
Completion of 6-8 Terminals Production	Oct. '92
Installation and Calibration of Terminals	Dec. '92
ACTS Launch	Late '92
Start of Data Collection	Early '93

#### Data Collection Sites

Rain climate zones without prior propagation data will receive special consideration. Sites with an ongoing environmental sensing program employing radiosondes, weather radars, etc., will be given higher priority.



### **Additional ACTS-Related Tasks**

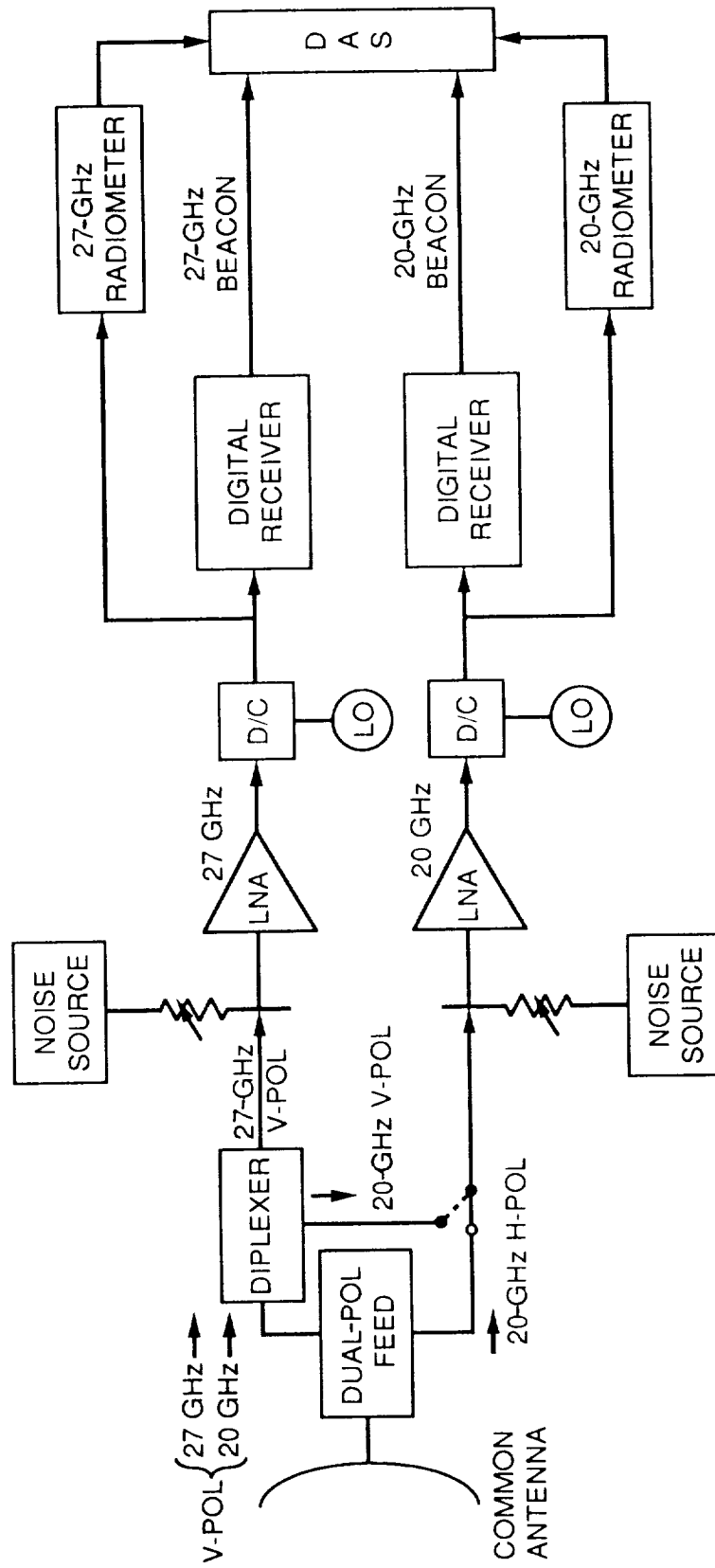
In addition to the planning discussed above, the following tasks need to be completed:

- Plan propagation study pertinent to mobile environment
- Plan fade detection and compensation via uplink power control
- Support ACTS Conference in August '91 and organize ACTS Workshop in late 1991 or early 1992
- Possibly organize a 20-/30-GHz Technology Workshop in GLOBCOM '92
- Select a central processing site for ACTS data reduction and analysis

### **Conclusions**

The ACTS Propagation Study Planning and developmental efforts are highlighted. No major constraint is foreseen at this time.

# FUNCTIONAL BLOCK DIAGRAM OF THE ACTS TERMINAL



## PROPAGATION MEASUREMENTS IN ALASKA USING ACTS BEACONS

Charles E. Mayer

Electrical Engineering Department  
University of Alaska Fairbanks  
Fairbanks, Alaska 99775

**Abstract**--The placement of an ACTS propagation terminal in Alaska has several distinct advantages. First is the inclusion of a new and important climatic zone to the global propagation model. Second is the low elevation look angle from Alaska to ACTS. These two unique opportunities also present problems unique to the location, such as extreme temperatures and lower power levels. These problems are examined and compensatory solutions are presented.

### 1. Introduction

Alaska has always been, and will continue to be, at the forefront of high technology satellite resource usage. From the first U.S. tracking of Sputnik to the installation of more than 200 remote video and voice C-band earth stations throughout rural Alaska, the unique location and population diversity of Alaska require innovative solutions to realize the State's telecommunications needs. New technologies, such as ACTS, provide additional opportunities for new solutions. Alaska is reliant on satellites for communications to its remote regions, and the State is committed to providing educational and health communications throughout the state. The location of a large teleconnected research university with three major campuses (Fairbanks, Anchorage, and Juneau) and many smaller campuses across the State, the demand for transportable USAT earth stations and mobile satellite service (Hills, 1988), and the growing demand for video and audio communications throughout the State, all point to the need for expansion into Ka-band communications. Accordingly, propagation statistics for Ka-band frequencies in Alaska are essential. Alaska offers two major advantages to the ACTS Propagation Program. The first is the addition of a new and important climatic zone to the global propagation model. The second is the low elevation look angle to the satellite. These two advantages provide a unique opportunity for collection of Ka-band propagation data from ACTS.

### 2. History

Alaska was the first state to enter the satellite communications age. The first satellite, Sputnik, was launched into a highly inclined orbit ( $65^\circ$ ) and passed over Alaska on October 4, 1957. Given 2 hours of advance notice by NASA Goddard, the EE faculty and students assembled receivers and recorders. Bob Merritt, Engineer on the Radio Astronomy Techniques project at the University of Alaska Fairbanks (UAF), and now Professor Emeritus of Electrical Engineering, fabricated 2 dipole antennas, arranged them into a baseline interferometer, and connected the antenna system to both 20 and 40 MHz receivers. Using a chart recorder, Merritt and his team were able to give NASA 0.1 second accuracy on the Sputnik transit time. Additional studies with the Sputnik data provided an estimate of the electron density of the ionosphere along the propagation path to the ~120 mile altitude satellite. A few days after launch, the tumbling Sputnik was visually observed reflecting the sun in the predawn light.

NASA then funded Minitrack System at UAF. Minitrack consisted of an array of antennas and was used to provide precision tracking position data and telemetry for the overhead passage of satellites. Array calibration was performed by flying an airplane-

born transmitter over the site. NASA built its first 85-foot reflector at the Gilmore Creek Tracking Station, some 20 miles from Fairbanks. The reflector tracked NIMBUS, for the short lifetime of the satellite. Other data were downlinked from the TIROS weather satellites, LANDSAT, and SEASAT, as they passed overhead in highly inclined orbits. Also satellites, such as the Canadian ALOET were used in top side sounder experiments. The array and the reflector were also used to study ionospheric propagation effects at 135, 404, and 1705 MHz, where new high latitude effects were discovered. Gilmore Creek remains operational today.

Alaska participated with ATS-1, with its push-to-talk 135.6 and 149.2 MHz downlink and uplink frequencies. The Alaska Public Health Service contracted to provide emergency communications to remote villages inaccessible by road or any form of communications except unreliable (due to solar activity) HF radio. From these beginnings, Merritt and others developed the Alaska Village Satellite System, a C-band satellite star network connecting some 200 villages with audio connection to the state, and world, telephone grid (Hills, 1983). Later, this network was expanded to include delivery of 2 channels of television, one educational and one entertainment, to all the remote Alaskan villages with a population over 25 people. Today, systems similar to the Alaska Village System are being deployed in developing countries and in countries with rugged and remote regions. Propagation studies at C-band were conducted at Sitka, where some noteworthy features of high latitude propagation were measured.

Current activities include the Alaska SAR Facility, a receive only earth station to collect data from polar orbiting SAR satellites. The United States did not launch a SAR satellite, but an agreement has been reached with other countries giving US researchers access to SAR data in exchange for the collection of data by the Alaska downlink facility. The foreign countries and organizations include ESA (Earth Resources Satellite), Japan, and Canada (RADARSAT).

### **3. ACTS Propagation Opportunities**

The placement of an ACTS propagation terminal in Alaska offers several unique opportunities for the collections of Ka-band data. The first is the climatic zone of the state. According to the Crane global model (Crane, 1985), Fairbanks is in region B1, close to the region A boundary. Very little data has been collected in either of these two climatic zones, and yet they are important for several reasons. Convergence of the global model will be benefitted by data from all the zones. Scientific research work in the arctic and antarctic regions is increasing rapidly, partially due to the global warming issue. Rapid data transfer to the supercomputers used for global modelling will require satellite links. Furthermore, basic communications in these isolated and often harsh areas of the world is heavily dependent upon satellite links. Design of reliable communications links requires adequate knowledge of propagation statistics. Therefore, collection of propagation data from this Alaska climatic zone is of utmost importance.

A second opportunity lies in the advantage of a low elevation look angle from Fairbanks to ACTS. At no other location in the United States does the opportunity exist for low elevation propagation studies. The power level from ACTS is still fairly high in Alaska, as shown in Figure 1 from GE Astro (Cashman, 1990). Alaska delivers a large range of look angles across the state ( $0^\circ < \theta < 22^\circ$ ), as shown in Figure 2. Fairbanks provides a look angle of  $7.9^\circ$  to ACTS, scheduled for a geosynchronous orbital slot at  $100^\circ$  West Longitude. While a look angle of  $7.9^\circ$  is not considered extremely low, it does require propagation through more than 7 air masses, many more air masses, by a factor of  $>3$ , than possible anywhere in the contiguous 48 states. Hawaii provides a look angle on the order of  $20^\circ$ , but is much farther down on the radiation pattern from ACTS.

A third opportunity would be a short term study of extremely low elevation Ka-band propagation effects. The location of a mobile terminal at a site such as Barrow,

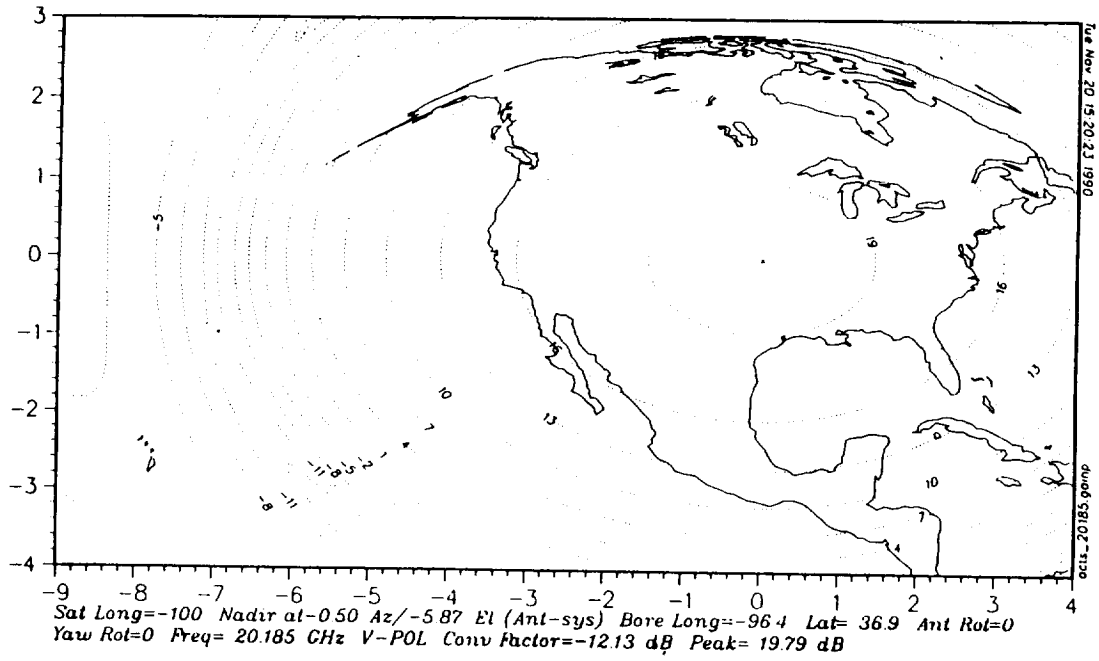


Figure 1. ACTS 20.185 GHz Beacon EIRP Levels in dBW.

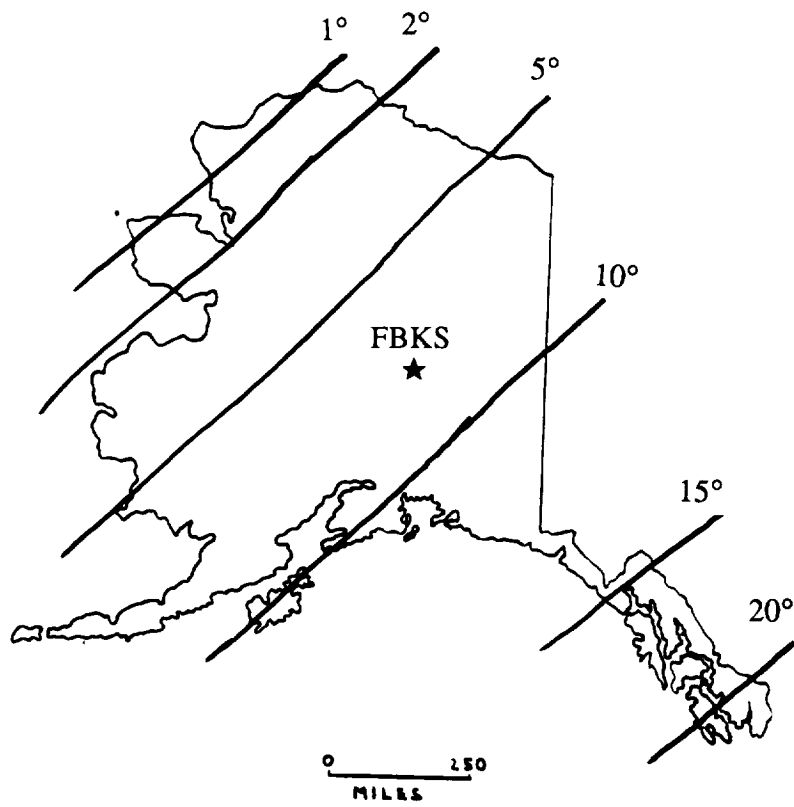


Figure 2. ACTS Elevation Look Angles in Alaska.

with a look angle of  $1.2^\circ$ , would provide a supply of very low angle data. The standard ACTS beacons could be used for this experiment, or the steerable antenna could furnish a greater EIRP for the time that it could be allocated.

Clearly, there are attractive advantages to the placement of an ACTS propagation terminal in Alaska. An examination of the link budget from Fairbanks explains how well such a propagation terminal would function.

#### 4. Link Budget

As seen in Figure 1, the ACTS EIRP in Fairbanks is less than in the contiguous states. There are three components of the link budget which are affected by the location of the receive site, which will cause the received beacon power to be less in Fairbanks than in the contiguous states. These three components are beacon antenna gain (given as EIRP), free space or path loss, and clear sky loss. We will compare the ACTS beacon levels available in Fairbanks with those available in two representative lower 48 locations, specifically Blacksburg and Seattle. Defining  $dB_{BB}$  as decibels relative to Blacksburg and  $dB_{SEA}$  as decibels relative to Seattle, Table 1 presents the EIRP levels in Fairbanks relative to Blacksburg and Seattle. Additionally, Fairbanks is located farther from ACTS than either Blacksburg or Seattle, thereby increasing the path loss by the amounts listed in Table 1. The third component is clear sky attenuation due to gaseous absorption by the atmosphere on the path length. Calculations according to the NASA Propagation Handbook (Ippolito, et al.) show that there is slightly more clear sky loss in Fairbanks during the worst case summer conditions as displayed in Table 1. In the winter months, there will be only miniscule clear sky losses in the cold, dry Alaskan air. The total worst case Fairbanks beacon power level deficit relative to Blacksburg and Seattle is tabulated in the last column of Table 1.

Table 1. Fairbanks Signal Levels Relative to Blacksburg and Seattle.

Frequency GHz	EIRP		Path Loss		Clear Sky		Total Deficit	
	$dB_{BB}$	$dB_{SEA}$	$dB_{BB}$	$dB_{SEA}$	$dB_{BB}$	$dB_{SEA}$	$dB_{BB}$	$dB_{SEA}$
20.2	-7.5	-5.0	-0.7	-0.5	-0.2	0.0	-8.4	-5.5
27.5	-7.0	-5.5	-0.7	-0.5	-0.2	0.0	-7.9	-6.0

All other parameters of a link budget calculation would be identical between the various locations. Given identical receiver stations, the C/N available in Fairbanks will be less than that available in Blacksburg or Seattle by 5.5 to 8.4 dB, as given in Table 1. There are two methods of making up this deficit, namely the use of a larger ground station antenna and/or the use of a lower noise receiver. The advantages/disadvantages of these two methods will now be examined.

A large fraction of the power level deficit can be readily restored with the use of a larger antenna. Harris Corporation manufactures both 1.2-m and 2.4-m antennas for their LBR-2 ACTS terminal. Harris lists a 6.0 dB increase in gain for the larger antenna (Koenig, 1990). Both antennas are of the same offset reflector geometry, and use the same feed horn. The surface tolerance error for both reflectors is the same,  $< 11$  mils rms. This surface error would give a surface tolerance loss of 0.24 dB at 20.2 GHz and

0.45 dB at 27.5 GHz, still well up on the gain vs. frequency curve. There are differences between the two antennas. The first is the difference in wind loading. The 2.4-m antenna can remain operational for winds >40 mph, whereas the 1.2-m antenna is operational for winds of 60 mph. The no-damage state for the two antennas are >80 and 100 mph, respectively. This does not represent any limitation or danger in Fairbanks, because of the low level of local winds. A more serious effect is the smaller beamwidth of the larger antenna. ACTS is specified to be maintained within  $\pm 0.05^\circ$  in both azimuth and elevation of its assigned orbital position. The maximum offset from the assigned position is therefore  $0.07^\circ$ . GE Astro expects the station keeping to be tighter than the maximum specified above. Calculations of estimated antenna beamwidths, given in degrees, are listed in Table 2, below.

Table 2. Antenna Beamwidths in Degrees

Antenna Diameter	1.2 m		2.4 m	
Frequency (GHz)	20.2	27.5	20.2	27.5
0.25 dB BW	0.26	0.19	0.13	0.10
1 dB BW	0.49	0.36	0.24	0.18
3 dB BW	0.89	0.65	0.45	0.33
10 dB BW	1.62	1.19	0.82	0.60

Examining the worst case situation, the beamwidth of the larger antenna at the higher frequency, and extrapolating between the tabulated values, the maximum variation in received beacon level due to satellite movement within the antenna beam is found to be <0.5 dB. GE Astro expects the satellite drift to be  $<\pm 0.03^\circ$ , which would give a maximum variation at the higher frequency of <0.25 dB. The lower frequency beacon variations would be less by about a factor of 2.

The second method of increasing the signal-to-noise ratio in Fairbanks is to use a lower noise receiver. The most straight forward way to accomplish this is to add low noise preamps at 20.2 and 27.5 GHz before the respective mixers. There are several disadvantages to this approach, however. First, to effect a 6 dB C/N difference requires a change in the system temperature by a factor of 4. The system temperature of the proposed VPI receiver is  $\sim 1800$  K, estimating  $T_{ANT} \approx 80$  K. A quick calculation gives a noise figure of <3.7 dB for the lower noise receiver. Another disadvantage is that gain variations in the amplifier would induce calibration problems into the data. With the temperature extremes of Fairbanks, there would most certainly be amplifier gain variations.

Using either the larger antenna or the lower noise receiver, it is possible to get back most if not all of the signal reduction caused by the remote location of Alaska. Furthermore, the fade depth in the Fairbanks climatic zone is not expected to be as deep as those found in coastal climatic zone.

## 5. Problems specific to Fairbanks

There are several problems specific to Alaska. The first is the extreme temperatures. The temperature range extends for a record high of  $99^\circ$  F to a record low of  $-67^\circ$  F. Typical yearly variations include highs in the 80's to lows in the 40 belows.

While the upper temperatures will be experienced at other ACTS propagation terminal sites, the lows will not. The outdoor components must be maintained within their specified thermal ranges. One solution would be to wrap the receiver with heat tape and another layer of insulation. The amount of excess heat applied would be held constant, ie turned on all winter, off in summer, so that temperature induced gain variations would not be a problem.

The lower levels of received beacon power were already addressed in the link budget discussion, Section 5. A larger antenna and/or a lower noise receiver prove to be relatively straight forward solutions.

A potentially more serious problem is caused by the change in pointing of the satellite throughout the day. This would cause variations in the received beacon power, due to the time changing antenna gain contours. Fortunately, because of its spot beam capabilities, ACTS is specified to keep true pointing within  $\pm 0.025^\circ$ , which will induce negligible variations in received power levels.

## 6. Conclusions

Alaska presents a unique opportunity to the ACTS Propagation Program. The understanding of high latitude effects is vital to reliable communications system design. Major advantages to the location of an ACTS propagation terminal in Alaska are the inclusion of a new and important climatic zone to the global propagation model. Also the low elevation angle would give a longer propagation path through the atmosphere in general, and clouds, rain, and snow events in particular. The beacon power levels are reduced from those of lower 48 sites. However, the C/N ratios available can be increased to comparable values through the use of a larger antenna or a lower noise receiver. The choice of a larger antenna seems to present a more stable and less troublesome solution. Any problems due to the location or climate of Alaska can be solved. Therefore, there are no technical obstacles to prevent the placement of an ACTS propagation terminal in Alaska, only great opportunities to contribute to the understanding of high frequency propagation.

## 7. References

- Cashman, W.F., "Spacecraft Beacon Characteristics," Presentations of the Second ACTS Propagation Studies Workshop, D. Chakraborty and F. Davarian, eds., JPL D-8041, pp. 37-63, Dec. 1990.
- Crane, R.K., "Comparative evaluation of several rain attenuation prediction models," Radio Science, Vol. 20, No. 4, pp. 843-863, 1985.
- Hills, A., "Alaska's giant satellite network," IEEE Spectrum, pp. 50-55, July, 1983.
- Hills, A., "Feasibility of mobile satellite service in Alaska," Telecommunications Policy, pp. 369-378, Dec., 1988.
- Ippolito, L.J., R.D. Kaul, and R.G. Wallace, Propagation Effects Handbook for Satellite Systems Design, NASA Reference Publication 1082(03), pp. 216, 1983.
- Koenig, W.R., "ACTS LBR-2 design," Presentations of the Second ACTS Propagation Studies Workshop, D. Chakraborty and F. Davarian, eds., JPL D-8041, pp. 247-283, Dec. 1990.



**Planned LMSS Propagation Experiment Using ACTS:  
Preliminary Antenna Pointing Results During Mobile Operations**

John R. Rowland <sup>+</sup>, Julius Goldhirsh<sup>+</sup>, Wolfhard J. Vogel<sup>#</sup>, Geoffrey W. Torrence <sup>#</sup>

<sup>+</sup>The Johns Hopkins University, Applied Physics Laboratory, Laurel, Maryland

<sup>#</sup>The University of Texas, Electrical Engineering Research Laboratory, Austin, Texas

**Abstract** – An overview and a status description of the planned LMSS mobile K band experiment with ACTS is presented. As a precursor to the ACTS mobile measurements at 20.185 GHz, measurements at 19.77 GHz employing the Olympus satellite were originally planned [Goldhirsh et al., 1990]. However, because of the demise of Olympus in June of 1991, the efforts described here are focused towards the ACTS measurements. In particular, we describe the design and testing results of a gyro controlled mobile-antenna pointing system. Preliminary pointing measurements during mobile operations indicate that the present system is suitable for measurements employing a 15 cm aperture (beamwidth  $\approx 7^\circ$ ) receiving antenna operating with ACTS in the high gain transponder mode. This should enable measurements with pattern losses smaller than  $\pm 1$  dB over more than 95% of the driving distance. Measurements with the present mount system employing a 60 cm aperture (beamwidth  $\approx 1.7^\circ$ ) results in pattern losses smaller than  $\pm 3$  dB for 70% of the driving distance. Acceptable propagation measurements may still be made with this system by employing developed software to flag out bad data points due to extreme pointing errors. The receiver system including associated computer control software has been designed and assembled. Plans are underway to integrate the antenna mount with the receiver on the University of Texas mobile receiving van, and repeat the pointing tests on highways employing a recently designed radome system.

## 1. Introduction

Since 1983, the authors have been involved in 11 experimental campaigns dealing with mobile satellite measurements at UHF and L band (see references). As a natural follow-on, mobile propagation measurements are important at K band in that they will provide information at a frequency where none exists. In particular, mobile communications and data transfer at K band will result in significantly larger bandwidths accommodating more users. As a consequence of employing higher gain antennas, larger fade margins will also be available to overcome precipitation and tree attenuation.

## 2. Link Margin Characteristics

The link parameters for the beacon and high gain transponder mode of ACTS for different receiver antenna sizes are tabulated in Table 1. Three antenna sizes are planned for the ACTS K band mobile campaigns; 61 cm (2'), 30.5 cm (1'), and 15.25 cm (6"). Repeat runs will be made for each of these antennas as these will provide information of the increased multipath

Table 1: Link Parameters for ACTS-K Band Mobile System

PARAMETER	BEACON			HIGH GAIN		
	Receiver Antenna Diameter (cm)					
	60	30	15	60	30	15
<b>Satellite:</b>						
Longitude (°W)	100					
Frequency (GHz)	20.185					
Polarization	Vertical					
<b>Receiver:</b>						
Latitude (°N)	39.25					
Longitude (°W)	77.0					
Elevation Angle (°)	38.7					
Azimuth Angle (°)	213.9					
Polarization	Horizontal					
Antenna Efficiencies	0.6					
Antenna Gains (dB)	40	34	28	40	34	28
Beamwidth (°)	1.7	3.4	6.8	1.7	3.4	6.8
Nominal System Temperature (K)	430					
<b>Link Budget:</b>						
EIRP (dBW)	20			50		
Free Space Loss (dB)	210.1					
Atmospheric Gas Loss (dB)	0.5					
Radome Loss (dB)	0.5					
Modulation Loss (dB)	3.0					
Mobile G/T (dB/K)	13.6	7.6	1.6	13.6	7.6	1.6
Signal Power (dBW)	-154.2	-160.2	-166.2	-124.2	-130.2	-136.2
Noise Power (dBW/Hz)	-202.2					
Carrier/Noise (per Hz)	48.0	42.0	36.0	78.0	72.0	66.0
<b>Carrier/Noise (400 Hz)</b>	22.0	16.0	10.0	52.0	46.0	40.0

contributions for various beamwidth sizes. Measurements employing transmissions from the ACTS beacons (20 dB e.i.r.p.) and the high gain transponder ( $\approx 50$  dB e.i.r.p.) are also planned. The latter mode will require a ground station to transmit to the satellite a cw signal which will be transponded down to the receiving van. Since planned experimental mobile runs are individually short, reserved time slots for this transmission of approximately 4 hours or less are required.

### 3. Gyro-Antenna Mount Tracking System

#### 3.1 Block Diagram

In Figure 1 is a block diagram depicting the logic of the antenna mount control. The mount is an "elevation" over "azimuth" system. The antenna and vertical gyro (Block #2) are located on the elevation assembly and the azimuth gyro and flux gate compass (Block #1) are on the azimuth assembly. The synchro outputs represent the actual pointing direction of the antenna axis. A single output exists for the azimuth gyro (relative to magnetic north) and there are two outputs, pitch and roll, (relative to true vertical) for the vertical gyro.

The gyro outputs are fed into corresponding synchro/digital converters (Blocks #5, #7, #8) whose outputs are connected to a digital input/output (I/O) PC interface card (Block #10). The PC (Block #11) compares the azimuth, pitch, and roll angles of the mount with the respective "true values" and generates digital error signals for each which are in-turn fed back through the interface card (Block #10) to the azimuth (Block #6) and elevation (Block #9) mount control drivers. These drive the azimuth (Block #3) and elevation motors (Block #4) in such a direction as to reduce the error signal. Ultimately this feedback system results in a condition of zero pointing error and the antenna is pointed in the true direction.

#### 3.2 Computer Control Features

If the differences between true and actual pointing in azimuth and elevation are each within  $0.1^\circ$ , no error signals are generated by the computer. This feature eliminates small angle hunting. More efficient tracking and further mitigation of hunting is achieved by controlling (via the PC) the speed of the elevation and azimuth mounts in the following manner: [1] For pointing errors greater than  $2^\circ$ , the slew rate is  $10^\circ/\text{s}$ . [2] For pointing errors between  $1^\circ$  and  $2^\circ$  the slew rate is  $5^\circ/\text{s}$ . [3] For pointing errors smaller than  $1^\circ$ , the slew rate is  $2^\circ/\text{s}$ . The above logic is software selectable and is based on the present PC (80286 processor with 12 MHz clock). The above conditions are expected to be modified for a planned faster computer system (80486 processor with a 33 MHz clock) and improved mount system having faster motor speeds.

### 4. Preliminary Mobile Tracking Tests

Several pointing tests were executed with the tracking antenna system during mobile operation. The objectives of these tests were to establish preliminary pointing accuracies of the designed tracking system during mobile operations and to establish requirements for

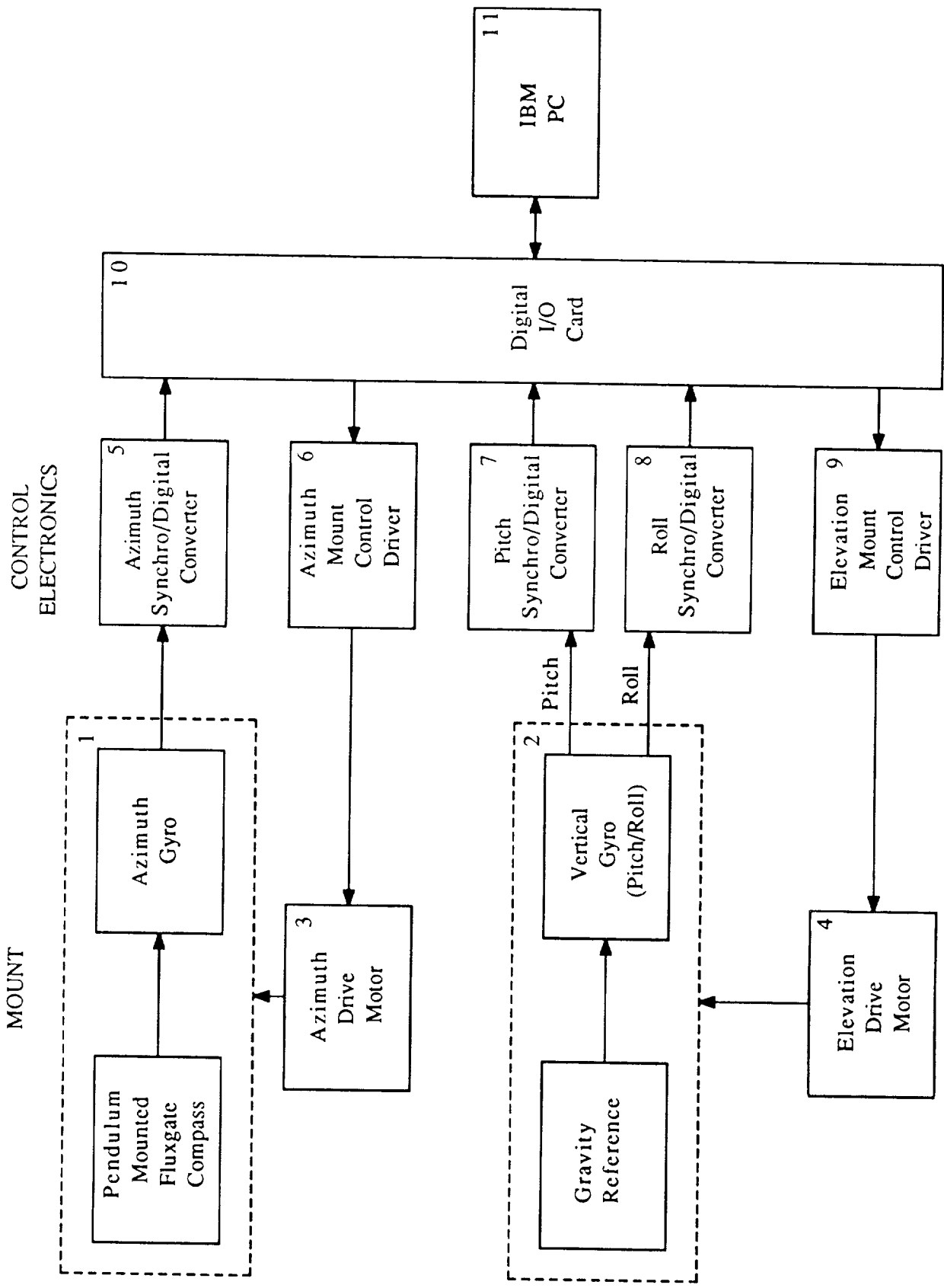


Figure 1: Block diagram of gyro-controlled antenna mount system to operate at K-Band.

improving the system. Since the radome was unavailable, all mobile tests were made within APL grounds at speeds smaller than 15 mph. The mount and controlling computer (and staff) were placed atop a pick-up truck and a sequence of runs were made along a relatively rough road having frequent sloping surfaces.

The mobile runs were made at fixed speeds (e.g., 0, 5, 10, and 15 mph) and included: [1] tracking the sun and [2] pointing towards the Olympus satellite. As these measurements were made prior to the demise of Olympus, ACTS pointing measurements were not made. The pointing results for the Olympus pointing are expected to be similar to those of ACTS. Prior to these runs, software was developed to operate with "Quickbasic" enabling the measurement of the actual pointing and true pointing angles, and subsequently the pointing errors for both the sun and satellite runs [Miller, 1991, Sterner, 1991a, 1991b, 1991c]. During the mobile runs, the mount azimuth and elevations were sampled at a 50 Hz rate. These positions were compared with the true values, and the mount pointing was updated (at this rate) following the logic described in Section 3 and Figure 1. The "actual" and "true" pointing angles were stored in computer memory at a selectable sampling rate and subsequently written into files.

In Figure 2 are cumulative distributions describing the percentage number of samples for which the pointing error is smaller than the abscissa values for repeated sun tracking runs. As mentioned, because no radome was available, these runs were made at slow speeds along an approximate one km road stretch. The sample sizes ranged between 100 to 200 at a sampling rate 1 to 10 seconds. The circular and bell shaped data points in Figure 2 represent the azimuth and elevation pointing error cases, respectively. The upper, middle, and bottom curves for azimuth and elevation represent zero vehicle speed, 5 mph, and 10 mph. In Figure 3 are shown a similar set of distributions describing the pointing errors for mobile-Olympus runs (azimuth of  $111.6^\circ$  and elevation of  $15.9^\circ$ ). As mentioned, it is expected that pointing errors for mobile-ACTS run (azimuth of  $213.9^\circ$  and  $38.7^\circ$ ) will give similar results.

We note that over approximately 98% of the driving distance, pointing errors are implied smaller than  $2^\circ$  for both the azimuth and elevation cases. These errors imply pattern losses of less than  $\pm 1$  dB employing a 15 cm aperture ( $\approx 7^\circ$  beamwidth). Using the high gain transponder mode of ACTS with the 15 cm aperture will provide a nominal 40 dB carrier to noise ratio (Table 1). For the 60 cm aperture (2' dish), Figures 1 and 2 imply an approximate  $\pm 3$  dB pattern loss over approximately 70% of the driving distance. Even if the present mount system were used with ACTS (which it will not be), a software has been developed which flags receiver data for which the pointing errors are unacceptable. We note from the figures that an increase of the vehicle speed results in a monotonic increase of the pointing errors. This increase is due the combination of slow mount and computer speeds. As mentioned, plans are underway to correct both of these deficiencies.

## 5. Receiver and Data Acquisition

### 5.1 Block Diagram

We describe here the receiver system which, at this writing, has been designed, the

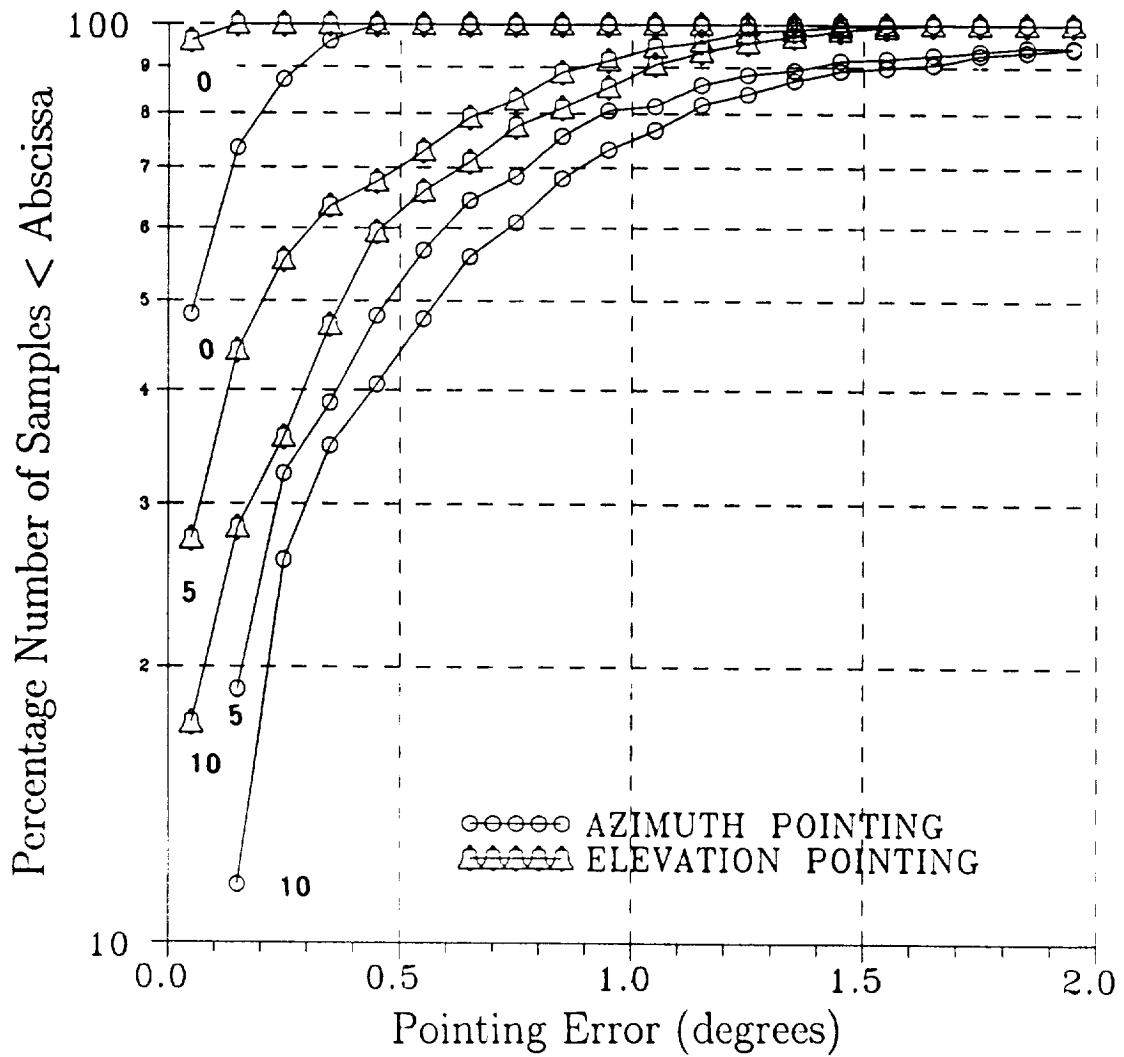


Figure 2: Cumulative distributions of pointing errors for mobile-sun-track runs for drive speeds of 0, 5, and 10 mph.

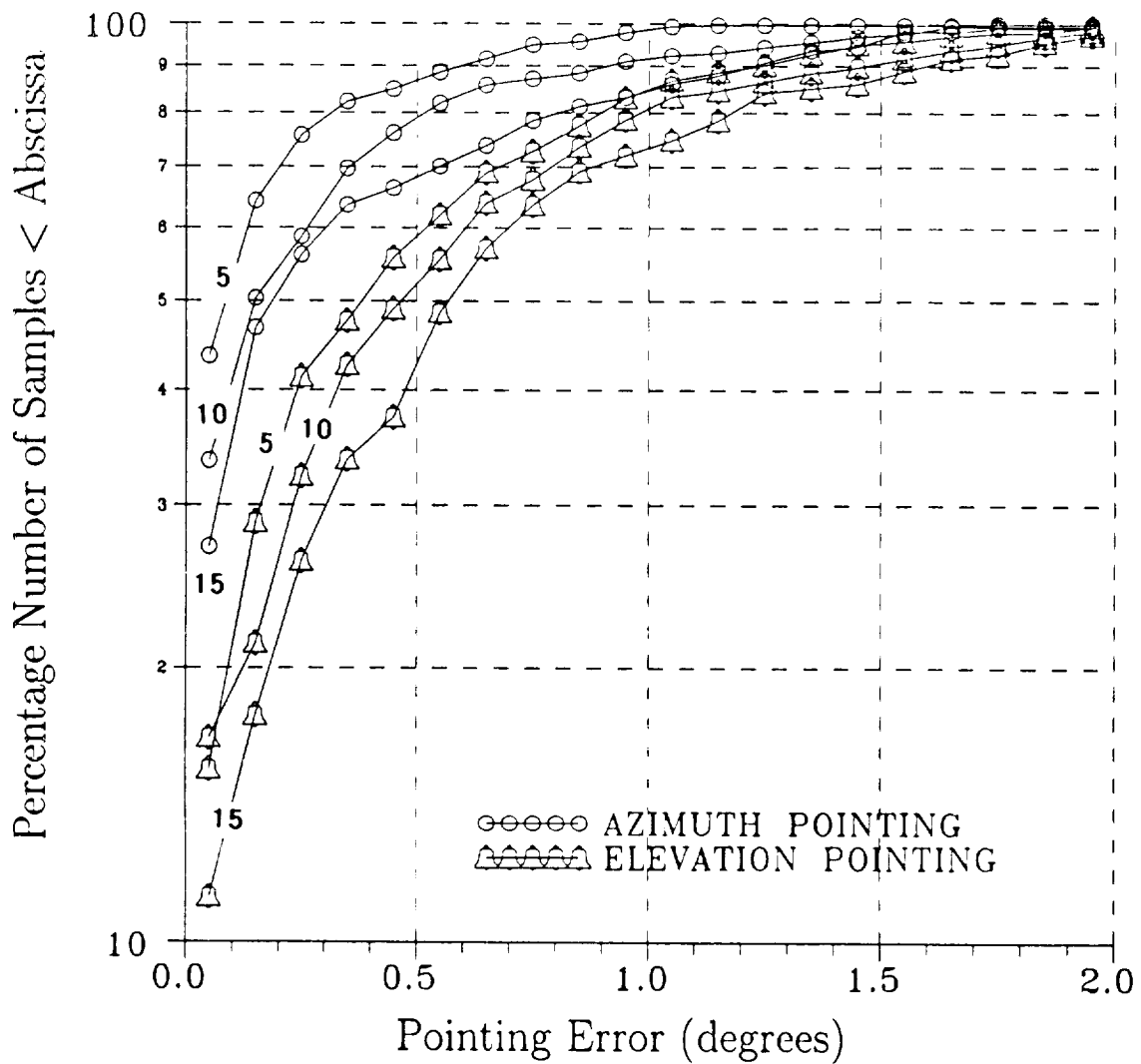


Figure 3: Cumulative distributions of pointing errors for mobile-Olympus runs at drive speeds of 5, 10, and 15 mph.

components integrated (with the exception of the mount system), and tested. With reference to Figure 4, the received signal enters the antenna-feed assembly (Block #1) and is then passed through a low noise amplifier mounted near the antenna (Block #2). The output signal is fed through a 1.7 to 2.2 GHz downconverter (Block #3). The amplified output signal from the low-noise converter is fed to a microwave spectrum analyzer (Block #4). Using a spectrum analyzer in the IF chain significantly enhances the functionality of the receiver by supplying built-in RF diagnostics, easy signal identification, and flexible receiver tuning. Once the correct signal has been acquired under computer control (Block #6) over the General Purpose Interface Bus (GPIB) interface, the spectrum analyzer mode is changed to non-sweeping and is centered at the desired beacon signal frequency. The 10 MHz IF output from the spectrum analyzer is converted to 10 kHz at the frequency tracking down-converter (Block #5). At that frequency, a filterbank comprised of eleven narrow filters has been implemented for the automatic frequency tracking function. The differential signal voltage from the two filter-channels straddling the center filter is used to tune an oscillator in the 10MHz to 10 KHz converter. On another path, the signal is quadrature detected, 500 Hz low-pass filtered, and fed to the data acquisition board in the PC (Block #6). The vehicle's speed will sensed (Block #7) and recorded once per second by the PC.

The antenna mount control system (Blocks #1, #8, #9, #10) is presently interfaced with a separate computer system (Block #10) which has an 80286 processor and 12 MHz clock). It is the intention to eliminate this system for further planned pointing tests and the ACTS experiment and to interface the mount control system with the existing receiver PC (Block #6) which has as 80486 processor and a clock speed of 33 MHz. This and planned mount improvements should improve the pointing accuracy allowing for more rapid updates.

## 5.2 Doppler Spread

For an omni-directional antenna, the maximum Doppler spread of a CW signal due to the range of relative motion in an environment filled with multipath scatterers is twice the speed divided by the wavelength. At 20 GHz, a maximum spread of 3.3 kHz results at 25 m/s speed ( $\approx$  55 mph). The receiving antenna does not couple into all directions, however, and therefore acts as a filter. With a high gain antenna practically all the power will be received from directions very close to the direction to the transmitter and the spread will be small. Although the transmitter frequency will be shifted by an amount proportional to the relative speed of the vehicle and the transmitter platform, the receiver AFC will be capable of tracking changes in this shift brought about by vehicle speed or direction variations.

## 6. System Integration with Van

The van to be used is the same in which eleven land-mobile measurement campaigns have been conducted. It is equipped with a shock-mounted standard equipment rack, a 115 vac primary power system, a video recorder and an electronic speed transducer. The video recorder captures the scene in front of the vehicle and the speed transducer enables a recording of the vehicle speed every second. The receiver data acquisition software, originally written in Microsoft Fortran, has been converted to a LabWindows/QuickBasic environment to take advantage of more modern and efficient software technology. As mentioned, the PC



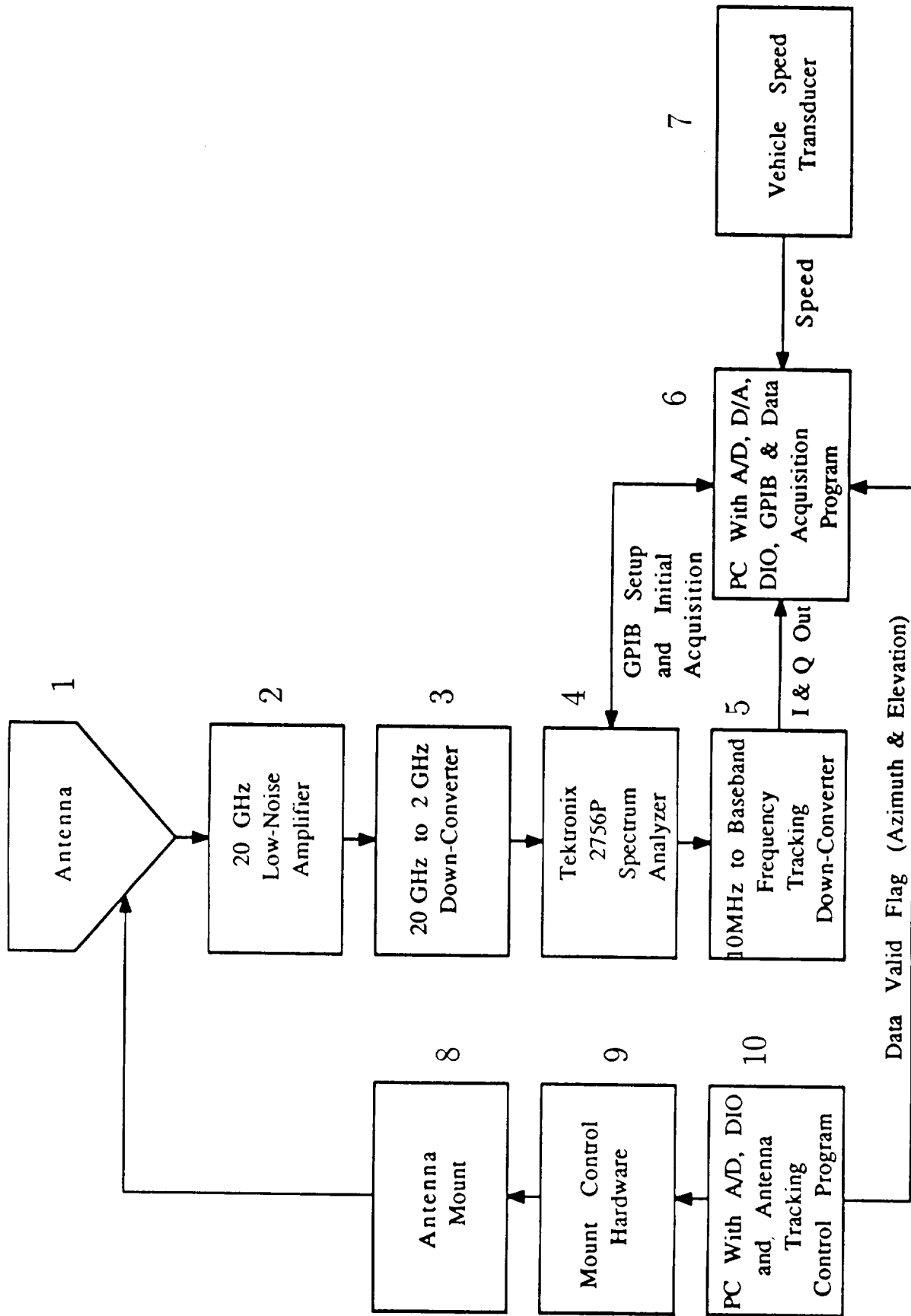


Figure 4: Block diagram of mobile K-band receiver system.

inside the van has a 80486 processor with a 33 MHz clock. It will serve the function of controlling both the receiver and the mount and will write data to 20 MHz Bernoulli Box disks. Plans are underway to integrate the mount-antenna control system with the van and its receiver system during the summer of 1991.

## 7. Planned Measurements

### 7.1 Pointing Measurements After System Integration with Van

As mentioned in Section 4, preliminary pointing measurements were executed using a slow speed computer system with the mount-antenna system having no radome placed atop an open truck. These preliminary measurements indicated the need for an improved mount system with faster motors and a higher speed computer; both changes of which are planned. In the meantime, the present antenna-mount control system will be integrated with the receiver and computer system within the van (described in Section 5.). A radome, which has already been designed and fabricated will be placed over the antenna-mount system atop the van and pointing measurements of the type described in Section 4 will be made using the integrated system on a highway traveling at normal speeds (e.g., 25 m/s).

### 7.2 LMSS Propagation Experiments with ACTS

Roadside tree propagation measurements will be instituted employing transmissions from the ACTS satellite for a system of roads in Central Maryland (Routes 295, 108 and 32). Under the NASA Propagation Program, attenuation measurements have been executed for this system of roads at 870 GHz and 1.5 GHz employing a helicopter and MARECS-B2 geostationary satellite as transmitter platforms [Goldhirsh and Vogel, 1991, 1989, 1987; Vogel and Goldhirsh, 1990]. It is planned to use the beacon measurements (20 dB e.i.r.p.) for making preliminary measurements and to follow these by repeat measurements with the high gain transponder (nominal 50 dB e.i.r.p.). The high gain measurements will enable the employment of a 15 cm antenna (6 inches) and result in a 40 dB carrier/noise at a 400 Hz bandwidth (Table 1). Since the beamwidth will be nominally 7° for the reduced aperture, minimal pattern losses are expected during tracking under mobile operation.

The analytical aspects will involve characterizing the fade distributions for the various road types, establishing the fade durations, combining the results with previous measurements at UHF and L band, and extending "frequency scaling" concepts from UHF to K Band. Analyses will be performed which are, in part, similar to those described by Vogel and Goldhirsh [1990], and Goldhirsh and Vogel [1991, 1989].

Some examples of propagation results to be derived for mobile-propagation experiments at K-band using ACTS are as follows: [1] cumulative fade distribution at 20 GHz due to roadside trees, [2] equi-probability cross polarization discrimination measurements, [3] cumulative fade distributions for different antenna size demonstrating the effects of enhanced multipath, [4] simulation of antenna diversity employing measured time-series fade data at K-Band, [5] equi-probability frequency scaling of cumulative fade distributions, [6] effects of foliage on cumulative fade distributions (measurements at different seasons), [7] fade

reduction statistics versus side of road, [8] fades caused by individual trees (static case), and [9] possible extension of the empirical roadside shadowing model to include K-Band.

## 8. Summary and Conclusions

A first generation gyro-controlled antenna tracking system has been designed and has undergone preliminary mobile testing by tracking the sun and the Olympus satellite. Although these measurements were performed before the demise of Olympus, the pointing results for ACTS are believed to be approximately similar. These measurements indicate that the present system may be used as is with a 15 cm aperture antenna ( $\approx 7^\circ$  beamwidth) employing the high gain transponder mode of ACTS. Minimal pattern loss due to pointing errors will ensue (e.g.,  $< \pm 1$  dB) for this mode which should result in a carrier to noise ratio of approximately 40 dB. Beacon measurements employing the present system and the 60 cm antenna ( $1.7^\circ$ ) will experience enhanced pattern losses (e.g.,  $\pm 3$  dB for 75% of the distance), although acceptable measurements may even be made with this system by generating *pointing error flags* and not using propagation data during pointing degraded periods.

Plans are presently underway to: [1] Integrate the present system with the receiving antenna, the van, and a radome, [2] Repeat mobile pointing measurements on highways with the integrated system, [3] Update the present mount system by interfacing higher speed mount motors and connecting the system to a higher speed computer system (80486 processor, 33 MHz clock). The possibility of further updating the system to receive the ACTS 27.5 GHz beacon during mobile operations is also being explored.

**Acknowledgements** This work was funded by the Communications and Information Systems Divisions of NASA Headquarters for the Applied Physics Laboratory of the Johns Hopkins University (Contract #N000039-89-C-0001) and the Jet Propulsion Laboratory for the Electrical Engineering Research Laboratory of the University of Texas (Contract #JPL956520). The authors are grateful to R. E. Miller and R. Sterner of the Applied Physics Laboratory for their hardware and software development and to W. Charbonneau for integrating and testing the mount components.

## References

- Goldhirsh, J., W. J. Vogel, and J. R. Rowland, "Planned Olympus and ACTS Mobile Propagation Experiments at K Band," *Proceedings of the Second ACTS Propagation Studies Workshop* Santa Monica, California, November 27-28, 1990, pp 204-215 (JPL Publication D-8041, December 15, 1990).
- Goldhirsh, J and W. J. Vogel, "Propagation Handbook for Land-Mobile-Satellite Systems - Preliminary," *APL/JHU Technical Report S1R-91U-012*, April 1991.
- Goldhirsh, J. and W. J. Vogel, "Roadside Tree Attenuation Measurements at UHF for Land-Mobile Satellite Systems," *IEEE Trans. Antennas Propagat.*, AP-35, pp 589-596, 1987.

- Goldhirsh, J. and W. J. Vogel, "Mobile Satellite System Fade Statistics for Shadowing and Multipath from Roadside Trees at UHF and L-band," *IEEE Trans. Antennas Propagat.*, AP-37, pp 489-498, 1989.
- Hase, Y., W. J. Vogel, and J. Goldhirsh, "Fade-Durations Derived from Land-Mobile Satellite Measurements in Australia," *IEEE Trans. on Commun.*, May, 1990.
- Miller, R. E., "Antenna Tracker Hardware and Operating Software for a Mobile Antenna System," *APL/JHU Technical Memorandum F2E-91-2-280* July, 1991.
- Sterner, R., "Solar Position Software in Quick-Basic," *APL/JHU Technical Memorandum STR-91-009*, April 3, 1991.
- Sterner, R., "Computing the Altazimuths of Geosynchronous Satellites," *APL/JHU Technical Memorandum STR-91-012*, May 2, 1991.
- Sterner, R., "Roll Angle Correction for a Mobile Antenna Tracking System," *APL/JHU Technical Memorandum STR-99-11*, June 11, 1991.
- Vogel, W. J., and J. Goldhirsh, "Tree Attenuation at 869 MHz Derived from Remotely Piloted Aircraft Measurements," *IEEE Trans. Antennas Propagat.*, AP-34, pp 1460-1464, 1986.
- Vogel, W. J., and J. Goldhirsh, "Mobile Satellite System Propagation Measurements at L-Band Using MARECS-B2," *IEEE Trans. Antennas Propagat.*, AP-38, pp 259-264, 1990.
- Vogel, W. J., and J. Goldhirsh, "Fade Measurements at L-band and UHF in Mountainous Terrain for Land Mobile Satellite Systems," *IEEE Trans. Antennas Propagat.*, vol. AP-36, pp 104-113, 1988.
- Vogel, W. J., J. Goldhirsh, and Y. Hase, "Land-Mobile-Satellite Fade Measurements in Australia," *AIAA Journal of Spacecraft and Rockets*, May-June, 1991.

# PROPAGATION-RELATED AMT DESIGN ASPECTS AND SUPPORTING EXPERIMENTS

Khaled Dessouky and Polly Estabrook

Jet Propulsion Laboratory  
California Institute of Technology  
4800 Oak Grove Drive  
Pasadena, California 91109

## 1. Introduction

The ACTS Mobile Terminal (AMT) is presently being developed with the goal of significantly extending commercial satellite applications and their user base. A thorough knowledge of the Ka-band channel characteristics is essential to the proper design of a commercially viable system that efficiently utilizes the valuable resources. To date, only limited tests have been performed to characterize the Ka-band channel and they have focused on the needs of fixed terminals. (See for example [1,2] as well as the articles in these proceedings.) As part of the value of the AMT as a Ka-band test bed is its function as a vehicle through which tests specifically applicable to the mobile satellite communications can be performed. The exact propagation environment with the proper set of elevation angles, vehicle antenna gains and patterns, roadside shadowing, rain and Doppler is encountered. The ability to measure all of the above, as well as correlate their effects with observed communication system performance, creates an invaluable opportunity to understand in depth Ka-band's potential in supporting mobile and personal communications. This paper discusses the propagation information required for system design, the setup with ACTS that will enable obtaining this information, and finally the types of experiments to be performed and data to be gathered by the AMT to meet this objective.

## 2. Experimental Setup

The AMT experimental setup with ACTS is shown in Figure 1. To support the FDMA architecture adopted (at least in the earliest experiments), an unmodulated pilot is transmitted from the fixed station to the AMT. This pilot is used by the mobile terminal for antenna tracking, as a frequency reference for Doppler correction and pre-compensation, and in measuring rain attenuation. For system efficiency, a pilot is transmitted only in the forward direction; i.e., from the fixed to the mobile terminal. Hence, in the AMT system setup two signals will exist in the forward direction, the pilot and the information link which could be voice or data. In the return direction (mobile to fixed) only the information channel (commonly referred to as the data channel) is transmitted. The data rate is selectable among 2.4, 4.8 and 9.6 kbps depending on channel conditions. A separate higher rate of 64 kbps will also be supported but under restricted link conditions.

Consistent with a Ka-band test bed approach, the AMT links have been designed to maximize utilization of the available ACTS resources to support as wide an array of channel measurements as possible. This is reflected in the link budgets of Table 1. ACTS was designed to support high data rate communications; as a result, even with the lowest TWT drive levels in the HBR-LET, the single user forward link has ample margin. This margin can be utilized to investigate the deleterious effects of the 20 GHz channel by permitting signal tracking through 15 - 20 dB of attenuation. Thus the range of channel impairments of practical interest can be studied with the AMT. (The different measurements will be discussed in Section 4.) In contrast to the forward link, the need to minimize radiation hazard in the neighborhood of the vehicle and practical limits on amplification in the user unit lead to a modest margin on the return link under normal operation. This is evidenced in Table 1. Nevertheless, under restricted experimental conditions this margin

could be boosted by up to 10 dB. Hence 30 GHz propagation investigations initiated at the mobile terminal will cover channel effects of up to 10-15 dB of attenuation.

To support an extensive system/channel data gathering campaign, the AMT experimental setup will be equipped with a state of the art data acquisition system (DAS). The DAS will be capable of capturing and recording up to half a Mbyte/s of channel and system information. In addition, it will record half a Mbyte/s of synchronized video information from a camera designed to observe the physical link. It was learned from MSAT-X experience that one of the most painstaking (and time consuming) aspects of experiment analysis is correlation of the gathered data with the channel that was encountered. Not only is keeping track of the various propagation environments hard to do, but also identifying the events that result in peculiar data is practically impossible. The camera will be mounted on a slave platform that follows the pointing of the AMT antenna. The camera platform will be located near the rear of the van outside the field of view of the antenna. In addition to the video, experimenters' voices will be recorded on the DAS and synchronously time tagged for easy logging and retrieval of comments. Thus, a multitude of data types augmented with synchronized video and audio annotation will be available to the post experiment analyst. To support the transfer of the data to analysis workstations, either the compact tapes will be duplicated at the workstations or an Ethernet interface will be included in the DAS. To complement all of the above, the DAS will have substantial real time and near real time analysis and display capabilities. These are primarily intended to assist the experimenters in the field. They can, however, serve as starting points for the more detailed analysis that will follow.

At present a six month initial experimentation phase with ACTS has been planned. From March to September of 1993 mobile experiments will be performed using the AMT van. Another set of experiments will be performed using the sedan; however, the sedan will not be equipped with a DAS and will therefore be more suited to subjective quality tests. This phase is currently planned for 1994.

### **3. Channel Information Required for Mobile System Design**

A commercially viable system must efficiently utilize the available resources while providing the user with an acceptable grade of service. Highest possible system capacity is critical to exploiting the economies of mass markets, and consequently to reducing user cost. Also, a careful balance has to exist between the design, capabilities, and cost of the different system segments, namely, user terminals, spacecraft, and fixed ground station(s). In general, more robustness means higher cost, either through the allocation of extra resources or added system or subsystem complexity.

To enable the careful design required, as much as possible detailed knowledge about the physical channel is required. This is particularly true for the AMT which operates in a challenging propagation environment that can have a very significant impact on terminal performance, terminal design and implementation cost. This propagation environment is central to the determination of link requirements, link operation and protocols, and ultimately, system capacity and overall viability.

The two most obvious propagation effects in the Ka-band mobile channel are shadowing and rain attenuation. Shadowing is handled in the AMT at different levels, in the pilot tracking/acquisition circuits, in the antenna controller, and in the modem and speech coder. The pilot tracking and antenna pointing schemes have to withstand a certain degree of signal drop-out due to shadowing. Frequent loss of tracking and/or switching to an acquisition mode is disruptive to terminal operation. The duration and depth of the typical shadowing events are extremely important for the proper design of these subsystems. Shadowing is also handled through the design of a modem that can "freewheel," i.e., not lose symbol synchronization through a deep fade and reproduce valid data soon thereafter. The statistics of fade length and the nature of the onset and recovery of shadowing episodes for a variety of road types are important parameters required for proper

modem design. Short duration statistics of light fading are also useful in the design of the speech codec, particularly frame repetition or other schemes employed to enhance operation for brief outages. Finally, sufficient information should be available about shadowing profiles to support the design of robust communication protocols (link setup, etc.) and the rain compensation algorithm (RCA) which has to distinguish between rain and shadowing.

Very limited information is available about shadowing in the Ka-band land-mobile channel. In the design of the AMT a rough estimate of the extent of shadowing is being obtained by applying an empirical formula<sup>1</sup> [4] to L-band data collected with a medium gain antenna [5]. In addition models of signal outage produced by periodic sequences of utility poles are being generated. Both estimates of shadowing data will be used as testing sequences for the AMT. However, this data falls far short of the accurate, reliable statistics sought, particularly for light to moderate shadowing which is of the most interest in AMT design.

Rain attenuation is handled in the AMT primarily through data rate reduction. This is complemented with power control on the forward uplink. Due to the power limitations of the user terminal, the most critical link is that between the mobile unit and the satellite. The AMT's RCA relies on real time pilot power measurement at the mobile terminal and satellite beacon power measurement at the fixed station. Proper design of the RCA rests on the availability of rain and rain rate statistics. The probability of rain, the temporal characteristics of rain events, the impact of vehicle motion on temporal rain statistics are all required for the proper design of the RCA. Measurement averaging periods, decision criteria and regions, interaction between the RCA and the communication protocol, as well as the data rate change procedure within the communication protocol itself, are all detailed aspects of AMT design that require the applicable rain information. This information has to be for the proper range of elevation angles and locations that the AMT will operate in. The measurements and analysis being performed at VPI are a step in the direction of understanding Ka-band rain at low elevation angles. Some of the theoretical models [6,7] are also useful for the initial design of the RCA. There is, however, no substitute to experimentation using the actual mobile terminal to refine and validate any rain compensation procedures for Ka-band mobile terminals.

#### **4. Propagation Related AMT Experiments**

The emphasis during AMT experiments will be on collecting propagation data that directly impacts AMT operation, and as explained above, is necessary for optimizing system design. The channel conditions experienced in the operational locations, and hence with the pertinent elevation angles, will be observed through the actual antenna of the mobile terminal, i.e., with the proper gain and beam characteristics. A conscious effort will be made to correlate the operation of the various AMT algorithms with the observed propagation characteristics.

A typical set of AMT experiments is summarized in Table 2. The experiments combine propagation measurements with system and subsystem performance characterization. The detailed definition of the complete set of experiments will evolve in parallel with the latter phases of AMT development, namely, subsystem implementation and terminal integration and checkout.

As can be seen from Table 2, pilot signal measurements are central to all propagation related experiments. At the mobile terminal both coherent and non-coherent measurements of the pilot will be recorded. Sampling rates will be chosen to significantly exceed any possible pilot frequency variation or spreading due to Doppler or channel scatterers (such as tree tops or

---

<sup>1</sup> This formula was derived by Weissberger [3] to predict the attenuation at various frequencies of a signal between 200 MHz to 95 GHz through groves of trees.

branches, poles, etc.).<sup>2</sup> The pilot tracking loop is being designed for a nominal C/N0 of 50 dB Hz, but will continue to track at lower C/N0s. Hence, in the absence of rain (98% of the time in L.A.), shadowing-induced fades of up to 30 dB could be measurable.

The data or voice channel signal will be measured by means of a power meter as well as through a received signal quality estimate obtained in the modem. Modem bit error rate performance will be measured quantitatively by using preselected PN sequences.

## **5. Future Experiments and Propagation Related Information**

Several institutions have expressed the desire to use the AMT for land mobile experimentation. One of the possible applications would involve mounting the AMT onto a satellite news gathering truck to enable the exchange of FAX and compressed video, in addition to voice and data messages. These services would be provided between the newsroom and the truck while it is en route to the news event. The impact of the mobile Ka-band channel on these services and the AMT protocols that handle them will be evaluated.

Other experiments are being proposed to utilize much of the AMT equipment after the van and sedan tests are performed. One experiment would involve mounting the AMT on an aircraft in order to measure the Ka-band aeronautical channel. This would permit several channel characteristics to be measured, e.g., shadowing due to the aircraft body, multi-path at low aircraft-to-satellite elevation angles, and Doppler and Doppler rate. The tracking performance of electronically and mechanically steered aircraft antennas could also be ascertained. A second experiment would seek to demonstrate seamless handover of a satellite-initiated call to a cellular mobile system and vice-versa. Operation of such a hybrid satellite/terrestrial system would be tested and the effects of the two distinct channels assessed. The required equipment and protocols would then be recommended.

## **6. References**

- [1] Stutzman, W. L., "Olympus Propagation Studies in the U.S.- Propagation Terminal Hardware and Experiments," Proceedings of NAPEX XIV, JPL Pub. 90-27, July 1, 1990.
- [2] Westwater, E. R., et al., "Attenuation Statistics Derived from Emission Measurements by a Network of Ground-Based Microwave Radiometers," Proceedings of NAPEX XIV, JPL Pub. 90-27, July 1, 1990.
- [3] Weissberger, M. A., "An Initial Critical Summary of Models for Predicting the Attenuation of Radio Waves by Foliage," ECAC-TR-81-101, Electromagnetic Compatibility Analysis Center, Annapolis, MD, August, 1981.
- [4] Report 236-6, "Influence of Terrain Irregularities and Vegetation on Tropospheric Propagation," International Radio Consultative Committee (CCIR), Recommendations and Reports of the CCIR, Volume V, Propagation in Non-Ionized Media, Geneva, 1986.
- [5] ALEX-1 Cumulative Distributions, Memorandum from W. J. Vogel, Electrical Engineering Research Laboratory, University of Texas at Austin, 3/23/89.

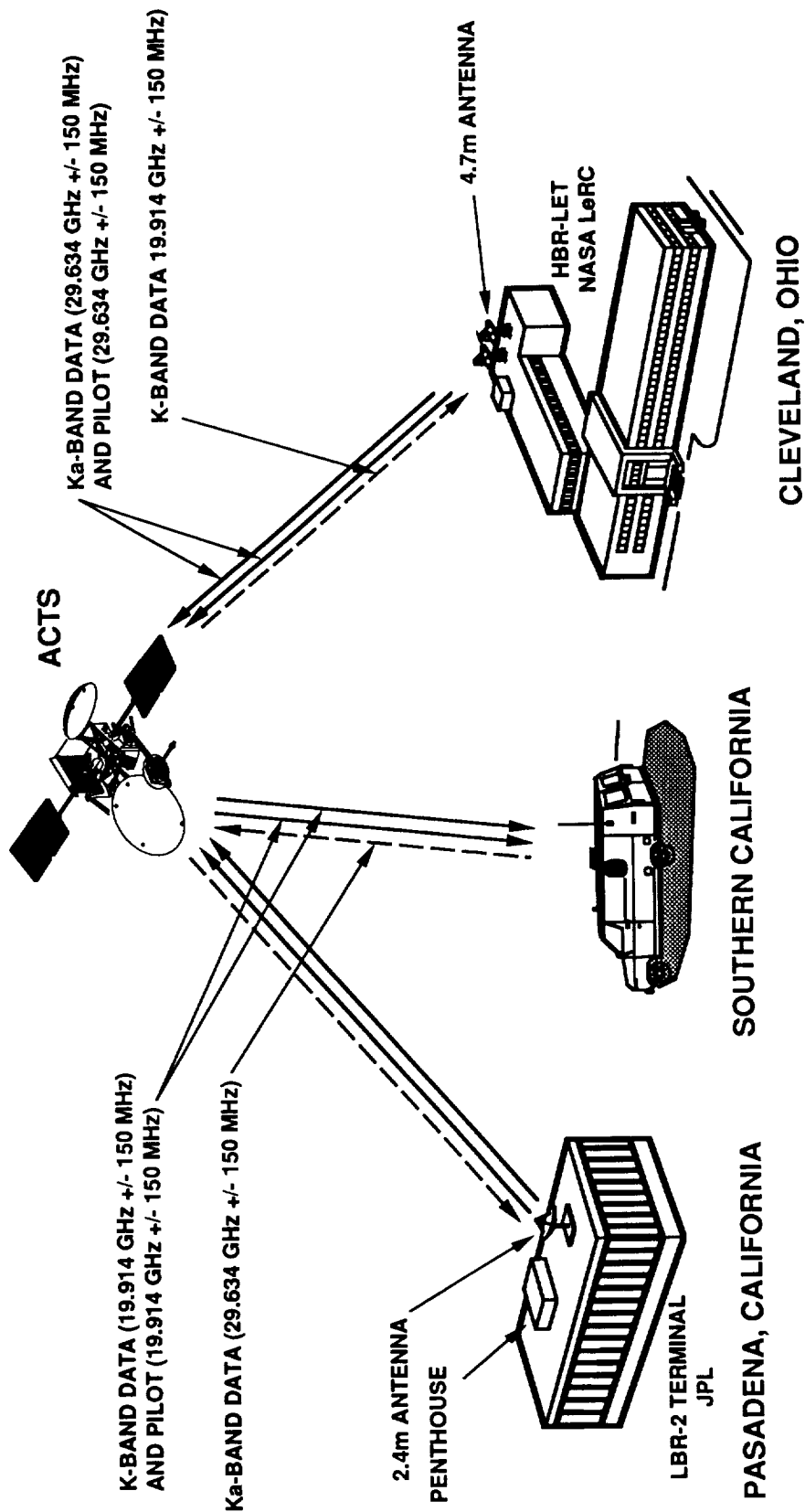
---

<sup>2</sup> For the AMT, and mobile Ka-band terminals in general, user antenna gains of at least 20 dB are required. Multi-path scattering from the surrounding environment is therefore very limited. Scatterers would typically be objects that are at least partially in the field of view of the antenna.



[6] Manning, R. M., "A Unified Statistical Rain Attenuation Model for Communication Link Fade Predictions and Optimal Stochastic Fade Control Design Using a Location Dependent Rain Statistics Data Base," International Journal of Satellite Communications, Vol. 8, pp. 11-30, 1990.

[7] Manning, R. M., "Rain Compensation for Mobile and Personal Satellite Communication Systems -- Application of the ACTS Rain Fade Algorithm," submitted to the Journal on Selected Areas in Communications.



ACTS GENERATED BEACONS AT 20.185, 20.195, AND 27.505 GHz ARE NOT SHOWN.

FIGURE 1. AMT Experiment Setup With ACTS

Table 1. AMT Link Budgets for Propagation-Related Experiments

FORWARD (LeRC-TO-ACTS-TO-AMT) 9.6 KBPS VOICE AND PILOT IN CLEAR WEATHER DBPSK, CODED R=1/2, K=7, BER=1E-3 AMT AT L.A., EL=46, SUPPLIER AT CLEVELAND			RETURN (AMT-TO-ACTS-TO-LeRC) 9.6 KBPS VOICE, CLEAR WEATHER DBPSK, CODED R=1/2, K=7, BER=1E-3 SUPPLIER AT CLEVELAND, AMT AT L.A., EL=46	
UPLINK: LeRC SUPPLIER-TO-ACTS			UPLINK: AMT-TO-ACTS	
	<i>DATA</i>	<i>PILOT</i>		<i>DATA</i>
<b>TRANSMITTER PARAMETERS</b>				
EIRP, DBW	65.00	65.00	EIRP, DBW	22.00
POINTING LOSS, DB	-0.39	-0.39	POINTING LOSS, DB	-0.50
<b>PATH PARAMETERS</b>				
SPACE LOSS, DB	-213.48	-213.48	RADOME LOSS, DB	-0.40
(FREQ., GHZ/MHZ	29.63	29.63	<b>PATH PARAMETERS</b>	
RANGE, KM)	38000.00	38000.00	SPACE LOSS, DB	-213.34
ATMOSPHERIC ATTN, DB	-0.92	-0.92	(FREQ., GHZ/MHZ	29.63
<b>RECEIVER PARAMETERS</b>				
POLARIZATION LOSS, DB	-0.50	-0.50	RANGE, KM)	37408.00
G/T, DB/K	19.60	19.60	ATMOSPHERIC ATTN, DB	-0.61
POINTING LOSS, DB	0.00	0.00	<b>RECEIVER PARAMETERS</b>	
BANDWIDTH, MHZ	900.00	900.00	POLARIZATION LOSS, DB	-0.50
RECV'D C/NO, DB.HZ	97.91	97.91	G/T, DB/K	17.30
TRANSPONDER SNR IN, DB	8.37	8.37	POINTING LOSS, DB	0.00
EFF. LIM. SUPPRESSION, DB *	-3.80	-3.80	BANDWIDTH, MHZ	900.00
HARD LIM. EFF. SNR OUT, DB	4.57	4.57	RECV'D C/NO, DB.HZ	52.55
			TRANSPONDER SNR IN, DB	-37.00
			LIM. SUP'RSS FACT. GAMMA **	0.79
DOWNLINK ACTS-TO-AMT			DOWNLINK ACTS-TO-SUPPLIER (CLEVELAND)	
<b>TRANSMITTER PARAMETERS</b>				
EIRP, DBW	56.22	56.22	EIRP, DBW	29.45
POINTING LOSS, DB	0.00	0.00	POINTING LOSS, DB	0.00
<b>PATH PARAMETERS</b>				
SPACE LOSS, DB	-209.89	-209.89	SPACE LOSS, DB	-210.03
(FREQ., GHZ/MHZ	19.91	19.91	(FREQ., GHZ/MHZ	19.91
RANGE, KM)	37408.00	37408.00	RANGE, KM)	38000.00
ATMOSPHERIC ATTN, DB	-0.61	-0.61	ATMOSPHERIC ATTN, DB	-0.92
<b>RECEIVER PARAMETERS</b>				
POLARIZATION LOSS, DB	-0.50	-0.50	<b>RECEIVER PARAMETERS</b>	
RADOME LOSS, DB	-0.20	-0.20	POLARIZATION LOSS, DB	-0.50
ANT. DIRECTIVITY (MIN.), DBI	23.50	23.50	ANT. DIRECTIVITY (MIN.), DBI	
SYS. TEMP (REF TO ARRAY), K	1400.00	1400.00	SYS. TEMP (REF TO ARRAY), K	
G/T, DB/K	-7.96	-7.96	G/T, DB/K	27.30
POINTING LOSS, DB	-0.50	-0.50	POINTING LOSS, DB	-0.50
DOWNLINK C/NO, DB.HZ	65.15	65.15	DOWNLINK C/NO, DB.HZ	73.90
OVERALL C/NO, DB.HZ	65.15	65.15	OVERALL C/NO, DB.HZ	51.47
REQ'D EB/NO (AWGN--SIM.), DB	5.75		REQ'D EB/NO (AWGN--SIM.), DB	5.75
MODEM IMPLEMENT. LOSS, DB	0.75		MODEM IMPLEMENT. LOSS, DB	0.75
REQUIRED EB/NO (TOTAL), DB	6.50		REQUIRED EB/NO (TOTAL), DB	6.50
FADE ALLOWANCE (OVERALL), DB	2.50		FADE ALLOWANCE (OVERALL), DB	2.50
DATA RATE, BPS	9600.00		DATA RATE, BPS	9600.00
REQ'D EFFECTIVE C/NO, DB.HZ	48.82	50.00	REQ'D EFFECTIVE C/NO, DB.HZ	48.82
PERFORMANCE MARGIN, DB	16.33	15.15	PERFORMANCE MARGIN, DB	2.65
* CASE OF TWO EQUALLY STRONG SIGNALS IN NOISE			** CASE OF ONE SIGNAL IN NOISE	

Table 2. Top-Level Summary of AMT Propagation-Related Experiments

TEST CONFIGURATION/CONDITIONS	TO MEASURE
<p><b>I. CLEAR SKY TESTS</b></p> <p>1. PILOT SIGNAL STRENGTH</p> <p>2. PILOT + FORWARD DIRECTION DATA</p> <p>3. PILOT + RETURN DIRECTION DATA</p> <p>4. PILOT + VOICE</p>	<p>A. SHADOWING CHARACTERISTICS            - ATTENUATION STATISTICS            - DURATION STATISTICS            - SIGNAL STRUCTURE FOR SPECIFIC LIGHT SHADOWING CASES</p> <p>B. ANTENNA SUBSYSTEM PERFORMANCE</p> <p>A. PILOT AND DOPPLER TRACKING (IN AMT IF)</p> <p>B. MODEM PERFORMANCE (BER, SYNC, ETC.)            - RESIDUAL DOPPLER TRACKING            - FREEWHEELING THROUGH SHADOWING</p> <p>A. TWO-WAY DOPPLER CORRECTION (IN AMT IF)            - L.O.S. AND SHADOWING CONDITIONS</p> <p>B. MODEM PERFORMANCE (SIMILAR TO ABOVE)</p> <p>A. SPEECH CODEC PERFORMANCE            - L.O.S. AND SHADOWING CONDITIONS</p>
<p><b>II. RAIN (ON ONE LINK) TESTS</b></p> <p>1. PILOT SIGNAL STRENGTH            - CLEAR IN CLEVELAND</p> <p>- CLEAR IN L.A.-UPLINK POWER CONTROL OFF AT LeRC</p> <p>2. PILOT + RETURN DIRECTION DATA            - SAME AS PRECEDING</p> <p>- POWER CONTROL ON AT LeRC</p> <p>3. PILOT + FORWARD DIRECTION DATA</p> <p>4. PILOT + VOICE</p>	<p>A. L.A. TEMPORAL RAIN CHARACTERISTICS            - ATTENUATIONS AND DURATIONS AT 20 GHZ            - ATTENUATION SLOPES AT 20 GHZ</p> <p>B. CLEVELAND TEMPORAL RAIN CHARACTERISTICS            - ATTENUATIONS AND DURATIONS AT 30 GHZ            - ATTENUATION SLOPES AT 30 GHZ</p> <p>A. CORRELATION OF 20 AND 30 GHZ SIGNALS</p> <p>B. OPERATION OF AMT COMM. PROTOCOL AND RCA</p> <p>A. OPERATION OF AMT COMM. PROTOCOL AND RCA</p> <p>A. FULL TESTING OF RCA &amp; COMM. PROTOCOL WITH VOICE DATA RATE CHANGE ON THE FLY</p> <p>B. FULL SUBSYSTEM PERFORMANCE TESTING (MODEM, CODEC, IF PILOT TRACKING, AND TERMINAL CONTROLLER)            - L.O.S. AND SHADOWING CONDITIONS</p>

**NAPEX XV**

**Session 2**

**TOPICS IN PROPAGATION  
STUDIES AND MEASUREMENTS**

Chairman:

John Kiebler  
NASA Consultant



# WHAT IS HAPPENING AT CCIR STUDY GROUP 5?

David V. Rogers

Communications Research Centre  
Department of Communications, Ottawa, Canada

ABSTRACT--At the Plenary Meeting of the International Radio Consultative Committee (CCIR) in 1990, significant changes in the organization were adopted. These changes will affect working methods and consequently impact to some degree the technical aspects of the CCIR. Changes specific to CCIR Study Group 5 (Propagation in Non-Ionized Media) are summarized.

## 1. INTRODUCTION

At the XVIIth Plenary Meeting of the CCIR in Düsseldorf in May-June 1990, new working procedures were adopted (CCIR, 1990). The new format, forged somewhat in response to criticism of CCIR reliance on Reports (instead of Recommendations) and the time required to develop Recommendations, is still evolving as part of a general restructuring of the ITU. The CCIR itself has restructured into 10 Study Groups (e.g., Barclay, 1990); the main changes are the merging of Study Group (SG) 3 into SG 9 and SG 2 into SG 7, and creation of a new SG 12 on Interservice Sharing and Compatibility. SG 5 is now defining its own work areas and nature of its documentation. Changes in SG 5 technical information and its dissemination will be of concern to many users of CCIR Recommendations and Reports.

## 2. CCIR STUDY GROUP 5

### 2.1 Organization

Each SG receives study Questions from the CCIR Plenary Assembly, which the SG then assigns either to a Working Party (somewhat permanent bodies that address long-range concerns) or a Task Group (for short-term, single-topic tasks). The work of SG 5 is now divided among 3 Working Parties: WP 5A (Radiometeorology) replaces Interim Working Party (IWP) 5/3; WP 5B (Terrestrial broadcast and mobile, and mobile-satellite) assumes elements of IWP 5/1 *plus the mobile-satellite area*; and WP 5C (Fixed, fixed-satellite and broadcast-satellite) replaces IWP 5/2, *and mobile-satellite*. WPs 5A, 5B, and 5C are respectively chaired by Gert Brussaard (The Netherlands), John Cavanagh (USA), and Martin Hall (UK). At present there are no SG 5 Task Groups.

Previously, during each 4-year CCIR cycle SG 5 held Interim and Final Meetings lasting 2-3 weeks. Numerous technical input documents were discussed and acted on, and the Interim ("MOD I") and Final ("MOD F") versions of the documents were agreed.

In the new structure, essentially final versions of documents will be decided within the WP responsible for a given topic. The Interim and Final Meetings will now be brief (a few days), held mainly to either approve or reject the proposals submitted by WPs; set the SG's program of work for the next 2 years; and draft proposed new Questions or Recommendations for the CCIR Plenary. The SG is also *empowered to approve new Recommendations* provided they have been selected by the CCIR for the accelerated-approval procedure. Participation in WP deliberations appears essential to influence the technical content of CCIR Volume 5, since little if any drafting will be possible at the Interim and Final Meetings.

## 2.2 Organization of SG 5 Technical Information

In the past the main technical content of Vol. 5 was embodied in Reports that contained engineering advice, prediction methods, assorted measured data, and even provisional advice (perhaps "to be used with caution"). Prior to the 1990 CCIR Plenary Meeting, the CCIR's reliance on Reports (instead of Recommendations) was criticized as was also the length of time required for the CCIR to approve its Recommendations. Furthermore, the CCIR itself had recognized that providing advice that had "to be used with caution" was not likely to be useful to systems designers.

Therefore SG 5 has recently emphasized Recommendations as the primary source of information for users of its propagation information, and is in the process of transferring much of the information now in Reports to corresponding Recommendations. Data in Recommendations must be sufficiently well-developed to justify confidence in its application to systems design. Less-developed or provisional material will not transfer to the corresponding Recommendation. Reports will persist as a repository for support or developing information, mainly for internal use by the SG, and will not be formally published (but will appear in the Interim booklets). Conversely, new or revised Recommendations will be disseminated as soon as they are approved. A loose-leaf format might perhaps be selected for easy incorporation of modifications.

At a joint meeting of WPs 5A and 5C in Rio in December 1990, guidelines were adopted to promote transfer of much of the existing material in SG 5 Reports to Recommendations. Some of the ground rules that were adopted by WPs 5A and 5C for creating SG 5 Recommendations from existing Reports may be of interest, and are summarized here:

- a. Recommendations should be brief, and recommend the use of the prediction methods, engineering advice, etc. in the Annex.
- b. Support or provisional information or advice is to be in a supporting Report.
- c. Texts are to be clear and unambiguous.



- d. Repetition among Recommendations is to be minimal to avoid inconsistencies resulting from revisions.
- e. Cross-references (to equations, etc.) are to be stated in both the Source and Quoting Recommendation.
- f. Literature references are to be avoided in Recommendations unless they are a prime source (e.g., for a table or map); support information should be in the supporting Report.
- g. Basic radio meteorology is to appear in the texts of WP 5A.
- h. Basic radio engineering and service-oriented predictions, including geometry and specific algorithms in texts of WP 5C.
- i. Explanatory notes that are not part of the Recommendation may be labelled and inserted in the text where required.

### 3. RECENT TECHNICAL ACTIVITIES

IWP 5/2, now WP 5C (Chaired by Martin Hall) and IWP 5/3, now WP 5A (then Chaired by R.K. Crane, USA) convened a joint meeting in Rio de Janeiro, Brazil, during 10-14 December 1990, mainly to address the problem of rain attenuation prediction. The impact of new tropical propagation data on the CCIR rain attenuation method is a major WP 5C assignment for the current study period (the other is interference prediction and determination of coordination distance, discussed below). The meeting immediately followed an URSI Commission F Special Open Symposium in Rio on "Regional Factors in Predicting Radiowave Attenuation due to Rain," with an emphasis on predicting rain attenuation in tropical regions of the world (J. Allnutt et al., 1991).

New data available at the Rio meeting were insufficient to generate proposals for modification to the current method for predicting rain attenuation, but 4 critical areas were identified for study:

- use of the 0.1% rain rate for prediction of attenuation in tropical regions, where the 0.01% rain rate can be extreme and difficult to measure (approach may also be beneficial for low-margin satellite communication systems);
- possible application of a vertical reduction factor to increase climate sensitivity of the existing method;
- study of the nonmonotonic behavior of path attenuation vs rain rate exhibited at high rain rates on terrestrial paths by the current prediction method;
- comparison of the slope of measured attenuation distributions with the CCIR slope (which is constant for all cases).

Based on the current availability of relevant data, the main focus in the coming period will be on the first two areas above.

WP 5C held another meeting in Abingdon, UK, during 7-14 March 1991 to focus on the problem of interference prediction and the determination of coordination distance. This meeting followed an international symposium on "Influence of the Atmosphere on Interference Between Radio Communication Systems at Frequencies Above 1 GHz," held at Leeds Castle on 5-6 March 1991, to provide the final results of the COST Project 210 (Hall, 1991).

For Report 724 ("Propagation data required for the evaluation of coordination distance in the frequency range 1-40 GHz"), WP 5C proposed that the existing procedure for calculating the Mode 1 (great-circle propagation) contours be extended up to a time percentage of 20% from the current 1%, and that the graphical methods for prediction be deleted from the Report. For Report 569 ("The evaluation of propagation factors in interference problems between stations on the surface of the Earth at frequencies above about 0.5 GHz"), which is to be converted to a Recommendation, the following proposals were offered:

- introduce the COST-210 method for duct propagation (after extension worldwide using Bean-Dutton refractivity gradient statistics), provided testing of the method is successful;
- possibly introduce COST-210 method for diffraction after testing;
- introduce the CCIR method for rain scatter interference as modified by COST-210;

The background for the new methods proposed for incorporation into the Recommendation and the background for the old methods of Report 724 is to be included in a draft Report.

The results had significant impact on CCIR Task Group 12/3 (Appendix 28) that met in Geneva during 13-22 May 1991. T. Hewitt of the UK, coordinator of the WP 5C project group on interference, chaired the Working Group on propagation at the TG 12/3 meeting.

#### 4. TECHNICAL ISSUES FOR THE FUTURE

The near-term commitments of SG 5 concern mainly the meetings of WPs 5A, 5B and 5C that will be held in Geneva in December 1991, and the SG 5 Interim Meeting scheduled for 20-22 May 1992 in Geneva. Additional requirements are associated with the second meeting of Task Group 12/3 on possible revisions to Appendix 28 of the ITU Radio Regulations in mid-January 1992, and some input to preparations for WARC-92 (Frequency Allocations in Certain Parts of the Spectrum) that will commence in Spain in February 1992.

As to technical issues that CCIR SG 5 must address in support of the above meetings and its own program of work, the following are likely examples. In WP 5A (Radiometeorology), transfer of data on gaseous absorption and atmospheric refractive effects will be necessary. There will continue to be critical studies of the horizontal and vertical structure of rainfall, with emphasis on features in tropical climates that affect prediction methods. With continuing evolution of small-margin satellite communication systems, data will be required on propagation mechanisms for percentages of time greater than, say, 1% of the year, including clear-air effects and rain rate statistics.

WP 5B will address the areas of propagation over the Earth's surface, including the electrical characteristics; diffraction; and propagation over irregular terrain, with a particular emphasis on the application of digital terrain databases. With its new responsibilities in the increasingly important area of mobile-satellite systems, a program to attack related technical issues will be needed. As mobile-satellite systems will now be removed somewhat from deliberations on the other slant-path topics, a mechanism for coordination between WPs 5B and 5C to ensure that technical data are exchanged will be required.

In WP 5C, a traditional domain of user Recommendations and Reports, as indicated above attention must be concentrated in the near future on regional (mainly tropical) aspects of rain attenuation prediction, and prediction of intersystem interference and evaluation of coordination distance. Continuing developments in small-margin communication systems will stimulate interest in propagation impairments for higher time percentages and dynamic features of propagation events (especially for application to adaptive impairment mitigation techniques). For the fixed services, work will continue on propagation distortion, diversity, a variety of clear-air effects, and fading distributions.

#### REFERENCES

1. CCIR Administrative Circular A.C./306, 17 August 1990; Corr. 1, 23 August 1990; Corr. 2, 8 November 1990.
2. L.W. Barclay, "The Working of the CCIR," *Electronics and Communication Engineering Journal*, Vol. 2, No. 6, pp. 244-249, December 1990.
3. J.E. Allnutt et al., "Report on Workshops: Regional Factors in Predicting Radiowave Attenuation Due to Rain," *IEEE Antennas and Propagation Magazine*, Vol. 33, No. 2, pp. 17-21, April 1991.
4. COST Project 210, "Influence of the Atmosphere on Interference Between Radio Communication Systems at Frequencies Above 1 GHz," Commission of the European Communities, Publication EUR 1347 EN, Luxembourg, 1990.

## Propagation Research in Japan

By Hiromitsu Wakana

Communications Research Laboratory, MPT  
893-1 Hirai, Kashima, Ibaraki 314 Japan

**Abstract** L-band propagation measurements for land-mobile, maritime and aeronautical satellite communications have been carried out by using the Japanese Engineering Test Satellite-Five (ETS-V) which was launched in August 1987. This paper presents propagation characteristics in each mobile satellite communications channel.

### 1. Introduction

In the Communications Research Laboratory, propagation research has been carried out for many years by using various satellite beacons at many different frequencies. Since the launch of the ETS-V satellite, L-band propagation measurements are mainly being carried out for future mobile-satellite communications systems. This paper presents experimental results of propagation characteristics for vehicles, trains, airplanes and vessels.

Propagation effects between a geostationary satellite and mobile earth stations are: (1) blockage and shadowing (2) multipath scattering and reflections (3) ionospheric scintillation or Faraday rotation, and (4) Doppler frequency shifts.

In land-mobile satellite channel, multipath fading, shadowing and blockage from roadside trees, utility poles, buildings and terrains are typical problems. Maritime satellite channel has multipath fading caused by reflections from the sea surface at low elevation angles. In aeronautical satellite channel, multipath fading is caused by reflection from the sea surface and from airplanes' wings. It is shown that ionospheric scintillation is still of significance at frequencies above 1GHz and can impair mobile satellite communications channels.

### 2. Land-mobile satellite communications channel

#### 2.1 Propagation characteristics for motor cars

L-band left-hand circularly polarized CW transmitted from the ETS-V satellite was received at a propagation measurement van with various antennas. Elevation angles of measurements along urban, suburban and rural roads and freeways are about 46 to 47 degrees.

Figure 1 shows a cumulative distribution of a receiving signal power with respect to the line-of-sight level, measured by a mechanically stirred four-element spiral array antenna (12dBi). Data were sampled with equidistance sampling pulses of a period of 3.14cm. Therefore, the results are independent of the vehicle speed.

Data in Tokyo urban areas show the fades of more than 5dB at the 33% probability level, which are mostly caused by blockage by ten-storied buildings and shadowing due to roadside

trees and utility poles. At a suburban area, it is found that for 13% of the distance the fade exceeds 5dB due to trees, utility poles and houses. On the other hand, the fade exceeds 5dB at only 3% probability along freeways. Main obstacles are overpasses and trees.

Figure 2 shows probability density functions of the received signal. It shows that the fade statistics can be divided into two parts. One is statistically described by a Rician distribution around the line-of-sight level. In mobile satellite channels, when both a dominant line-of-sight signal and scattered signal are received, the composite signal has a Rician distribution. The other is characterized by the fades larger than about 6 to 8dB, which are caused by blockage and shadowing. These data show that an effective fading margin is about 5dB for land-mobile satellite channels, although this value may depend on gains or patterns of the vehicle's antennas.

Based on a given threshold of a signal level, it can be determined whether a propagation channel is on a fade state (below the threshold) or on a non-fade state (above the threshold). Figures 3 and 4 show cumulative distributions of fade and non-fade durations, respectively. In Tokyo urban areas, the fade state continues over 10 meters at the 8% probability for all the fade-duration distributions. Such long fades are caused by blockage from buildings. Cumulative distributions of fade duration in suburban areas and freeways show moderate vegetative shadowing and can be presented by a lognormal fit (Vogel et al., 1989; Hase et al., 1991).

Except data in freeways, cumulative distributions of non-fade durations can be also approximated with the cumulative distribution of the lognormal distribution, which differs from that measured in Australia by Vogel et al. (1989).

Figure 5 shows a receiving noise measured in urban areas with omni-directional, mechanically stirred and phased array antennas. Impulsive noise, most of which may be generated by ignition of motorcars or motorcycles, has been observed, except for the phased array antenna. It shows that this effect depends on radiation patterns of mobile antennas. As a result of measuring bit error rates with 4.8kbps BPSK, it is found that this impulsive noise causes bit errors. In urban areas, impulsive noise is one of the effects which impair mobile communication channels.

## **2.2 Propagation characteristics for trains**

A new satellite-based train control system is going to be introduced. In train-satellite communications channels, blockage and shadowing due to power poles, overpasses and noise generated from pantographs and motors impair communications quality. Figure 6 shows measured C/No ( carrier-to-noise-power-density ratio ) with an omni-directional antenna installed away from pantographs. Blockage due to trolley beams occurred periodically but impulsive noise was not observed. Except for blockage due to bridge's structures, overpasses and tunnels, durations of most fades are very short. The cumulative distribution shows the fades of more than 5dB at the 5% probability level.

## **3. Aeronautical satellite communications channel**

In the CRL's experiment, the aircraft earth station was installed on a B-747F freighter of Japan Air Lines. A phased-array antenna of G/T of about 13dB/K was installed on the top of the fuselage. In-flight experiments were started in November 1987 and were conducted 24 times until March 1989, mainly on flight routes between Narita and Anchorage (Ohmori, 1990).

Most data show constant  $C/N_0$  and no fading except the period when the direction of the ETS-V satellite coincides with that of the main wings. Figure 7 shows standard deviations of signal levels versus antenna-beam directions and Figure 8 shows antenna-beam directions during flights between Narita and Anchorage and between Narita and Singapore. These figures show that signal level fluctuations occur only when antenna-beam directions coincide with that of the main wings and are caused by reflections from the main wings, vibrations of the wings and rolling of the airplane. Except at very low elevation angles below  $0^\circ$ , fading caused by reflections from the sea surface has never been detected. The reason is that waves reflected from the sea surface are blocked out by the fuselage and wings.

Yasunaga et al. (1989) have carried out propagation measurements using a helicopter with several antennas installed at both sides of the fuselage. Figure 9 shows statistics of multipath fading caused by sea reflections as a function of elevation angles. At an altitude of 10km and  $5^\circ$  elevation angle, the 99% fading level is less than that in the maritime satellite channel only by 2dB.

#### 4. Maritime satellite communications channel

Multipath fading characteristics in maritime satellite communications channels have been studied by many authors and a lot of the literature has been published (Sandrin and Fang, 1986). Here, we present a brief introduction of our ETS-V's experiments. The ship earth station employs an improved short-backfire antenna of 40 cm in diameter (antenna gain of 15dBi) and has a two-axis mount (AZ/EL) with a program tracking function slaved to the ship-borne navigation system. It can compensate ship motions and keep the antenna pointing toward a satellite with a motion detector installed at the center of gravity of the ship. The CRL has developed a multipath fading reduction technique by using reflected cross-polarized components (Ohmori and Miura, 1983).

Figure 10 shows cumulative distributions of the received signal at several elevation angles. These data are found to be a good fit to the Rician distribution with a Rice factor, which is the direct-power-to-multipath-power ratio, of 5-9 dB, 6-12 dB and 15 dB at  $3^\circ$ ,  $6^\circ$  and  $10^\circ$  elevation angles, respectively.

The generalized model for fading statistics proposed by Sandrin (1986) is described for antennas with gains ranging from 0 to 16 dBi as follows:

$$K = El + 4 \quad \text{for } 2^\circ < El < 4^\circ,$$

where  $K$  is the Rice factor in decibels and  $El$  is an elevation angle in degrees. Therefore, as shown in Fig. 10, our measured data can be fit into this relationship at elevation angles less than 10 degrees.

Figure 11 shows a cumulative distribution of the  $C/N_0$  with respect to the medium of the  $C/N_0$  measured without the fading reduction technique. The fading depth is improved from 10.9 dB to 1.4 dB by the fading reduction technique. Both cumulative statistics without and with the fading reduction follow the Rician distribution with Rice factors of 6 dB and 20 dB, respectively. An increase of the Rice factor indicates reduction of reflected co-polarized components. This technique has a definite advantage at elevation angles lower than  $6^\circ$ .

## 5. Ionospheric scintillation

Figure 12 shows ionospheric scintillation measured on 30 November 1988 (Wakana and Ohmori, 1991). Both enhancement and negative fades with respect to the line-of-sight level were observed. The maximums of enhancement and fades are 6dB and -34dB, respectively. Mobile-satellite communication systems have only a small link-margin of about 4dB. Therefore, the fade due to ionospheric scintillation provides serious impairment in mobile-satellite communication channels.

Figure 13 shows observed places, frequencies and periods when the scintillation occurred. The data were measured by using signals transmitted from several satellites at different frequencies. Numbers above the periods show peak-to-peak variations of the signal level in decibels. As shown in this figure, ionospheric scintillation started simultaneously from low to middle latitudes at different frequencies, except at the Kashima earth station. The scintillation was observed even at the frequencies of 20GHz: this frequency is the highest frequency of ionospheric scintillation observed in Japan until now.

Since the ETS-V satellite is not always transmitting a beacon, we cannot monitor the propagation condition continuously. However, we have observed scintillation of about 2dB once every several months. From a satellite communication point of view, service availability which is the fraction of time that satisfactory satellite service is obtained on demand, is very important for users. Typically, systems in the fixed-satellite services are expected to achieve availability of 99.9% or better. Therefore, large attenuations produced by rare events of ionospheric scintillation can be ignored for the mobile satellite system design.

## 6. Conclusions

Mobile satellite communications experiments using the ETS-V satellite have provided fruitful experimental data about communication qualities and propagation characteristics. This paper presents the results of propagation measurements for land-mobile, aeronautical and maritime satellite communications.

In land-mobile satellite channels, blockage and shadowing by trees, buildings and terrains are a serious impairment rather than multipath fading, and a large link margin to combat blockage and shadowing is ineffective for providing acceptable services. Other aspects such as fade rate, fade and non-fade duration, delay spread and impulsive noise are important for the error correction scheme, data rate and data format.

In aeronautical satellite channels, propagation conditions are superior to those of land-mobile and maritime satellite channels because of no obstacles in link between a satellite and mobile stations. It was found that multipath fading due to sea-surface reflections can be ignored when the antenna is installed on the top of the fuselage, while a small amount of fading occurred due to reflections from main wings.

For maritime satellite channels, multipath fading statistics due to reflections from the sea surface are presented. Fading statistics can be modeled by the Rician model for most of the time. Furthermore, a technique to combat multipath fading which is applicable to commercial maritime communications links is presented.

Ionospheric effects are very important for radio communications systems operated at the frequencies below 1GHz. It was shown that this effect is still of significance at frequencies above

1GHz and can impair mobile satellite channel. However, from service availability point of view, large attenuation produced by rare events can be ignored for the mobile satellite system design.

## References

- Hase, Y., Vogel, W. J. and Goldhirsh, J., "Fade Duration derived from Land-Mobile-Satellite Measurements in Australia," IEEE Trans. Commun. (forthcoming).
- Ohmori, S. and Miura, S., "A Fading Reduction Method for Maritime Satellite Communications," IEEE Trans. Antennas Propagat., vol. AP-31, No.1, pp. 184-187, Jan. 1983.
- Ohmori, S., Hase, Y. and Wakana, H., "The World's First Experiments on Aeronautical Satellite Communications using the ETS-V Satellite," Denshi Tokyo, No. 29, pp.113-116, 1990.
- Sandrin, W.A. and Fang, D.J., "Multipath Fading Characterization of L-band Maritime Mobile Satellite Links," Comsat Tech. Rev., Vol.16, No.2, pp.319-338, Fall 1986.
- Yasunaga, M., Karasawa, Y., Matsudo, T. and Shiokawa, T., "Characteristics of Multipath Fading due to Sea Surface Reflection in Aeronautical Satellite Communications," Trans. IEICE, B-II, Vol. J72-B-II No. 7, pp.297-303, July 1989. ( in Japanese )
- Vogel, W. J., Goldhirsh, J. and Hase, Y., "Land-mobile-satellite propagation measurements in Australia using ETS-V and INMARSAT-Pacific," Johns Hopkins University, Applied Physics Laboratory Tech. Rep. S1R89U-037, August 1989.
- Wakana, H., Ikegami, T., Kawamata, F., Ide, T. and Matsumoto, Y., "Experiments on Maritime Satellite Communications using the ETS-V Satellite," J. Commun. Res. Lab. ( to be published ).
- Wakana, H. and Ohmori, S., "Signal Variation due to Ionospheric Scintillation on L-band Mobile Satellite Channels," Electronics Letters (submitted).

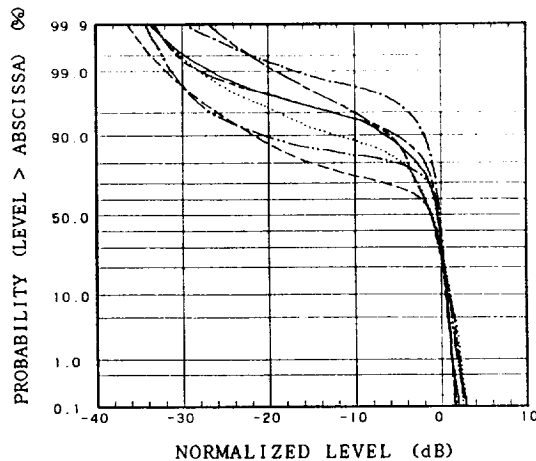


Figure 1 Cumulative distribution of receiving signal powers with respect to the line-of-sight level, measured by a mechanically stirred antenna of 12 dBi.

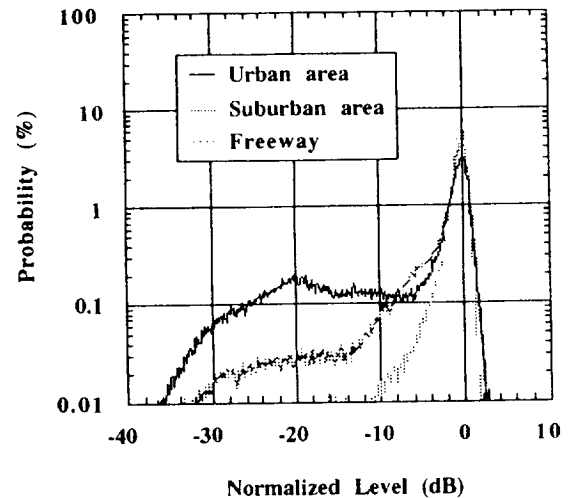


Figure 2 Probability density of receiving signal powers with respect to the line-of-sight level, measured by a mechanically stirred antenna of 12 dBi.

- Higashi-kantou (expressway, Ibaraki)
- Ohno village (rural area, Ibaraki)
- Tachikawa city (suburban area, Tokyo)
- Mito city (urban and suburban area, Ibaraki)
- Kyoto city (urban and suburban area, Kyoto)
- Chiba city (urban area, Chiba)
- Oumckaidou-Yasukunidohri (urban area, Tokyo)



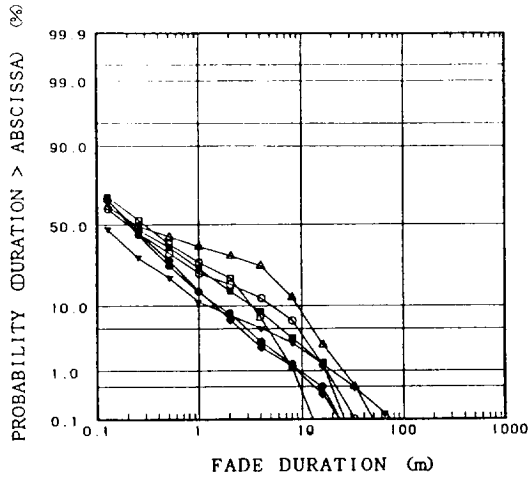


Figure 3 Cumulative distribution of fade duration: threshold level=-4dB.

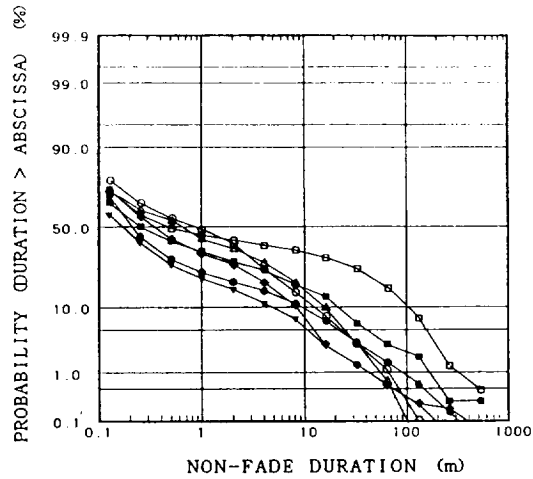


Figure 4 Cumulative distribution of non-fade duration: threshold level=-4dB.

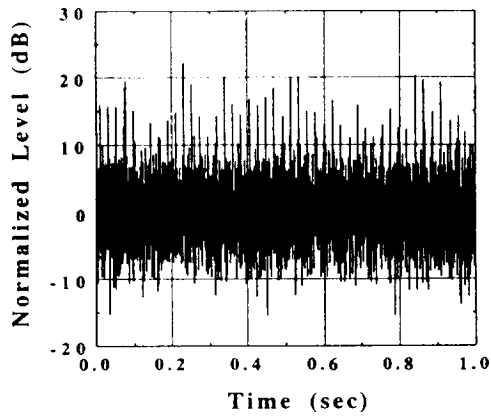


Figure 5 Receiving noise measured by an omni-directional antenna.

- △ Oumekaidou-Yasukunido (urban area, Tokyo)
- Chiba city (urban area, Chiba)
- ▼ Kyoto city (urban and suburban area, Kyoto)
- Mito city (urban and suburban area, Ibaraki)
- ◆ Tachikawa city (suburban area, Tokyo)
- Ohno village (rural area, Ibaraki)
- Higashi-kantou (expressway, Ibaraki)

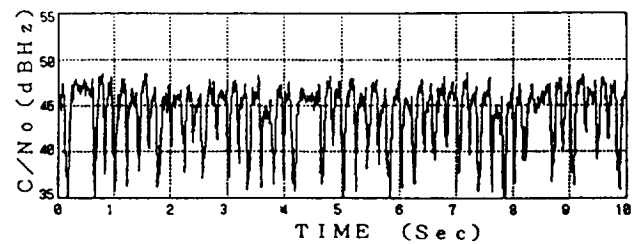
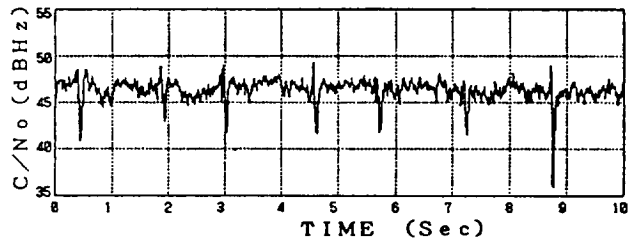


Figure 6 C/No measured on a train with an omni-directional antenna.

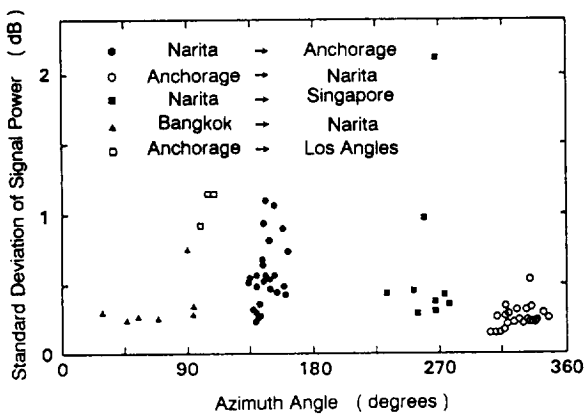


Figure 7 Standard deviation of signal level versus azimuth angle.

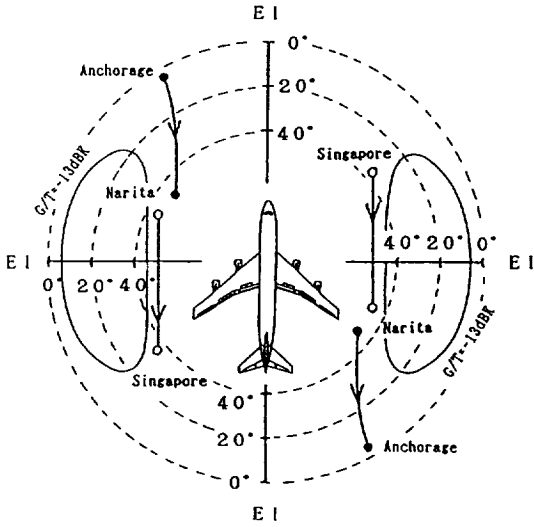


Figure 8 Antenna-beam direction during flight.

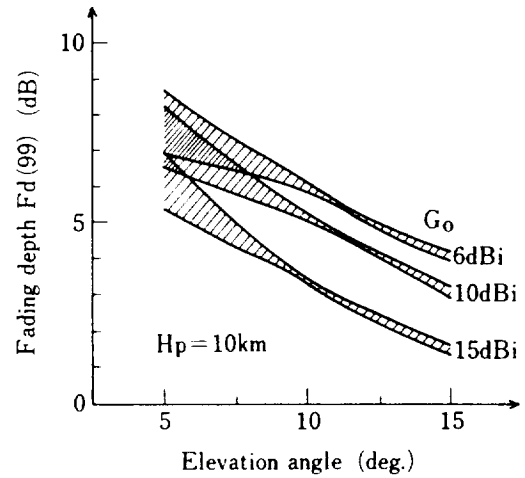


Figure 9 Fading depth versus elevation angle under rough sea condition

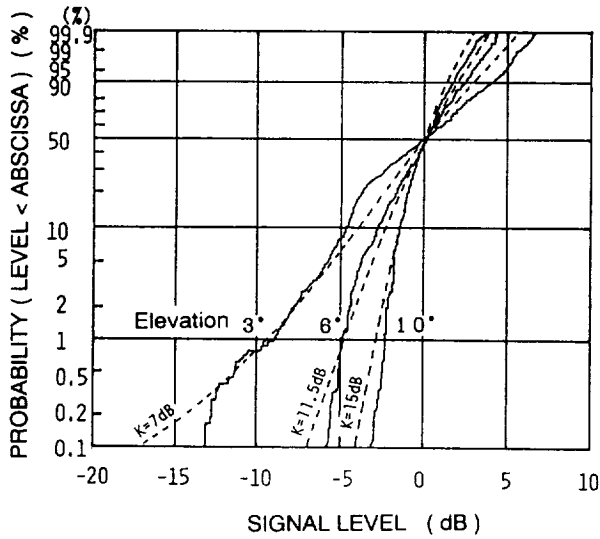


Figure 10 Cumulative distributions of receiving signal power with respect to the medium value. Dashed lines are the Rician distribution with several Rice factors (referred to as K).

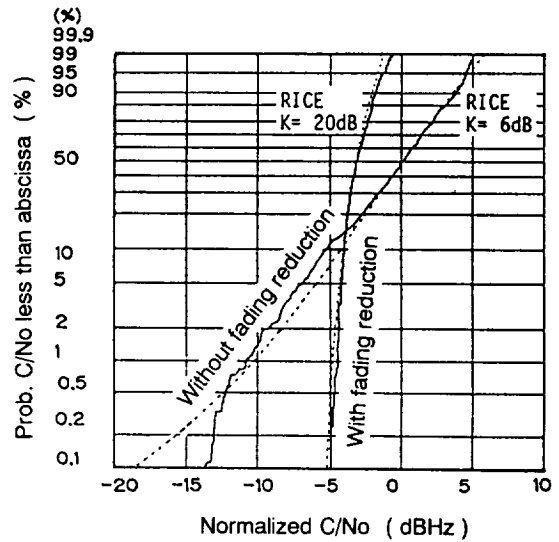


Figure 11 Cumulative distribution of C/No. Dashed lines are the Rician distribution with Rice factors K of 20 dB and 6 dB.

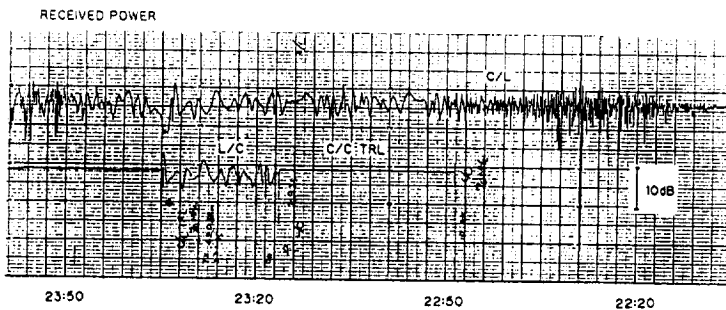


Figure 12 Ionospheric scintillation measured on 30 November 1988.

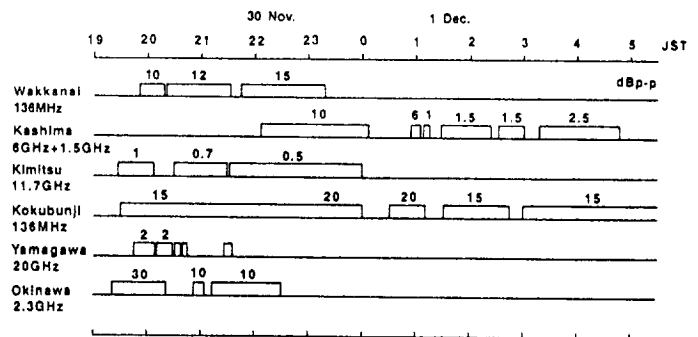


Figure 13 Ionospheric scintillation on 30 Nov., 1988. This figure shows observed places, frequencies and periods when the scintillation occurred.

# A Comparison of Cloud Attenuation Models Using Measured Cloud Data

G.C. Gerace  
E.K. Smith  
E.R. Westwater

Dept. of Electrical and Computer  
Engineering  
Campus Box 425  
University of Colorado  
Boulder CO 80309-04325  
(303) 492-7123 (Smith, Gerace)

Wave Propagation Laboratory  
National Oceanic and Atmospheric  
Administration, Boulder CO 80302  
(303) 497-6527 (Westwater)

## Abstract

Simultaneous measurements of surface atmospheric parameters and cloud liquid water are used to test and compare the accuracy of three different cloud models.

## 1. Brief Review of Cloud Attenuation Models

Numerous models for predicting the attenuation of electromagnetic waves propagating through clouds were developed over the years from a variety of theoretical and empirical methods. Cloud modeling for the purposes of assessing attenuation can be divided into essentially three different categories: 1) attenuation is computed by using a Rayleigh approximation to Mie scattering theory [Gunn, East, 1954], [Staelin 1966], [Liebe, Manabe, Hufford, 1989]; 2) attenu-

ation is directly correlated to surface absolute humidity [Altshuler, Marr, 1989]; 3) Meteorological data and computations are used to determine cloud liquid and then attenuation is computed using a slightly modified version of the category 1 models described above. [Slobin, 1982], [Dintelmann, Ortgies, 1989].

Although their mathematical form and predictions vary over a fairly large range, a parameter common to all models is the liquid water content of the cloud. Unfortunately, this fundamental parameter is also the most difficult to predict and to measure.

A detailed comparison of five prominent cloud models developed over the last forty years shows good agreement at frequencies below 40 GHz for light to medium clouds conditions [Gerace, Smith, 1990]. However, for heavy to very heavy clouds and frequencies above 10 GHz, the models diverge from each other.

The recent availability of radiometric measurements of atmospheric parameters and the worldwide availability of surface atmospheric measurements have inspired the development of new cloud attenuation models. These new models strive to relate surface atmospheric measurements to cloud attenuation. The overall underlying assumption is that the liquid water content of clouds is in some way related to the water vapor present at the earth's surface.

This paper describes how three of these new cloud models

perform on a cloud event that was in no way related to the empirical data used to develop the models. The preliminary results presented below are an attempt to qualitatively verify both the mathematical cloud models (types 2 and 3) and the latest methods available for extracting data from an independent cloud event. A complete statistical analysis is forthcoming when we complete our analysis using cloud data measured at numerous sites worldwide.

We begin by introducing the Altshuler-Marr, Dintelmann-Ortgies, and GSW cloud attenuation models and briefly discussing a method for measuring cloud liquid water. We then present our methods for comparing the models along with graphical results. The results are also cross checked with the well established Slobin cloud models [Slobin, 1982].

## 2. Altshuler Model

By correlating data of absolute surface humidity with measurements of zenith cloud attenuation in the Boston area, Altshuler derived the following empirical model for a nominal cloud temperature of 10°C [Altshuler, 1989]:

$$\alpha = \left[ -0.0242 + 0.00075\lambda + \frac{0.403}{\lambda^{1.15}} \right] (11.3 + \rho) \quad (1)$$

where

$\alpha$  = zenith attenuation (dB)  
 $\lambda$  = wavelength (mm)  
 $\rho$  = surface water vapor density (g/m<sup>3</sup>)

To account for elevation angles other than 90 degrees, eq. 1 must be multiplied by the following:

$$D(\theta) = \begin{cases} \text{CSC}(\theta) \\ \left[ (a_e + h_e)^2 - a_e^2 \cos^2(\theta) \right]^{\frac{1}{2}} \\ -a_e \sin(\theta) \end{cases} \quad (2)$$

where

$\theta$  = elevation angle  
 $a_e$  = effective radius of the earth (4/3 earth taken as 8497 km)  
 $h_e = 6.35 - 0.302\rho$  effective cloud height (km)  
 $\rho$  = surface absolute humidity (g/m<sup>3</sup>)

While the Altshuler model is primarily an empirical model the next model is more appropriately classified as a semiempirical model.

## 3. Dintelmann-Ortgies Model

Using standard meteorological equations along with radiometer attenuation and concurrent meteorological measurements, Dintelmann and Ortgies derived the following semiempirical model for cloud attenuation prediction [Dintelmann, Ortgies, 1989]:

$$M = \rho_o \frac{T_o}{T} \left( 1 - \frac{\kappa - 1}{\kappa} \frac{gH}{RT_o} \right)^{\frac{\kappa}{\kappa - 1}} - 3.82 \quad (\text{g/m}^3) \quad (3)$$

where

M = cloud liquid water  
(g/m<sup>3</sup>)

T<sub>0</sub> = surface temperature

T = cloud temperature

ρ<sub>0</sub> = surface water vapor  
density (g/m<sup>3</sup>)

K = the ratio of the  
specific heat of water at  
constant pressure to the  
specific heat of water at  
constant volume (approximately  
= to 4/3)

g=acceleration of gravity  
(9.8 m/s<sup>2</sup>)

R=gas constant for air  
(approximately 287 J/K-Kg)

H = height of the 0 degree  
isotherm (m)

The height of the 0 degree  
isotherm can be approximated  
by:

$$H=0.89+0.165(T_0-273) \quad (4)$$

where

T<sub>0</sub> = Surface Temp. (K)

Then the attenuation  
through the cloud can be  
computed using an equation  
Dintelman borrowed from  
[Slobin, 1982]:

$$\alpha = \frac{4.343 \cdot 10^{0.0122(291-T)-1}}{\lambda^2} \cdot 1.16M \quad (5)$$

where α is now in dB/km, T is  
the cloud temperature in  
Kelvin, and λ is the wavelength  
in centimeters.

To obtain the total attenuation  
through the cloud, Dintelman  
used radiometer measurements to  
obtain the following empirical  
formula for the cloud vertical

extent:

$$\Delta=0.15-0.023M+0.0055M^2 \quad (km) \quad (6)$$

where M is the cloud liquid in  
g/m<sup>3</sup>.

Inherent in this model is  
the assumption that clouds form  
around the 0°C isotherm. The  
next model attempts to refine  
the Dintelman-Ortgies model by  
including a calculation aimed  
at predicting more accurately  
the altitude of cloud  
formation.

#### 4. GSW Model

The altitude at which the  
actual water vapor density  
exceeds the saturated water  
vapor density for the  
temperature and pressure at  
that point is called the  
lifting condensation level. The  
GSW (initials of authors' last  
names) model assumes that this  
is the altitude at which clouds  
begin to form. The model can  
be described as follows:

The initial version of the  
GSW model assumes a linear  
adiabatic temperature lapse  
rate of 6 deg C per kilometer:

$$T(h) = T_0 - \gamma T$$

$$\gamma = 6^\circ / Km$$

(7)

Then a vertical saturated  
water vapor profile can be  
computed as follows:

$$p_s = \frac{e_s}{RT} \quad (8)$$

where  $e_s$  is the water vapor pressure and is given by the following formula due to [Nordquist, 1973]:

$$e_s = 10^x \quad \text{where}$$

$$x = c_1 - 1.3816e^{-7 \cdot 10^{p_1}} + 8.1328e^{-3 \cdot 10^{p_2}} - \frac{2949.076}{T} \quad (9)$$

where

$$p_1 = 11.344 - 0.0303998T \quad (10)$$

$$p_2 = 3.49149 - \frac{1302.8844}{T} \quad (11)$$

$$c_1 = 23.832241 - 5.02808 \log(T) \quad (12)$$

Now a vertical water vapor profile can be computed as follows:

$$\rho(h) = \rho_o \frac{T_o}{T} \left( 1 - \frac{\kappa-1}{\kappa} \frac{gh}{RT_o} \right)^{\frac{\kappa}{\kappa-1}} \quad (13)$$

One can compute the lifting condensation level by equating equations (8) and (13) and solving for the height,  $h$ . This is where the saturation vapor density equals the actual vapor density and is most likely the altitude at which the cloud begins to form.

Above the lifting condensation level, water vapor continues condensing as long as the actual vapor density exceeds the saturated vapor density. Loosely based on actual measurements of total integrated cloud liquid water and typical values of cloud liquid water densities, an estimate of the cloud liquid water content can be computed as follows:

$$M = \rho(h') - \rho_s(h') \quad (14)$$

where  $h'$  is the altitude at which  $\rho = 1.25 \rho_s$ .

Then cloud attenuation can be computed using equations 5 and 6 with equation 6 modified by multiplying all of the coefficients by a factor of ten. This factor of ten will most likely be refined as we

average in more data sets from various sites to improve our model.

Next, we describe a method for measuring the amount of liquid water in a cloud.

### 5. Cloud Liquid Water Measurements

Radiometer measurements of atmospheric absorption at two frequencies, a water vapor sensitive frequency and a cloud liquid water sensitive frequency (say 20.6 and 31.65 MHz), can lead to a determination of total integrated cloud liquid water,  $L$  [Westwater, 1978]. The computation can be summarized as follows:

$$L = \frac{(-\kappa_{vu}f_l + \kappa_{vl}f_u)}{(\kappa_{vl}\kappa_{Lu} - \kappa_{vu}\kappa_{Ll})} \quad (15)$$

where

$$f_v = -\tau_{dv} - \ln \left[ \frac{(T_{mr} - T_{bv})}{(T_{mr} - T_{bb})} \right] \quad (16)$$

for  $v = l, u$

where

$\kappa_{vu}$  = path averaged absorption coefficient of vapor at the upper liquid water sensitive frequency,  $u$ .

$\kappa_{Lu}$  = path averaged absorption coefficient of liquid at the upper liquid water sensitive frequency,  $u$ .

$\kappa_{vl}$  = path averaged absorption coefficient of vapor at the lower water vapor sensitive frequency,  $l$ .

$\kappa_{Ll}$  = path averaged absorption coefficient of liquid at the lower liquid water sensitive frequency,  $l$ .

$T_{mr}$  = mean radiating temperature

$T_{bb}$  = cosmic background "big bang" brightness temperature (2.8 K)

$T_{bv}$  = measured value of the microwave brightness temperature at frequency,  $v$ .

$\tau_{dv}$  = dry absorption at frequency,  $v$ .

Measurements of cloud liquid water using the above algorithm are currently being made by the Wave Propagation Laboratory (WPL) of the National Oceanic and Atmospheric Administration (NOAA) at San Nicolas Island, CA, and Denver Colorado. We are now intensively analyzing data that was collected throughout the 1980s. The results in this report are based on data taken in July 1984.

### 6. Method of Comparison

Figure 1 depicts our method of comparison. Using surface atmospheric measurements taken in Denver CO, cloud liquid water contents

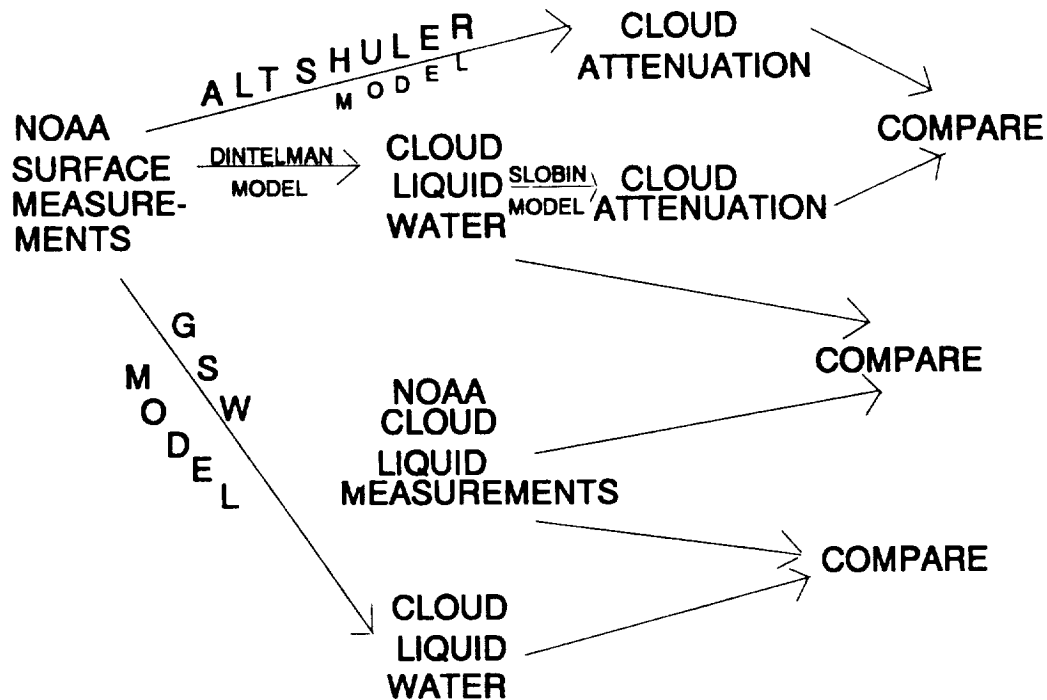


**Figure 1.** Method of Comparison

computed using the Dintelmann-Ortgies and GSW models were compared to measurements of cloud liquid present at the time the surface measurements were recorded. Attenuation predicted by the Altshuler model was compared to that predicted by the Dintelmann-Ortgies model (via the Slobin approximation discussed above).

**7. Results.**

A time series of the surface measurements taken during a sample cloud event is shown in figure 2. Figure 3 shows a comparison of the Dintelmann predictions to NOAA's measurements of cloud liquid water. Figure 4 shows a similar comparison for the GSW model. Note that the order of magnitude of the total integrated liquid (cm) for all

three models is correct. However, the shape of the curves agree qualitatively only

during the last half of the three hour measurement period. Also note that the Dintelmann-Ortgies model predicts high liquid water content (g/m<sup>3</sup>) and low vertical cloud extent as compared to the Slobin models described in figure 5. But the two effects sort of cancel each other out when computing the total integrated liquid (cm) because the units conversion from g/m<sup>3</sup> to cm is as follows:

$$M \left( \frac{g}{m^3} \right) = \frac{10M (cm)}{\Delta (Km)} \tag{17}$$

where M is the cloud liquid and Δ is the extent of the cloud.



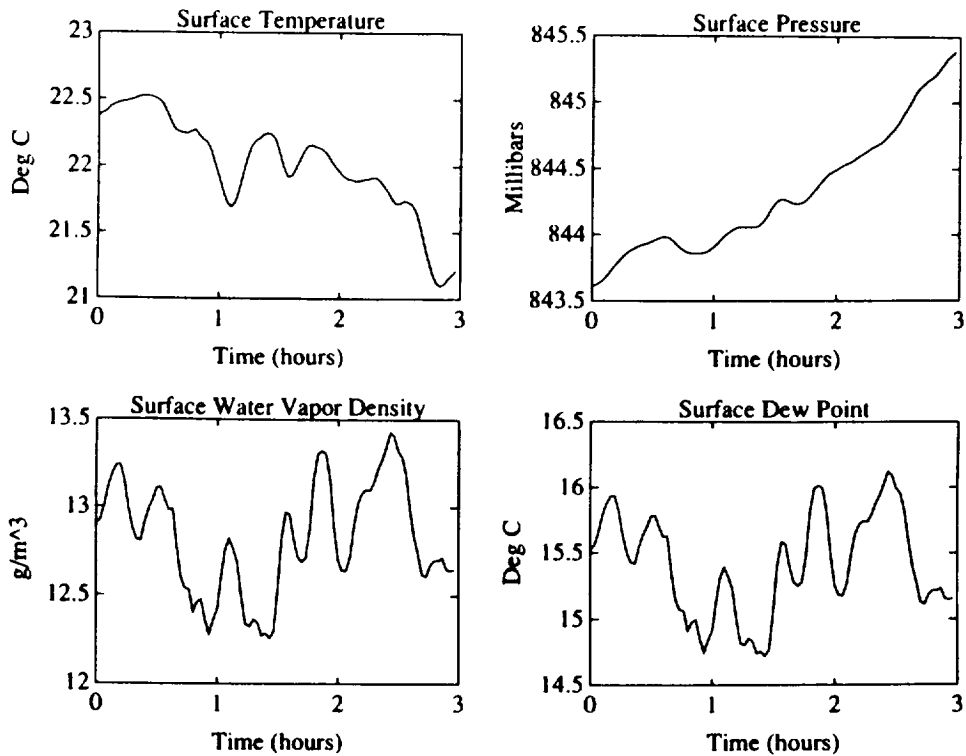


**Figure 2.** Surface Measurements of Atmospheric Parameters During the Cloud Event.

The GSW predictions are a little closer to the Slobin models but also exhibit some disagreement during the first half of the time period.

All of this probably points to some physical phenomena that is not being accounted for in these simple "state equation" models. Improvements in modeling the vertical temperature profile, for example, might help matters. We are currently using simultaneous measurements of vertical temperature gradients and cloud liquid to improve the model.

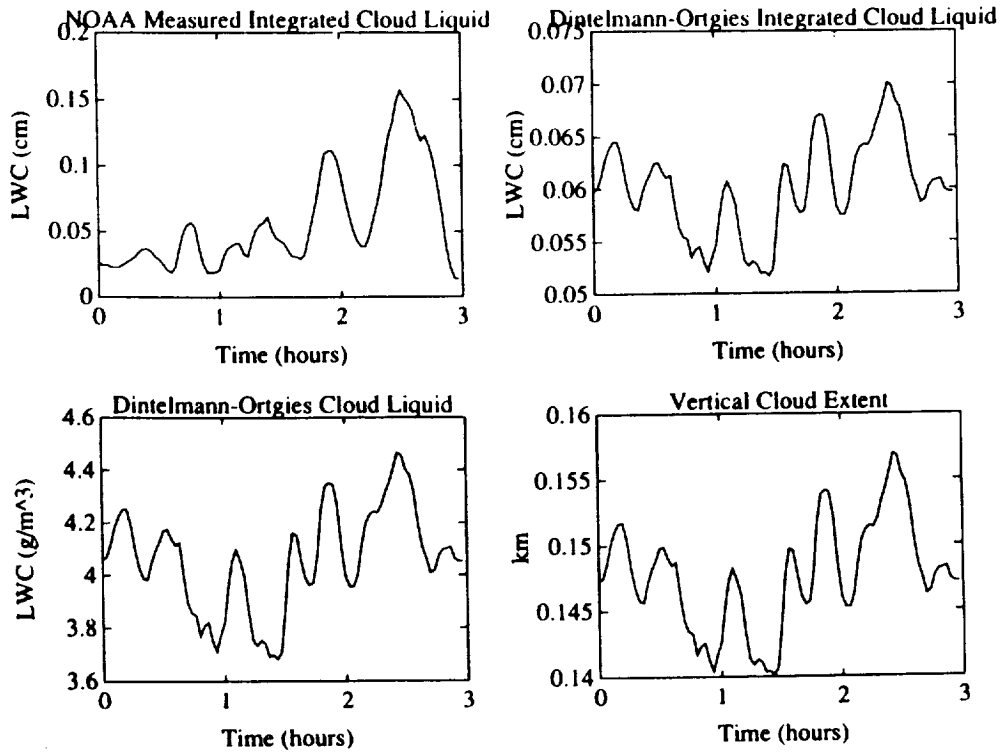
It is also of interest to note that the GSW model predicts the lifting condensation level to be a kilometer or so below the zero degree isotherm as shown in

figure 6. We are now analyzing measurements of the lifting condensation level to improve cloud base altitude predictions.

A striking result is shown in figure 7. Although the Altshuler and Dintelmann-Ortgies models were derived quite differently, they predict almost identical cloud attenuation time series patterns during the cloud event. Note however that the absolute magnitudes and the dynamic range of the patterns do differ.

## 8. Continuing Work

The complexity of cloud physics and the lack of



**Figure 3.** Cloud Liquid and Vertical Cloud Extent Predicted by Dintelmann-Ortgies Model and NOAA Measurements of Cloud Liquid.

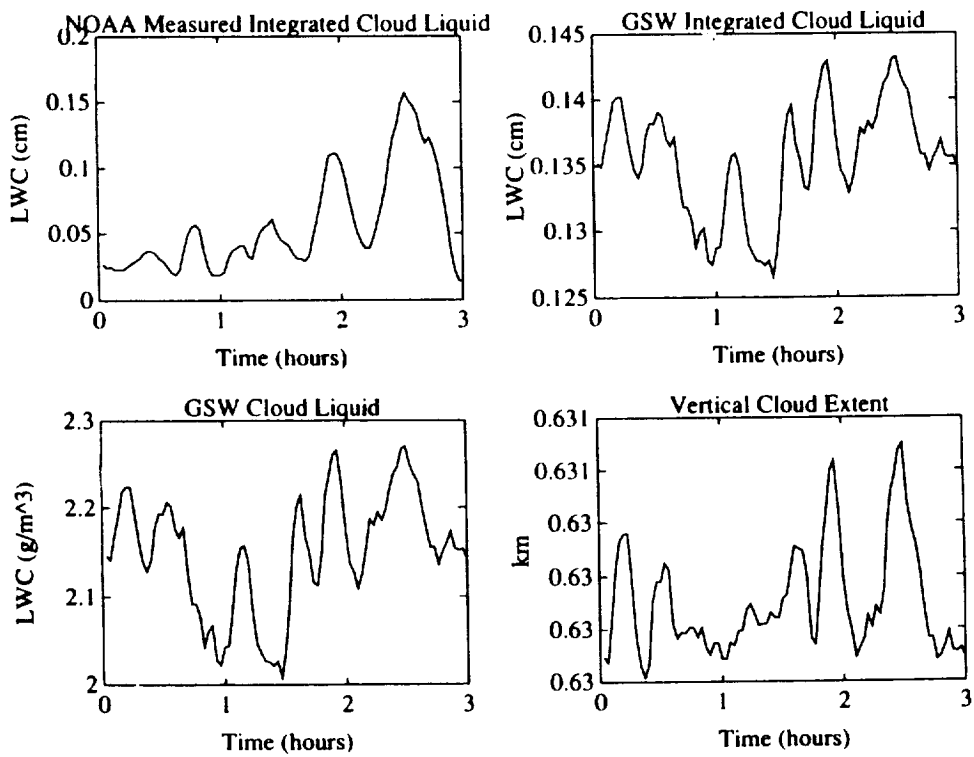


**Figure 4.** Cloud Liquid and Vertical Cloud Extent Predicted by GSW Model and NOAA Measurements of Cloud Liquid.

Sample Clear-Air and Cloud Models With Associated Zenith Microwave Effects

Case	Lower Cloud				Upper Cloud				10 GHz		20 GHz		30 GHz		40 GHz		50 GHz	
	Density (g m <sup>-3</sup> )	Base (km)	Top (km)	Thickness (km)	Density (g m <sup>-3</sup> )	Base (km)	Top (km)	Thickness (km)	T (K)	A (dB)	T (K)	A (dB)	T (K)	A (dB)	T (K)	A (dB)	T (K)	A (dB)
1	...	...	...	...	...	...	...	...	305	0.049	14.73	0.232	13.76	0.219	23.20	0.383	78.14	1.481
2	0.2	10	12	0.2	...	...	...	...	3.22	0.052	15.37	0.242	15.20	0.242	25.67	0.424	81.17	1.545
3	...	...	...	...	0.2	30	32	0.2	3.28	0.053	15.60	0.247	15.72	0.252	26.55	0.441	82.22	1.572
4	0.5	10	15	0.5	...	...	...	...	4.12	0.066	18.80	0.298	22.84	0.367	38.53	0.646	96.63	1.892
5	...	...	...	...	0.5	30	35	0.5	4.50	0.073	20.24	0.326	26.01	0.430	43.73	0.758	102.57	2.067
6	0.5	10	20	10	...	...	...	...	5.27	0.084	23.12	0.370	32.29	0.529	54.05	0.934	114.68	2.342
7	...	...	...	...	0.5	30	40	10	6.06	0.098	26.06	0.428	38.57	0.660	63.97	1.168	125.42	2.708
8	0.5	10	20	10	0.5	30	40	1.0	8.25	0.133	34.10	0.566	55.40	0.970	89.96	1.719	153.47	3.569
9	0.7	10	20	10	0.7	30	40	1.0	10.31	0.166	41.42	0.700	70.06	1.271	111.21	2.254	174.40	4.404
10	1.0	10	20	10	1.0	30	40	1.0	13.35	0.216	51.97	0.900	90.17	1.722	138.36	3.055	198.77	5.656
11	1.0	10	25	15	1.0	35	50	1.5	19.66	0.326	72.67	1.338	126.26	2.708	181.57	4.908	232.20	8.395
12	1.0	10	30	20	1.0	40	60	2.0	26.34	0.457	94.35	1.864	159.18	3.891	214.08	6.912	251.92	11.682

Cases 2-12 are clear air and clouds combined

Figure 5. Slobin Cloud Models [Slobin, 1982].

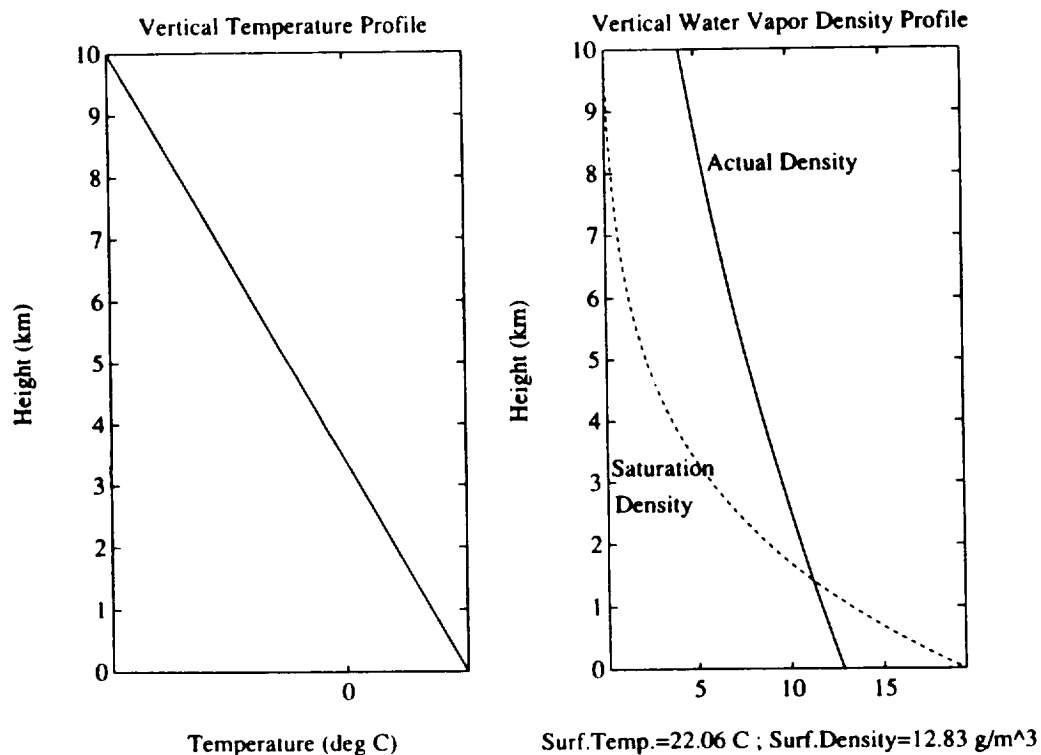
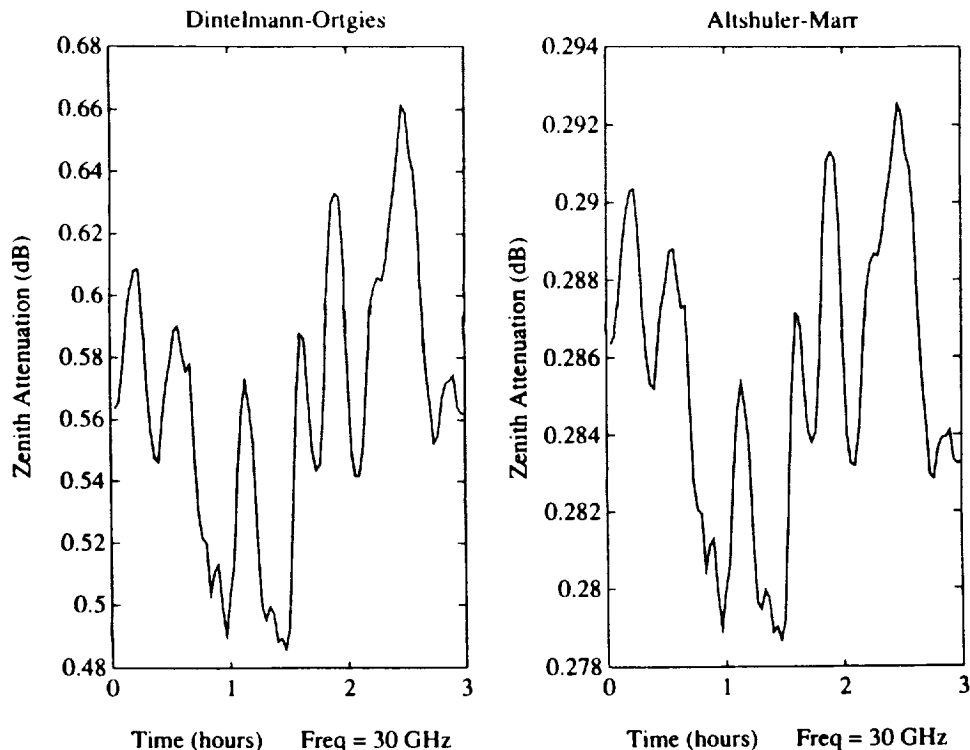


Figure 6. Vertical Profiles of Temperature, Saturation Water Vapor Density, and Actual Water Vapor Density as Predicted by the GSW Model.



**Figure 7.** Comparison of Zenith Attenuation Predicted by the Dintelmann-Ortgies and Altshuler-Marr Models.

measured data has always hampered cloud liquid research. Now as data begins to trickle in, we are seeing the beginnings of a new cloud liquid science--a blend of theory and experiment. The models presented here are a building block toward the understanding of cloud attenuation. As we continue working with more data sets at various locations, we are seeking to improve temperature profiling and condensation level predictions. Gradually we hope to incorporate and validate more detailed cloud physics to describe the condensation and mixing processes associated with clouds. We openly welcome your critiques and ideas.

#### References

- Altshuler, E. and Marr, R., 1989: "Cloud Attenuation at Millimeter Wavelengths," *IEEE Transactions on Antennas and Propagation*, vol 37, no. 11, Nov pp. 1473-1479.
- Altshuler, E.E., 1984: "A Simple Expression for Estimating Attenuation by Fog at Millimeter Wavelengths," *IEEE Transactions on Antennas and Propagation*, vol 32, no. 7, Jul., pp. 757-758.
- Dintelmann, F. and Ortgies, G., 1989: "Semiempirical Model For Cloud Attenuation Prediction," *Electronics Letters*, vol 25, no. 22, Oct., pp. 1487-1488.
- Flock, W.L., 1987: *Propagation Effects on Satellite Systems at Frequencies below 10 GHz*, NASA

Ref. Pub. 1108(02), pp. 5.1-5.24.

Gerace, G.C. and Smith, E.K., 1990: "A Comparison of Cloud Models," *IEEE Antennas and Propagation Magazine*, Oct., pp. 32-38.

Gunn, K.L. and East, T.W., 1954: "The Microwave Properties of Precipitation Particles," *Quarterly Journal of the Royal Meteorological Society*, vol 80, pp. 522-545.

Hopponen, D.H. and Liebe, H.J., 1986: "A Computational Model for the Simulation of Millimeter-Wave Propagation Through the Clear Atmosphere," *National Telecommunications and Information Administration Report 86-204*, U.S. Department of Commerce, pp. 1-5.

Hufford, G.A., 1989: "Millimeter-Wave Attenuation and Delay Rates Due to Fog/Cloud Conditions," *IEEE Transactions on Antennas and Propagation*, vol 37, no. 12, Dec., pp. 1617-1623.

Ippolito, L.J., 1989: *Propagation Effects Handbook for Satellite Systems Design*, NASA Ref. Pub. 1082(04), pp. 6.62-6.72.

Iribarne, J.V. and Godson, W.L., 1989: *Atmospheric Thermodynamics*, D. Reidel Publishing Company, Boston MA.

Kerr, D.E. (ed.), Goldstein, H., 1951: *Propagation of Short Radio Waves*, McGraw-Hill Book Company, Inc. NY, pp. 671-692.

Liebe, H.J. and Hufford, G.A., 1989: "Modeling Millimeter-Wave Propagation Effects in the Atmosphere," *Agard Fall*

*Symposium on Atmospheric Propagation*, Copenhagen, Denmark, Oct 9-13.

Liebe, H.J., Manabe, T., Manabe, T., Liebe, H.J., Hufford, G.A., 1987: "Complex Permittivity of Water Between 0 and 30 THz," *Twelfth International Conference on Infrared and Millimeter Waves Conference Digest*, 14-18 Dec., Session W6.6 IEEE Catalog Number: 87CH2490-1, pp. 229-230.

McIlveen, R., 1986: *Basic Meteorology*, Van Nostrand Reinhold Co, Ltd, Berkshire, England.

Mie, G., 1908: "Beiträge Zur Optik Trüber Medien, Speziell Kolloidaler Metallösungen," *Ann. der Physik*, 25, Mar.

Pruppacher, H.R. and Klett, J.D., 1980: *Microphysics of Clouds and Precipitation*, D. Reidel Publishing Company, Boston MA.

Rogers, R.R. and Yau, M.K., 1989: *A Short Course in Cloud Physics*, Pergamon Press, Oxford.

Slobin, S., 1982: "Microwave Noise Temperature and Attenuation of Clouds: Statistics of these Effects at Various Sites in United States, Alaska, and Hawaii," *Radio Science*, vol 17, no. 6, Dec., pp. 1443-1454.

Smith E.K., 1982: "Centimeter and Millimeter Wave Attenuation and Brightness Temperature due to Atmospheric Oxygen and Water Vapor," *Radio Science*, vol 17, no. 6, Nov-Dec., pp. 1455-1464.

Staelin, D.H., 1966:  
"Measurements and  
Interpretation of the Microwave  
Spectrum of the Terrestrial  
Atmosphere near 1-Centimeter  
Wavelength," *Journal of  
Geophysical Research*, vol 71,  
no. 12, Jun., pp. 2875-2881.

Van de Hulst, H.C., 1981:  
*Light Scattering by Small  
Particles*, Dover Publications,  
Inc., NY.

Westwater, E.R., 1978: "The  
Accuracy of Water Vapor and  
Cloud Liquid Determination by  
Dual-Frequency Ground-Based  
Microwave Radiometry," *Radio  
Science*, vol 13, no. 4, Jul.-  
Aug., pp. 677-685.

Zufferey C.H., 1972: "A Study  
of Rain Effects on  
Electromagnetic Waves in the  
1-600 GHz Range," Master's  
Thesis, University of Colorado,  
pp. 139-142.

BRIGHTNESS TEMPERATURE AND ATTENUATION  
STATISTICS AT 20.6 AND 31.65 GHzE. R. Westwater and M. J. Falls  
NOAA/ERL/Wave Propagation Laboratory  
Boulder, CO

Abstract--Attenuation and brightness temperature statistics at 20.6 and 31.65 GHz are analyzed for a year's data that were collected in 1988 at Denver, and Platteville, Colorado. The locations are separated by 49 km. Single-station statistics are derived for the entire year. Quality control procedures are discussed and examples of their application are given.

I. Introduction

In previous NAPEX meetings, we have presented attenuation and attenuation diversity statistics for a limited number of station months (Westwater et al., 1988; Westwater et al., 1989; Snider et al., 1989). Because of an extensive data base of radiometric observations at 20.6 and 31.65 GHz in the front range of eastern Colorado, we are currently developing monthly and yearly statistics at these frequencies. Our goal is to develop statistics representing each of four locations, as well as appropriate diversity statistics for pairs of stations for the year 1988. This paper is a status report in which 1988 data from Denver and Platteville, stations 49 km apart, are analyzed. Details of the characteristics of our radiometers and our calibration procedures are reported in Westwater et al. (1990).

II. Quality Control

The radiometric data were taken by radiometers that operated in an unattended mode, although bimonthly on-site calibrations were done. For the most part, the data were of high quality, although occasional outliers had to be removed from the data. Such outliers can arise from liquid and ice buildup on the antennas, spurious signals of electromagnetic origin, calibration drifts in the receivers, and data transmission errors. To eliminate obvious erroneous data, we plotted and inspected daily time series of the following quantities: brightness temperature  $T_b$  at 20.6 and 31.65 GHz; derived attenuation  $\tau$  at 20.6 and 31.65 GHz; and precipitable water vapor and cloud liquid. If a record had an obvious error at either or both frequencies, data from the entire record were removed. Next, scatter plots of  $T_b$ s at both frequencies were constructed; usually, suspicious points were easily identified from these plots. We show in Fig. 1 scatter plots showing both (A) original data and (B) data with outliers removed. During cold conditions, the total range of  $T_b$  is much less than 300 K. Therefore, for these cold conditions, we also constructed scatter plots over a 15 K range. In Fig. 2, obvious

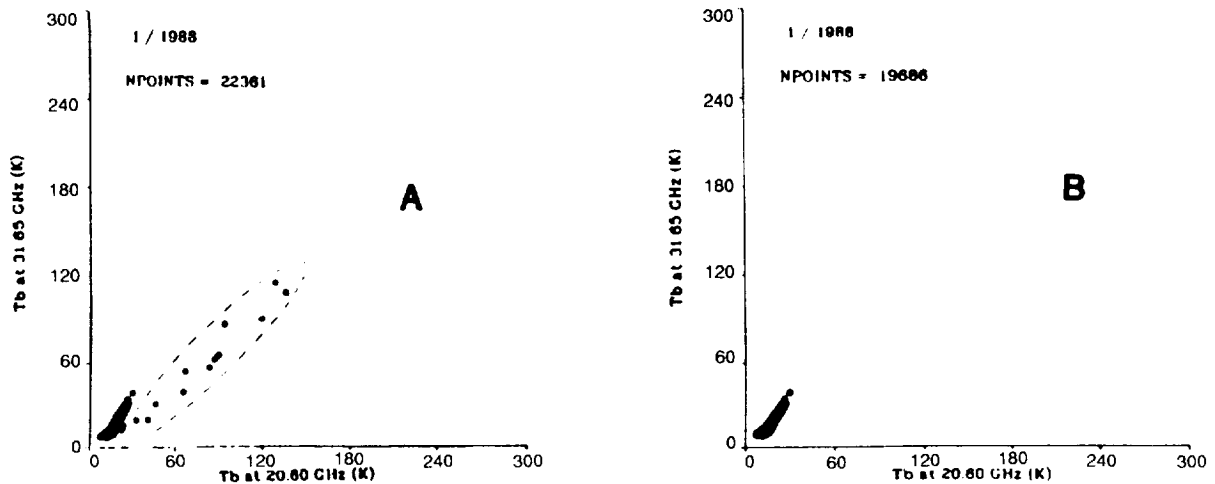


Fig. 1. Examples of brightness temperature scatter plots for quality control. (A) scatter plots with encircled outliers; (B) scatter plots with outliers removed. Denver, CO, 1/88.

outliers with 31.65 GHz  $T_b$ s less than  $\sim 8.5$  K are shown. Finally, in Fig. 3, we show scatter plots of quality-controlled  $T_b$ s for a year's data taken at Denver and Platteville. The potential of using these plots for quality control is apparent. The general behavior of the scatter plots may be explained as follows: due to far wing absorption from  $O_2$  and for clear, dry conditions,  $T_b$  (31.65 GHz) may be larger than  $T_b$  (20.6). For increasing water vapor concentration,  $T_b$  (20.6) rapidly becomes the larger of the two. Finally, since cloud attenuation is greater at 31.65 GHz than at 20.6 GHz, during many cloudy situations  $T_b$  (31.65) will again be the larger of the two.

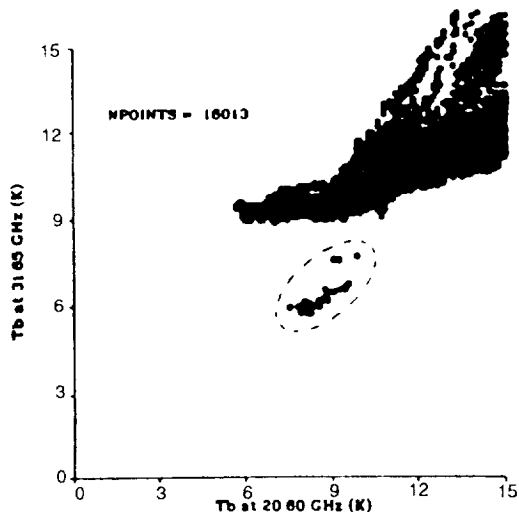


Fig. 2. Scatter plots of brightness temperatures for  $T_b < 15$  K. Note the approximately 6 K and 9 K minimum  $T_b$ s at 20.6 and 31.65 GHz. Outliers are encircled. Platteville, CO, 1/1 - 12/31/88.

### III. Brightness Temperature Statistics

The first paper in which the climatological variations of brightness temperatures were considered was given by Slobin (1982), who constructed statistics of  $T_b$  at a variety of locations and frequencies. His work was based on climatological radiosonde data. Since conventional radiosondes do not measure cloud liquid, modeling of this component requires additional assumptions: Slobin assumed a modified adiabatic cloud liquid distribution. We will compare later his results with ours.

For a given location, the dominant variable in determining the range of  $T_b$  is cloud liquid.



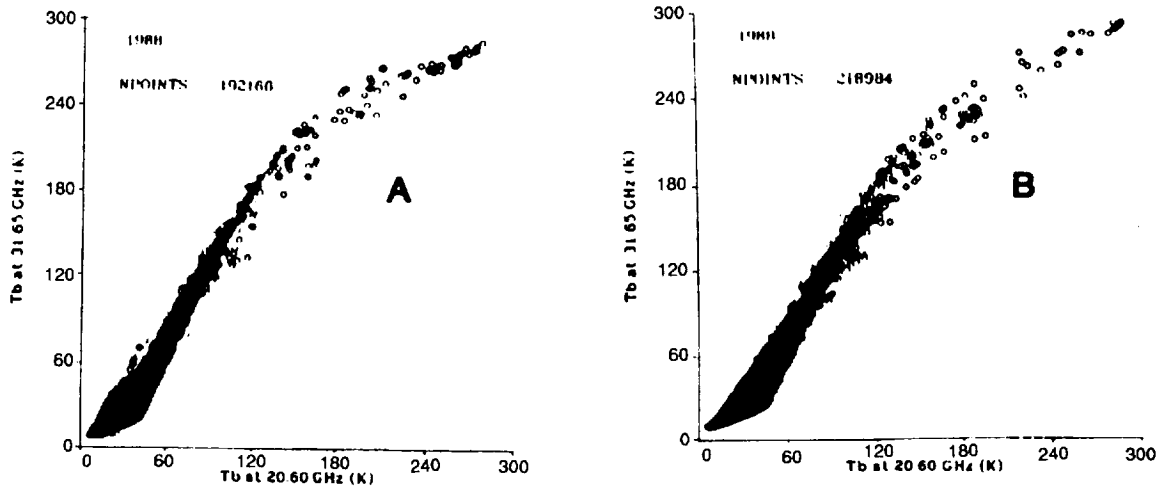


Fig. 3. Scatter plots of  $T_b$  at 20.6 and 31.65 GHz for (A) Denver, and (B) Platteville, CO for 1/1 - 12/31/88.

At Denver, in the winter, cold temperatures limit the amount of liquid that clouds can hold; hence, in the winter months,  $T_b$  values are limited to a range of less than ~75 K. During warmer months, cloud liquid greatly increases as does the range of  $T_b$ . Figs. 4 and 5 show scatter plots of  $T_b$  for each month of 1988 at Denver; similar results were obtained for Platteville.

The cumulative  $T_b$  statistics at 20.6 and 31.65 GHz for Denver and Platteville are shown in Fig. 6. For percentages of time greater than 0.1%, the probability distributions are almost identical. We also show in Fig. 6 (B) Slobin's estimated probability distribution for Denver. Given the uncertainties in modeling cloud liquid statistics from radiosonde data, the agreement is remarkable.

#### IV. Attenuation Statistics

We also derived attenuation  $\tau$  (dB) from brightness temperature by using the well-known formula (Westwater et al., 1990)

$$\tau \text{ (dB)} = 4.34 \ln\{(T_m - T_c)/(T_m - T_b)\} \quad , \quad (1)$$

where

$T_m$  = medium temperature (K),

and

$T_c$  = cosmic background temperature = 2.75 K.

In deriving  $\tau$ , we used monthly mean values of  $T_m$  that were calculated from our radiative transfer and cloud models. Yearly cumulative probability distributions of  $\tau$  are shown in Fig. 7. Since water vapor attenuation at 20 GHz is larger than 31.65 GHz

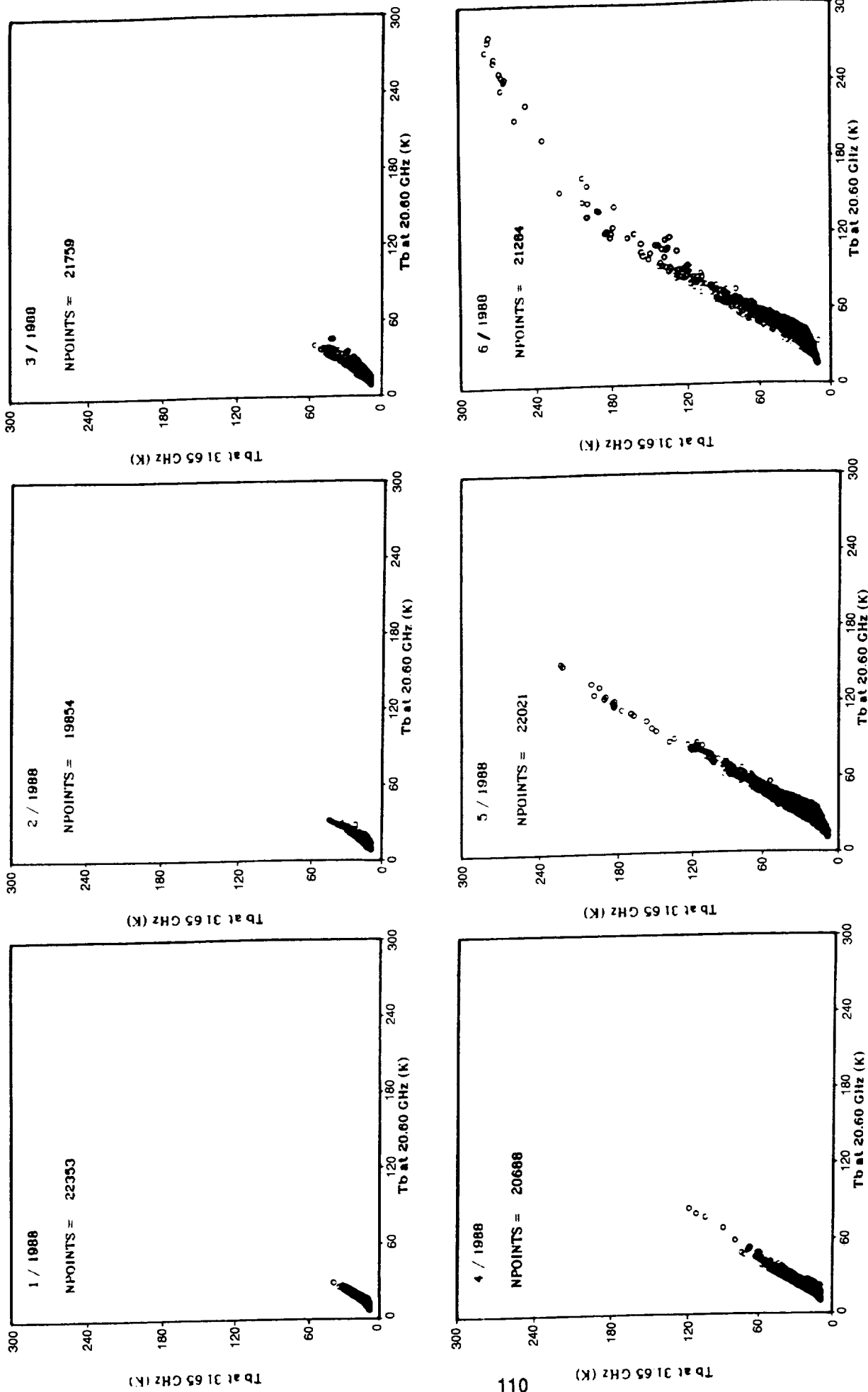


Fig. 4. Monthly scatter plots of 20.6 and 31.65 GHz  $T_b$ s for Denver, CO, for the first six months of 1988.

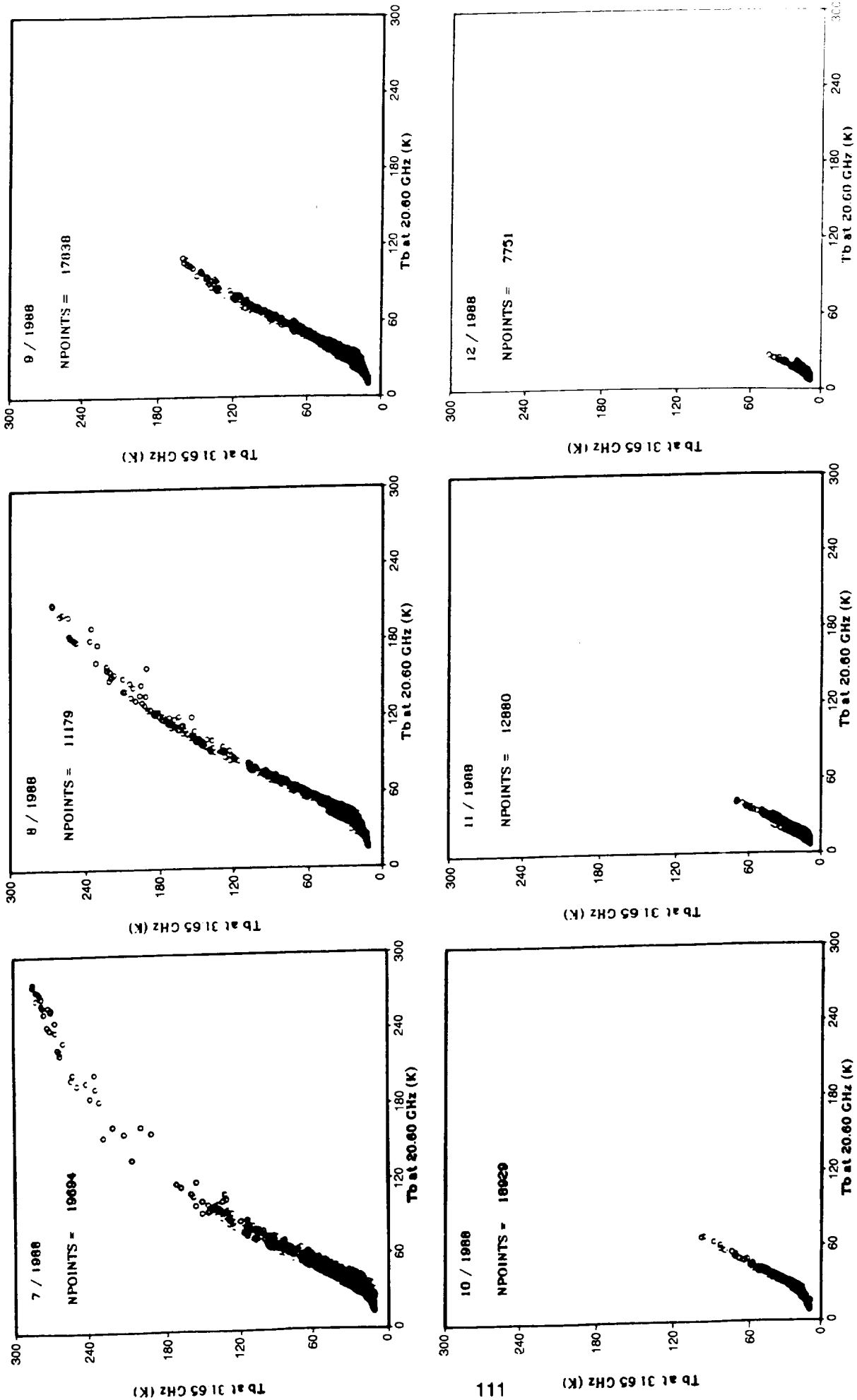


Fig. 5. Monthly scatter plots of 20.6 and 31.65 GHz for Denver, CO, for the last six months of 1988.

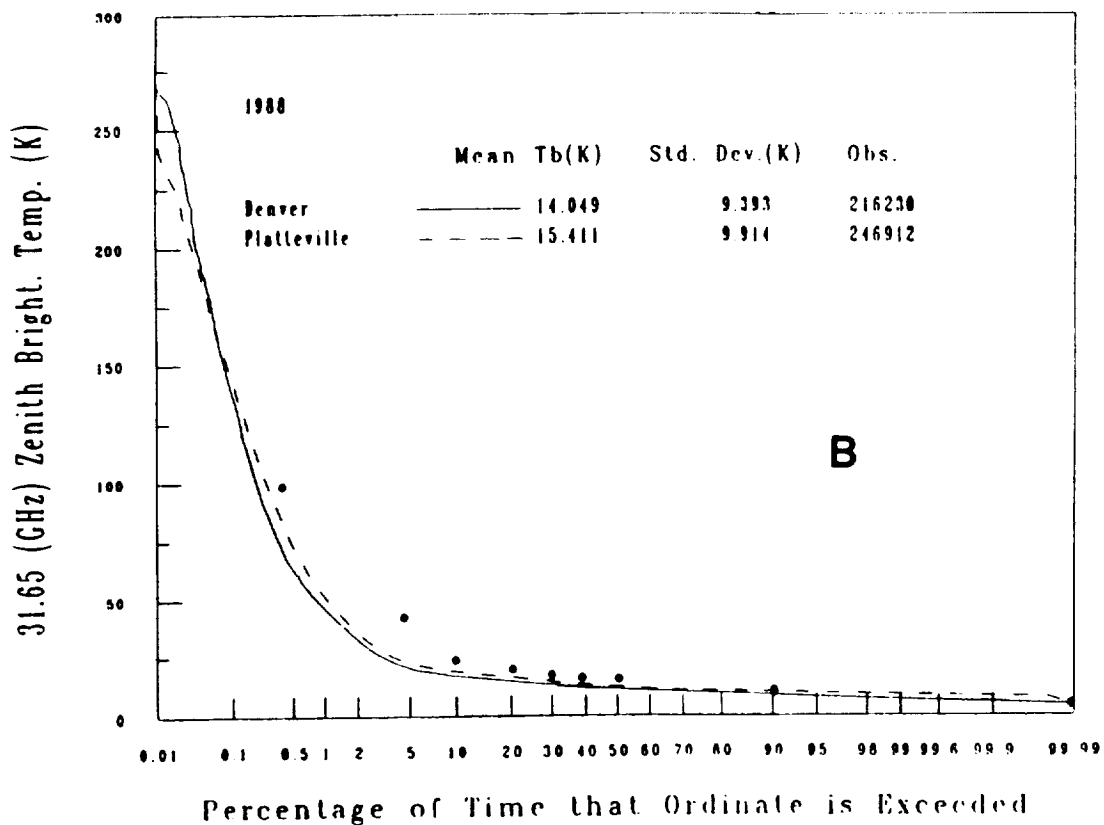
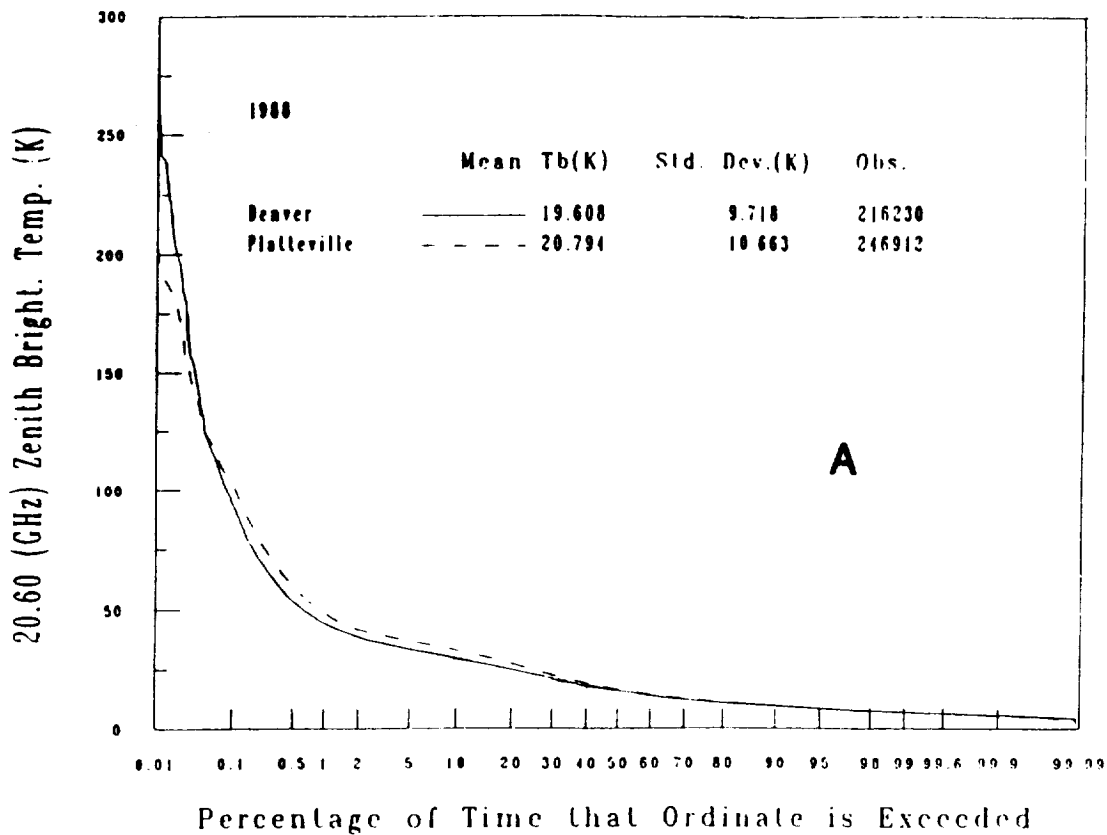


Fig. 6. Percentage of time that brightness temperature levels are exceeded at (A) 20.6, and (B) 31.65 GHz. Data represent measurements taken during 1/1 - 12/31/88, at Denver, and Platteville, CO. Comparisons with the estimates of Slobin (1982) are shown by dots in (B).

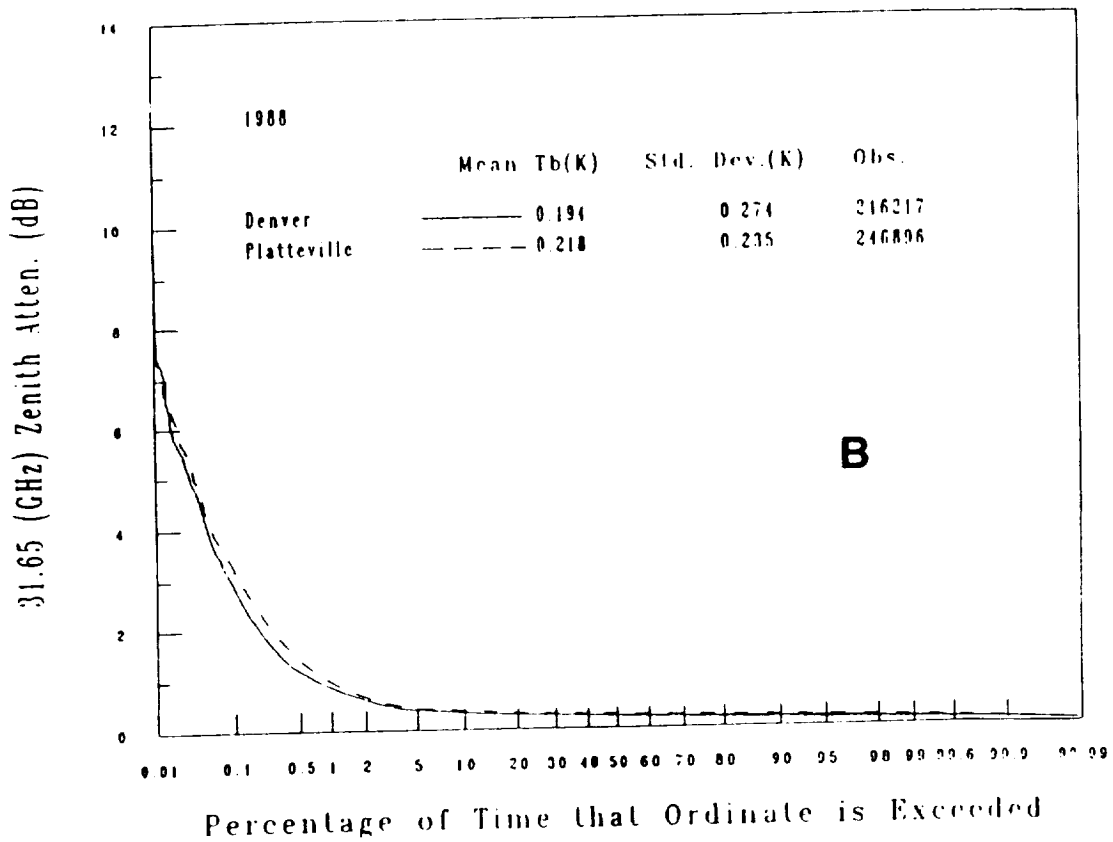
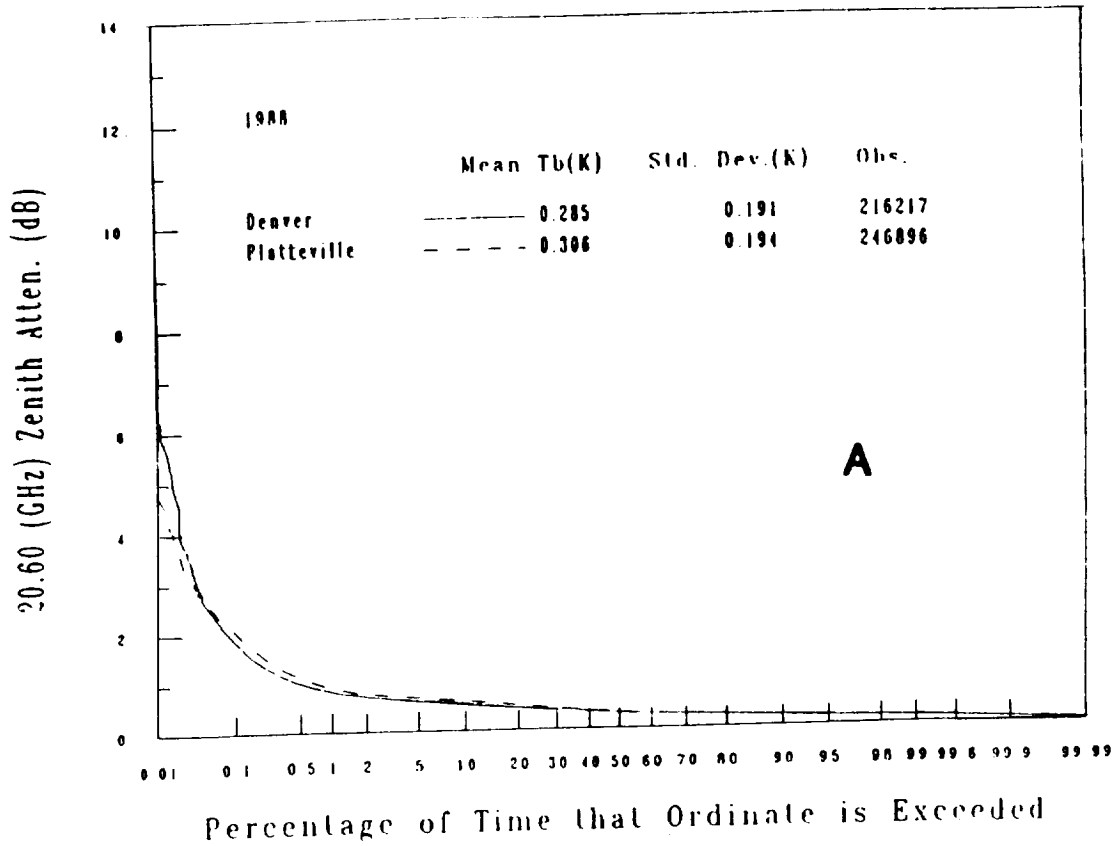


Fig. 7. Percentage of time that attenuation levels are exceeded at (A) 20.6, and (B) 31.65 GHz. Data represent measurements taken 1/1 - 12/31/88, at Denver, and Platteville, CO.

and since the situation is reversed for cloud liquid attenuation, there are crossovers in the cumulative probability distributions.

Another crossover occurs for the very low attenuations that occur during dry, cold conditions when 31.65 GHz is again larger than 20. We note that 8 dB is exceeded at the 0.01% level for the 31.65 GHz channel.

#### V. Summary and Plans

For the first time, we derived yearly brightness temperature and attenuation statistics at 20.6 and 31.65 GHz for Denver and Platteville, two Colorado locations separated by 49 km. A strong seasonal variation in attenuation was observed and maximum values in the summer months exceeded those in the winter by a factor of three or four. In our NAPEX XIV report, we reported on attenuation diversity between Denver and Platteville for three summer months. We are currently developing single station statistics and joint-station diversity statistics for all four stations of the Colorado Research Network for the 1988 data.

We have also shown the utility of using 20 vs. 31.65 GHz scatter plots for quality control. We plan to extend the procedure by developing confidence intervals as a function of attenuation and brightness values. Strict confidence intervals are required when precipitable water vapor and cloud liquid are derived from the radiometric data.

#### VI. Acknowledgements

The authors thank Joseph Shaw for reviewing the manuscript and for his help in preparing the figures.

#### References

- Slobin, S. D., 'Microwave noise temperature and attenuation of clouds: Statistics of these effects at various sites in the United States, Alaska, and Hawaii,' Radio Science, 17:6, pp 1443-1454, 1982.
- Snider, J.B., M.D. Jacobson, and R.H. Beeler, "Observations of Attenuation at 20.6, 31.65 and 90.0 GHz - Preliminary Results from Wallops Island, VA," Proc. XIII NAPEX, San Jose, California, pp 138 - 144, 1989.
- Westwater, E.R. and J.B. Snider, 'Microwave Radiometer Facilities at the Wave Propagation Laboratory,' Proc. of NAPEX XI, Virginia Polytechnic Institute and State University, Blacksburg, Virginia, pp 24-27, 1987.
- Westwater, E.R., J.B. Snider, and M.J. Falls, 'Ground-Based Radiometric Observations of Emission and Attenuation at 20.6, 31.65, and 90.0 GHz,' Proc. of NAPEX XII, Syracuse, New York, pp 114-125, 1988.

Westwater, E.R., M. Falls, E. Fionda and J. Snider, 'Radiometric Observations at 20.6, 31.65 and 90.0 GHz: Continuing Studies,' Proc. XIII NAPEX, San Jose, California, pp 145-151, 1989.

Westwater, E.R., J.B. Snider, M.J. Falls and E. Fionda, 'Attenuation statistics derived from emission measurements by a network of ground-based microwave radiometers,' Proc. NAPEX XIV, Austin, Texas, pp 102-109, 1990.

COMPARISON OF OLYMPUS BEACON AND RADIOMETRIC ATTENUATION  
MEASUREMENTS AT BLACKSBURG, VIRGINIAJ. B. Snider, M. D. Jacobson,  
R. H. Beeler, and D. A. HazenNOAA/ERL/Wave Propagation Laboratory  
Boulder, Colorado 80303

Abstract - Measurements of attenuation of the 20 and 30 GHz beacons on board the OLYMPUS satellite are compared to simultaneous observations of atmospheric attenuation by a multichannel microwave radiometer along the same path. Departures from high correlation between the two measurements are believed to be related to differences in antenna beamwidths. Mean equivalent zenith attenuations derived from the slant path data are compared to zenith observations made at previous locations.

### *I. Introduction*

The availability of the OLYMPUS satellite with beacons operating near 12.5, 20, and 30 GHz offers an opportunity for high frequency propagation measurements in the eastern United States. In cooperation with the NASA Propagation Program, The Satellite Communications Group at Virginia Polytechnic Institute and State University (Virginia Tech) at Blacksburg, VA, has constructed receivers and is performing a one year period of measurements of the beacon signal levels. In addition, the receivers are equipped with microwave radiometers to permit the measurement of low values of attenuation by the clear atmosphere and liquid-bearing clouds. The radiometric measurements also allow determination of a clear sky reference level for the beacon measurements. The Virginia Tech OLYMPUS propagation study program and receiver/radiometer design is discussed in more detail by Stutzman (1990) and McKeeman (1990).

The Virginia Tech radiometers employ the same antennas and share some of the RF circuitry in the beacon receivers. As the antennas are designed for fixed angle operation, it is not possible to employ "tipping curve" calibrations which inherently include calibration of the antenna and front-end losses. For this reason, the National Oceanic and Atmospheric Administration/Wave Propagation Laboratory (NOAA/WPL) steerable beam, multichannel radiometer (20.6, 31.65, and 90.0 GHz), was employed to assist in the calibration of the Virginia Tech radiometers operating near 20 and 30 GHz. In addition, the WPL radiometer was used to obtain attenuation statistics at 20, 31, and 90 GHz for Blacksburg, VA to add to the database begun in 1987 at San Nicolas Island (Snider et al., 1989).

### *2. Experimental Plan and Instrument Configuration*

The NOAA/WPL transportable radiometer with steerable antenna (Hogg et al., 1983) was moved to Blacksburg, VA where it was



operated from 8 August to 13 September 1990. The separation between the WPL radiometer and the three beacon receivers was about 20 m. Antennas were directed along the slant path to the OLYMPUS satellite (13.9 deg elevation, 109.4 deg azimuth). Thus, all instruments viewed approximately the same region of the sky. However, because of the different antenna sizes employed by the various instruments (see Table I), each instrument observed slightly different fields of view. The antennas of the NOAA/WPL radiometer are designed to produce approximately equal 2.5 deg beamwidths at each frequency (Hogg, et al., 1983). Further details of the WPL radiometer have been discussed at previous NAPEX meetings and will not be repeated here. However, it should be noted that the NOAA/WPL radiometers are calibrated using the "tipping curve" method which includes the effects of the antenna.

Radiometers in the OLYMPUS beacon receivers are total power systems that measure atmospheric emission in a 25 MHz bandwidth within a few tens of MHz from the beacon operating frequencies. The radiometers are operated in temperature controlled enclosures to maintain a constant gain without switching. Components ahead of the input to the radiometers include the antenna, low noise amplifier, and bandpass filter. The antennas used with the beacon receivers are not capable of being moved over a sufficient range of elevation angles to perform tipping curve calibrations. Instead, initial calibrations were performed using cold (~80 K) loads and hot loads (273-303 K). This technique does not allow for calibration of the antenna system. In addition, uncertainties about the emissivity of the cold and hot loads reduce the absolute accuracy of the calibration to about  $\pm 1$  K. One objective of the participation by NOAA was to help reduce the uncertainty in calibration of the 19.77 and 29.65 GHz radiometer channels.

Table I. Characteristics of Microwave Radiometers Employed in OLYMPUS Propagation Observations at Blacksburg, VA.

<u>Frequency(GHz)</u>	<u>Antenna</u>		<u>Bandwidth (MHz)</u>	<u>Approximate Sensitivity (K)</u>	<u>Integration Time (s)</u>
	<u>Aperture (m)</u>	<u>Beamwidth (deg)</u>			
Virginia Tech					
12.50	4.0	0.44	25	$\leq 1.0$	1-3
19.77	1.5	0.72	25	$\leq 1.0$	1-3
29.65	1.2	0.60	25	$\leq 1.0$	1-3
NOAA/WPL					
20.60	0.51	2.50	500	$\leq 0.3$	1
31.65	0.51	2.50	500	$\leq 0.3$	1
90.00	0.15	2.50	500	$\leq 0.4$	1

### 3.0 Initial Results

It had been planned to present a preliminary comparison of brightness temperatures measured by the NOAA and Virginia Tech radiometers at NAPEX XV. However, as the Virginia Tech radiometric data are not yet available, we shall instead discuss observations of attenuation made by the two instruments during August and September 1990.

#### 3.1 Comparison of Beacon and Radiometric Attenuation Observations

Examples of beacon fade data and simultaneous observations of attenuation at 20 and 31 GHz by the WPL radiometers are shown in Figs. 1 and 2. The relative values of the radiometric attenuation data have been adjusted with a constant offset in order to match approximately the beacon levels during clear weather. Excellent correlation between the beacon and radiometer is found up to an attenuation of about 15 dB. Higher values of radiometric attenuation were not calculated due to uncertainties in the brightness measurement and the mean radiating temperature of the atmosphere. In general, the beacon and radiometer attenuation measurements of Fig. 1 vary in synchronism during a fade. However, Fig. 2 reveals several cases where radiometer and beacon attenuations do not track closely. These instances are believed to be caused by regions of attenuation by clouds or precipitation on relatively small spatial scales which do not simultaneously fill the different antenna beamwidths of the various instruments. Attenuation measured by the radiometers in the beacon receivers would be expected to track more closely with the beacon level since common antennas are used. We will determine if the latter expectation is the case when the Virginia Tech radiometer data become available.

#### 3.2 Attenuation Statistics

Cumulative distributions of attenuation at 20, 30, and 90 GHz derived from the WPL radiometer are shown in Figs. 3-5. Although the data were measured along a slant path, they have been normalized to equivalent zenith values for comparison with previous measurements at other geographic locations. The distributions appear to have the same shape as seen previously. Mean attenuation data at Blacksburg and mean values for locations previously examined are shown in Table II. Note that the values include both clear and cloudy data. The greater mean equivalent zenith attenuation at Blacksburg may be due to measurements being made along a slant path with frequent rain showers present. Future analyses shall compare only the clear sky attenuation data to determine the relative background attenuations at the different locations.

Table II. Comparison of Mean Attenuation Observed at 20.6, 31.65, and 90.0 GHz for Locations Examined to Date. Clear and Cloudy Data Combined.

<u>Location</u>	<u>Mean Zenith Attenuation (dB)</u>		
	<u>20.6 GHz</u>	<u>31.65 GHz</u>	<u>90.0 GHz</u>
San Nicolas Island July 1987	0.398	0.321	1.128
Denver, Colorado December	0.159	0.158	0.411
August	0.497	0.278	1.190
Wallops Island, Virginia April/May	0.428	0.398	1.239
Blacksburg, Virginia* August/September	0.661	0.444	1.711

\*Blacksburg data are normalized to zenith from 13.9 deg slant path

---

#### 4.0 Summary

In general, excellent correlation was observed between direct measurements of OLYMPUS satellite attenuation by the Virginia Tech beacon receivers and radiometric attenuation observations by the NOAA/WPL multichannel microwave radiometer. Occasional differences are likely to be the result of different antenna beamwidths employed by the two measurement systems. Equivalent zenith attenuation values observed at Blacksburg are greater than seen at previous locations. This result may be due to observations being made on a slant rather than a vertical path.

#### 5.0 Future Plans

Future analysis will include comparison of NOAA and Virginia Tech brightness temperature observations to determine if systematic differences exist. Based upon these comparisons, the feasibility of calibrating the beacon receiver radiometers with an independent radiometer will be evaluated. Finally, the radiometric attenuation statistics recorded during clear weather will be analyzed to determine the variability of the background attenuation as a function of path-integrated water vapor.

References:

- Hogg, D. C., F. O. Guiraud, J. B. Snider, M. T. Decker, and E. R. Westwater, 1983: A steerable dual-channel microwave radiometer for measurement of water vapor and liquid in the troposphere. *J. Climate Appl. Meteorol.*, **22**, 789-806.
- McKeeman, John C., 1990: Olympus propagation studies in the U. S. - Receiver development and the data acquisition system. Proceedings of the Fourteenth NASA Propagation Experimenters Meeting (NAPEX XIV), JPL Publication 90-27, 43-53.
- Snider, J. B., M. D. Jacobson, and R. H. Beeler, 1989: Observations of attenuation at 20.6, 31.65, and 90.0 GHz - Preliminary results from Wallops Island, VA. Proceedings of the Thirteenth NASA Propagation Experimenters Meeting (NAPEX XIII), JPL Publication 89-26, 138-144.
- Stutzman, Warren L., 1990: Olympus propagation studies in the U. S. - Propagation terminal hardware and experiments. Proceedings of the Fourteenth NASA Propagation Experimenters Meeting (NAPEX XIV), JPL Publication 90-27, 36-42.

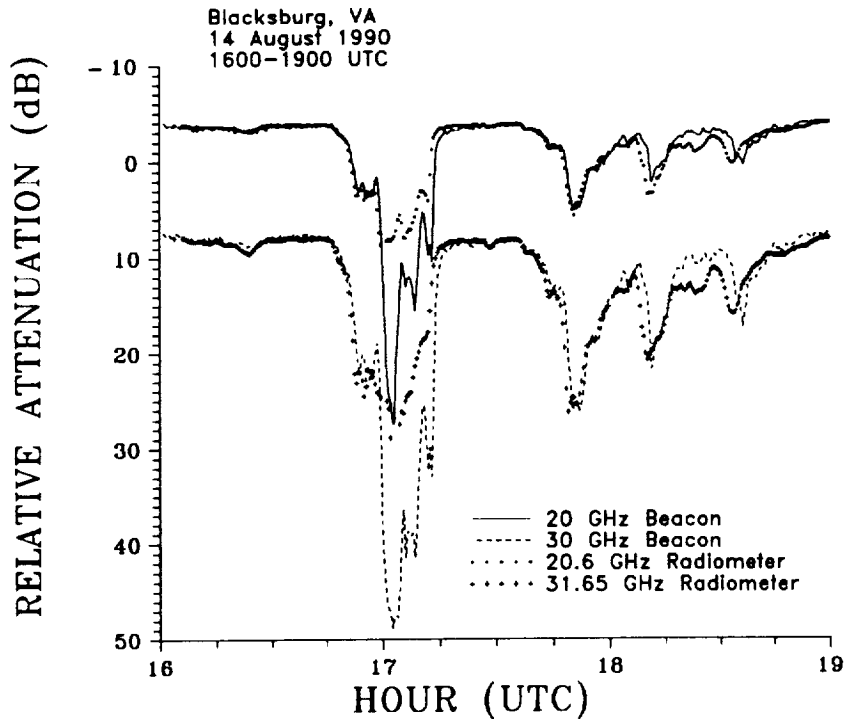


Figure 1. Comparison of attenuation of OLYMPUS satellite beacons measured by Virginia Tech receivers and by NOAA/WPL microwave radiometer on 14 August 1990 during periods of clear skies, clouds, and precipitation.

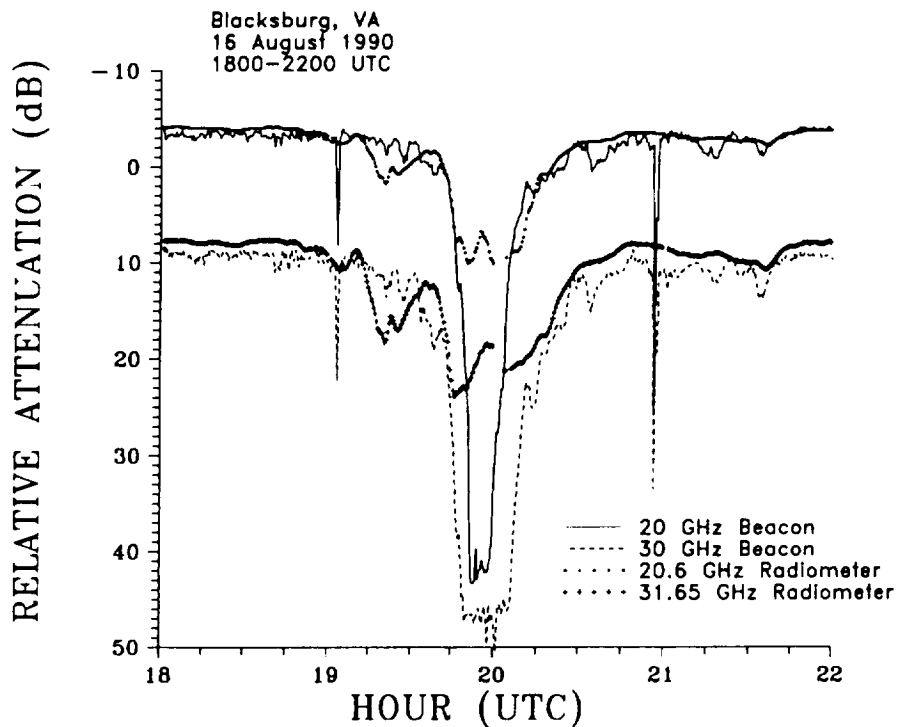


Figure 2. Comparison of attenuation of OLYMPUS satellite beacons measured by Virginia Tech receivers and by NOAA/WPL microwave radiometer on 16 August 1990 during periods of clear skies, clouds, and precipitation.

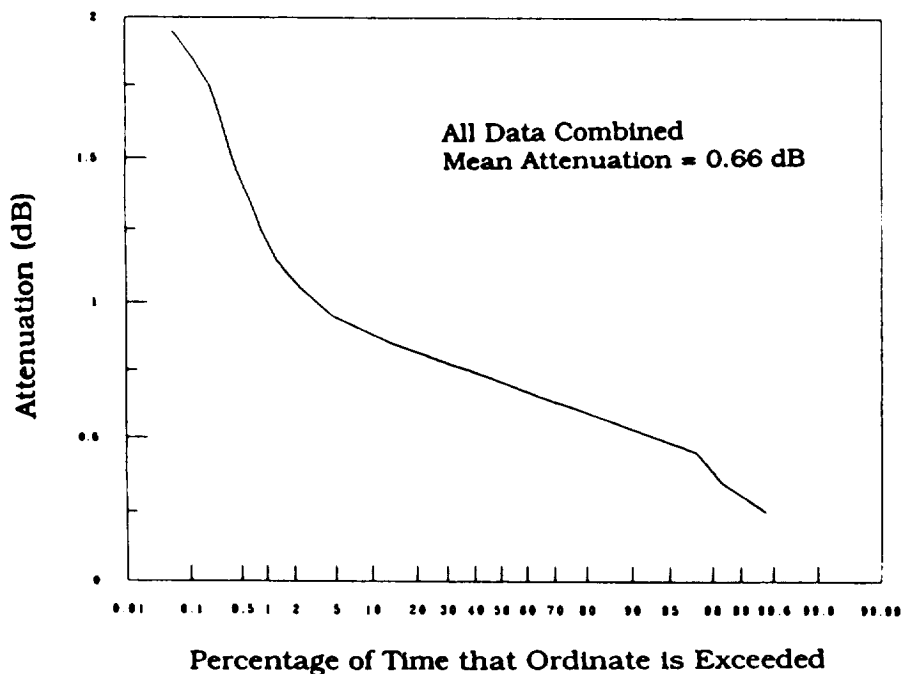


Figure 3. Cumulative distribution of zenith-normalized attenuation at 20.6 GHz measured by NOAA/WPL microwave radiometer during both clear and cloudy weather at Blacksburg, VA, 7 August - 12 September 1990.

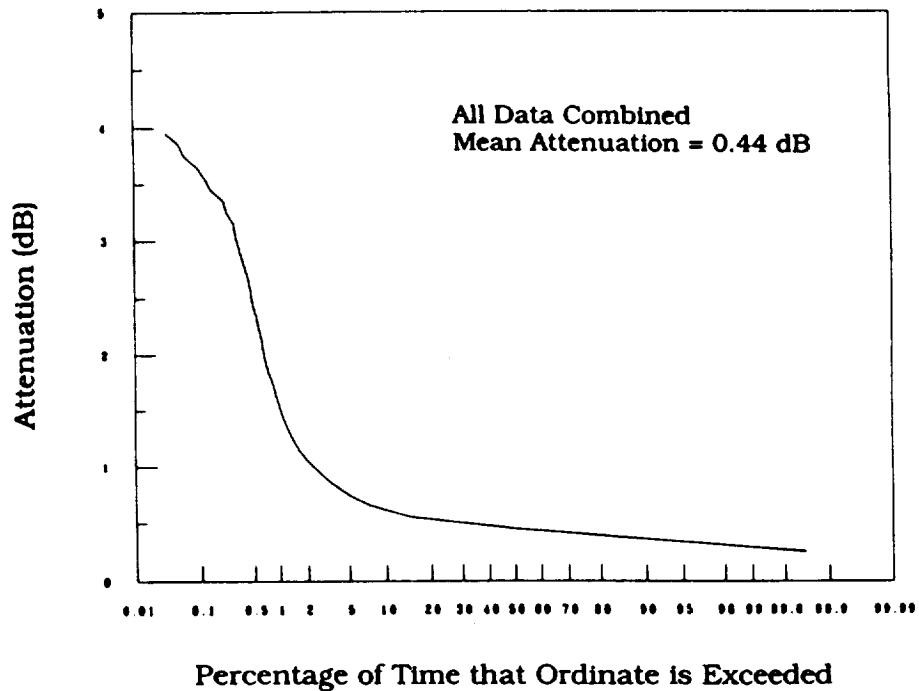


Figure 4. Cumulative distribution of zenith-normalized attenuation at 31.65 GHz measured by NOAA/WPL microwave radiometer during both clear and cloudy weather at Blacksburg, VA, 7 August - 12 September 1990.

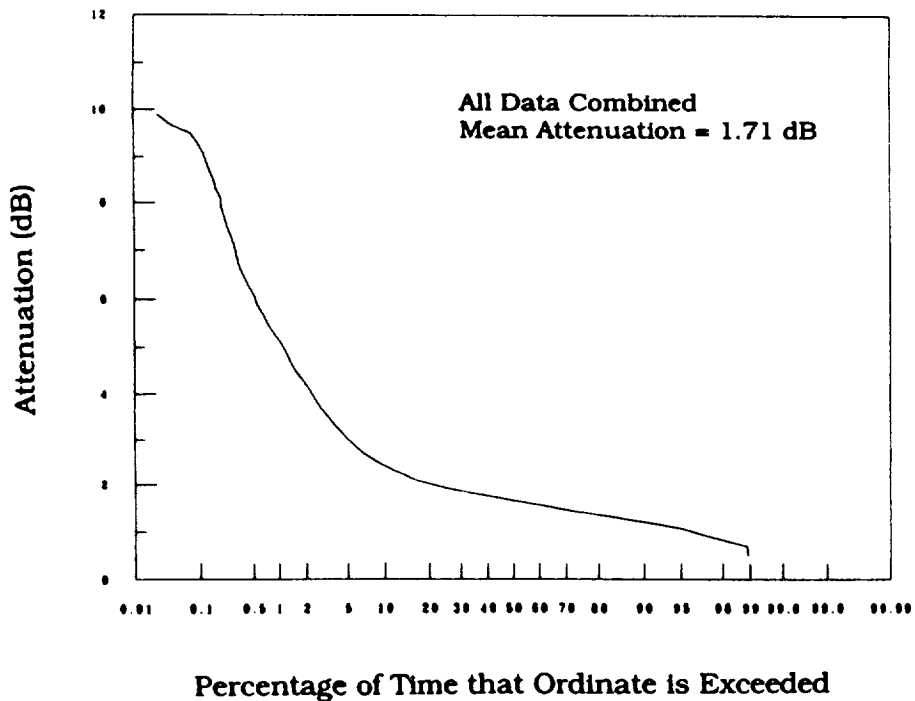


Figure 5. Cumulative distribution of zenith-normalized attenuation at 90.0 GHz measured by NOAA/WPL microwave radiometer during both clear and cloudy weather at Blacksburg, VA, 7 August - 12 September 1990.

## Satellite Sound Broadcast Propagation Measurements

Wolfhard J. Vogel and Geoffrey W. Torrence  
 Electrical Engineering Research Laboratory, The University of Texas  
 10100 Burnet Road, Austin, TX 78758-4497

**Abstract**-Power transmitted from atop a 17.9 m tower in simulation of a satellite signal, emitted by a tone generator sweeping from 700 to 1800 MHz, was received using a 90° beamwidth linearly scanning antenna at many locations inside six buildings of solid brick, corrugated sheet-metal, wood-frame, mobile home, and concrete wall construction. The signal levels were found to have much structure in the spatial and frequency domain, but were relatively stable in time. Typically, people moving nearby produced less than 0.5 dB variations, whereas a person blocking the transmission path produced 6 to 10 dB fades. Losses, which at an average position in a room increased from 6 to 12 dB over 750 to 1750 MHz, could be mitigated to 2 to 6 dB by moving the antenna typically less than 30 cm. Severe losses (17.5 dB, mitigated to 12.5 dB) were observed in a concrete wall building, which also exhibited the longest multipath delays (>100 ns). Losses inside a mobile home were even larger (>20 dB) and independent of antenna orientation. The losses showed a clear frequency dependence.

### I. Introduction

Several efforts [1]-[3] are underway to develop systems for direct broadcasting of radio programs from geostationary satellites (BSS-Sound) to inexpensive personal receivers in houses and cars. Such features as a shareable space-segment in a safe location, tailored footprints from global to local using multiple spot-beams, and flexible sound quality through digital signal processing combine to make this an attractive technology. Three potential frequency bands for BSS-Sound have been proposed by the FCC: 728-788 MHz, 1493-1525 MHz, and 2390-2450 MHz. This paper reports on signal strength measurements made inside six buildings over the 700-1800 MHz band, using a tower-mounted transmitter in simulation of a satellite. Radio wave building attenuation measurements were reported [4] at 860, 1550, and 2569 MHz, using the ATS-6 geostationary satellite as a source platform. The average attenuation into wood-frame houses with and without brick veneer was found to be 6.3 dB for elevation angles from 36° to 55° and increasing by 3 dB from 860 to 2569 MHz. The widely spaced, single frequency results presented were spatially averaged, however, allowing no conclusions about the fine structure of signal levels within a room. The experiment described here has been carried out to determine the excess path loss associated with reception inside buildings. Such information is needed for the preparation of international standards [5].

### II. Experimental Aspects

#### **A. Instrumentation**

The measurement system makes use of an erectable 17.9 m tall tower attached to a van which has been outfitted with radio transmission and reception equipment as well as a data acquisition and control computer. Continuous wave (constant frequency or swept) signals from a tracking generator synchronized to a microwave spectrum analyzer are fed through a cable to the top of the tower, amplified, and transmitted towards the location under test. There they are received by an antenna which is mounted to a linear positioner about 1.4 m above ground and pointed towards the transmitter. After amplification the received power is conducted through an 80 m cable back to the spectrum analyzer in the van. The positioner can be manually oriented to allow computer controlled antenna motion along any arbitrary axis. For the measurements presented here the receiving antenna position was varied in 16 steps of 0.05 m, resulting in a

total scan distance of 0.8 m along either the vertical direction or in the horizontal plane parallel with or at right angles to the propagation path.

The measurement system, shown as a block diagram in Figure 1, functions like a scalar network analyzer. It is capable of determining transmission loss over a maximum frequency span from 700 to 1800 MHz with a resolution bandwidth of between 10 kHz and 1 MHz and an overall accuracy of better than 0.5 dB. By varying the transmitter to receiver range from 15 to 75 m, elevation angles of 12° to 48° can be obtained. Both antennas are circularly polarized cavity-backed spirals with 90° half-power beamwidth and gain increasing from -2.5 to 4.5 dB over the 700 to 1800 MHz frequency range. They were chosen because of their wide bandwidth and relatively constant directivity characteristics. The pertinent system parameters are summarized in Table I below.

**Table I: Pertinent System Parameters**

Frequency	
Coverage:	700 MHz to 1800 MHz
Span:	0 Hz to 1100 MHz
Resolution:	1 MHz to 10 kHz
Amplitude	
Range:	45 dB
Resolution:	0.2 dB
S/N Ratio:	>45 dB
Error:	<0.5 dB
Antennas	
Type:	Cavity Backed Spiral
Polarization:	Right-hand Circular
Beamwidth:	90° (3 dB)
Gain:	-2.5..+4.5 dB
Elevation Angle:	12° to 45°

## B. Calibration Method

The system was calibrated to power levels relative free space with height-gain measurements performed over the entire 1100 MHz frequency range at distances from 15 to 75 m in a flat open field. In this situation the received signal mainly consists of a combination of two waves: the direct wave and the specular ground reflection. Increasing the height of the receiver causes additional delay of the reflected relative to the direct wave and changes the pattern of con- and destructive interference as a function of frequency. Typical peak-to-peak received power variations in a full frequency sweep were 10 dB at 75 m and 1.5 dB at 15 m. The free space level was determined by linearly averaging the composite maximum and minimum of the power levels versus frequency obtained at 16 vertical positions from 2.0 to 2.8 m.

An example of such a procedure for the distance of 25 m (elevation angle 32°) is depicted as Figure 2. The vertical scale has been adjusted relative to free space using the overall calibration results. Absolute power levels consistent with propagation loss calculations and with errors of typically less than 0.5 dB for all frequencies and distances were obtained. Some of the remaining ripple is due to the residual impedance mismatch between the receiving antenna and the cable to the low-noise amplifier.

## C. Measurement Sites

The measurement campaign covered six locations and many positions at each location. The characteristics of the receiving locations are as follows:



**BRC 16-4:** A corner room office (about 6x7 m) with two large windows in a single story building. The exterior walls are of concrete-block masonry. They are covered with plasterboard on the inside. The ceiling is formed by acoustic tiles suspended at 3 m height from metal hangers. The double-glazed reflective window in the wall exposed to the transmitter has a modern aluminum frame, but no screening, and takes up about 3/8 of the wall. The roof of the building is flat, consisting of concrete panels supported by steel beams. The room contains wooden office furniture and two large plants. Trees and shrubs on the outside of the building did not obstruct the line-of-sight (LOS) between transmitter and receiver. The transmitter was at a distance of 33 m from the closest inside receiver location, resulting in an elevation angle of 27.5°. The azimuth angle between the wall and the line-of-sight was 50°.

**BRC 15-24:** A small room (about 3x4 m) with two windows taking up about 5/8 of the exterior wall. A cable chase separates the two windows. The construction is similar to that of BRC 16-4. The room is furnished with metal filing cabinets. The location was illuminated over the top of several trees at an elevation angle of 18° from a distance of 52 m, but the LOS between transmitter and receiver was clear. The azimuth angle between the wall and the LOS was 50°.

**Commons:** A 5x5 m corner foyer with a large reflective glass door taking up half of one outside wall. Wooden double doors lead from this room to the interior of the building. The external walls are of concrete tilt-wall construction; internal walls have metal frames covered with plasterboard. The ceiling consists of acoustic tile suspended at 3.5 m height. Several small trees in front of the measurement location did not shadow the propagation path. The transmitter was 57 m from the building at an azimuth angle of 45°, making both sides of the outside corner visible. The elevation angle was 16°.

**Metal Shack:** A 3x6 m shack (approximately 2.5 m high) with corrugated sheet-metal walls and roof on the outside and plywood on the inside. The shack stands in an open field. It has one small, unscreened window on each of the two narrow sides and a metal covered door centered between two windows (also unscreened) on one of the long sides, which was in the direction to the transmitter. The distance to the transmitter was 35 m, the elevation angle 25°, and the azimuth angle between the wall and the LOS was 60°.

**Farm House:** An 1870 vintage restored and furnished 2-story ranch house with wood siding. The walls are filled with rock wool and covered with sheetrock on the interior and wood siding on the exterior. No metallic heat-shield is installed. The attic is insulated. The gabled roof is covered with wood shingles. Windows have wooden sashes and are not covered with metallic screens. There are two large trees near the house, but the propagation path was not shadowed. Measurements were made in two rooms on the ground floor and one room on the second level. The distance to the transmitter was 35 m, the elevation angle 25°, and the azimuth angle between the wall and the LOS was 45°.

**Mobile Home:** A 40'x8' empty mobile trailer home with sheet-metal exterior and aluminum frame windows with metal screens. The distance to the transmitter was 35 m, the elevation angle 25°, and the azimuth angle between the wall and the LOS was 45°.

### III. Measurement Results

#### **A. Data Examples**

An example of the power received versus frequency from 700 to 1800 MHz during a vertical position scan near a window in BRC 15-24 is given in Figure 3. The two outside traces in the plot are the composite maximum and minimum signal levels measured at 16 positions with 5 cm spacing. The trace meandering between the outside two represents the received power versus frequency at just one of the positions. At best, the signal was attenuated by 0 to 5 dB; at worst troughs of over 20 dB were found. Figures 4 and 5 more clearly show signal levels in this scan at two positions separated by 50 cm. In the first case, the deepest troughs happen to be located near 800 and 1100 MHz; in the second case one is close to 1400 and another to

1500 MHz. Over a frequency span of about 25 MHz, from 725.3 to 749.5 MHz, a trough near the center position of the scan changes its location and depth only slightly, as depicted in Figure 6.

Taken in a different building, the Metal Shack, two frequency sweeps from a horizontal position scan which were separated by 50 cm are shown in Figures 7 and 8. In contrast to the similarity of the two previous scans, these two scans are quite dissimilar. At position 2 the receiving antenna was looking through the open door, at position 12 it was shielded by the wall between the door and the window, resulting in the loss of most of the direct signal and consequently greater variations due to multipath scattering across the entire frequency span. A scan taken in Commons in the vicinity of the window at a position where the LOS penetrated the exterior wall is shown in Figure 9. As in Fig. 8, the average attenuation was 15 to 20 dB, but the variations with frequency are faster, indicating multipath contributions arriving from greater distances. Moving the antenna by 50 cm resulted in a LOS path through the window, and as can be seen in Figure 10, the signal level increased across the band, with some frequencies being enhanced to above the free space level by constructive interference, probably from the specular ground reflection. Figure 11 illustrates the high degree of correlation with frequency for a span of 25 MHz at 1500 MHz over an 80 cm motion, except at very low signal levels.

It is easy to calculate that in the case where both a direct wave and a reflected wave are received, the resulting linear power has a sinusoidal variation across the bandwidth of the receiver with a frequency-periodicity that is inversely proportional to the delay of the reflection relative to the direct path. The periodogram of the signal level versus frequency, therefore, represents an estimate of the time delay spread spectrum. This has been determined for the scans of Figs. 4, 8, and 9, and the results, shown in Fig. 12, give the percentage of the delayed power with delays less than the abscissa. The small room, BRC 15-24, suffered the shortest delays with 95% of the multipath power delayed by less than 15 ns. In the Metal Shack, the percentage increased rapidly after about 17 ns, which corresponds to the turn-around time between the receiver and the walls. In the Commons building, a large structure, more than 10% of the multipath power was received with delays greater than 80 ns (24 m distance).

## B. Time Variations

In order to assess the time-variability of the received power, repeated frequency sweeps were obtained at many measurement locations while keeping the receiving antenna stationary. Statistics of amplitude changes at each frequency were determined from 99 sweeps taken over a period of about 6.5 minutes, with each sweep lasting 1 s. Some typical results are shown in Figs. 13 and 14, which give the maximum, average, and minimum power versus frequency and the standard deviation versus the average, respectively. The gross structure of the losses remains quite stable, whereas the standard deviation increases with falling average power level, presumably as more distant and variable multipath components become effective.

By making single frequency measurements over durations of 100 seconds, it was determined that power variations within the 1 s full sweep time of the receiver tended to be smaller than the 0.5 dB measurement accuracy of the equipment to signal levels of about -15 dB. Variations brought about by scattering from people walking in the vicinity of the receiving antenna were also quite small, except when someone moved directly into the LOS, in which case fades of 6 to 10 dB were observed. We conclude that time variations of near free-space-level power levels transmitted into buildings are not of primary importance in characterizing the transmission channel.

## C. Losses

In each of the six buildings, at between eight and twenty locations, horizontal and vertical scans were taken. The power levels obtained were analyzed to derive losses at the average and at the best position in the scans for bandwidths of 1, 2, 5, 9, 18, 45, and 90 MHz from 700 to 1800 MHz. As no bandwidth dependence of the losses was found, Figure 15 gives probability contours for the signal level being less than the ordinate at 99, 90, 50, 10, and 1% at the average position in the scan for BRC 15-24 averaged over all the bandwidths

listed above. The median loss increased from 5 dB at 750 MHz to 13 dB at 1750 MHz. Assuming that the receiving antenna was placed at the best position in a scan, the median losses were reduced, varying from 1.5 dB to 7 dB over the same frequency span. The central percentiles at that position show less variability than those at the average position, especially at the low frequency end. Table II summarizes the losses observed in all buildings. By moving from the average position to the best position, the signal level can be improved by about 3 to 6 dB. The trend is for higher frequencies to suffer more attenuation when losses are moderate. In Commons losses are rather uniformly high across the full frequency span.

**Table II: Median Power Levels as a Function of Frequency.**

<u>Building</u>	Average Position	Best Position
	<u>750..... 1750 MHz</u>	<u>750..... 1750 MHz</u>
BRC 16-4	-5.....-11 dB	-2.....-6 dB
BRC 15-24	-5.....-14 dB	-2.....-5 dB
Metal Shack	-9.....-11 dB	-5.....-6 dB
Commons	-17.....-18 dB	-12.....-13 dB
Farm House	-5.....-11 dB	-3.....-5 dB
Mobile Home	-20.....<-24 dB	-16.....-22 dB

After averaging over all frequencies, the probability distribution functions (PDF) at the average and best positions were calculated for each building and the results for the Metal Shack have been plotted against a normal probability scale in Figs. 17 and 18. The means and standard deviations derived with linear regressions are summarized in Table III.

**Table III: Signal Distributions at the Average and Best Position.**

<u>Building</u>	Average Position	Best Position
	<u>Mean.....STD</u>	<u>Mean.....STD</u>
BRC 16-4	-7.9 dB .... 5.5 dB	-4.2 dB .... 4.2 dB
BRC 15-24	-9.1 dB .... 4.4 dB	-5.4 dB .... 3.7 dB
Metal Shack	-9.7 dB .... 6.3 dB	-5.2 dB .... 4.9 dB
Commons	-15.4 dB .... 8.4 dB	-9.7 dB .... 6.7 dB
Farm House	-9.0 dB .... 4.5 dB	-5.4 dB .... 3.7 dB
Mobile Home	-24.9 dB .... 3.8 dB	-19.8 dB .... 3.4 dB

In the first three buildings all distributions deviate from normal at the upper signal level tails, as can be seen in the examples of Figs. 17 and 18; in Commons the fit is poor across the entire range. Loss measurements performed at 900 MHz [6] into a well shielded metal building have shown the signal amplitudes in a multipath environment to be Rayleigh distributed, but all amplitude data collected in this experiment except for the Mobile Home case were obtained under less severe attenuation conditions and the Rayleigh distribution did not provide a better fit than the normal one.

For each building, using all the data collected, the percentage of positions P (%) at which the average received power was less than a given threshold THR (from -3 to -18 dB) has been determined. For example in the Metal Shack as a function of frequency F (in GHz) from 50 to 65 percent of positions had signals lower than -9 dB. At all six buildings P can be approximated by the relations:

$$P = A + B * F, \tag{1}$$

where

$$A = A_0 + A_1 * THR, \tag{2}$$

and

$$B = B_0 + B_1 \cdot \text{THR.} \quad (3)$$

Table IV summarizes the coefficients derived for the six buildings, including the rms error of P in percentage points.

**Table IV: Fit Coefficients for the % Positions at Which the Signal is Below a Threshold**

Building	A0	A1	B0	B1	RMS-Error
BRC 16-4	66.2	5.3	16.0	-0.54	4.0
BRC 15-24	74.1	7.0	20.3	-1.2	8.4
Metal Shack	97.8	6.2	-3.8	-1.5	3.4
Commons	105.7	3.1	-7.8	-0.34	2.8
Farm House	67.2	5.2	24.9	-0.1	6.1
Mobile Home	61.9	-1.3	11.1	-0.02	13.2

#### IV. Summary and Conclusion

The experiment described has been performed to allow a more detailed description of radio wave propagation into buildings than has been hitherto available in the literature. Such comprehensive information is needed for the design of BSS-Sound systems, which will have to mitigate unfavorable propagation characteristics with additional power, coding, or space- and frequency-diversity. Although measurements were made into dissimilar buildings of brick, metal, wood-frame, or concrete construction, many similarities among the results were uncovered. Temporal variations at levels within about 15 dB of the free space value were only of the order of 0.5 dB. Only in one of the buildings were delays greater than 50 ns of importance. The predominating effects of short delays for satellite systems have previously been observed in the land mobile case [7] and are a feature of near free-space propagation.

Losses increased with frequency, although many specific counter examples could be found. In light of the demonstrated frequency insensitivity of multipath effects, increased losses at higher frequencies are believed to be due to greater absorption by the walls of the buildings studied. By moving the receiver to a position of a signal strength crest, losses could be reduced.

#### **References**

- [1] Arora, O. P. and Narayanan, K., "Sound Broadcasting-Satellite System for a National Coverage in Developing Countries," *Telecommunication Journal*, Vol. 51, No. 12, Dec 1984, pp. 645-649
- [2] Ratliff, P. A., "UHF satellite sound broadcasting technology," *IEEE Int. Conf. on Comm.*, Philadelphia, PA, 12-15 June 1988, pp. 141-146
- [3] Miller, J. E., "Application of coding and diversity to UHF satellite sound broadcasting systems," *IEEE Trans. on Broadcasting*, Vol. 34, No. 4, Dec 1988, pp. 465-475
- [4] Wells, P. I., "The Attenuation of UHF Radio Signals by Houses," *IEEE Trans. on Veh. Technology*, Vol. VT-26, No. 4, Nov. 1977, pp. 358-362
- [5] CCIR, "Technical Information to define the practical system parameters for satellite sound broadcasting (Recommendation No. 2 of WARC ORB-85)," *CCIR Doc. JIWP/ORB(2)/90-E*, Geneva, Switzerland, Dec. 1987
- [6] Hoffman, H. D. and Cox, D. C., "Attenuation of 900 MHz Radio Waves Propagating into a Metal Building," *IEEE Trans. on Ant. and Prop.*, Vol. AP-30, No. 4, July 1982, pp. 808-811
- [7] Vogel, W. J. and Hong, U.-S., "Measurement and Modeling of Land Mobile Satellite Propagation at UHF and L-Band," *IEEE Trans. on Ant. and Prop.*, Vol. AP-36, No. 5, May 1988, pp. 707-719

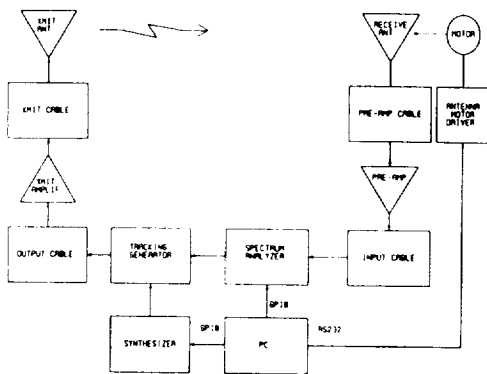


Fig. 1. The DBS-R measurement system functions like a scalar network analyzer in the 700-1800 MHz frequency range.

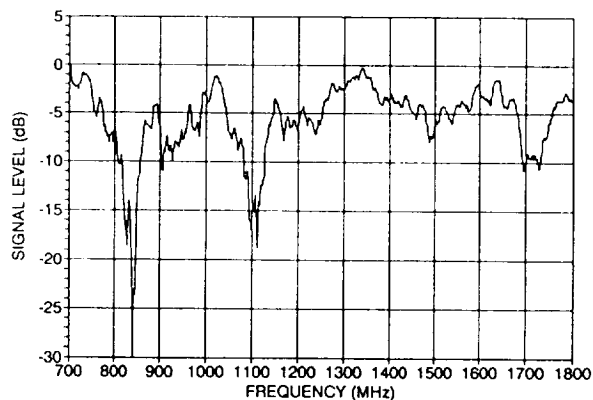


Fig. 4. The received power at one position in the vertical scan of Fig. 3 shows the deepest fade troughs near 850 and 1100 MHz.

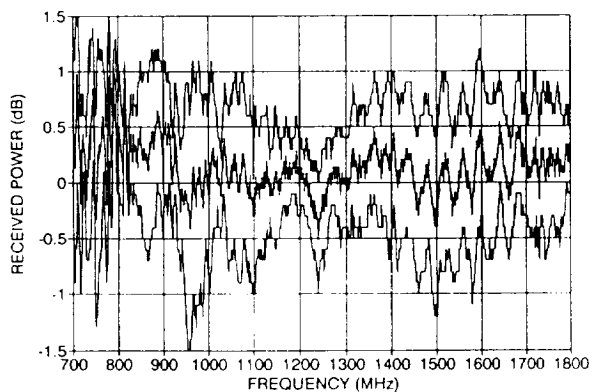


Fig. 2. Equipment calibration to 0.5 dB accuracy accounts for specular ground reflections observed in an open field.

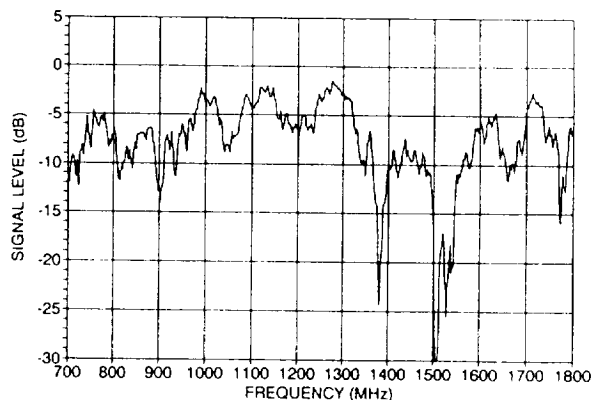


Fig. 5. At another position, some 50 cm higher than in the previous figure, the deepest fade troughs appear close to 1400 and 1500 MHz.

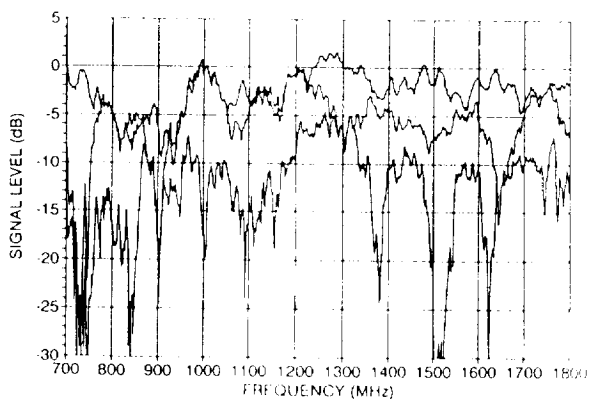


Fig. 3. The composite maximum and minimum of the received power in a vertical position scan near window in BRC 15-24, and a single position trace.

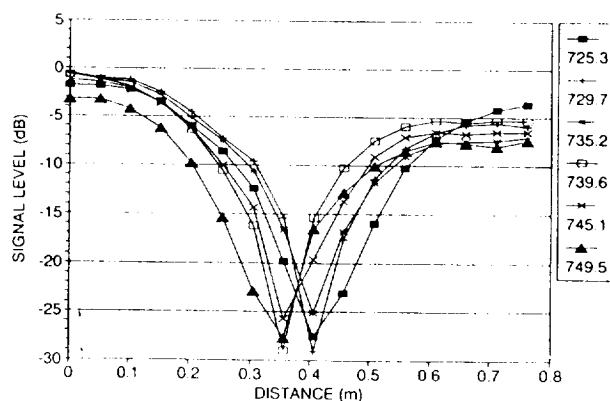
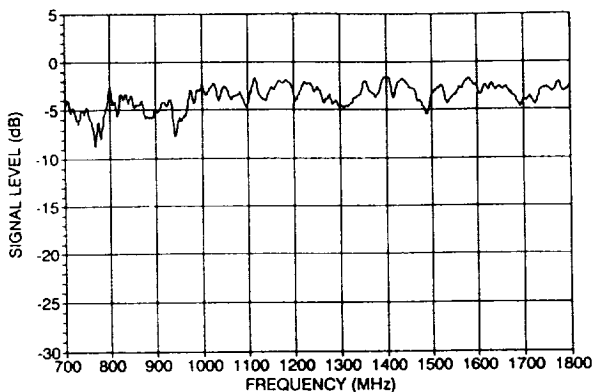
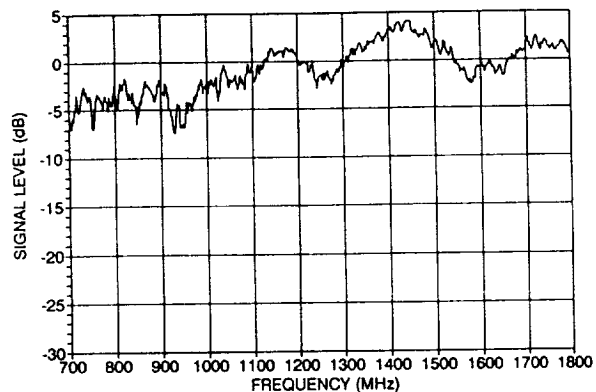


Fig. 6. The received signal level in a fade trough versus distance at six frequencies from 725.3-749.5 MHz spaced by about 5 MHz. The scan is same as shown in Fig. 3.



**Fig. 7.** The signal level observed at position 2 during a horizontal position scan near the open door, but inside of the Metal Shack.



**Fig. 10.** A frequency sweep taken in Commons 50 cm from the previous example, but now the line-of-sight path penetrated the window.

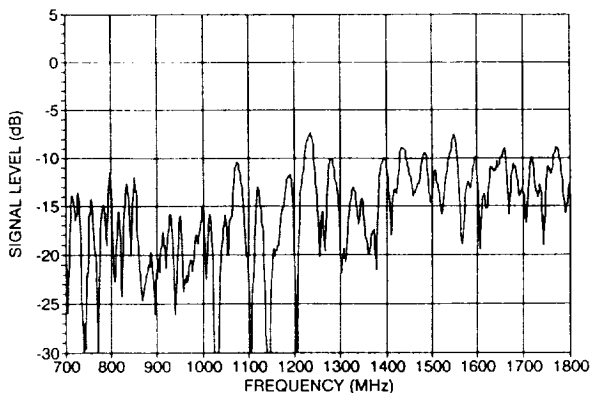


**Fig. 8.** The signal level observed at position 12, 50 cm from the previous location, with the path now obstructed by a corrugated sheet-metal wall.

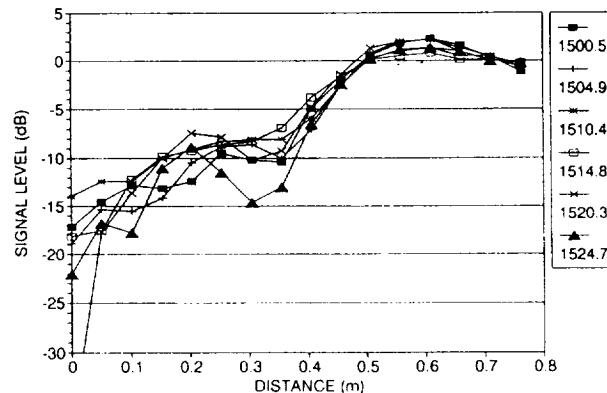


**Fig. 11.** The signal level versus distance, at six frequencies from 1500.5-1524.7 MHz. The receiver LOS moves from behind the wall of Commons to the window.

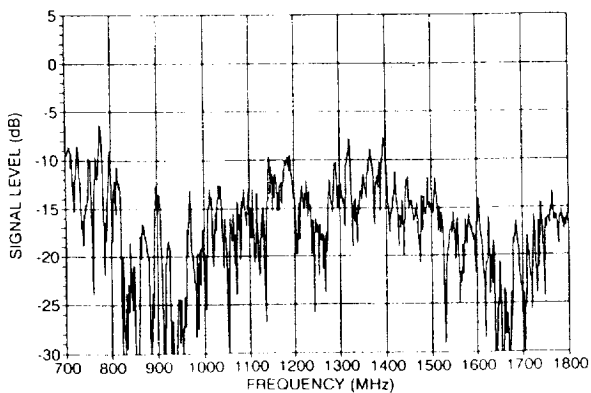


**Fig. 9.** A frequency sweep taken in Commons in the vicinity of the large window, but where the line-of-sight path penetrated the exterior concrete wall.

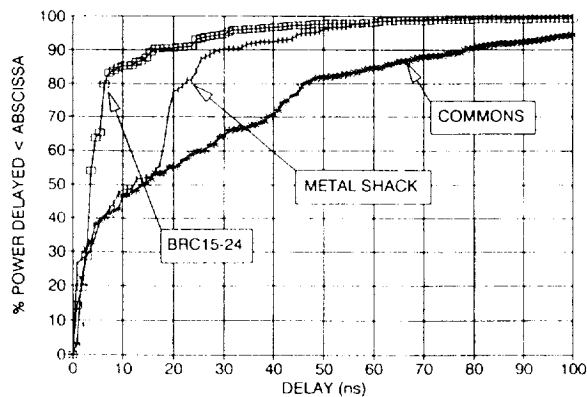


**Fig. 12.** The CPF of time delay spread at one position in three buildings. The most lossy structure, Commons, had the longest delays.

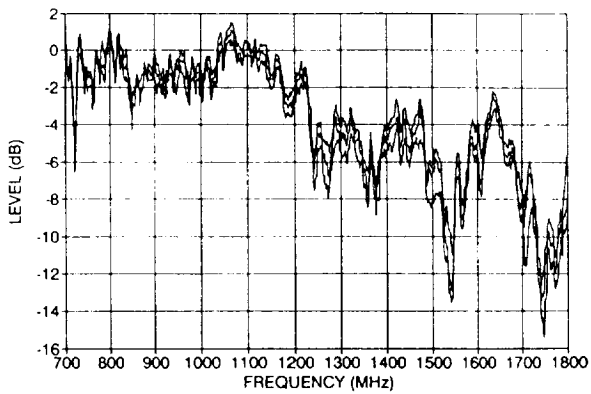


Fig. 13. Maximum, average, and minimum for 99 frequency sweeps taken in BRC 16-4 over a period of about 6.5 minutes, with each sweep lasting one second.

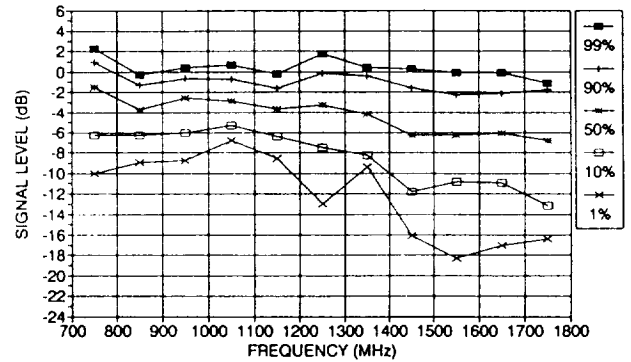


Fig. 16. Probability contours for the signal level being less than the ordinate at 99, 90, 50, 10, and 1% at the best position in the scan for BRC 15-24.

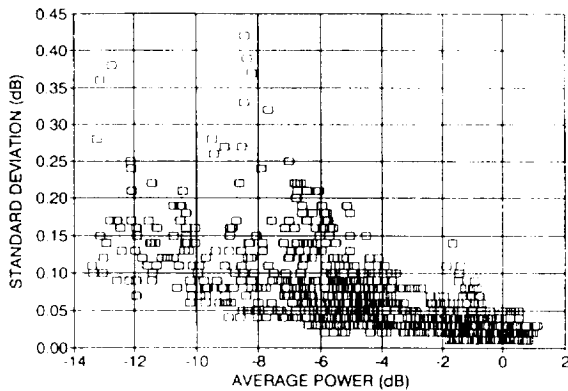


Fig. 14. The standard deviation of time variations gets larger in the deeper fade troughs, where more distant and variable multipath components become relevant.

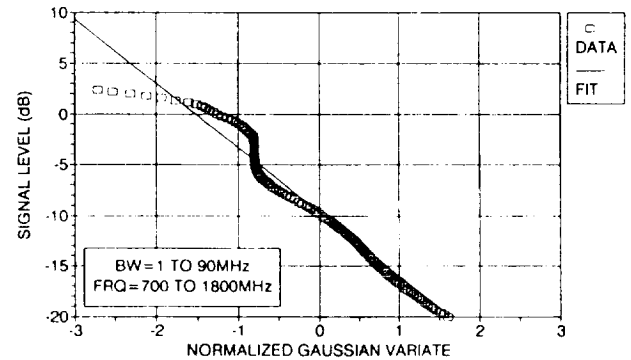


Fig. 17. Gaussian scaled distribution of the signal level at all average positions in the Metal Shack, with a mean of -9.7 dB and a standard deviation of 6.3 dB.

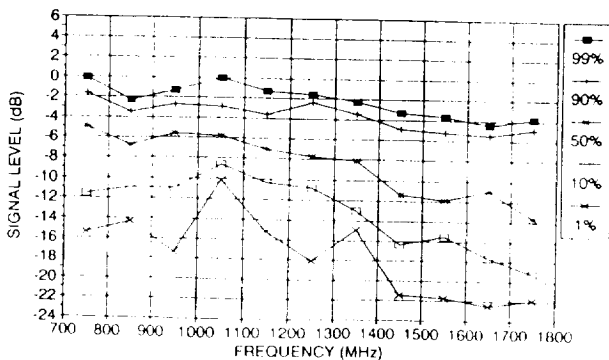


Fig. 15. Probability contours for the signal level being less than the ordinate at 99, 90, 50, 10, and 1% at the average position in the scan for BRC 15-24.

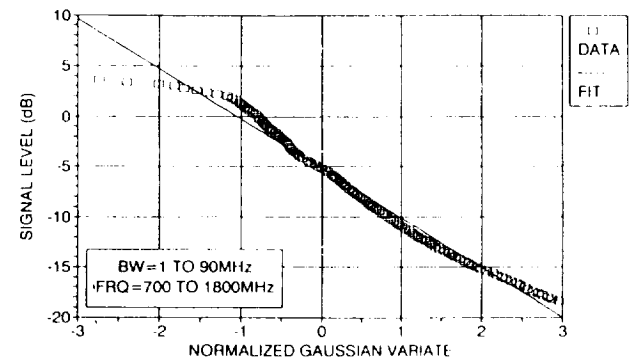


Fig. 18. Gaussian scaled distribution of the signal level at all best positions in the Metal Shack, with a mean of -5.2 dB and a standard deviation of 4.9 dB.

**AN OVERVIEW OF THE TEXT  
"PROPAGATION EFFECTS FOR LAND-MOBILE-SATELLITE SYSTEMS:  
EXPERIMENTAL AND MODELING RESULTS"**

Julius Goldhirsh\* and Wolfhard J. Vogel#

\*The Johns Hopkins University, Applied Physics Laboratory, Laurel, Maryland

#The University of Texas, Electrical Engineering Research Laboratory, Austin, Texas

**Abstract** – We present an overview of the contents of the text having the above title and which is now in the form of a *preliminary document* titled, "Propagation Handbook for Land-Mobile-Satellite Systems-Preliminary" [Goldhirsh and Vogel, 1991]. At this writing the text is undergoing peer review, and the final revised manuscript will be published in the near future as a NASA document. The text was inspired by a series of Land-Mobile-Satellite System (LMSS) experiments by the authors and other investigators at UHF and L-Band. The rationale for its writing is to place in a single document an overview of the previous propagation related salient experimental and modeling results pertaining to LMSS scenarios (see References).

It is apparent that LMSS propagation at UHF and L-Band can be seriously degraded because of attenuation (e.g., greater than 10 dB) caused by roadside tree shadowing. The extent of attenuation is shown to depend on such factors as the elevation angle to the satellite, the bearing of the line-of-sight path to the satellite relative to the line of roadside trees, the side of the road in which the vehicle is driven, the season, and the frequency. Multipath effects during line-of-sight communications are shown to cause less serious fading (e.g., smaller than 3 dB for 90% of the driving distance).

## 1. Introduction

During the period 1983-88 a series of experiments (Table 1) were undertaken by the Electrical Engineering Research Laboratory of the University of Texas and the Applied Physics Laboratory of The Johns Hopkins University in which propagation impairment effects were investigated for Land Mobile Satellite Service (LMSS) configurations. Prior significant LMSS propagation investigations were performed in Canada [Butterworth, 1984a; 1984b], and in Europe [Jongejans et al., 1986]. More recently, LMSS propagation measurements were reported from Australia [Bundrock, 1988], England [Renduchintala et al., 1990], and Spain, France, and Sweden [Benarroch et al., 1989].

The results described in this text are mostly derived from systematic studies of propagation effects for LMSS geometries in the United States associated with rural and suburban regions. Descriptions of these efforts have appeared in a number of technical reports, conference proceedings and publications (see References). The rationale for the writing of this text was to locate the salient and useful results in one single document for use by communications engineers, designers of planned LMSS communications systems, and modelers of propagation effects.



Table 1: Land-mobile propagation measurement campaigns of EERL, University of Texas, and APL, The Johns Hopkins University.

Date	Source	Location	Freq.	Objectives	Ref
10/83	Balloon	East Texas to Louisiana	UHF	First U.S. data set for, forested and rural roads (600 km), max el = 35°	V and H; 1988
1/84	Balloon	East Texas	UHF	150 km, max el = 30°	V and H; 1988
11/84	Balloon	East Texas to Alabama	UHF, L	Freq. comparison, El = 50°, variety of roads and terrain	
6/85	Remotely piloted aircraft	VA	UHF	Single tree attenuation, stationary receiver	V and G; 1986
10/85	Helicopter	Central MD	UHF	Systematic roadside tree, sampling, single tree attenuation in fall foliage	G and V; 1987
3/86	Helicopter	Central MD	UHF	Systematic roadside tree, sampling, no foliage	G and V; 1987
7/86	Balloon	East Texas to New Mexico	UHF, L	Open terrain, optical, sensor, 45°, scatter model	V and H; 1988
8/86	Helicopter	Colorado	UHF, L	Mountain roads, canyons multipath limits	V and G; 1988
6/87	Helicopter	Central MD	UHF, L	Systematic roadside tree sampling, full foliage	G and V; 1989
12/87	MARECS-B2	Central MD	L	Systematic roadside tree sampling, ERS model	V and G; 1990
10/88	ETS-V and INMARSAT	S.E. Austral.	L	Systematic roadside tree sampling, fade durations, diversity, cross pol	V et al.; 1991 H et al.; 1991

Where applicable, the authors have also liberally drawn from the results of the other related investigations. The results are presented in a “user friendly style” in the form of graphs, tables, and “best fit” analytic functions.

A “preliminary” version has been disseminated to reviewers for their comments and suggestions [Goldhirsh and Vogel, 1991]. The revised manuscript will be published as a NASA document in the near future.

## **2. Background**

The propagation experiments by the authors were performed in the Southern United States (New Mexico to Alabama), Virginia, Maryland, Colorado, and South-Eastern Australia. These experiments were executed with transmitters on stratospheric balloons, remotely piloted aircraft, helicopters, and geostationary satellites (INMARSAT B-2, Japanese ETS-v, and INMARSAT Pacific). The earlier experiments were performed at UHF (870 MHz), followed by simultaneous measurements at L-Band (1.5 GHz) and UHF. The satellite measurements were performed only at L-Band. During these experiments, the receiver system was located in a van outfitted with the UHF and L-Band antennas on its roof, and receivers and data acquisition equipment in its interior.

## **3. Objectives**

The general objectives of the above tests were to assess the various types of impairments to propagation caused by trees and terrain for predominantly rural and suburban regions where terrestrial cellular communication services are presently non-existent and commercially impractical. Data acquired from the above experiments and other investigations have provided insight into the following LMSS propagation related characteristics described in the planned text:

- Attenuation and attenuation coefficients due to various tree types for non-mobile cases and their relation to elevation angle and frequency (Chapter 2).
- Attenuation and related statistics of the attenuation of roadside trees, including seasonal and frequency effects (Chapter 3).
- Attenuation caused by mountainous and roadside tree environments where line-of-sight propagation is maintained (Chapter 4)
- Fade duration, non-fade duration and phase characteristics for road-side tree environments (Chapter 5)
- Effects on fade statistics employing different gain antennas, feasibility of frequency re-use, and space diversity modeling (Chapter 6)
- Modeling of propagation effects (Chapter 8)

Also included for completeness are fade distribution measurements obtained from various experimenters from different countries (Chapter 7).

We emphasize L-Band since The World Administration Radio Conference for Mobile Services (WARC-MOB-87) in 1987 has allocated frequencies in this band for both the uplink and downlink modes. In particular, the agreed uplink and downlink bands are: [1] 1631.5 to 1634.5 MHz and 1530 to 1533 MHz, respectively, and [2] 1656.5 to 1660.5 MHz and 1555 to 1559 MHz, respectively, where the first set of bands are to be shared with the maritime mobile satellite service [Bell, 1988].

The results and methods described here deal with propagation for mobile satellite geometries in suburban and rural environments for elevation angles generally above 15°. Results “not” covered are associated with measurements performed in urban environments which may efficiently be serviced by cellular communications. Also, not examined here are measurements which pertain to channel effects associated with wide bandwidth modulated signals; with the exception of fade and non-fade durations and phase spreads (Chapter 5).

#### **4. Table of Contents**

Although, as of this writing, the preliminary manuscript is undergoing peer review, the following contents (as they presently exist) should provide the flavor of the final text.

1. Introduction
  - 1.1 Why This Text?
  - 1.2 Background
  - 1.3 Objectives
2. Attenuation Due to Individual Trees - Static Case
  - 2.1 Background
  - 2.2 Attenuation and Attenuation Coefficient
  - 2.3 L-Band Versus UHF Attenuation Scaling Factor-Static Case
  - 2.4 Effects on Attenuation Caused by Season and Path Elevation Angle
3. Attenuation Due to Roadside Trees-Mobile Case
  - 3.1 Background
  - 3.2 Time Series Fade Measurements
  - 3.3 Empirical Roadside Shadowing Model
  - 3.4 Validation of the Empirical Roadside Shadowing Model
  - 3.5 L-Band Versus UHF Attenuation Scaling Factor-Dynamic Case
  - 3.6 Seasonal Effects on Attenuation - Dynamic Case
  - 3.7 Fade Reduction Due to Lane Diversity
4. Signal Degradation for Line-of-Sight Communications
  - 4.1 Background
  - 4.2 Multipath for A Mountain Environment
  - 4.3 Multipath Due to Roadside Trees
5. Fade and Non-Fade Durations and Phase Spreads
  - 5.1 Background
  - 5.2 Experimental Aspects

- 5.3 Cumulative Distributions of Fade Durations
- 5.4 Cumulative Distributions of Non-Fade Durations
- 5.5 Cumulative Distributions of Phase Fluctuations
- 6. Propagation Effects Due to Cross Polarization, Gain, and Space Diversity
  - 6.1 Background
  - 6.2 Frequency Re-Use
  - 6.3 Distribution from Low and High Gain Receiving Antennas
  - 6.4 Diversity Operation
    - 6.4.1 Joint Probabilities
    - 6.4.2 Diversity Improvement Factor, DIF
    - 6.4.2 Diversity Gain
- 7. Investigations from Different Countries
  - 7.1 Measurements in Australia
  - 7.2 Measurements in Canada
  - 7.3 PROSAT Experiment-Belgium, France, and Sweden
  - 7.4 Measurements Performed in the United States
  - 7.5 Measurements Performed in Japan
- 8. Modeling for LMSS Scenarios
  - 8.1 Background
  - 8.2 Background Information Associated with Model Development
    - 8.2.1 Diffusely Scattered Waves
    - 8.2.2 Faraday Rotation
    - 8.2.3 Ground Specular Reflection
  - 8.3 Empirical Regression Models
    - 8.3.1 Large Scale - Small Scale Coverage Model
    - 8.3.2 Empirical Roadside Shadowing Model
  - 8.4 Probability Distribution Models
    - 8.4.1 Density Functions Used in Propagation Modeling
    - 8.4.2 Loo's Distribution Model
    - 8.4.3 Total Shadowing Model
    - 8.4.4 Lognormal Shadowing Model
    - 8.4.5 Simplified Lognormal Shadowing Model
    - 8.4.6 Models with Fade State Transitions
  - 8.5 Geometric Analytic Models
    - 8.5.1 Single Object Models
    - 8.5.2 Multiple Object Models
  - 8.6 General Conclusions
- 9. References

## 5. Salient Results and Conclusions

Some of the major conclusions that may be gleaned from the results in the text are summarized as follows:

1. An Empirical Roadside Shadowing (ERS) model developed by the authors may be used

to arrive at fade levels ranging from 3 dB to 26 dB over elevation angles between 20° and 60° over percentages ranging from 1% to 20% (percentage of the distance driven over which fades are exceeded). This model, which has as inputs elevation angle and percentage of distance driven, gives the fade exceedance. The model corresponds to average driving conditions (left and right side driving along multiple roads), a maximum shadowing line-of-sight orientation, and roads in which the percentage of optical tree shadowing ranged between 55% to 75%. It was validated by independent measurements in Australia [Vogel et al., 1991].

2. The attenuation may be scaled upwards or downwards between UHF (870 MHz) and L-Band (1.5 GHz) employing the square root of the ratio of the frequencies [Goldhirsh and Vogel, 1989]. The results of Bundrock and Harvey [1988] indicate this scaling may be extended to S-Band (e.g., 3 GHz).
3. Measurements made during a full blossom period in the summer and in the winter time during which deciduous trees are devoid of leaves have demonstrated that in the 1% to 30% percentage interval, approximately 80% of the signal attenuation is caused by the wood part of the trees (branches and trunk).
4. Significant fade reductions (e.g., 8 dB at 60 degrees elevation at L-Band) may be achieved by switching lanes.
5. Signal fading due to multipath is generally less than 3 dB for both mountain and roadside tree environments for 90% of the driving distance. The dominant attenuation is hence caused by shadowing of the line-of-sight path. These results presume an azimuthal omni-directional antenna with a beamwidth in elevation over the interval 15% to 75%.
6. Simulations using real data show that separated antennas may lead to significant fade reductions for diversity mode operations. For example, a 5 dB single terminal fade may be reduced to 3 dB, for a 1 m separation employing diversity operation. Rapid switching is implied (e.g., 10 milliseconds).
7. When the line-of-sight is completely blocked by continuous obstacles such as mountains, buildings, or overpasses, not enough power is contributed by multipath scattering to enable communications through a satellite system with a commercially feasible fade margin of 6 to 12 dB. For such a case LMSS is not functional.
8. The model development efforts and comparison of experimental results with model results show:
  - When the propagation path is unshadowed, Rician statistics apply most of the time, although the K-factor (ratio of line-of-sight and multipath powers) cannot strictly be assumed constant.
  - When a single scatterer dominates, as might be the case with a utility pole, Rician statistics are no longer applicable.
  - Geometrical analytic models involving single point scatterers give time series fading results consistent with drive-by results associated with a single utility pole.

- More accurate model descriptions of “undshadowed propagation” than those given by existing Ricean multipath scatter models and geometric-analytic models are not necessary in that fading due to multipath is less than 3 dB for 90% of the driving distance.

## 6. Acknowledgments

This work was funded by the Communications and Information Systems Division of NASA Headquarters and by The Office of Commercial Programs for the Applied Physics Laboratory of the Johns Hopkins University (Contract #N00039-89-C-0001). Funding for the Electrical Engineering Research Laboratory of the University of Texas was provided by the Jet Propulsion Laboratory (Contract #JPL 956520).

## 7. References

- Bell, T.E., “Technology 88 - Communications,” *IEEE Spectrum*, pp 41-43, January 1988.
- Benarroch, A., L. Mercader, G. Sastre, “Propagation Measurements for Land Mobile Satellite Systems at 1.5 GHz; Rural Environment in Europe,” *Proceedings of the International Symposium of Antennas and Propagation, 1989 (ISAP '89)*, August 22-25, Tokyo Vol 3, pp 765-768, 1989.
- Bundrock, A. and R. Harvey, “Propagation Measurements for an Australian Land Mobile-Satellite System,” *Proc. of Mobile Satellite Conference*, pp 119-124, 1988.
- Butterworth, J. S., “Propagation measurements for land-mobile satellite systems at 1542 MHz,” *Commun. Res. Cent.*, Ottawa, Canada Tech. Note 723, August 1984a.
- Butterworth J. S., “Propagation measurements for land-mobile satellite services in the 800 MHz Band,” *Commun. Res. Cent.*, Ottawa, Canada Tech. Note 724, August 1984b.
- CCIR, “Recommendations and Reports of the CCIR, Volume V, Propagation in Non-Ionized Media,” International Telecommunications Union, Geneva, Switzerland, 1986.
- Goldhirsh, J. and W. J. Vogel, “Propagation Handbook for Land-Mobile-Satellite Systems - Preliminary,” *Applied Physics Laboratory, Johns Hopkins University, Technical Report #S1R-91U-012* April, 1991.
- Goldhirsh, J. and W. J. Vogel, “Roadside tree attenuation measurements at UHF for land-mobile satellite systems,” *IEEE Trans. Antennas Propagat.*, vol. AP-35, pp. 589-596, May 1987.
- Goldhirsh, J. and W. J. Vogel, “Mobile satellite system fade statistics for shadowing and multipath from roadside trees at UHF and L-band,” *IEEE Trans. Antennas Propagat.*, vol AP-37, No. 4, pp. 489-498, April 1989.
- Hase, Y., W. J. Vogel, and J. Goldhirsh, “Fade-durations derived from land-mobile-satellite measurements in Australia,” *IEEE Trans. Communications*, Vol 39, No. 5, May 1991.

- Jongejans, A., A. Dissanayake, N. Hart, H. Haugli, C. Loisy, and R. Rogard, "PROSAT-Phase 1 report," *European Space Agency Tech. Rep. ESA STR-216*, May 1986, (European Space Agency, 8-10 Rue Mario-Nikis, 75738 Paris Cedex 15, France.)
- Vogel, W. J., and J. Goldhirsh, "Tree attenuation at 869 MHz derived from remotely piloted aircraft measurements," *IEEE Trans. Antennas Propagat.*, vol. AP-34, No. 12, pp. 1460-1464. Dec. 1986.
- Vogel, W. J., and U.-S. Hong, "Measurement and modeling of land mobile satellite propagation at UHF and L-band," *IEEE Trans. Antennas Propagat.*, vol AP-36, No. 5, pp 707-719, May 1988.
- Vogel, W. J., and J. Goldhirsh, "Fade measurements at L-band and UHF in mountainous terrain for land mobile satellite systems," *IEEE Trans. Antennas Propagat.* vol. AP-36, No. 1, pp. 104-113, June 1988.
- Vogel, W. J., J. Goldhirsh, and Y. Hase, "Land-Mobile-Satellite Fade Measurements in Australia," *AIAA Journal of Spacecraft and Rockets*, July-August, 1991.
- Vogel, W. J., and J. Goldhirsh, "Mobile satellite system propagation measurements at L-band using MARECS-B2" *IEEE Trans. Antennas Propagat.*, Vol AP-38, no 2, pp 259-264, Feb. 1990.

## **Handbooks of the NASA Propagation Program, Past History and Thoughts to the Future**

Ernest K. Smith  
NASA Propagation Information Center  
ECE Department  
University of Colorado

In this contribution I would like to say something about the history of handbooks in the NASA Propagation Program, review our options, and report on a luncheon meeting at the University Club on June 27, 1991.

1. The "handbooks" of the NASA Propagation Program were initiated, I believe, by Dr. Louis J. Ippolito when he was program manager. The current "Ippolito" series has progressed through four editions. I believe the first three were produced at ORI, Inc. under contracts which Dr. Ippolito managed. The third edition of this series is:

A) NASA Reference Publication 1082(03). **Propagation Handbook for Satellite Systems Design** *A summary of Propagation Impairments on 10 to 100 GHz Satellite Links with Techniques for System Design*, by Louis J. Ippolito, R.D. Kaul and R.G. Wallace. June 1983 (468 pp).

The fourth edition was prepared by Dr. Ippolito personally after retiring from NASA in December 1983 through a contract from NASA/JPL to Westinghouse.

B) NASA Reference Publication 1082(04). **Propagation Effects Handbook for Satellite System Design** *A Summary of Propagation Impairments to 10 to 100 GHz Satellite Links with Techniques for System Design*, by Louis J. Ippolito, February 1989.

A second series of current handbooks was initiated by me when I became JPL program manager in 1980 and interest in UHF and L-band was beginning to surface. Warren Flock was spending a year with me at JPL and took on the job of preparing a parallel "handbook" for frequencies between 100 MHz and 10 GHz. This text has now gone through two editions.



C) NASA Reference Publication 1108. **Propagation Effects on Satellite Systems at Frequencies Below 10 GHz** *A Handbook for Satellite Systems Design* by Warren L. Flock, December 1983 (420 pp).

D) NASA Reference Publication 1108(02). **Propagation Effects on Satellite Systems at Frequencies Below 10 GHz** *A Handbook for Satellite Systems Design* by Warren L. Flock, 1987 (502 pp).

Earlier "Handbooks" produced for the NASA Propagation Program or its predecessors and referenced in the literature include:

E) R. Kaul, R. Wallace and G. Kinal. **A Propagation Effects Handbook for Satellite Systems Design**, NASA Headquarters, Washington, D.C., Rep. ORI TR 1679, Mar. 1980.

F) R. Kaul, D. Rogers and J. Bremer. **A Compendium of Millimeter Wave Propagation Studies Performed by NASA**, ORI, TR 1278, Nov. 1977.

G) R.K. Crane and D.W. Blood. **Handbook for the Estimation of Microwave Propagation Effects - Link Calculations for Earth-Space Paths**, Doc. No. P 7376- TR1, ERT, Inc (Prepared for NASA Goddard) June 1979.

A new series of "Handbooks" was initiated by Dr. Faramaz Davarian who commissioned Julius Goldhirsh and Wolf Vogel to undertake handbooks on propagation for the mobile services, the first volume to be on the land mobile service. The first draft of this text has been distributed for review.

The immediate questions, as I understand it are: (1) Should the Flock and Ippolito series of handbooks be combined into one handbook? (2) Should the MSS section in the Flock handbook be removed and offered to the Goldhirsh-Vogel handbook? (3) Should the Goldhirsh-Vogel (G/V) handbook be called something else?

Definition of "Handbook": A manual; A concise reference book covering a particular subject (Webster's New Collegiate Dictionary).

2. There were three important contributions to the June 27 meeting. Faramaz Davarian's memo laid out the options as
  - A. Status quo including an LMSS Handbook.
  - B. Status quo except LMSS section is transferred from Flock to Goldhirsh-Vogel (G/V).
  - C. The Ippolito handbook remains unchanged but Flock and G/V are combined.
  - D. Ippolito and Flock are combined and the G/V series covers all MSS.

John Kiebler's input memo pointed out:

- A. That it is difficult to combine handbooks.
- B. G/V is not yet comprehensive.
- C. Suggests integrating G/V into Flock or else publishing it as something other than a handbook.

Ernie Smith's contribution reviewed some texts called "handbooks" and suggested some other titles. He also pointed out that the Ippolito and Flock handbooks are written from two points of view. Ippolito is more directed to the systems engineer; Flock is more scholarly and gives the physical bases for model development. There is a lot of common ground in the two handbooks; both treat rain attenuation and depolarization, gaseous absorption, prediction techniques, and link budgets. There is relatively more attention to rain in the Ippolito handbook than in Flock. However, as would be expected, there is extensive treatment of the ionosphere and surface effects in Flock and not in Ippolito. There is also a difference in style. Ippolito is more of an engineer's approach, Flock has much more physics and is more academically oriented. As my undergraduate degree was in physics I relate more readily to Flock, but engineers may find the Ippolito approach more satisfying. There is some rationale for these two approaches. In the NBS Central Radio Propagation Laboratory (CRPL) the Radio Propagation Physics Division was concerned with ionospheric propagation while the Radio Propagation Engineering Division was concerned with tropospheric propagation. The two handbooks can be combined but something will be lost in the process.

Additionally, there is very little duplication of material between the Flock Chapter 6: Propagation Effects on Mobile-Satellite Systems, and the Goldhirsh/Vogel text; so the need to reduce duplication there is minimal.

3. At the luncheon meeting (attended by Davarian, Goldhirsh, David Rogers, Smith, and Vogel) Goldhirsh proposed the title for the G/V text: "Propagation Effects for Land Mobile Satellite Systems: Experiment and Modeling Results." Goldhirsh also suggested a hard cover for the volumes.

David Rogers, our advisory committee representative, made the following points:

1. Ionosphere scintillation will be very important at L-band at low latitudes and deserves mention in G/V.
2. The systems engineering approach is appropriate for the NASA Handbook series - they are the customers NASA is trying to reach.
3. A combined handbook 100MHz -100 GHz is desirable. It could be in two volumes.

The consensus, after discussion, was that of the cost of updating vs. combining the existing handbooks should be investigated. If the combining of the handbooks is possible then a good man willing to dedicate the order of 1 or more man-years would need to be identified.



**NAPEX XV**

**Session 3**

**COMPUTER-BASED  
PROPAGATION MODEL**

Chairman:

Faramaz Davarian  
Jet Propulsion Laboratory

**PRECEDING PAGE BLANK NOT FILMED**



**Database for Propagation Models**

**Anil V. Kantak  
Jet Propulsion Laboratory  
California Institute of Technology  
4800 Oak Grove Drive  
Pasadena, California 91109**

**1.0 Introduction:**

A propagation researcher or a systems engineer who intends to use the results of a propagation experiment is generally faced with various database tasks such as the selection of the computer software, the hardware, and the writing of the programs to pass the data through the models of interest. This task is repeated every time a new experiment is conducted or the same experiment is carried out at a different location, generating different data. Thus the users of this data have to spend a considerable portion of their time learning how to implement the computer hardware and software towards the desired end. This situation may be facilitated considerably if an easily accessible propagation database is created that has all the accepted (standardized) propagation phenomena models approved by the propagation research community. Also, the handling of data will become easier for the user.

Such a database construction can only stimulate the growth of the propagation research if it is available to all the researchers, so that the results of an experiment conducted by one researcher can be examined independently by another, without different hardware and software being used. The database may be made flexible so that the researchers need not be confined only to the contents of the database. Another way in which the database may help the researchers is by the fact that they will not have to document the software and hardware tools used in their research since the propagation research community will know the database already. The following sections show a possible database construction, as well as properties of the database for the propagation research.

**2.0 Objectives and Properties of the Database:**

The proposed database will contain all the accepted propagation phenomena models by the propagation research community. The database will also contain some example data for each model in the database, but it will not attempt to be an extensive database by any means. This is because of the fact that the database is intended to run on a personal computer which generally has memory restrictions. Thus every user will have to use his own storage

medium for storing his experimental data. The database will be modular in form, i.e., the propagation models will be kept in modules in the database and may be accessed easily by the user without his having to know the internal working of the database. The database will have enough bells and whistles to steer the user away from making incorrect inputs, thereby avoiding the confusion that results from the output of such a run of the database. The database will have on-screen help for the user that will guide the user step by step through the procedure necessary to run the database, allowing even the novice user of the database to obtain the same performance as the experienced user.

Many times the user only wants printouts of the models included and the data that is present to be used with the models; hence, printout either to a printer or to a file will be allowed for any module of the database. The database will be flexible enough to allow the users to change the default values of the models or change the model itself (the formula), and to run the database with either the data stored in the database or with their own data. The output of the database will be in terms of graphs as well as tables, depending on the model. The software selected for the database will be such that the graphs resulting from the models will be flexible, i.e., after creation of a graph, manipulation will be allowed to fit it to their own requirements. The graphs will be able to be printed out or stored for later use.

### **3.0 Database Hardware and Software:**

For maximum use, the database will be designed to run on a personal computer and not a work-station or a mainframe computer. Whether the personal computer be an IBM PC or Apple Macintosh, the database will work for it. A personal computer that has a clock speed of 16 MHz or more will be reasonable for this purpose. This does not indicate that the slower computers will not run this database, only that the slower-clock computers, such as 8-MHz speed, will take more time to run the database request. It is recommended that the computer have 4 MB of RAM so that the program can be properly loaded and there is enough memory space for it to work. It is also recommended that the PC should have a hard disk drive of at least 40 MB. To make the list of needed hardware complete, the setup should also have a monitor and a laser printer. The monitor may be a color monitor or just a monochrome monitor; it will not make any difference in the working of the database software. The laser printer is recommended for its clarity of printing and the control it offers in fonts, etc. However, other printers may be used.

The selection of software necessary for the database falls into two distinct categories: compiler-based software and spreadsheet-based software. Each category can do the complete job; however, there are advantages and disadvantages of each type of software. Microsoft's Professional Basic 7.1 compiler and Microsoft's Excel spreadsheet



were selected as possibilities for the database software. Following is a discussion of advantages and disadvantages of these two software.

Regardless of the PC selected, i.e., either the IBM PC or Apple, Windows 3.0 software for the IBM PC will make it operate virtually like the other. The Excel software is available for both types of computers. The Excel spreadsheet will use macros to do all the processing. The Excel macros have an impressive array of functions for the processing, as well as on-screen help for the user along with easy interactive input-output capability. It has 'message' capability also, which can be used to guide or advise the user through the steps necessary to execute the model. The Basic compiler does not have easy on-screen help capability. This capability may be created in Basic but only after extensive programming. Another problem the Basic compiler has is that it cannot use the 'mouse' to point and shoot when the program is in execution mode. The mouse is used extensively in Excel and can also be used for the input-output processing during interactive procedures.

Since Excel is a spreadsheet, it is well suited for the plotting with minimum efforts on the user's part. With the Basic compiler, on the other hand, as though it has the plotting commands in it, it is rather difficult to use these commands to produce a quality plot. Excel's internal software produces excellent plots and also allows the users to manipulate the plots after they are produced to fit their requirements. The plot produced by the compiler cannot be manipulated by the users and thus may fall short of what the users desire in that plot in terms of the plot's presentability. A similar situation is present as far as the database facility is concerned. Excel, being a spreadsheet, is naturally suitable for the database processing, with input-output in columns. The Basic compiler does have the database capability but it falls short of many desirable qualities the spreadsheet database has. It will take a considerable amount of programming in Basic to make it equivalent to the spreadsheet in terms of ease of use for the user.

The above discussion seems to be tilting towards selection of the Excel spreadsheet for the database. However, one should be aware of some disadvantages of the spreadsheet. As the programs become larger in size, the database program is expected to become larger, and the execution of the spreadsheet becomes slower than that of the compiler program. Another disadvantage the spreadsheet has is that the user needs the spreadsheet program as well as the spreadsheet software to run it, whereas with the compiler the user needs the executable file of the program only and does not need the Basic software itself. This situation may change in the future. Also, the spreadsheet macros are rather difficult to program as compared to the Basic compiler programming, and their files input-output processing is slow.

The following table shows the advantages and disadvantages of the Basic compiler and the spreadsheet.

MICROSOFT EXCEL SPREADSHEET	MICROSOFT PROFESSIONAL BASIC
On-screen help is easy	On-screen help is difficult
Plots are easy to create and manipulate	Plots are difficult to create and manipulate
Database facility is excellent	Database facility is present but not easy to operate
Tabular form of input and output are natural	Tabular form is not easy to obtain for input or output
Plots and outputs are very impressive	Plots and outputs are not impressive in general
Execution is rather slow when program size becomes large	Execution is fast
User needs the program as well as the spreadsheet	User needs only the executable file and not the compiler
It is difficult to program and file input-output is slow	It is easy to program and file input-output is fast

The following figures show a sample of a working database. This is only a sample; the actual database will have many other options. Figure 1 shows the first window with all the options the database may have; this is the main menu of the database. The window also includes the instructions needed to select the desired option of the options available to be executed. For this example the Land-Mobile system propagation models option was selected. Figure 2 shows the sub-options available in the option selected in Figure 1. For this example, the probability distribution models were selected from Figure 2. Figure 3 shows all available options under the sub-option selected in Figure 2. Here, the simplified lognormal shadowing model was selected. The result of that selection is shown in Figure 4. This figure shows the model itself and the parameters associated with it. Figure 5 shows the default parameter values and the place for user inputs. In the same window, the possibilities of plotting the default curve with the user's own curve and supplying

the user's own data are provided. Once this step is completed, the model is computed using the data selected and the graph is plotted (Figure 6). Note that at this time, the user can use Excel's graphics capabilities to manipulate the graph until it satisfies any requirement the user may have. After completion of the plotting, the next window (Figure 7) has the print and store options for the plot as well as the database. Also in the same window, the user may select to run the model again with a different database or different parameters, go back to the main menu, or exit the database.

#### **4.0 Conclusions:**

After understanding the limitations of the spreadsheet and the compiler, it seems imperative that the spreadsheet should be selected as the software for the database. This conclusion is not surprising because spreadsheets are naturally more suitable for the database-type operations than the compiler-based software. If desired, both database software may be produced, allowing the user to select the software he desires.

**AN EXAMPLE**


**WELCOME TO THE PROPAGATION MODELS AND DATABASE**

- IONOSPHERIC PROPAGATION MODELS.
- TROPOSPHERIC PROPAGATION MODELS.
- **LAND-MOBILE SYSTEM PROPAGATION MODELS.**
- EFFECTS OF SMALL PARTICLES ON PROPAGATION.
- RAIN MODELS.
- RADIO NOISE MODELS.

TO SELECT THE MODEL TO EXECUTE:  
BRING THE CURSOR TO THE BULLET AND PRESS ENTER OR  
POINT TO THE BULLET WITH A MOUSE AND CLICK.

Figure 1. Main Menu of the Database.

## **LAND-MOBILE SYSTEM PROPAGATION MODELS**

- DIFFUSELY SCATTERED WAVES MODELS.
- FARADAY ROTATION MODELS.
-  PROBABILITY DISTRIBUTION MODELS.
- EMPIRICAL REGRESSION MODELS.
- GROUND SPECULAR REFLECTION MODELS.
- GEOMETRIC ANALYTIC MODELS.

TO SELECT THE MODEL TO EXECUTE:  
BRING THE CURSOR TO THE BULLET AND PRESS ENTER OR  
POINT TO THE BULLET WITH A MOUSE AND CLICK.

**Figure 2. Available Options in Land-Mobile System Propagation Models.**

**PROBABILITY DISTRIBUTION MODELS**

- LOO'S DISTRIBUTION MODEL.
- LOGNORMAL SHADOWING MODEL.
- **SIMPLIFIED LOGNORMAL SHADOWING MODEL.**
- TOTAL SHADOWING MODEL.
- FADE STATE TRANSITION MODEL.

TO SELECT THE MODEL TO EXECUTE:  
BRING THE CURSOR TO THE BULLET AND PRESS ENTER OR  
POINT TO THE BULLET WITH A MOUSE AND CLICK.

Figure 3. Available Options in Probability Distribution Models.

## SIMPLIFIED LOGNORMAL SHADOWING MODEL

This model was developed by Barts et al. (1987). The probability distribution model is expressed in terms of the contributions for the "no shadowing" and "shadowing" cases in the following way:

$$\begin{aligned}
 P(A > A_q) = & (1 - S) \cdot \text{Exp} \left[ - \frac{A + 0.01 K^2 - 0.378 K + 3.98}{331.35 K^{-2.29}} \right] \\
 & + S (50 - A_q) \frac{(-0.006 \bar{K} - 0.008 m + 0.013 s + 0.121)}{-0.275 \bar{K} - 0.723 m + 0.336 s + 56.979}^{-1}
 \end{aligned}$$

where

S = Shadowed fraction of the total distance

s = Standard deviation of lognormal fading

K = Line of sight to average multi-path power ratio, K = (Average multi-path power)<sup>-1</sup>

Figure 4. Simplified Lognormal Shadowing Model.

**INPUTS TO THE SIMPLIFIED LOGNORMAL SHADOWING MODEL**

PARAMETER	RANGE OF VALUES	USER INPUT	DEFAULT
K	13 to 22 (dB)	?	17.5 (dB)
$\bar{K}$	18 to 21 (dB)	?	15.0 (dB)
m	-10 to -1 (dB)	?	- 5.5 (dB)
s	0.5 to 3.5 (dB)	?	2.0 (dB)
S	0.0 to 1.0	?	0.5

- ENTER 1 IN THE SQUARE IF THE DEFAULT CURVE IS TO BE PLOTTED  
ALONG WITH THE USER CURVE.
- ENTER 1 IN THE SQUARE IF USER WANTS TO SUPPLY HIS OWN DATA.

Figure 5. Table of Inputs and Defaults for the Simplified Lognormal Shadowing Model.



**MEDIUM HEAVY SHADOWING**  
 **$K = 17.5 \text{ dB}$ ,  $K' = 15 \text{ dB}$ ,  $m = 5.5 \text{ dB}$ ,  $s = 2 \text{ dB}$**

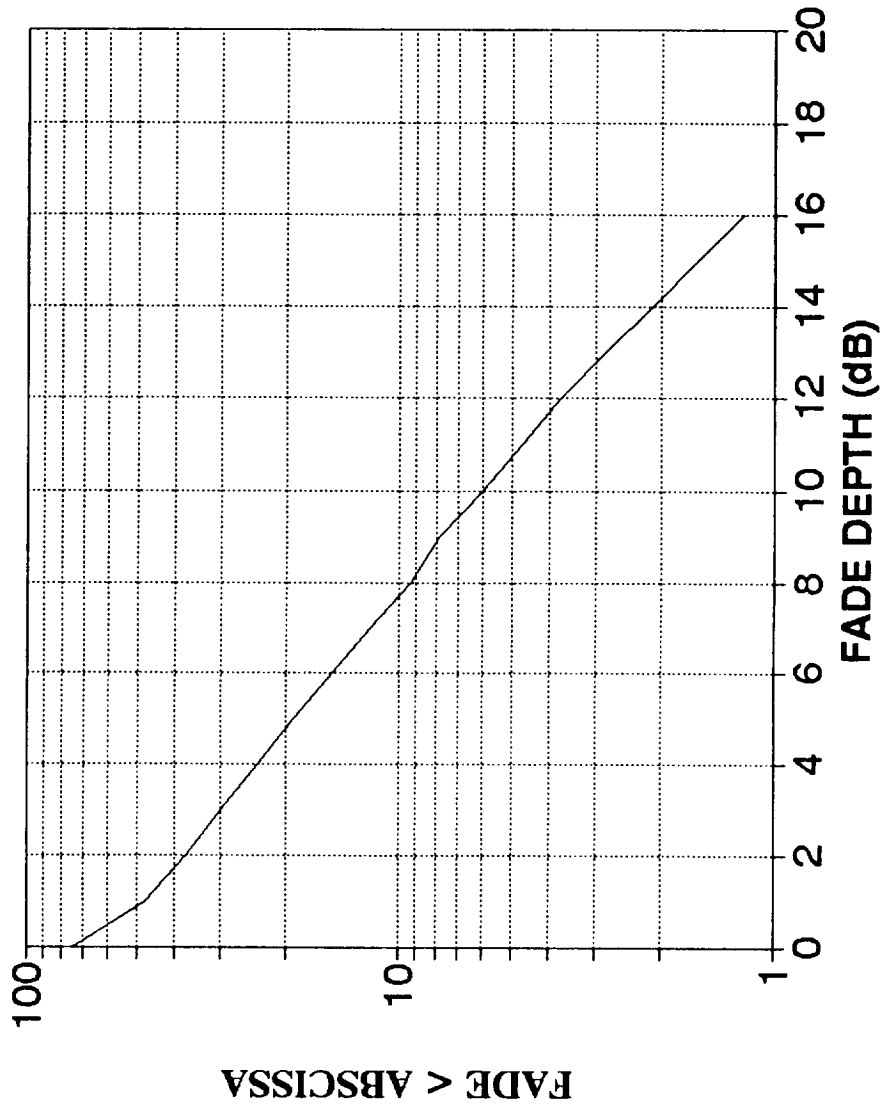


Figure 6. A plot of Fade < Abscissa Versus the Fade Depth.

## **SIMPLIFIED LOGNORMAL SHADOWING MODEL**

### **CHARTS:**

- **PRINT OPTIONS.**
- **STORE OPTIONS.**

### **DATABASES (INTERNAL + USER-SUPPLIED):**

- **PRINT OPTIONS.**
- **STORE OPTIONS.**

### **RUN POSSIBILITIES:**

- **RUN THE SAME MODEL WITH DIFFERENT DATABASE.**
- **RUN THE SAME MODEL WITH DIFFERENT INPUT PARAMETERS.**
- **GO BACK TO THE MODEL MENU.**

**Figure 7. Print and Store Options for Charts and Databases With Run Possibilities.**

# A CCIR-BASED PREDICTION MODEL FOR EARTH-SPACE PROPAGATION

Zengjun Zhang and Ernest K. Smith  
University of Colorado at Boulder

## 1. BACKGROUND

At present there is no single "best way" to predict propagation impairments to an Earth-Space path. However there is an internationally accepted way — namely that given in the most recent version of CCIR Report 564 of Study Group 5. This paper treats a computer code conforming as far as possible to Report 564. It was prepared for an IBM PS/2 using a 386 chip and for Macintosh SE or Mac II. It is designed to be easy to write and read, easy to modify, fast, have strong graphic capability, contain adequate functions, have dialog capability and windows capability.

Computer languages considered included the following

- Turbo BASIC
- Turbo PASCAL
- FORTRAN
- SMALL TALK
- C++
- MS SPREADSHEET
- MS Excel-Macro
- SIMSCRIPT II.5
- WINGZ

Microsoft Excel-Macro was chosen as the first phase simulation language for the following Characteristics

- strong graphic capability
- about 400 math or control functions
- sophisticated coordinate systems
- window and dialog capability
- easy to customize
- enough resolution and colors for our use
- not too fast at the beginning, because of on-screen processing

## 2. PROGRAM STRUCTURE

Shown in Figure 1 are the dialog boxes illustrating how the first part of the program would be run. The second part consists of consolidating gaseous attenuation and rain attenuation with the free-space value of the carrier  $C$ ; and brightness temperature with the noise temperature of the receiving system, to obtain the overall system noise density  $X_0$  or  $N_0$  to yield  $C/X_0$ .

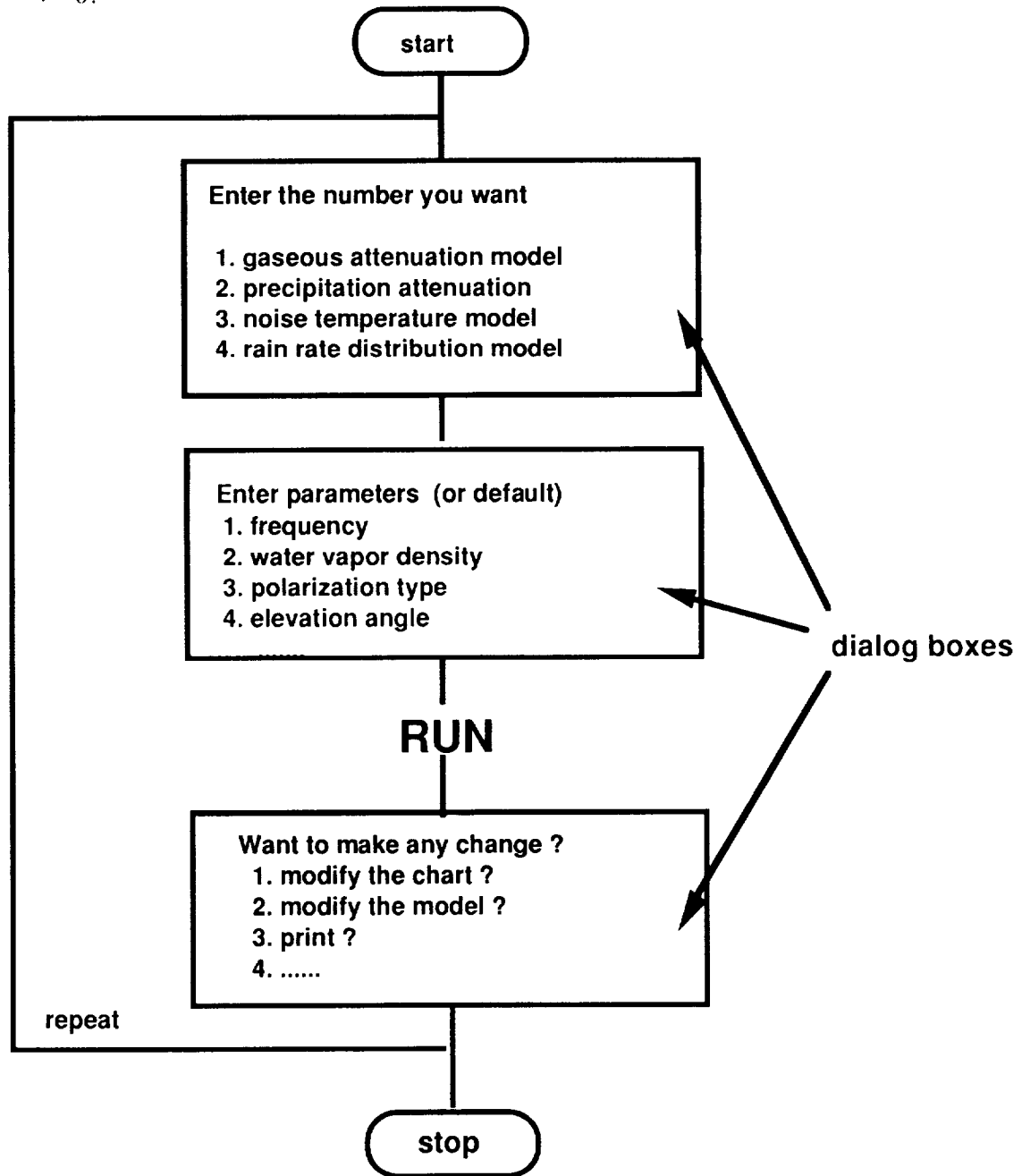


Figure 1 Program Diagram

### 3. METHOD AND RESULTS

(A) *Rain Rate as a Function of percentage of year:* CCIR Report 563 (1990) is used as the authority for rain rate. The formula used is

$$P(R>r) = \frac{a e^{-ur}}{b} \quad r \geq 2 \text{ mm/h} \quad (1)$$

where  $R$  is rain rate,  $r$  is a given rain-rate threshold,  $u$  is a parameter depending on climate and geographical features, and

$$a = 10^{-4} R_{0.01}^b e^{u R_{0.01}}$$

$$b = 8.22 (R_{0.01})^{-0.548}$$

Figure 2 illustrates this relation applied to 4 CCIR regions (found in Report 563), and Figure 3 illustrates the goodness of fit of equation (1) with the CCIR data in Report 563. As can be seen, beyond 2 mm/h the fit appears very good.

(B) *Attenuation due to Rain:* CCIR Report 564 (1990) is used to obtain rain attenuation. The specific attenuation  $\gamma_r$  is obtained from

$$\gamma_r = \kappa (R_{0.01})^\alpha \quad \text{dB/km} \quad (2)$$

where  $\kappa$  and  $\alpha$  are tabulated values and are a function of frequency and drop size distribution. The path attenuation  $A$  is then given by

$$A = \gamma_r L_s r_{0.01} \quad \text{dB} \quad (3)$$

where  $L_s$  is the adjusted path length through rain,  $R_{0.01}$  is the rain rate in mm/h for 0.01% of the time. Figure 4 illustrates these relations in a plot of attenuation vs frequency for four different rain rates.

(C) *Gaseous Attenuation:* According to the CCIR Report 719 (1990) version, specific attenuation due to oxygen and water vapor are determined as

$$\gamma_0 = \left[ 7.19 \times 10^{-3} + \frac{6.09}{f^2 + 0.227} + \frac{4.81}{(f-57)^2 + 1.5} \right] f^2 \times 10^{-3} \quad \text{dB/km} \quad f \leq 57 \text{ GHz} \quad (4)$$

$$\gamma_0 = \left[ 3.79 \times 10^{-7} f + \frac{0.265}{(f-63)^2 + 1.59} + \frac{0.028}{(f-118)^2 + 1.47} \right] (f+198)^2 \times 10^{-3} \quad \text{dB/km} \quad 63 \leq f \leq 350 \text{ GHz} \quad (5)$$

$$\gamma_w = \left[ 0.05 + 0.0021 \rho_w + \frac{3.6}{(f-22.2)^2 + 8.5} + \frac{10.6}{(f-183.3)^2 + 9.0} + \frac{8.9}{(f-325.4)^2 + 26.3} \right] f^2 \rho_w 10^{-4}$$

dB/km  $f \leq 350$  GHz

(6)

where  $\gamma_o$  and  $\gamma_w$  represent specific attenuation by oxygen and water vapor,  $f$  is frequency in GHz, and  $\rho_w$  is water vapor density. Total attenuation  $A_g$  due to gaseous then is determined as

$$A_g = \frac{\gamma_o h_o e^{-\frac{h_s}{h_o}} + \gamma_w h_w}{\sin \theta} \quad \text{dB} \quad \theta > 10^\circ$$
(7)

$$A_g = \frac{\gamma_o h_o e^{-\frac{h_s}{h_o}}}{g(h_o)} + \frac{\gamma_w h_w}{g(h_w)} \quad \text{dB} \quad \theta \leq 10^\circ$$
(6)

Figure 5 illustrates attenuation due to the gaseous atmosphere at four different elevation angles, and Figure 6 shows attenuation due to the gaseous atmosphere at four different station heights.

*D: Brightness Temperature (upward looking antenna):* The general formula used for brightness temperature was based on the model developed by Waters in 1976. Because it is quite complicated, we used a simplified formula which was the combination of two models developed by E. K. Smith (1982) and Waters (1974)

$$A = \int_0^\infty \sum_i \gamma_i dr \approx \int_0^\infty [\gamma_o + \gamma_w] dr$$
(7)

$$T_b = \int_0^\infty T(r) \gamma(r) e^{-\tau(r)} dr + T_\infty e^{-\tau_\infty}$$
(8)

where  $\tau(r) = \int_{\text{surf}}^r \gamma(r') dr'$

If  $T(r)$  is replaced by a mean path temperature  $T_m$ , it can be simplified as

$$T_b = T_m (1 - e^{-\tau})$$
$$\text{or } T_b = T_m (1 - 10^{[-A(\text{dB})/10 \sin\theta]}) \quad \theta \geq 10^\circ \quad (9)$$

where  $A$  is the attenuation at zenith direction,  $T_b$  is brightness temperature,  $\theta$  represents elevation angle,  $L$  is the loss factor, and  $\tau$  is the optical depth.

Figure 7 illustrates the brightness temperature at four different elevation angles, and Figure 8 is a comparison of computed results and CCIR data at the conditions of water vapor density 7.5 mm/h and elevation angle 30 degrees. As we can see, the fit is very good in lower frequency range.

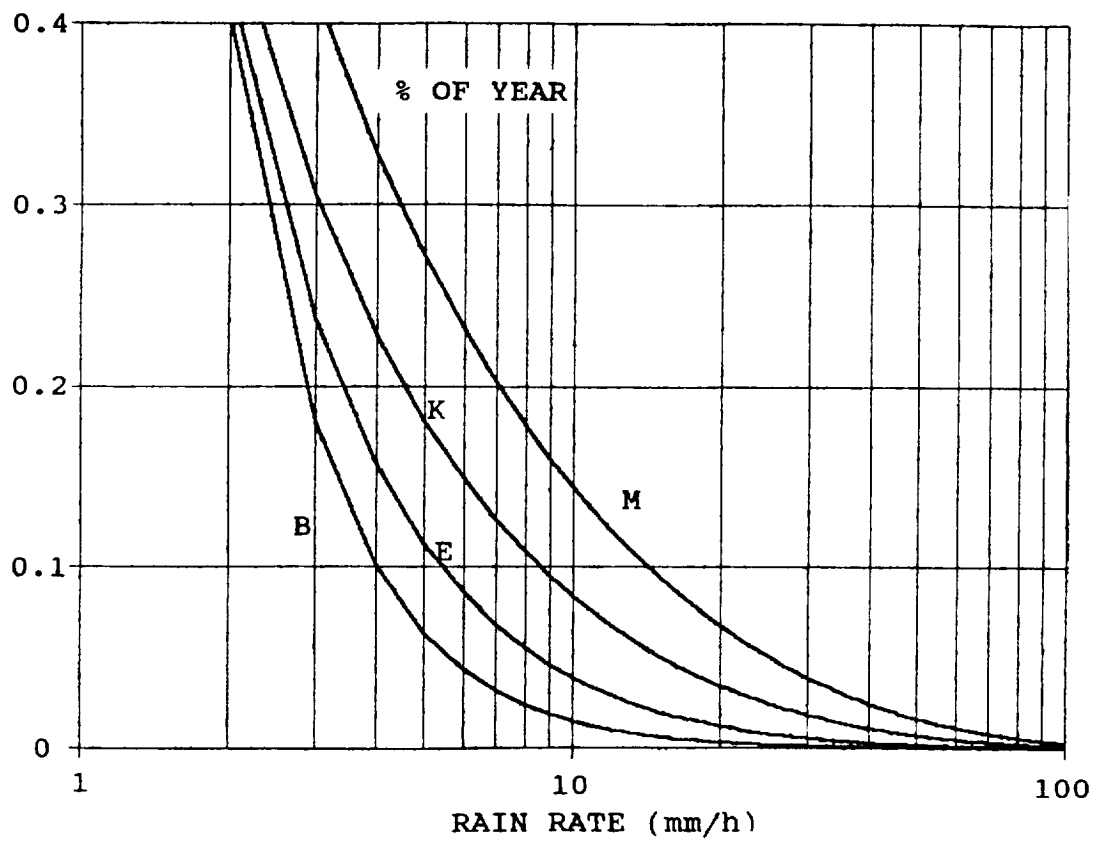


Figure 2 Rain Rate vs % of Year for Regions B, E, K, M



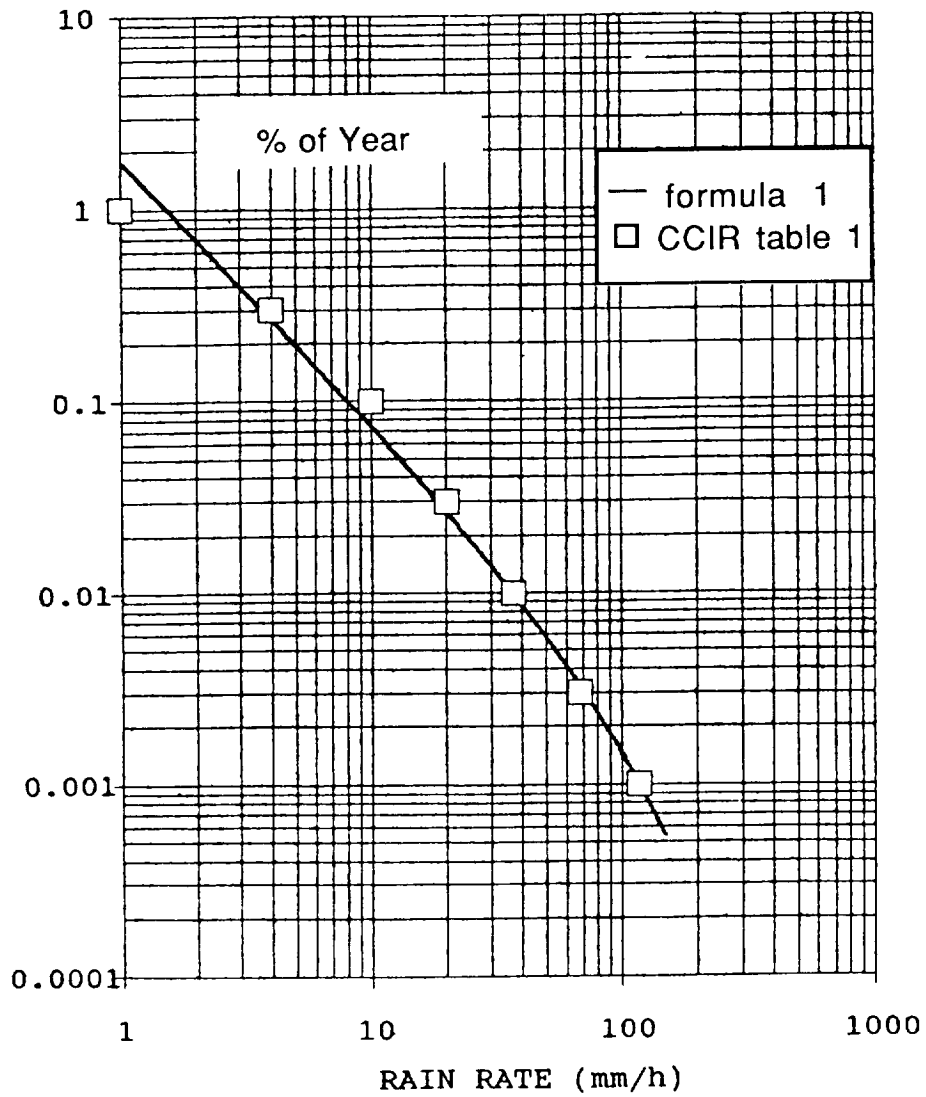


Figure 3 Analytical vs Experimental Results (CCIR region E)

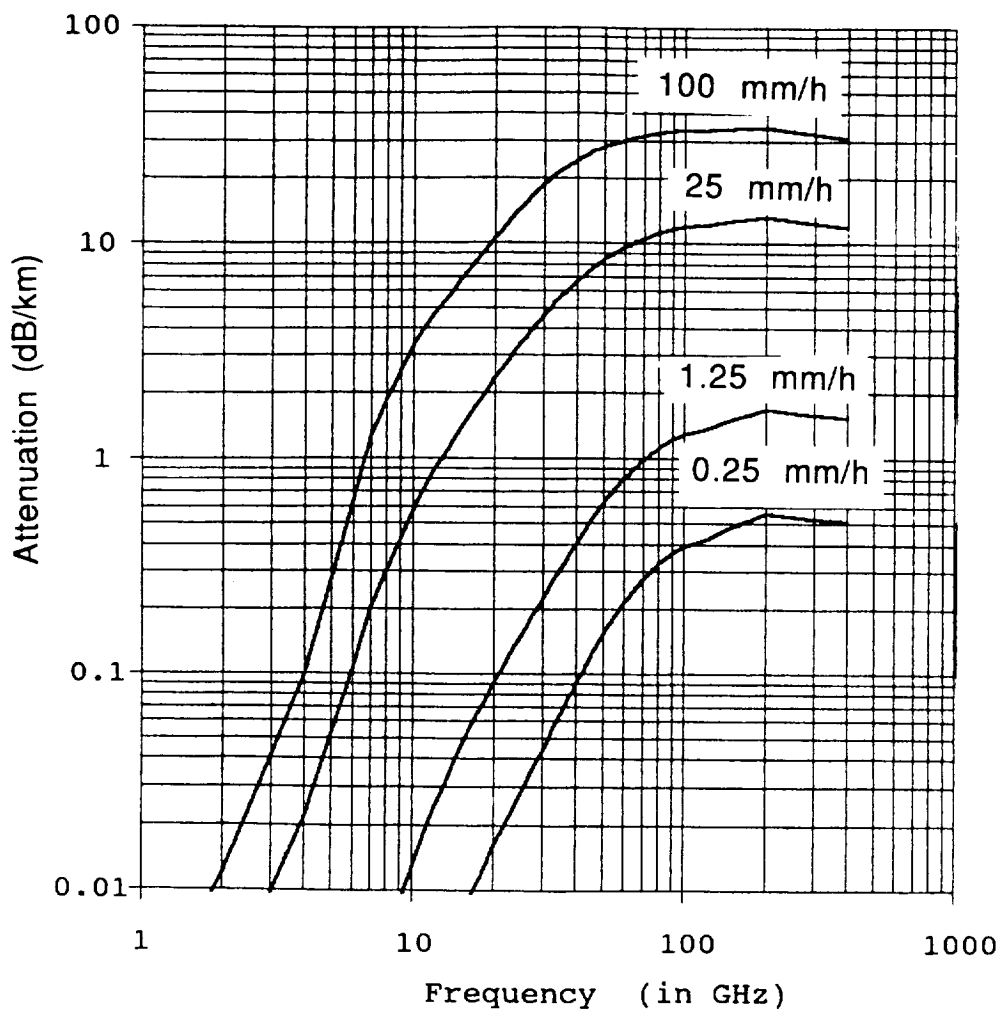


Figure 4 Specific Attenuation  $\gamma_r$  Due to Rain

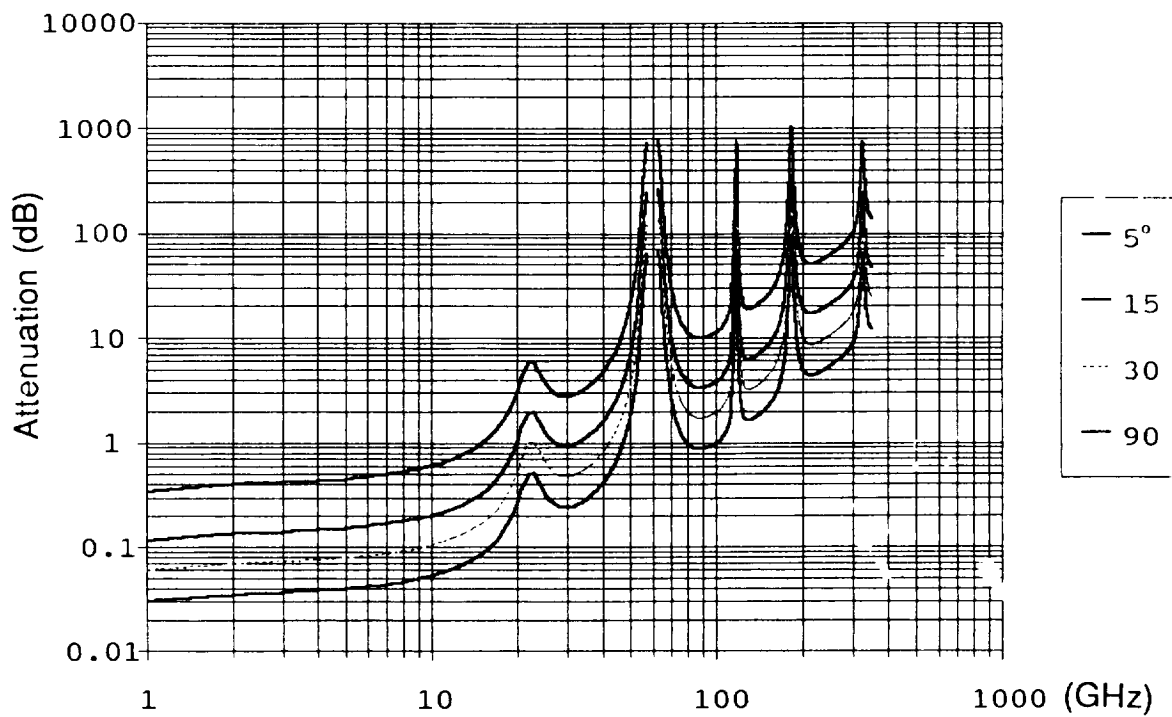


Figure 5 Gaseous Attenuation Transiting the Atmosphere  
 (pressure 1013 mb, temperature 15° C, Water Vapor 7.5 g/m<sup>3</sup>)

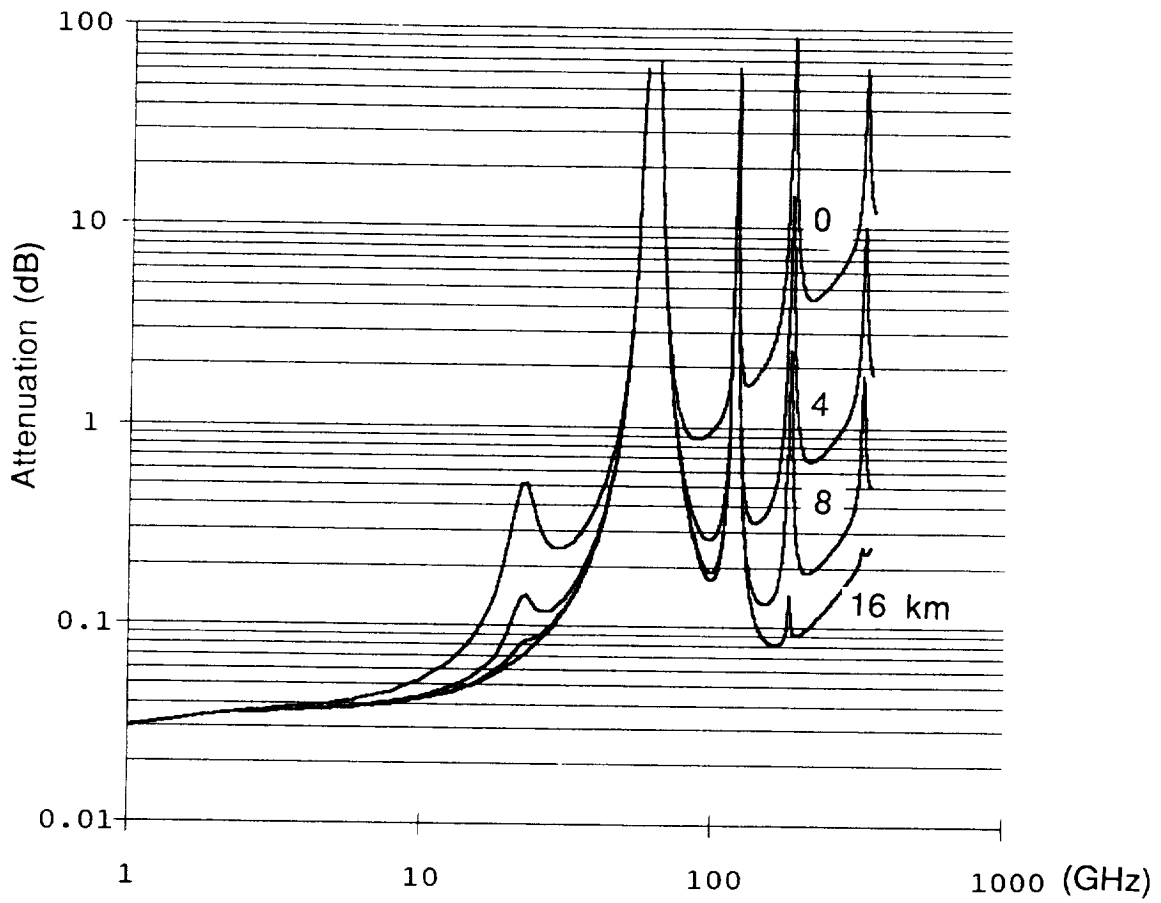


Figure 6 Zenith Gaseous Attenuation at Different Heights

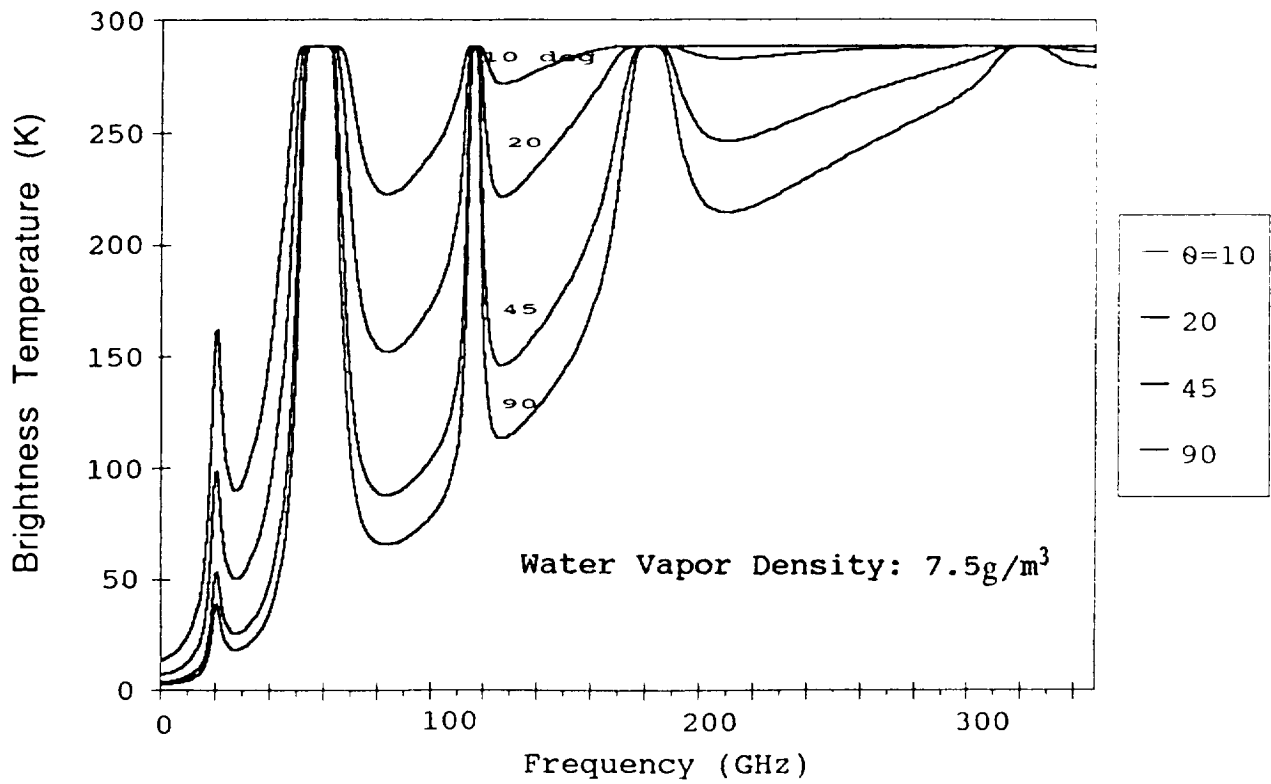


Figure 7 Brightness Temperature at Different Elevation Angles

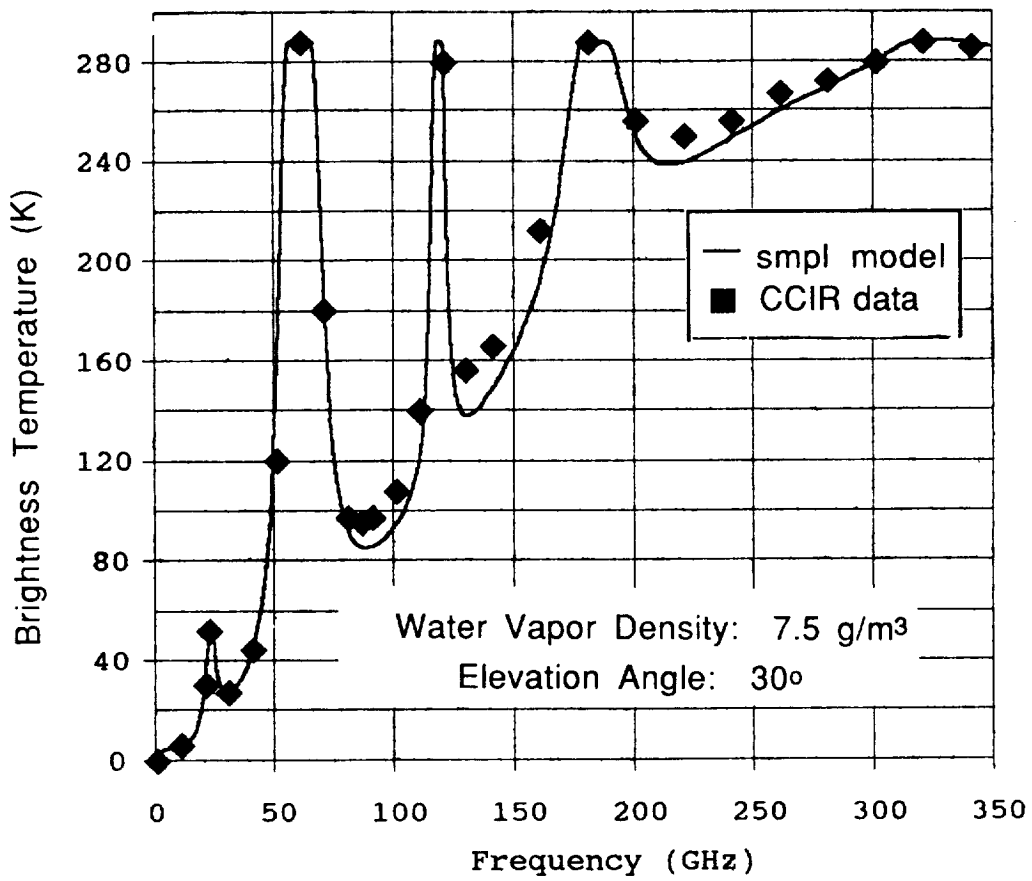


Figure 8 Brightness Temperature Comparison of the Simple Model and the CCIR Radiative Transfer Model

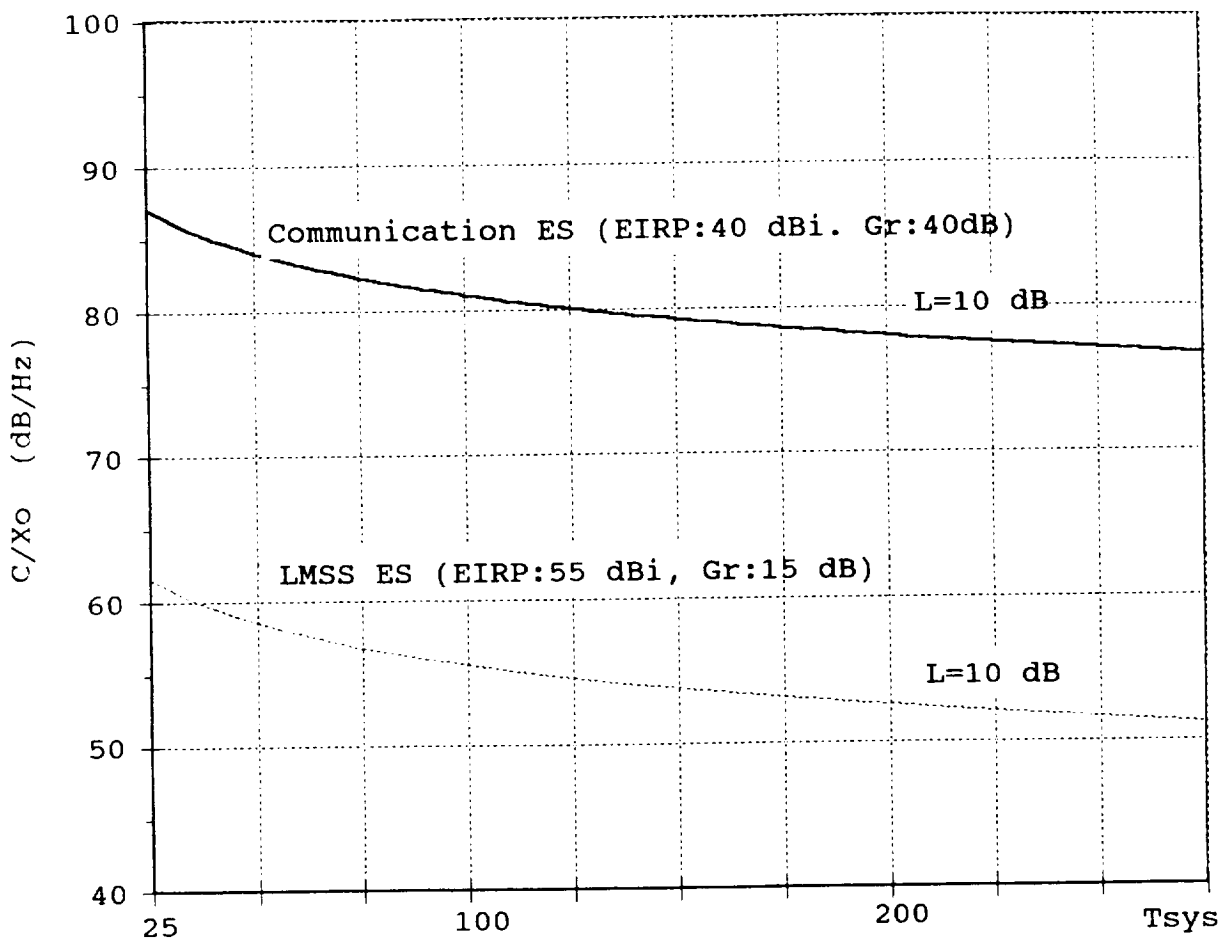


Figure 9 Two Examples of  $C/X_0$  as Received at Earth Stations  
 (—1.6 GHz, .... 30 GHz)

0-9

The program takes about 2-5 minutes to run for each application, depending on the parameters given. The program can be totally customized or manually controlled. In the former case, the program can open, run, and close automatically; the only thing needed to do is to input your options and answer questions asked.

#### References:

- [1] CCIR [1990] Recommendations and Reports of the 1990 Plenary Assembly, Dusseldorf (taken from pink documents), Reports 563, 564, 719, 720, 721.
- [2] Smith, E.K. [1982] "Centimeter and Millimeter Wave Attenuation and Brightness Temperature due to Atmospheric Oxygen and Water Vapor", Radio Science, vol.17, No.6, pp 1455-1464.
- [3] Waters, J.W. [1976] "Absorption and Emission by Atmospheric Gases", in Methods of Experimental Physics, vol. 12B, edited by M.L. Meeks, Chapter 2.3, Academic Press, N.Y.
- [4] Moupfouma F. [1985] "Model of Rainfall Rate Distribution for Radio System Design", IEE Proceedings, Vol.132, Pt. H, No 1.
- [5] Moupfouma F. [1987] "More about Rainfall Rates and Their Prediction for Radio System Engineering", IEE Proceedings, Vol.134, Pt. H, No 6.



## **Software for Propagation** **by W. Vogel, U. of Texas, Austin**

1. Choice of Hardware and Software Platform
2. Selection of Problems To Be Coded
3. Coding & Solicitation of Contributions
4. Testing & Documentation
5. Dissemination to Users
6. Technical Support
7. Revisions/Expansion

### 1. Hardware and Software Platform

- IBM/PC + Macintosh
- Spreadsheet:                   1-2-3, EXCEL, QUATTRO...
- Math:                            MATHCAD
- Special Purpose:            EE-PAC
- Language:                    Quick, FORTRAN
- Survey Users
- User Modifiable

## 2. Problem Selection

- CCIR Greenbook
- NASA Handbook
- Books: P+B, Ippolito...
- Models
- Orbits
- Footprints
- Propagation Database
- Call for Contributions

## 3. Coding & Solicitation of Contributions Standards

## 4. Testing & Documentation

Operation, Logical Errors,  $\beta$ -Testing

Easy To Use, Built-In Help, Example

User Knowledgeable

## 5. Dissemination

To Anybody

Mail, BBS

6. Technical Support

BBS, FAX

7. Revisions/Expansion

Useful Lifetime...

Enhance Functionality

Include New Developments

Advisory Panel

A Study of  
Land Mobile Satellite Service Multipath Effects  
Using SATLAB Software\*

Richard L. Campbell  
Department of Electrical Engineering  
Michigan Technological University  
Houghton, MI 49916

A software package is proposed that uses the known properties of signals received in multipath environments along with the mathematical relationships between signal characteristics to explore the effects of antenna pattern, vehicle velocity, shadowing of the direct wave, distributions of scatterers around the moving vehicle and levels of scattered signals on the received complex envelope, fade rates and fade duration, Doppler spectrum, signal arrival angle spectrum and spatial correlation. The data base may be either actual measured received signals entered as ASCII flat files, or data synthesized using a built in model. An example illustrates the effect of using different antennas to receive signals in the same environment.

## INTRODUCTION

If an elevated CW transmitter illuminates a typical mobile radio environment, with a vehicle moving past roadside trees and other scatterers, the received signal will have fast (multipath) and slow (shadow) fading, a Doppler spectrum related to the vehicle velocity and the distribution of signal arrival angles, and a spatial correlation. Each of these signal characteristics is important to a different set of engineers: the envelope fade rates are needed by system engineers to determine reliability and fade margins; the fade rates and Doppler spectrum are needed by the engineers who design robust modulation and coding; the angular spectrum is needed by the antenna engineers; and the spatial correlation is needed to evaluate the effectiveness of space diversity and adaptive arrays. All of these signal characteristics can be determined from a record of the received complex envelope as a function of time, as the receiver moves through the multipath environment. Since each characteristic is obtained from the same time record, all of the signal characteristics are related. The Doppler spectrum is the Fourier transform of the complex time record, the signal arrival angle spectrum (obtained from the Doppler spectrum) is the Fourier transform of the spatial correlation and the fast and slow fading envelope is the envelope of the complex time record. If any

\*Reprinted without oral presentation.

characteristic of the receiver is changed, it will affect all of the signal characteristics. For example: if the antenna is changed from an omni directional to a gain antenna, the distribution of signal arrival angles will change. This will change the Doppler spectrum, which is the Fourier transform of the received complex envelope. We can see that adding a gain antenna to a system not only increases the signal level; it also changes the fade statistics, the Doppler spread and the spatial correlation.

The proposed software package uses the known characteristics of received signals in multipath environments along with the mathematical relationships between the signal characteristics to allow the engineer to explore the effects of antenna pattern, vehicle velocity, various amounts of shadowing of the direct wave, distributions of scatterers around the vehicle and levels of scattered signals on each of the received signal characteristics. The actual time record of the received signal may be either real data, as collected by Vogel and Goldhirsh or Campbell, or synthesized data with the same properties as the real data.

#### RECEIVED SIGNAL COMPLEX TIME RECORD

The received signal is the sum of the direct wave and all of the scattered waves. The direct wave is attenuated by shadowing on the direct path, and is received at a frequency equal to the transmitted frequency plus or minus a Doppler shift obtained from the vehicle speed and the angle between vehicle velocity and the direct signal arrival angle. The scattered signals arrive from angles all around the receiver (Campbell 1989), so they are received at a spread of frequencies between a maximum (vehicle moving directly toward a scatterer) and minimum (vehicle moving directly away from a scatterer). The total power in the scattered waves is about 17 dB below the unattenuated direct wave (Stutzman and Barts 1988, Campbell 1989).

One application of this program is to explore the effects of different antennas and vehicle velocities on existing data bases. For example, the Vogel and Goldhirsh data were collected using crossed drooping dipole antennas. The fade statistics would be different if other antennas had been used. This program allows post processing of the Vogel and Goldhirsh data to see what they would have obtained with a different antenna, for example a 13 dB patch array.

Another application of this program is to explore the characteristics of received signals in environments that have not been measured. For example, in dense foliage, the direct wave might be attenuated by an average of 17 dB. Then the total signal is made up of equal parts, direct and scattered waves. The fade statistics will be dominated by multipath effects, and the signal arrival angle will be uniformly

distributed around the vehicle. A feedback type antenna aiming system would be lost in such an environment. The benefit obtainable from various antenna systems, such as gain, space diversity, and adaptive array, in this environment would depend on the modulation and coding used in the system.

To study signal environments that have not been measured, it is necessary to synthesize data having the correct properties. If the engineer specifies a carrier frequency, vehicle speed and direction relative to the direct wave and ratio of direct to total scattered wave power, the program can generate an appropriate complex time record with the properties of a signal received on an omni directional antenna. Shadowing effects may be included by making the ratio of direct to scattered wave power a function of time. The data may be generated using either the simple model developed by Campbell or a more correct scattering theory model (Wang, 1991). Once the basic time record is generated, it may be modified with different antenna patterns.

#### ANTENNA EFFECTS

The antenna system operates on the distribution of signal arrival angles. Antenna effects may be studied by multiplying the Doppler spectrum by the antenna pattern. This is equivalent to a convolution of the complex time record with the Fourier transform of the antenna pattern. For example, the Fourier transform of an omni directional antenna pattern is a delta function. Convolving a delta function with the complex time record leaves it unchanged. The Fourier transform of a narrow Gaussian beam antenna is a wide Gaussian. Convolving a wide Gaussian with the complex time record will tend to remove rapid fluctuations in the complex time record. This agrees with our intuition that narrow beam antennas may be used to reduce multipath effects.

To study the benefit of a narrow beam antenna, the antenna must be aimed in the direction of the direct signal arrival. Conversely, the effects of antenna aiming errors may be studied by purposely introducing an offset in the antenna pattern. The effect of an antenna aiming error is not only to reduce the received signal strength, but also to decrease the ratio of direct to scattered signal power available to the receiver. When an antenna aiming error is present, the signal strength goes down and the multipath effects go up.

The antenna patterns may be entered either as analytical functions or as ASCII flat files. A catalog of useful antenna patterns will be included in the software.

#### MODULATION AND CODING

In order to design robust modulation and coding for the

transmitted signals, the fade rates, fade durations and Doppler spectrum must be known. Each of these depends on the ratio of direct to scattered signal level, the antenna pattern, the vehicle velocity and direction and any antenna aiming errors. If feedback is used to aim the antenna, it may be useful to use different modulation on the antenna aiming pilot than for error free speech and data. Entirely different antenna systems may be optimum for intelligible real time speech and maximum data transfer.

The input and output files of SATLAB will be ASCII flat files and MATLAB .MAT files, allowing data transfer to and from other programs and industry standard signal analyzers (the latest Tektronix models communicate with MATLAB). This will permit simulating the entire signal environment, including the source, modulation and coding, multipath channel, antennas and demodulation and decoding in the laboratory.

#### EXAMPLE

Figure 1 shows a typical Doppler spectrum that might have been received by a 1.5 GHz receiver with an omni directional antenna moving at highway speeds with roadside trees. The vertical scale is in dB, with the receiver noise at -20 dB and the direct signal received at + 40 dB. The direct signal to noise ratio is about 60 dB, so receiver noise is not significant in this example. The horizontal axis is the frequency of the downconverted received signal in Hz. The scattered signals are displayed as a uniform spectrum between the minimum and maximum Doppler shifts.

Figure 2 shows the effect of receiving this same signal with a dipole antenna. The nulls of the dipole are toward the front and rear of the moving vehicle, so the minimum and maximum Doppler shifted scattered signals are attenuated. The dipole received spectrum is the solid line and the original omni spectrum is the dotted line. Note that the antenna has no effect on the receiver noise.

Figure 3 shows the effect of receiving this same signal on a 10 dB gain array. Once again the original omni signal is shown as a dotted line. The direct signal is now 10 dB stronger than for the omni case, and the scattered signals at arrival angles near the direct signal are also stronger, but by less than 10 dB. The scattered signals at angles far from the direct signal are greatly attenuated. Since the receiver noise is not affected by the antenna, the direct signal to noise ratio is now 70 dB.

Figure 4 shows the IF voltage as a function of time for each of these three cases. The signal from the dipole is offset by +2 and the signal from the omni is offset by -2. Note that the signal from the 10 dB gain array is not only stronger, it has smaller fluctuations than the signals from

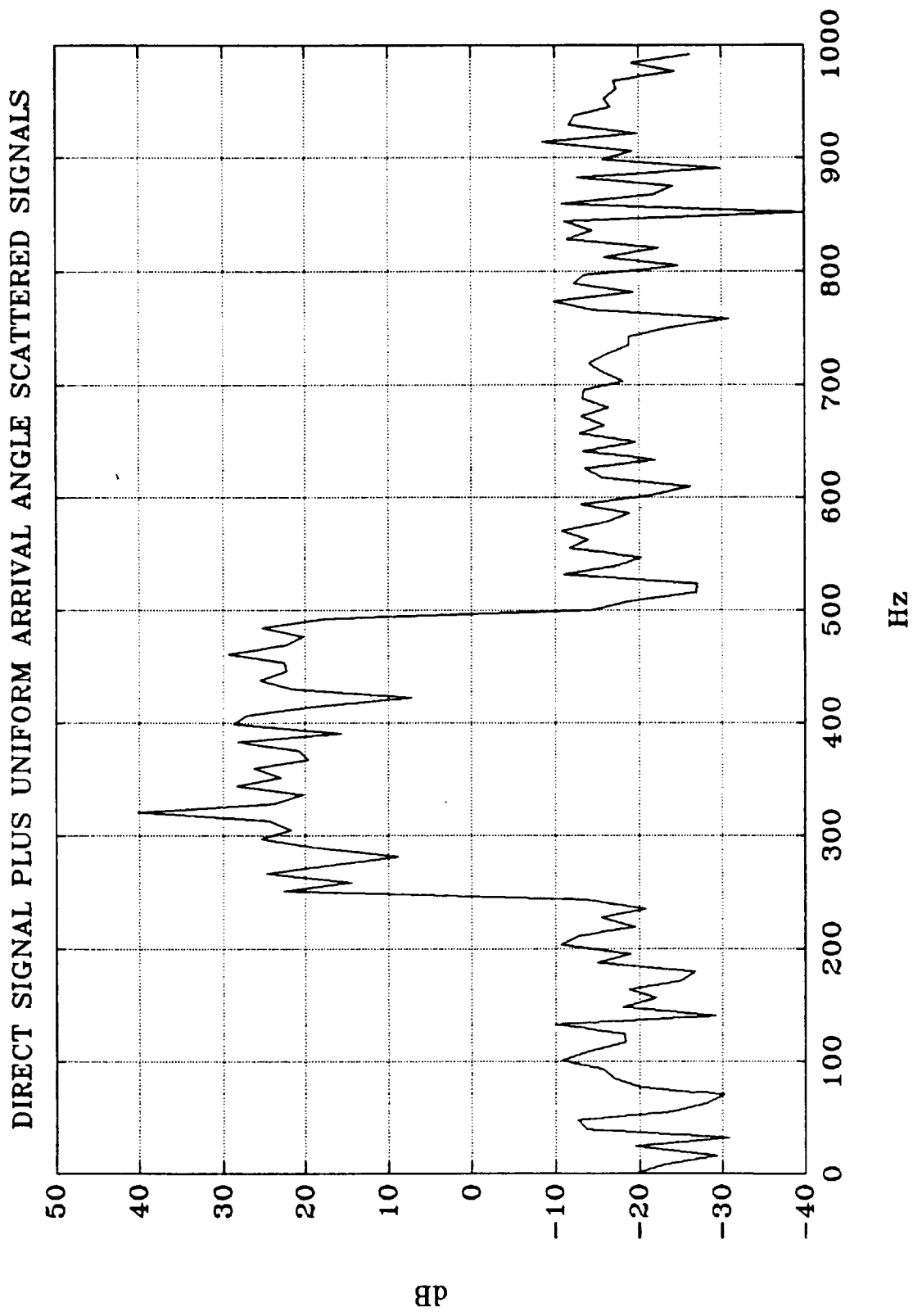
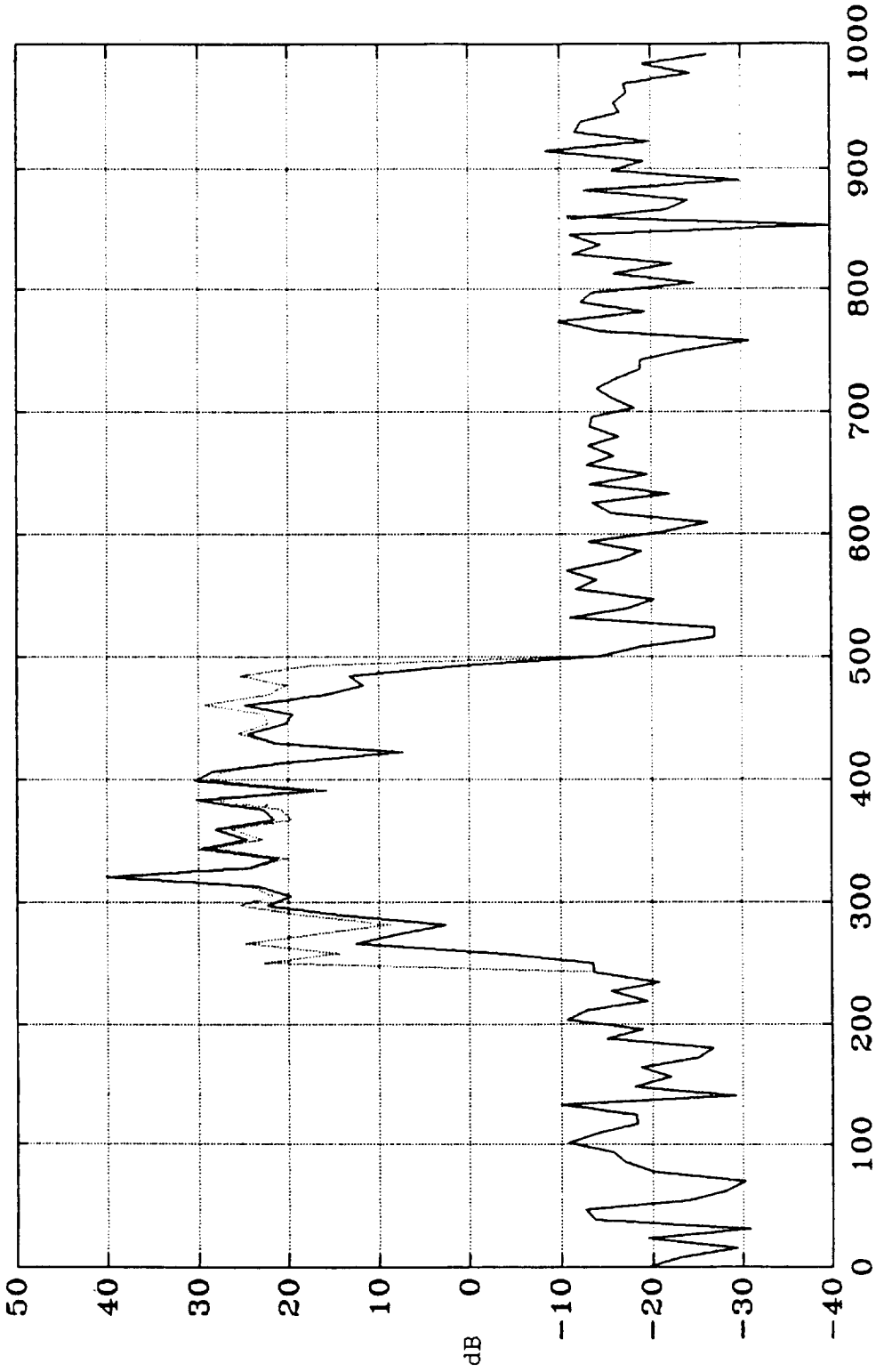


FIGURE 1

IF SPECTRUM RECEIVED ON OMNI DIRECTIONAL ANTENNA





Hz

FIGURE 2

IF SPECTRUM RECEIVED ON DIPOLE (SOLID)  
AND OMNI DIRECTIONAL ANTENNAS (DOTTED)

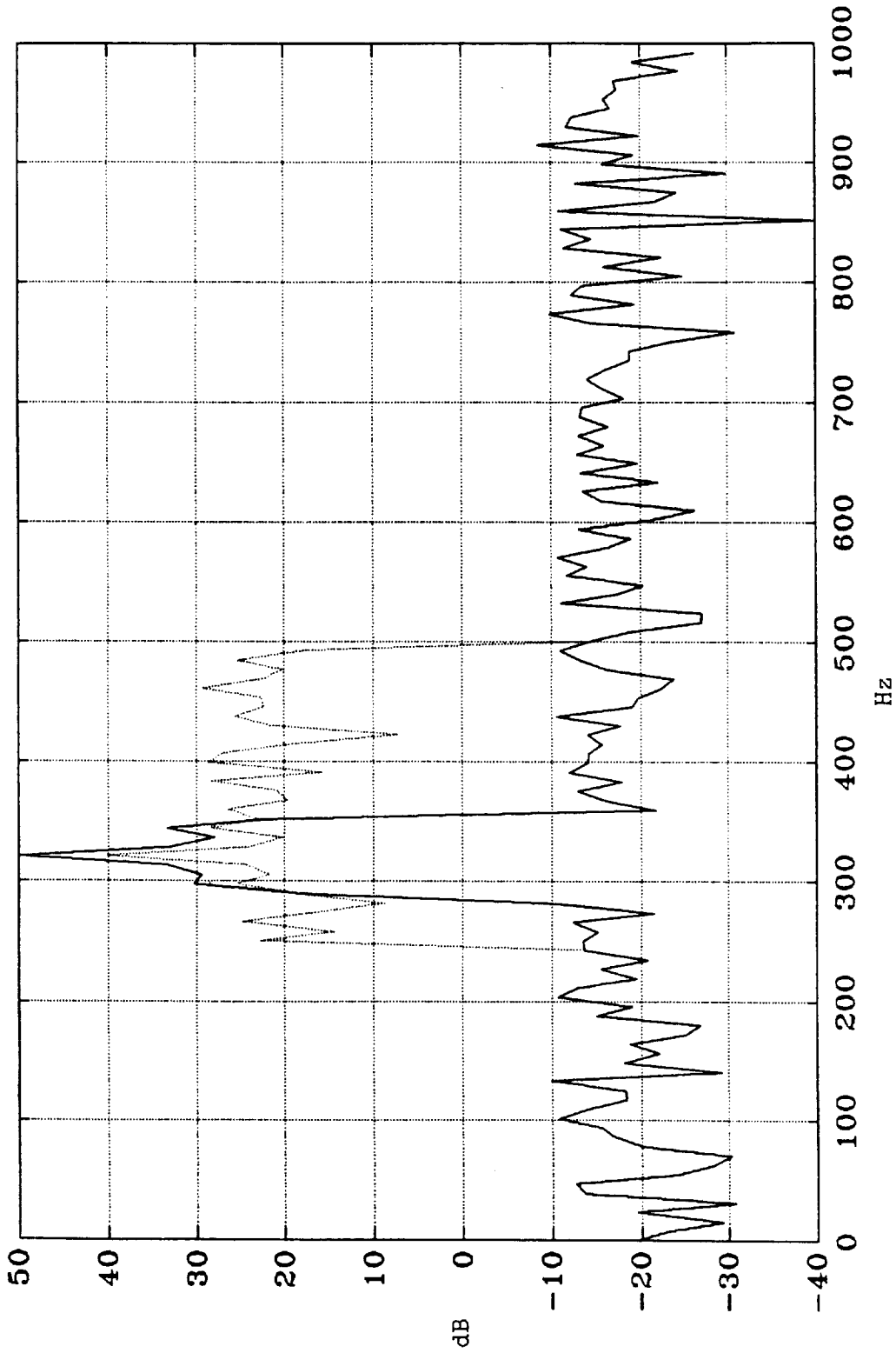


FIGURE 3  
 IF SPECTRUM RECEIVED ON 10 DB GAIN ANTENNA (SOLID)  
 AND OMNI DIRECTIONAL ANTENNA (DOTTED)

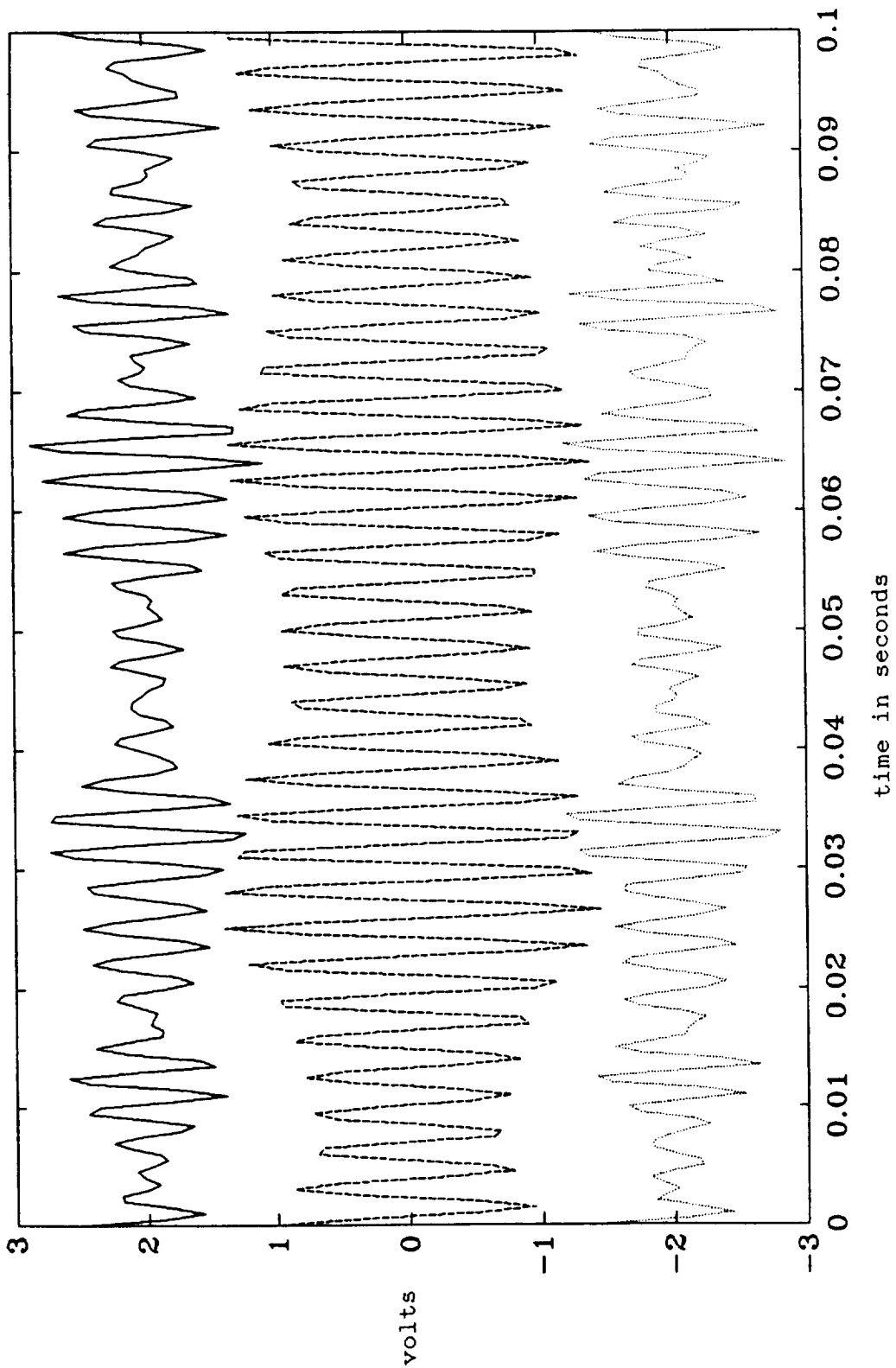


FIGURE 4

RECEIVED TIME RECORD SIGNALS ON DIPOLE (UPPER TRACE)

10 DB GAIN ANTENNA (MIDDLE TRACE)

AND OMNI DIRECTIONAL ANTENNA (LOWER TRACE)

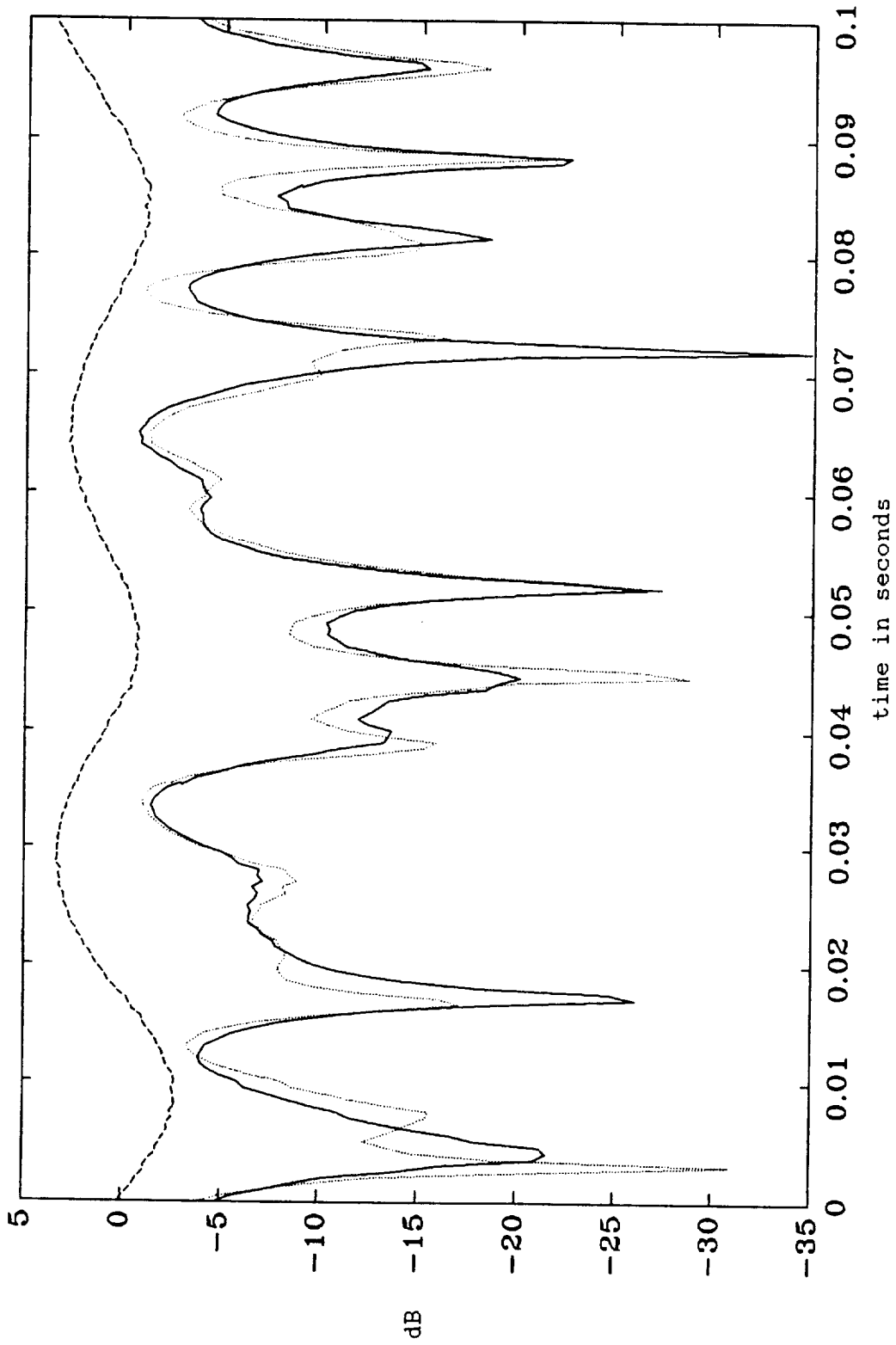


FIGURE 5

RECEIVED SIGNAL ENVELOPE USING DIPOLE (SOLID) 10 DB GAIN  
 (DASHED) AND OMNIDIRECTIONAL (DOTTED) ANTENNAS

the other two antennas.

Figure 5 is the received signal envelope as a function of time. Note the characteristic multipath rapid fading in the signals received on the omni and dipole antennas. The signal received on the 10 dB gain antenna is not only stronger than the other signals, it also has much less fading.

This example clearly illustrates the effect of different antenna patterns on the fade statistics of strong signals in a multipath environment. By modifying the signal parameters (signal to noise ratio, ratio of direct to scattered signals etc.) other signal environments may be studied.

## CONCLUSIONS

The proposed software package will be a useful tool for studying mobile radio signals in environments with direct and scattered waves. The interrelated effects of carrier frequency, vehicle speed, antenna gain and antenna pattern, antenna aiming errors, direct to scattered signal ratio, shadowing and receiver noise are all included. By modifying one parameter, the engineer may observe the effect on all the other signal characteristics.

This program will either generate synthetic data using one of several available models, or use actual received data files. The engineer may modify measured data to see the effect of different antennas.

## REFERENCES

Campbell, Richard L., R. Estus and H. Wang, "1300 MHz Propagation and Scattering in Trees," Final Report of NASA JPL Contract 957973, June 1989.

Stutzman, W. L., and R. M. Barts, "LMSS Modeling Status Report," in Proceedings of the Thirteenth NASA Propagation Experimenters Meeting (NAPEX XIII), San Jose, CA June 1989, JPL Publication 89-26.

Wang, H., "Experimental and Theoretical Study of UHF Radio Wave Propagation in a Forest Environment," Ph.D. Dissertation, Michigan Technological University, Houghton, MI, June 1991.



## CLOSING REMARKS ON THE NASA PROPAGATION PROGRAM

David V. Rogers  
Propagation Advisory Committee Representative  
Communications Research Centre  
Department of Communications, Ottawa, Canada

ABSTRACT--Several remarks on the current state of the NASA Propagation Program are offered.

### 1. INTRODUCTION

The Science Review of the NASA Radio Propagation Program that was held in September 1986 yielded 14 principal recommendations. It is perhaps worthwhile to reflect on those recommendations now in light of the current evolution of the program.

### 2. REMARKS

Almost five years have elapsed since the Science Review of the NASA Propagation Program (Booker et al., 1987). In reviewing the 14 Principal Recommendations of the report, one observes that some of the recommendations have become obsolete and some have been most successfully implemented; they seem to have been accorded the respect that they deserved. The recommendations were applied to focus the program, not hinder its flexible evolution.

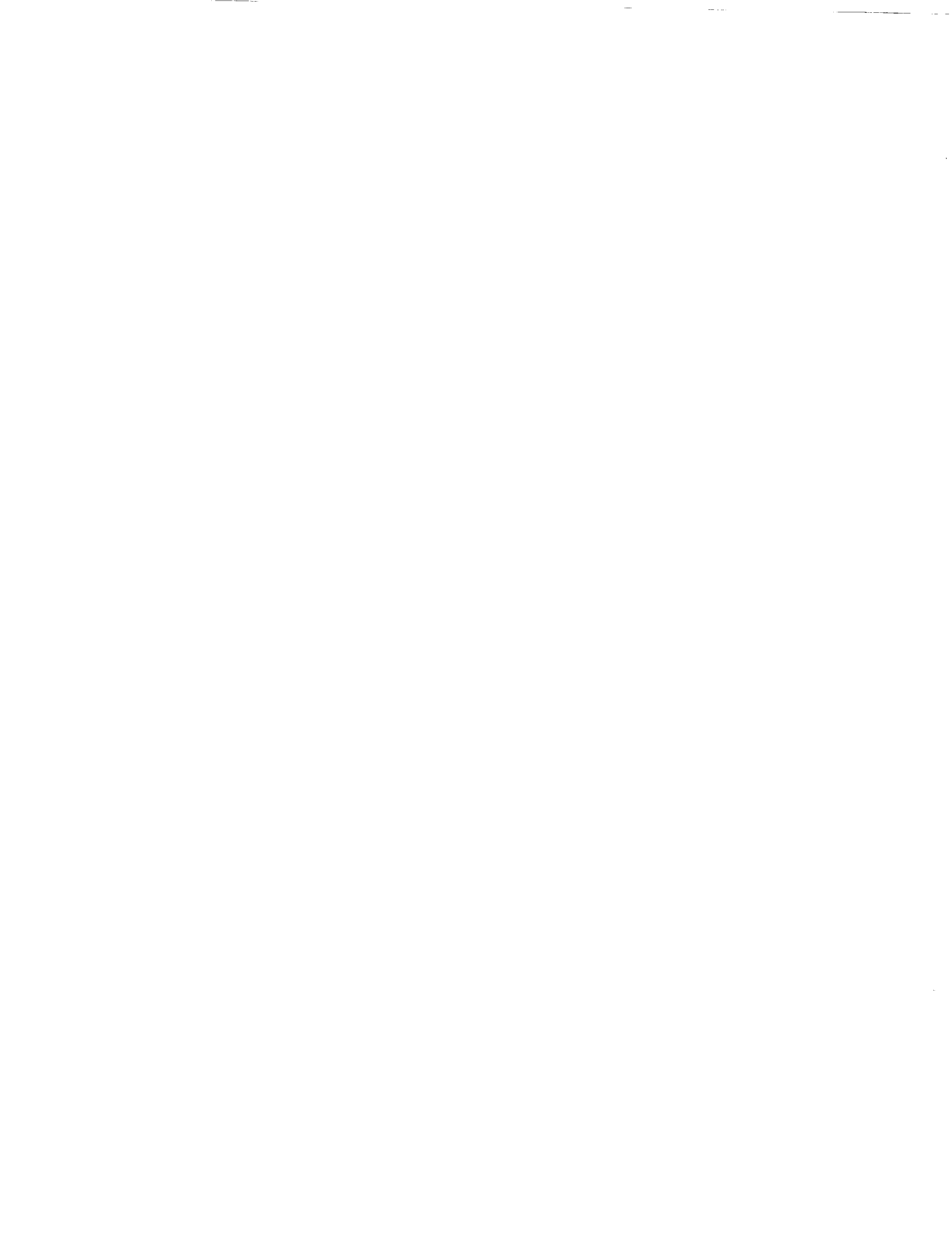
This latter aspect appears to be quite important considering the current broadbased coverage of propagation topics within the program. While much of NASA's early propagation work concerned higher frequencies, at the time of the science review the emphasis was on low-frequency mobile-satellite effects related to the MSAT-X program.

It is gratifying to observe that the current program covers a variety of topics. K-band slant-path propagation with the Olympus and ACTS satellites emphasizing requirements of emerging systems (e.g., low-availability applications); EHF radiometry, including cloud attenuation; continuing development of the NASA handbooks based on theoretical and empirical inputs; and a look ahead to K-band mobile propagation are being addressed. The attendance at NAPEX XV is proof of the recommended national and international cooperation. I am impressed with the current program.

### REFERENCE

1. H.G. Booker, G. Brussaard, K.S. McCormick, and D.V. Rogers, "Science Review of the NASA Radio Propagation Program," Report STC-2127, Science & Technology Corporation, Hampton, Virginia, February 1987.

PRECEDING PAGE BLANK NOT FILMED





**ADVANCED COMMUNICATIONS  
TECHNOLOGY SATELLITE  
PROPAGATION STUDIES MINIWORKSHOP**

Chairman:

D. (Jack) Chakraborty  
Jet Propulsion Laboratory

**PRECEDING PAGE BLANK NOT FILMED**

THE UNIVERSITY OF CHICAGO

INTRODUCTORY REMARKS FOR ACTS MINIWORKSHOP  
JOHN W. KIEBLER

PROGRESS SINCE LAST WORKSHOP

- GRANT AWARDED TO VPI FOR DEVELOPMENT OF ACTS PROPAGATION TERMINAL IN JANUARY
- PRELIMINARY DESIGN REVIEW CONDUCTED IN MAY
- NASA RESEARCH ANNOUNCEMENT IN NEAR FINAL FORM
  - INVITES PROPOSALS TO INSTALL, OPERATE TERMINALS, PREPROCESS DATA, PERFORM RESEARCH
  - INVITES PROPOSALS FOR OTHER PROPAGATION RESEARCH
  - DECISION SCHEDULED FOR SEPTEMBER ON WHETHER TO RELEASE AS STAND ALONE NRA OR COMBINED WITH COMMUNICATIONS EXPERIMENTS

ACTS CONFERENCE '91 AUGUST 29-30, 1991

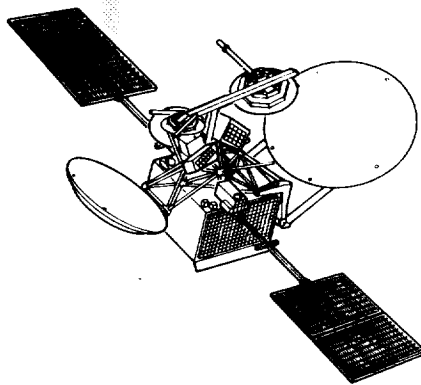
- PROPAGATION SESSION
- BRING ACTS PROPAGATION EXPERIMENTS PROGRAM INTO MAINLINE ACTS ACTIVITIES
- EXPECT THAT ACTS PROPAGATION WORKSHOPS WILL BE MERGED WITH ACTS ANNUAL MEETING STARTING IN 1992
- STRONGLY ENCOURAGE ALL OF OUR EXPERIMENTERS WHO ARE INTERESTED IN ACTS PROPAGATION STUDIES TO ATTEND

ISSUES TO BE RESOLVED WHICH NEED THE BENEFIT OF ADVICE FROM THIS GROUP

- WOULD LIKE TO SEE ACTS WORKSHOPS FOCUS ON PROBLEM SOLVING AND PLANNING-GOOD OPPORTUNITY TO MAKE PROGRESS ON SOME ISSUES TODAY
  - NEED FOR WEATHER INSTRUMENTATION AND ITS AVAILABILITY
  - RECOMMENDATIONS FOR DATA ACQUISITION DISPLAYS
  - REQUIREMENTS FOR DATA PREPROCESSING

PRECEDING PAGE BLANK NOT FILLED

# ADVANCED COMMUNICATIONS TECHNOLOGY SATELLITE (ACTS) PROGRAM



ROBERT BAUER  
ACTS PROGRAM UPDATE  
NAPEX XV  
LONDON, ONTARIO, CAN.  
06/29/1991

**ACTS**

NASA

**ACTS LAUNCH READINESS DATE**

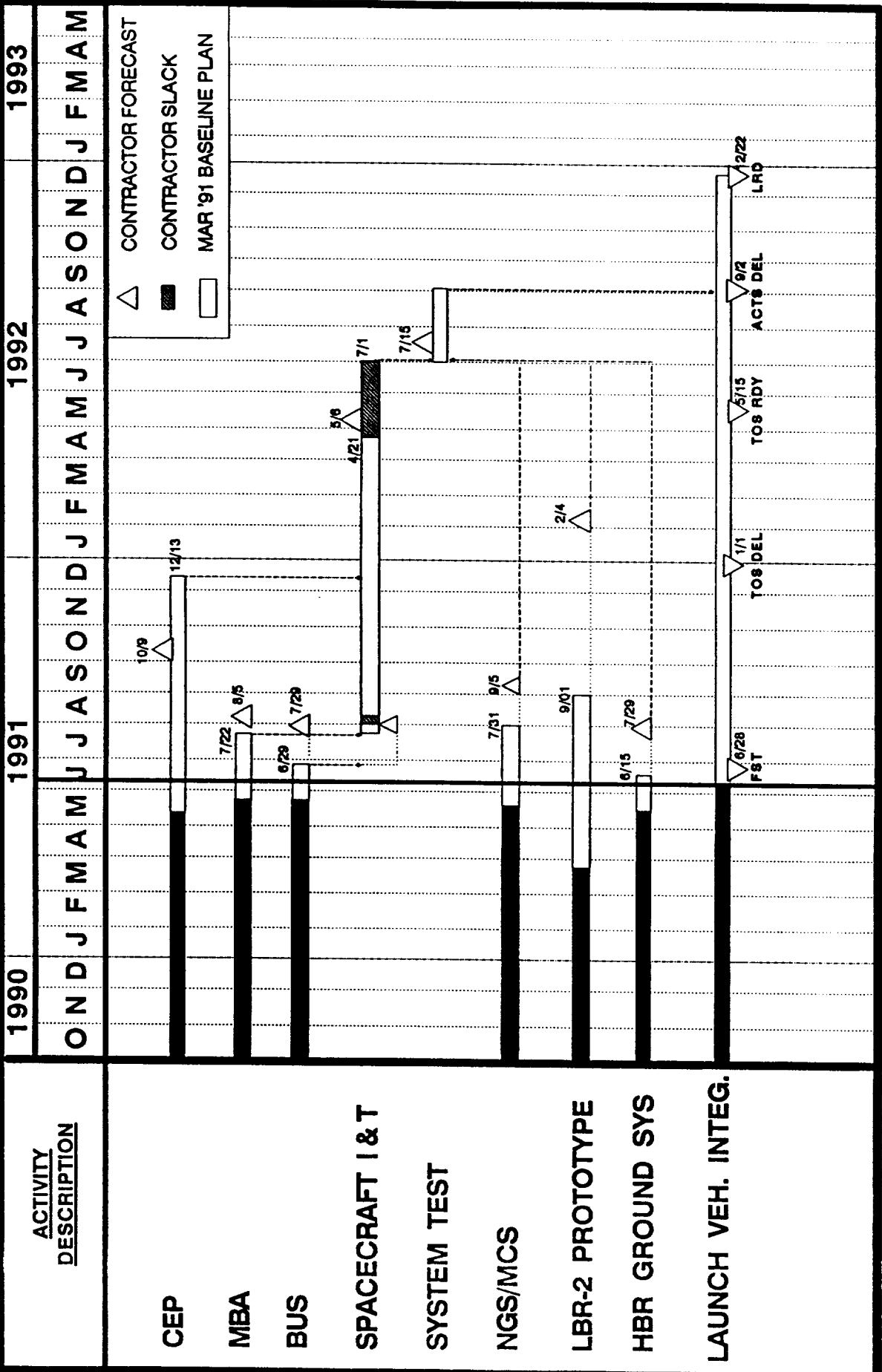
- CURRENT PLAN IS TO BE READY TO LAUNCH BY 22 DEC. 1992
- PLANNING MANIFEST INDICATES A FEB. 1993 LAUNCH
- DUE TO "CAP" CONSIDERATIONS, ACTS DESIRES TO LAUNCH AS CLOSE TO DEC. 1992 LRD AS POSSIBLE
- MARS OBSERVER MISSION, WITH A 16 SEPT. - 10 OCT. 1992 LAUNCH WINDOW IS DRIVING THE SCHEDULE
- MEETING WITH MSFC, KSC, LERC AND CONTRACTORS HAS BEEN HELD TO DEVELOP AN INTEGRATED/AGREED-TO-LAUNCH-SITE SCHEDULE - CURRENT DRAFT IS EXTREMELY CONSERVATIVE. KSC HAS AGREED THAT A JAN. 1993 LAUNCH IS POSSIBLE
- LERC PLAN IS TO MAINTAIN EARLY JAN. 1993 LAUNCH CAPABILITY

# ACTS STATUS

REV 1: 6/11/91

STATUS DATE: 6/11/91

ENGINEER: D.W. COOK



## **ACTS EXPERIMENTS PROGRAM**

**THE EXPERIMENTS PROGRAM IS BEING HANDLED IN 3 PHASES:**

**PHASE 1:** NASA MEETS WITH POTENTIAL EXPERIMENTERS TO EXPLAIN ACTS AND OPPORTUNITIES TO EXPERIMENT. RECEIVE INITIAL EXPERIMENT CONCEPT FROM EXPERIMENT.

**PHASE 2:** EXPERIMENTERS DEFINE EXPERIMENT CONCEPT IN FURTHER DETAIL AND SUBMIT FORMAL RESPONSE (E.G., EOA, NRA, OR MOU) TO SOLICITATION. RECEIVE APPROVAL FROM NASA ON REQUEST TO USE ACTS.

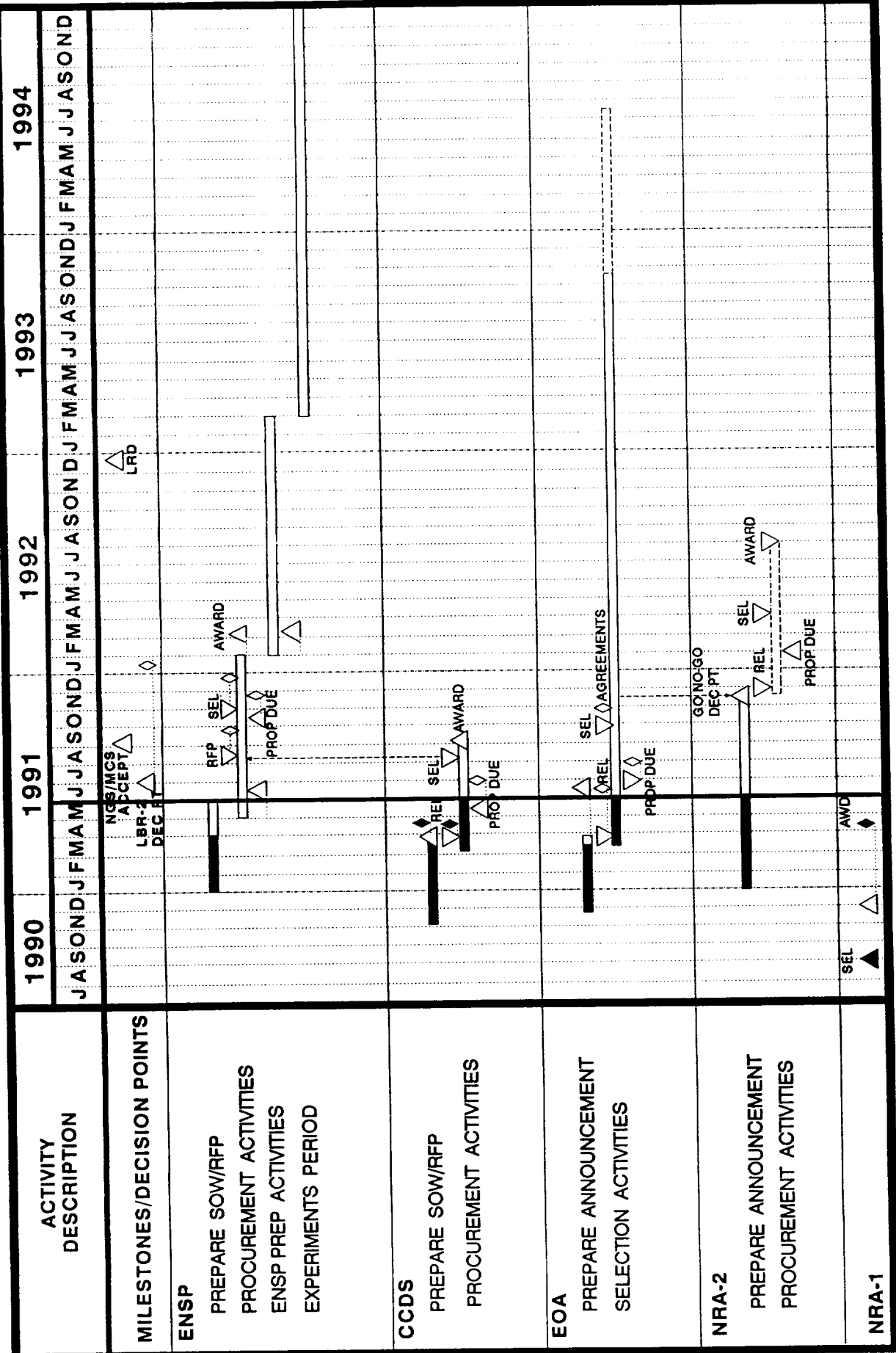
**PHASE 3:** NASA SCHEDULES THE EXPERIMENT, EXPERIMENTER PERFORMS ACTS EXPERIMENT AND SUBMITS RESULT OF EXPERIMENT TO NASA.

**PHASE 1 HAS BEEN COMPLETED (12-31-90) ALTHOUGH SOME SOLICITATION WILL CONTINUE IN SELECTED AREAS. EXPERIMENT CONCEPTS HAVE BEEN DEVELOPED AS A RESULT OF PHASE 1 AND FORMAL RESPONSES ARE BEING PREPARED TO RESPOND TO THE EXPERIMENT OPPORTUNITY ANNOUNCEMENT AND NASA RESEARCH ANNOUNCEMENT.**



# ACTS Experiments Program Solicitation Activities Schedule

BASELINE DATE: 03/01/91  
STATUS DATE: 06/07/91  
ENGINEER: D.W. COOK





# **Commercial Satellite Communications Program**

---

---

## **ACTS: Experiment Network Provider (ENP)**

### **Objectives**

- Reduce the Costs (equipment, learning curve) of Conducting an ACTS Experiment
- Incentivize an Industry Partner to Develop Potential Experimenters, and Encourage Commercial Focus

### **Structure**

- Selection Based on Level of Capitalization, Cost Recovery Charges, Network Versatility and Operations Experience
- Procurement Would be Modelled after Sea Wiffs
- Solicit Proposals for Post 2-Year Mission Utilization

### **Status**

- Draft and Schedule Under Development at LeRC
- Issue RFP after CCDS Selection – They May Team with a Carrier and Propose

## **ACTS EXPERIMENTS PROGRAM**

### **CENTER FOR THE COMMERCIAL DEVELOPMENT OF SPACE (CCDS)**

**DEFINITION:** NOT-FOR-PROFIT JOINT RESEARCH AND DEVELOPMENT INSTITUTION FORMED BY COMMERCIAL FIRMS, ACADEMIC AND RESEARCH INSTITUTIONS, AND NON-NASA GOVERNMENT ORGANIZATIONS DEVELOPED TO FOCUS ON AN IDENTIFIED TECHNOLOGY AREA.

**OBJECTIVE:** TO STIMULATE AND HELP SUSTAIN FURTHER DEVELOPMENT OF U.S. SPACE-RELATED ACTIVITIES CONTRIBUTING TO U.S. LEADERSHIP IN AN ECONOMIC SECTOR.

**ACTS CCDS AREA OF FOCUS IS SPACE-BASED TELECOMMUNICATIONS AT THE SYSTEMS OR SUBSYSTEMS LEVEL THAT PREFERABLY INCLUDES SOME LEVEL OF ACTS EXPERIMENTS ACTIVITY.**

**RELEASE DATE: APRIL 19, 1991**

**PROPOSALS DUE: JUNE 21, 1991**



# **Commercial Satellite Communications Program**

---

---

## **ACTS: Experiment Opportunity Announcement (EOA)**

### **Objectives**

- Provide for "Broadest Possible Participation"
- Establish Formal Working Arrangements Between NASA and Experimenters

### **Structure**

- Accommodate All U.S. Experimenters Who Bring Their Own Resources and Do Not Cause Technical Harm to the Network
- Technical Evaluation Will Include Scheduling of Spacecraft Resources to Support experiments

### **Status**

- Ready for Circulation to Other NASA Offices

# **Commercial Satellite Communications Program**

---

---

## **ACTS: NASA Research Announcement**

### **Objectives**

- **Meet Experiment Balance Objective: Exercise All Facets of ACTS New technologies**
- **Broaden Participation to Universities**
- **Support Non-product Oriented Experiments**

200

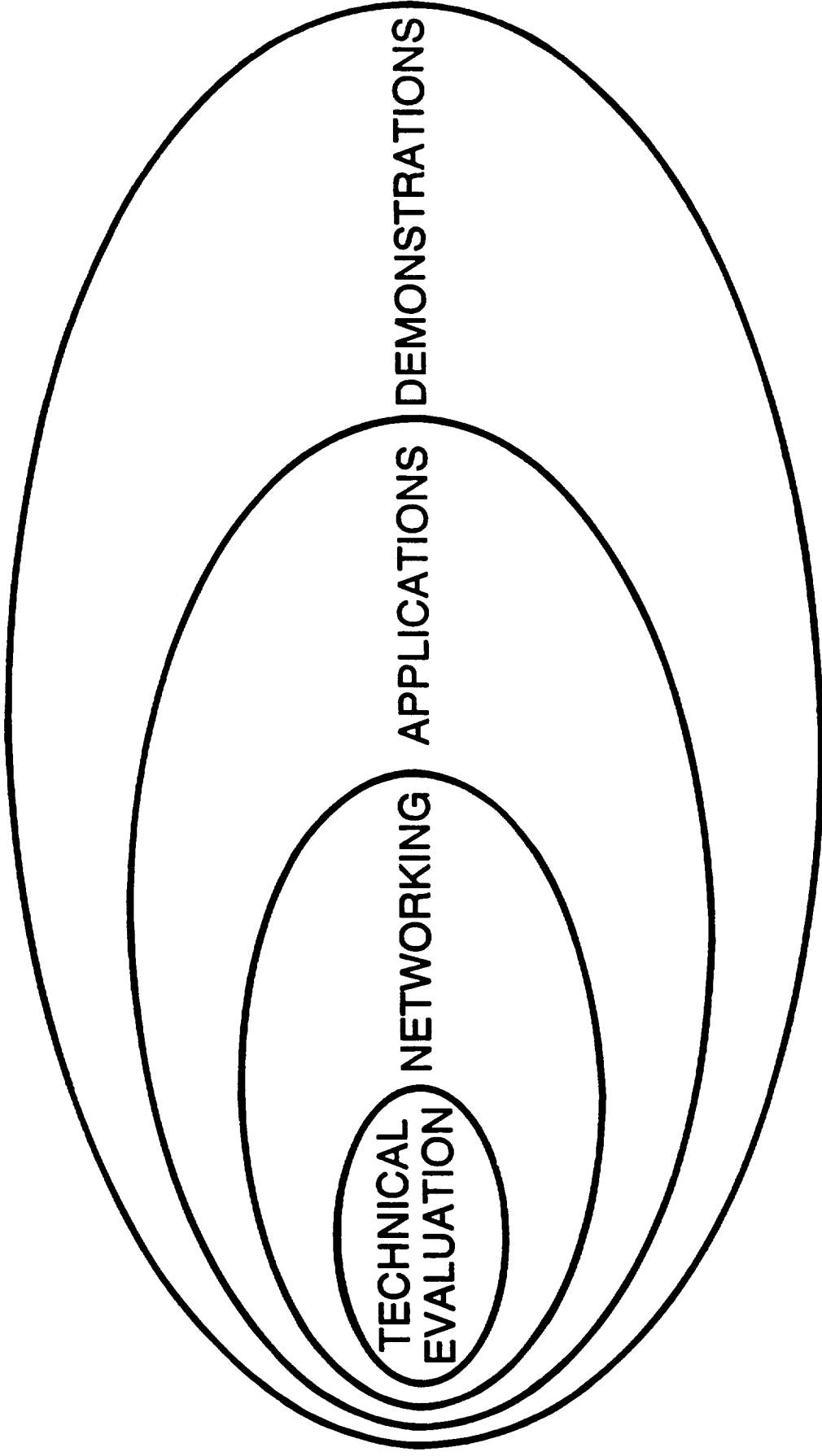
### **Structure**

- **Prefer Educational Institutions**
- **Encourage Resource-sharing**

### **Status**

- **Phase One: Selected 10 Proposals for Award**
- **Phase Two: Draft Under Development**

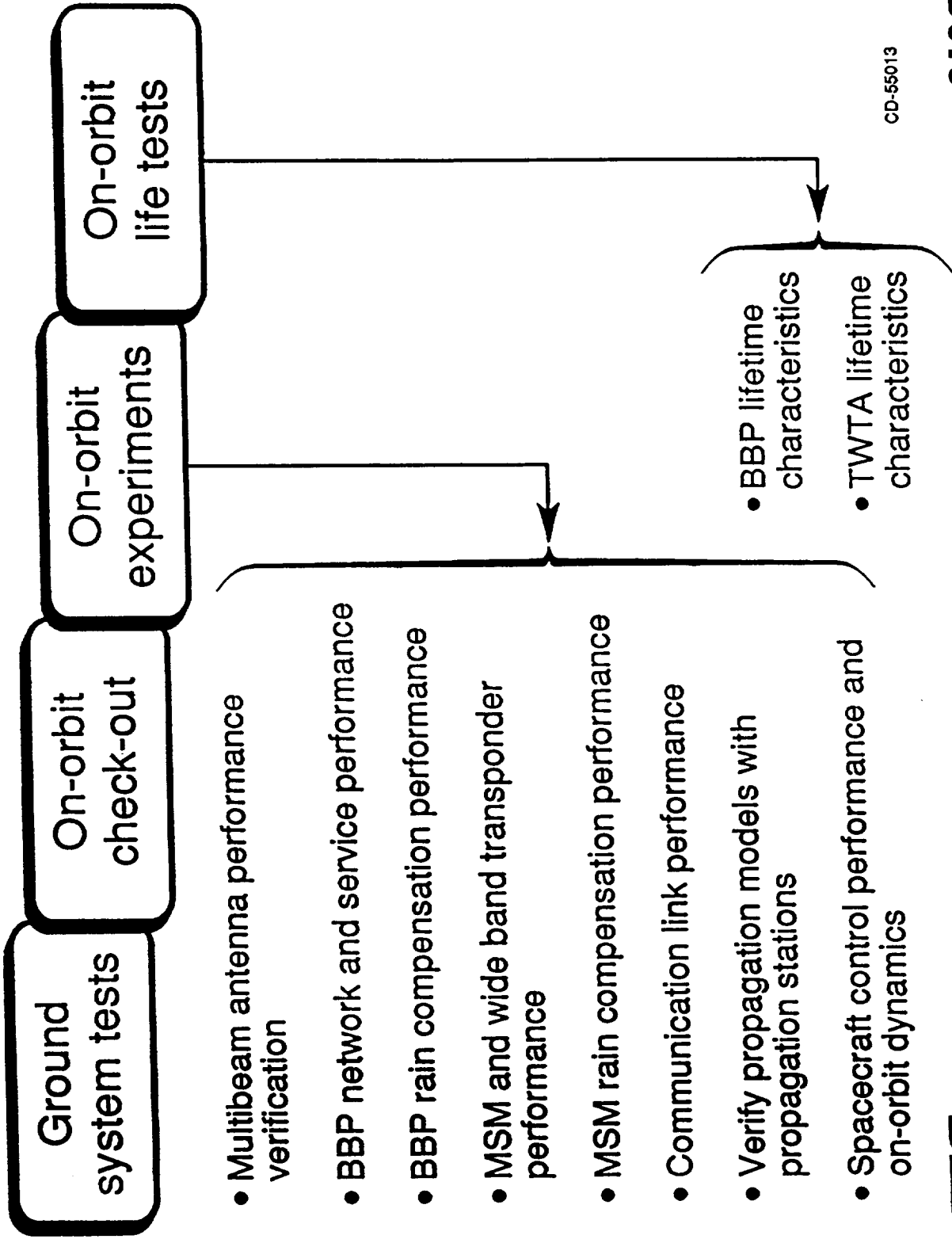
# THE SPECTRUM OF EXPERIMENTS



## EXPERIMENT CATEGORIES

- **TECHNOLOGY**
  - SYSTEM TECHNICAL EVALUATION AND VALIDATION  
FLIGHT  
GROUND
  - NETWORK CONTROL  
SWITCHING  
ACQUISITION AND SYNCHRONIZATION
  - PROPAGATION  
DYNAMIC RAIN FADE COMPENSATION  
TRANSMISSION IMPAIRMENTS
- **APPLICATIONS**
  - DYNAMIC, ON-DEMAND MESH INTERCONNECTIVITY (BBP)  
DATA, VOICE AND VIDEO  
WIDE AREA NETWORKS, LAN INTERCONNECTIVITY  
INTEGRATED DIGITAL SERVICES (ISDN)
  - BROADBAND SWITCHING (MSM)  
SUPERCOMPUTER INTERCONNECTION & DISTRIBUTION  
SCIENCE DATA NETWORKING  
HIGH DEFINITION TELEVISION TRANSMISSION
  - KA-BAND (30/20 GHz)  
PERSONAL COMMUNICATIONS  
AERONAUTICAL MOBILE COMMUNICATIONS
- **DEMONSTRATIONS**

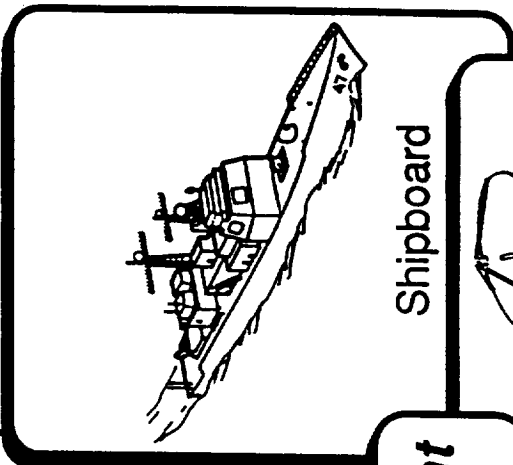
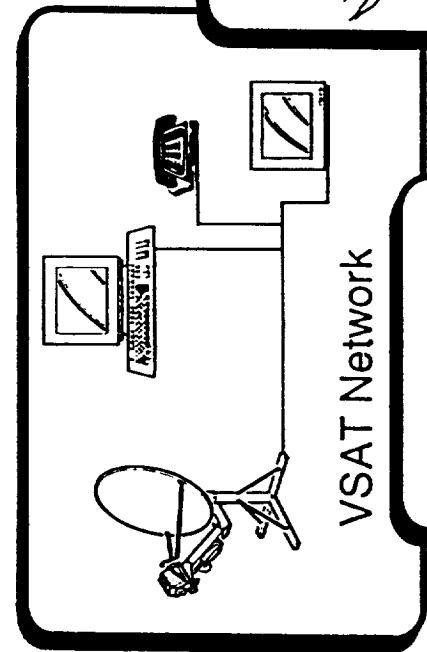
# ACTS Technology Verification



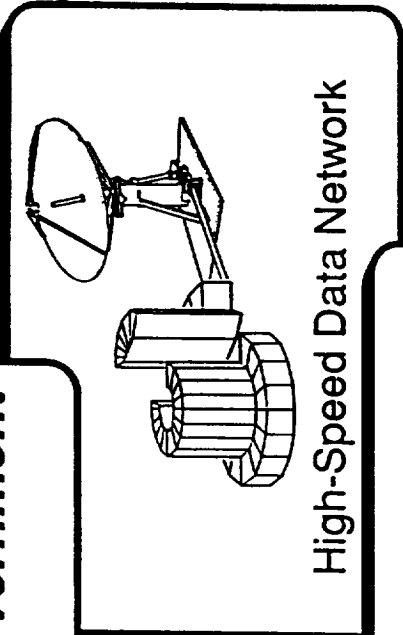
CD-55013



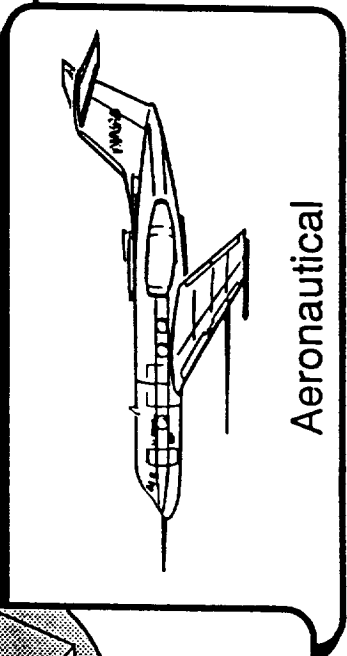
**Experiments  
Development**



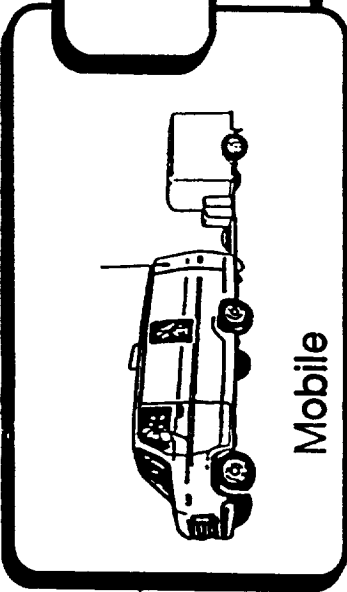
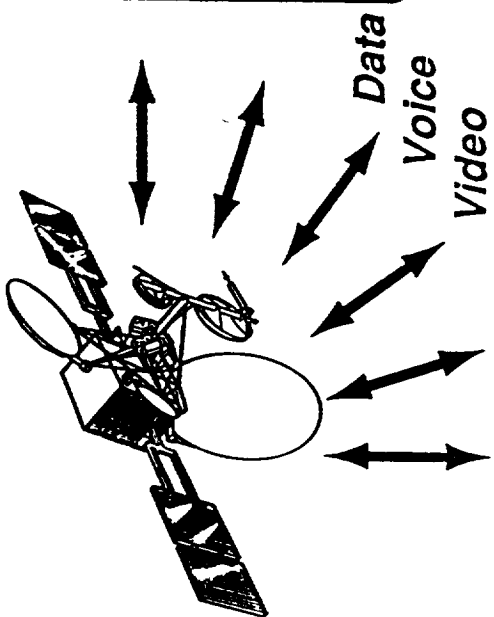
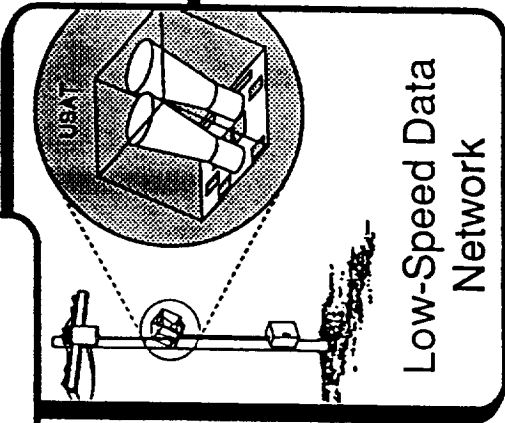
**Government**



CD-55006

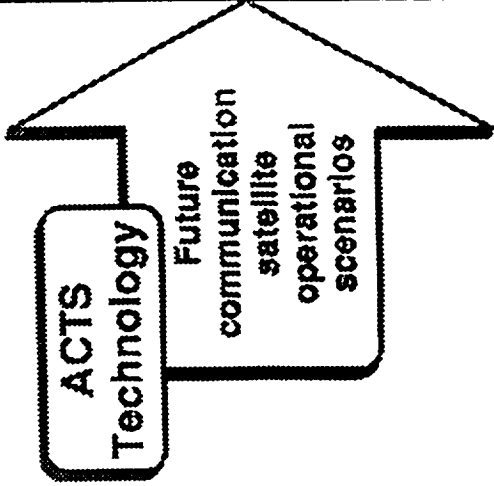


**Industry**





# ACTS Earth stations



## Potential high payoff application areas

1. T1 VSAT (1.544Mbps) full mesh network
  - Data voice and video
  - ISDN
2. High Data Rate (HDR) (300 Mbps)
3. Mobile
  - Aeronautical
  - Land
  - Shipboard
4. USAT (Kbps)
5. Personal communications

CD-55011

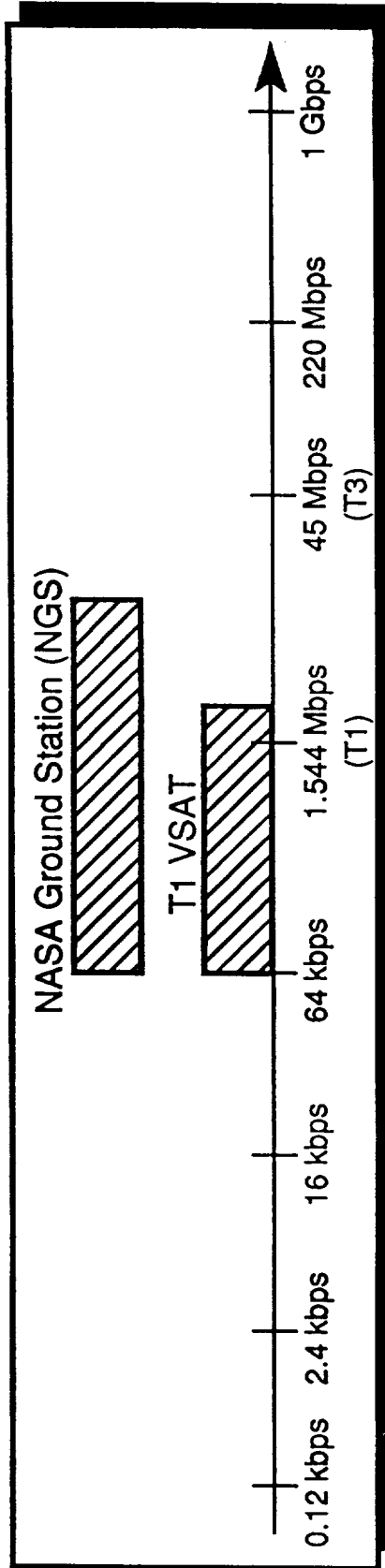
## Development of Earth stations

- NGS TT COMSAT
- T1 VSAT Harris
- ISDN-TIE COMSAT
- MSM-LET LeRC-SED
- HDR NASA/DARPA
- Aero LeRC-SED/JPL
- AMT JPL
- Shipboard NASA/Navy
- USAT NASA/Industry
- Propagation receive only VPI

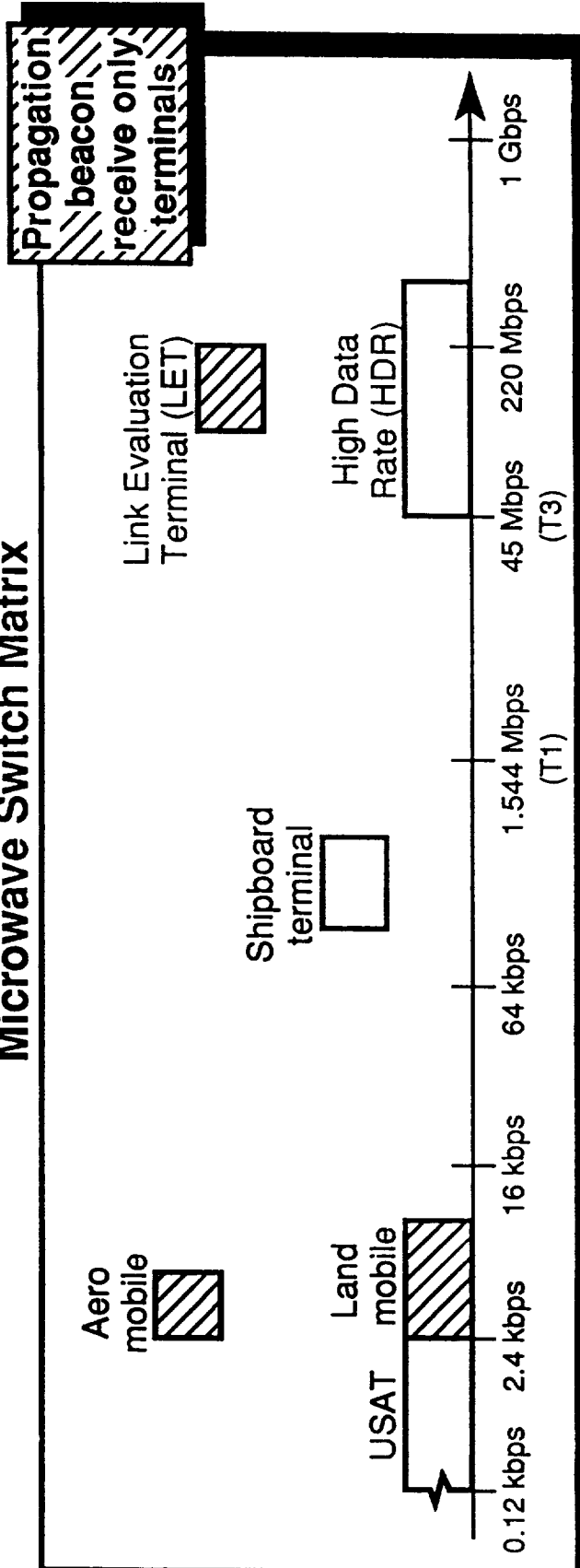


# ACTS Experimenter Terminal Types

## Baseband Processor Mode



## Microwave Switch Matrix

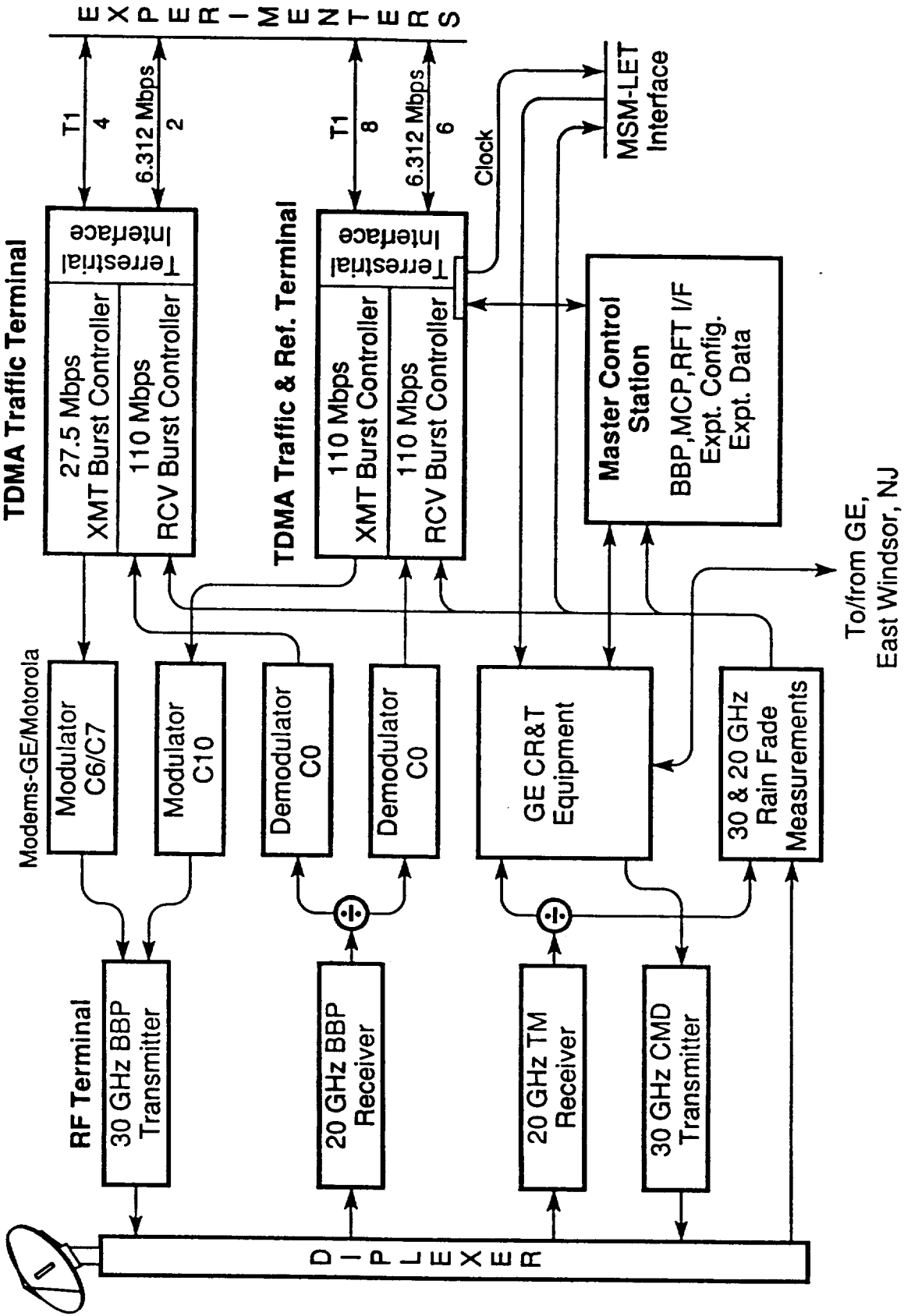


Prototype currently funded

CD-55038



# ACTS Master Ground Station (NGS/MCS)

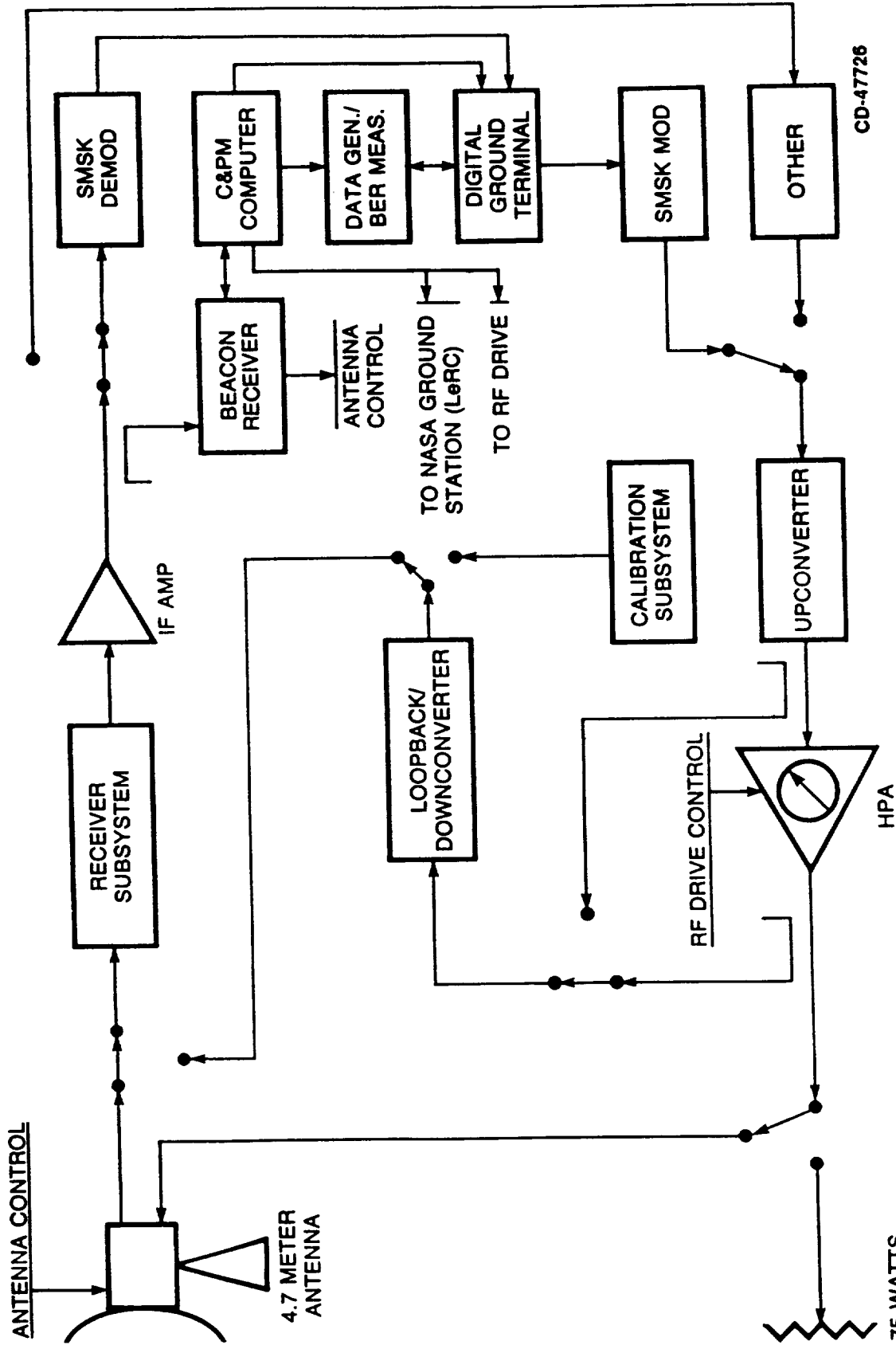


CD-55052



Provided by COMSAT except as noted

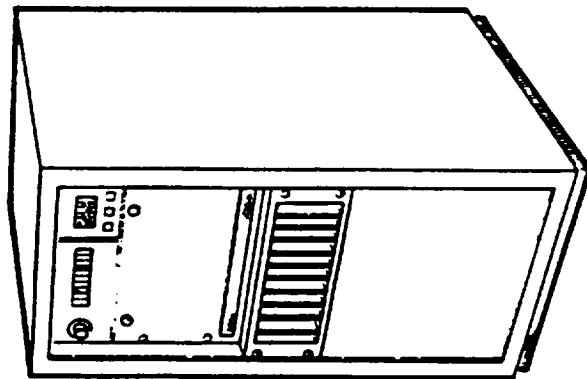
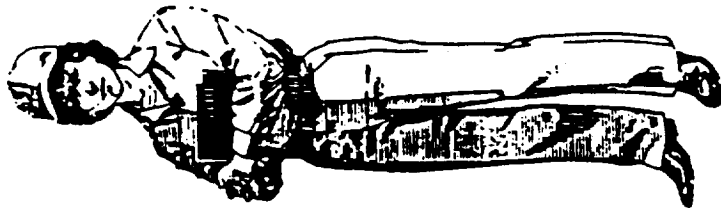
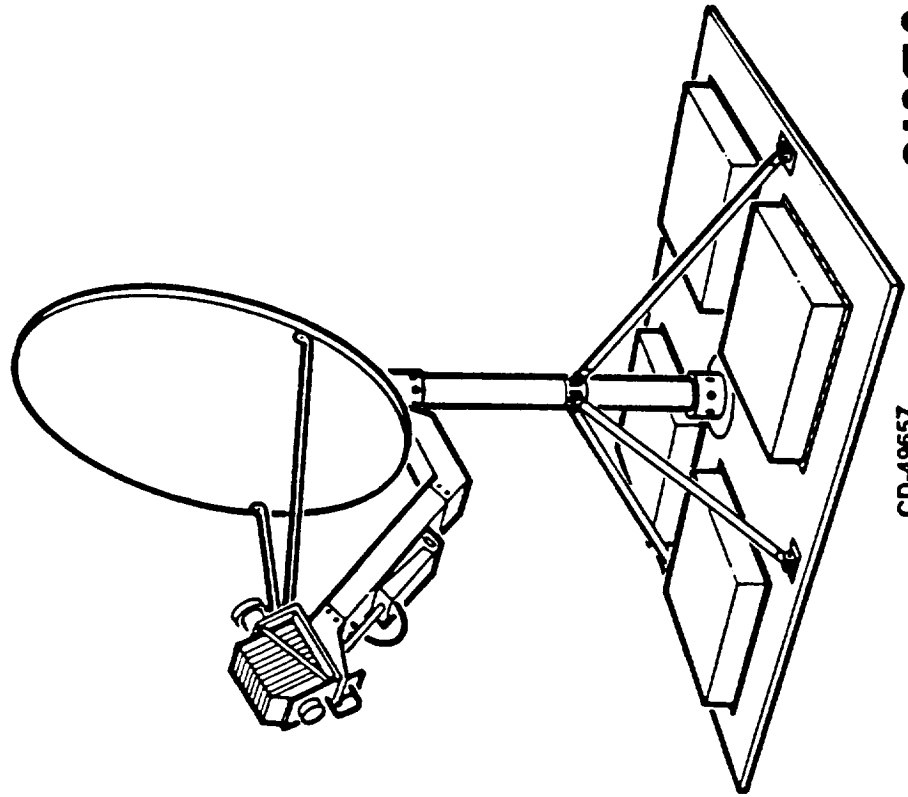
# HIGH BURST RATE LINK EVALUATION TERMINAL



BER	BIT ERROR RATE	RF	RADIO FREQUENCY
C&PM	CONTROL AND PERFORMANCE MONITOR	HPA	HIGH POWER AMPLIFIER
NGS	NASA GROUND STATION	SSK	SERIAL MINIMUM SHIFT KEY



# ACTS T1 VSAT EARTH STATION

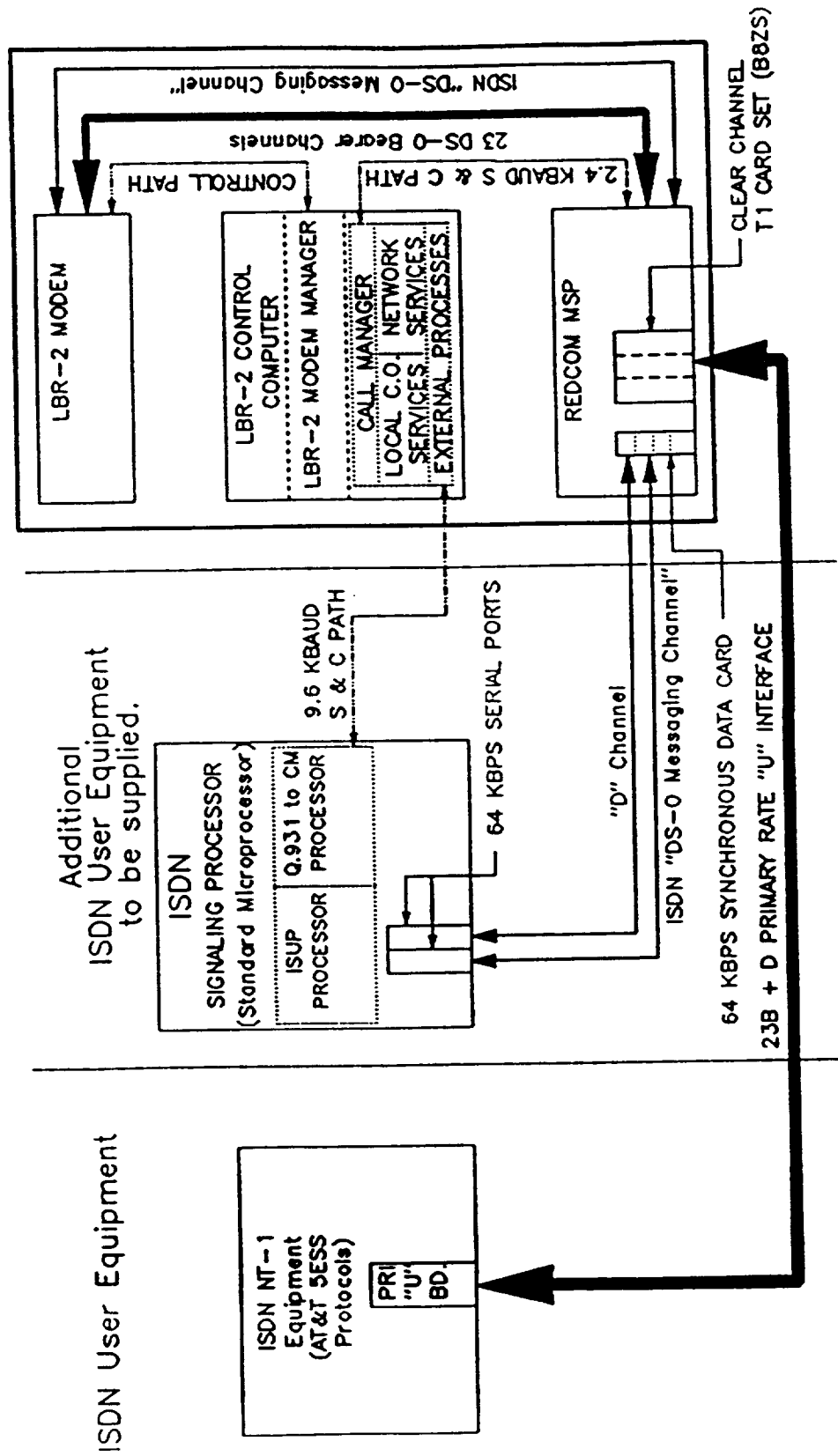


**ACTS**

CD-49657

**NASA**

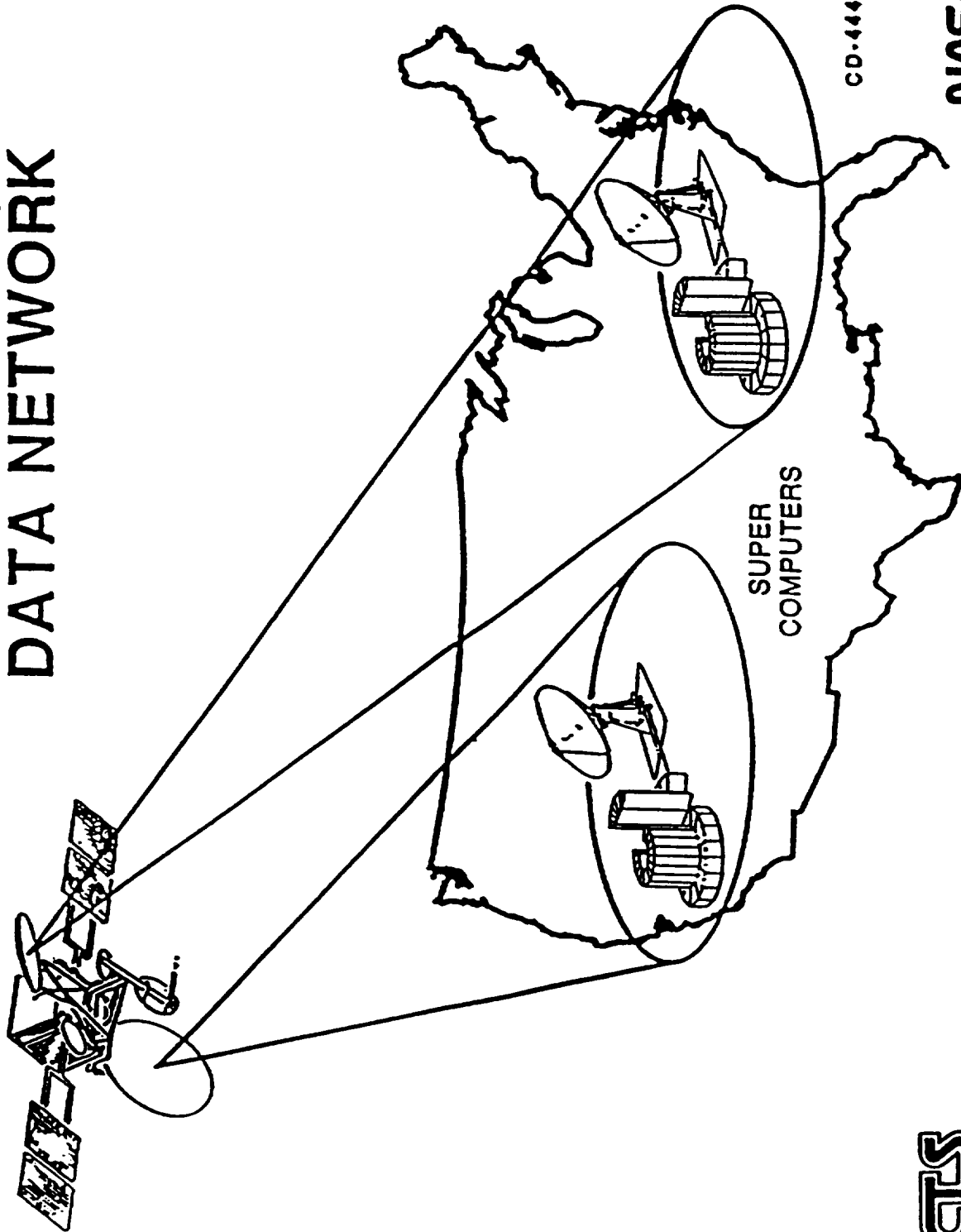
# ISDN User to Network Interface



S & C -- Signaling and Control

P. A. Lowry  
12/20/90

# HIGH THROUGHPUT (1 GBPS) DATA NETWORK

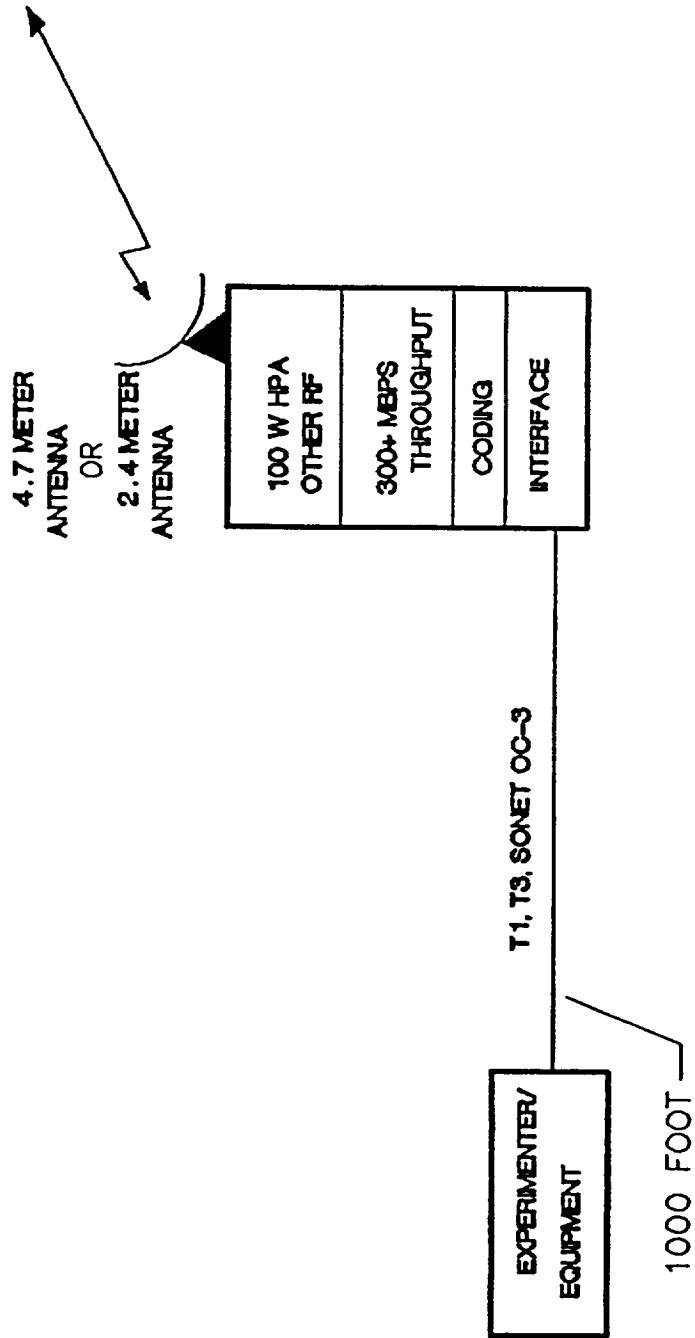


CD-44469

NASA

AGTS

# ACTS HIGH DATA RATE GROUND STATION CONCEPT





HIGH DATA RATE DESIGN CONCEPTS

THROUGHPUT RATE OF UP TO 311 MBPS - TWO OC-3 (155.5 MBPS) CHANNELS  
- SIX DS3 CHANNELS  
- SIX DS1 CHANNELS

THREE CHANNELS ACCOMMODATED IF NECESSARY ANTENNA(S) IS(ARE) AVAILABLE.

CURRENTLY PROPOSED GROUND STATION SITES ARE IN THE AREAS OF  
CHAMPAIGN, ILLINOIS; COLUMBUS, OHIO; KANSAS CITY, KANSAS;  
CLEVELAND, OHIO; LOS ANGELES, CA; WASHINGTON, D.C.

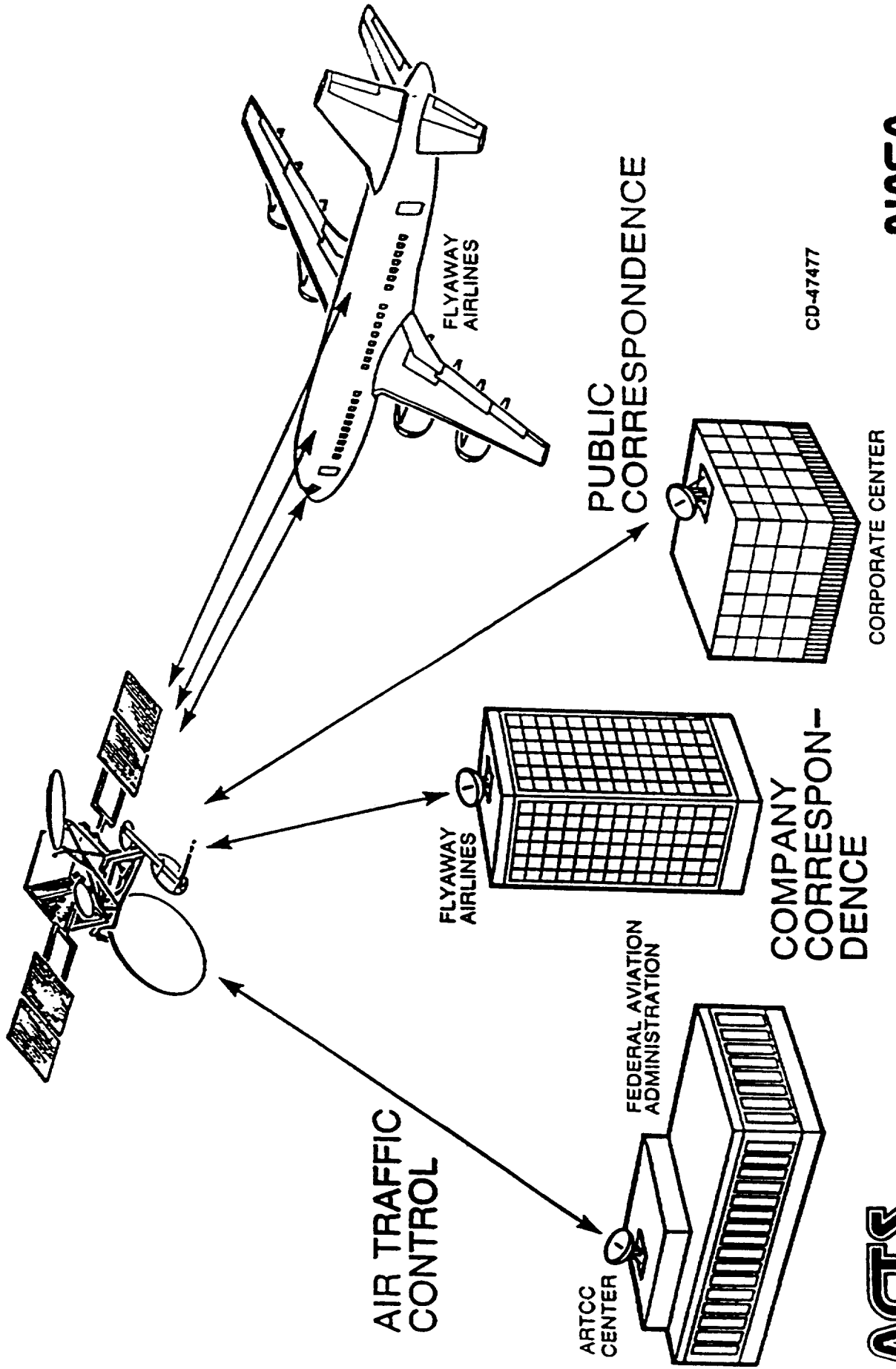
5 METER MAXIMUM DIAMETER ANTENNA

TDMA WITH RESERVATION WITH NASA REFERENCE STATION

SUPPORTS  $10^{-1}$  BIT ERROR RATE

TRANSPORTABLE

# AERONAUTICAL COMMUNICATIONS



CD-47477

NASA

STAN



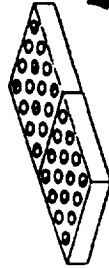
AEROSPACE TECHNOLOGY DIRECTORATE

# ACTS AERO EXPERIMENT



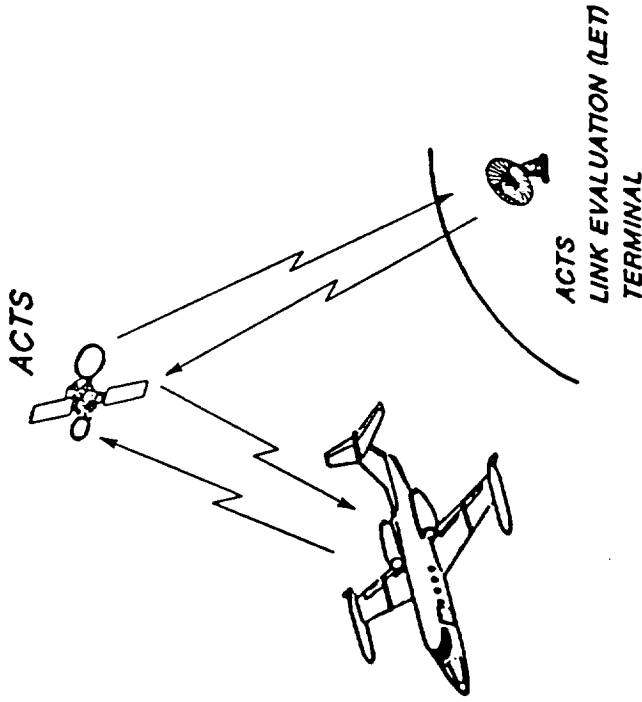
30 GHz MMIC XMIT ARRAY

TWO 4 x 4 TEXAS INSTRUMENTS SUBARRAYS - LeRC CONTRACT NAS3-25718



20 GHz MMIC REC'V ARRAYS (2)

GE AND BOEING ARRAYS ARE "ADD-ONS" TO EXISTING ROME LABS / MILSTAR ARRAY DEVELOPMENT CONTRACTS



## EXPERIMENT FEATURES

- ELECTRONICALLY STEERED MMIC ARRAYS:
- LEARJET AIRCRAFT PLATFORM
- FULL DUPLEX VOICE LINK
- OPEN LOOP BEAM STEERING

## OBJECTIVES

- DEMONSTRATE / EVALUATE MMIC ACTIVE PHASED ARRAYS ON AIRCRAFT PLATFORM  
 DEMONSTRATE FULL DUPLEX VOICE & DATA AT 2.4, 4.8 AND 9.6 Kbps  
 EVALUATE ANTENNA STEERING / AUTOMATIC ACTS BEAM TRACKING  
 MEASURE A/C-TO-E/T LINK PARAMETERS: BER, Eb/No, QUALITY, etc.
- DEMONSTRATE / EVALUATE ACTS TECHNOLOGY  
 EVALUATE PERFORMANCE OF ACTS SCANNING BEAM IN TRACKING AERONAUTICAL TERMINAL  
 EVALUATE EFFECTS OF ACTS WIDEBAND TRANSPONDER ON LOW DATA RATE SIGNALS

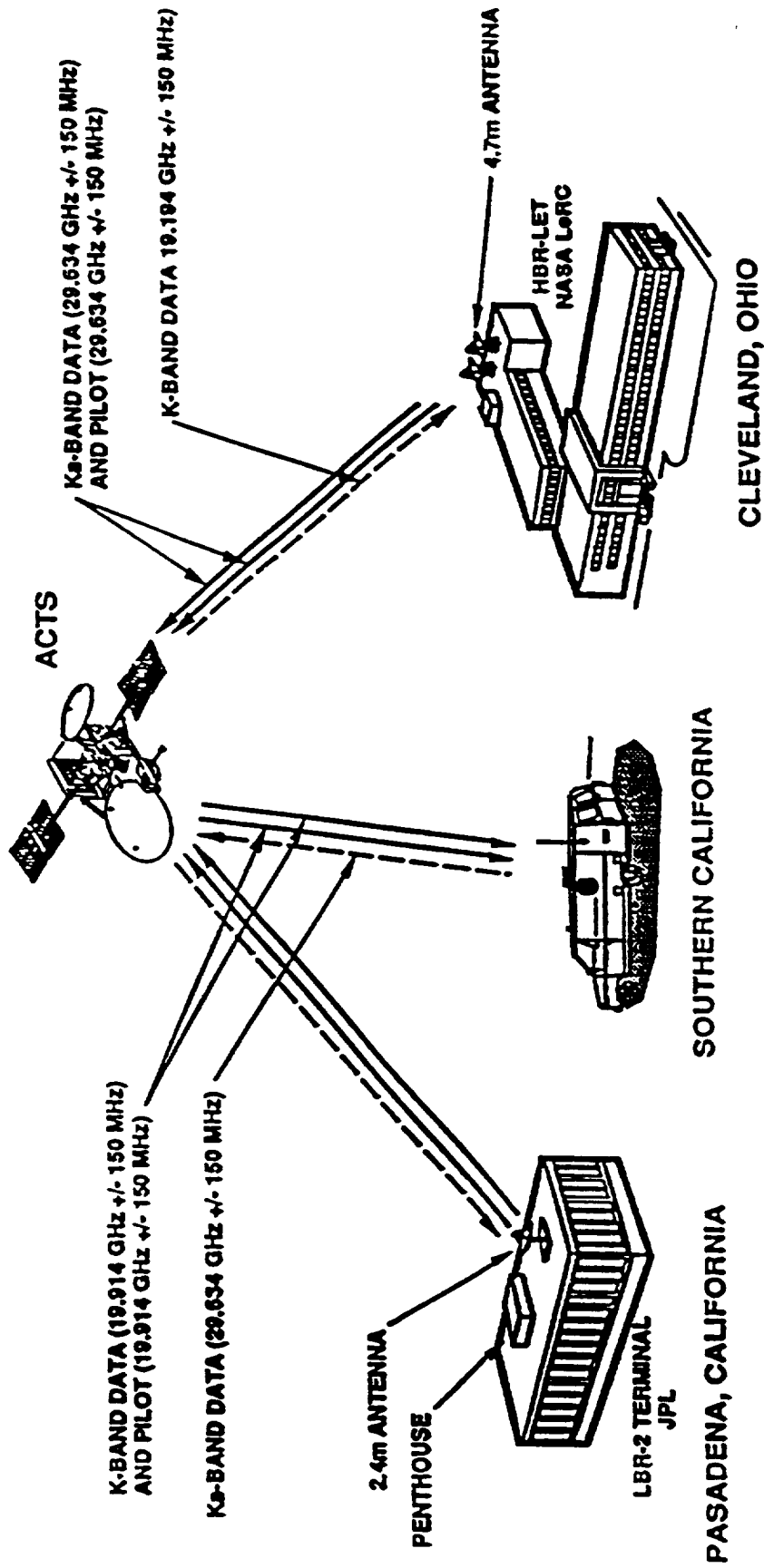
## ACCOMPLISHMENTS

- LeRC SPACE ELECTRONICS DIVISION / ACTS PROJECT OFFICE PLANNING TEAM ESTABLISHED
- EXPERIMENT OPTIONS DEVELOPED
- ROME LABS / MILSTAR COMMITMENT TO EXPERIMENT OBTAINED FOR 20 GHz RECEIVE ARRAYS

# JPL

## AMT PLANNED AND FUTURE EXPERIMENTS

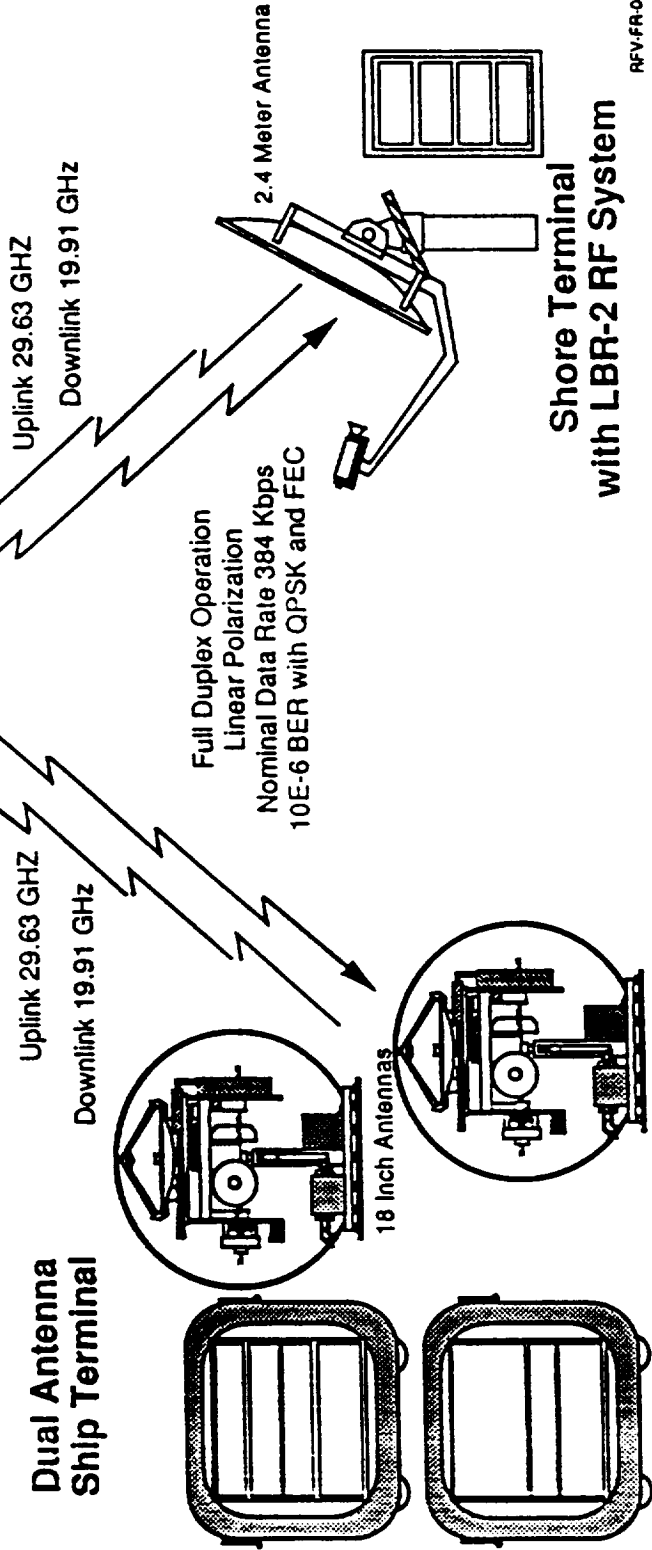
### EXPERIMENTAL SETUP



ACTS GENERATED BEACONS AT 20.185, 20.195, AND 27.505 GHz ARE NOT SHOWN.

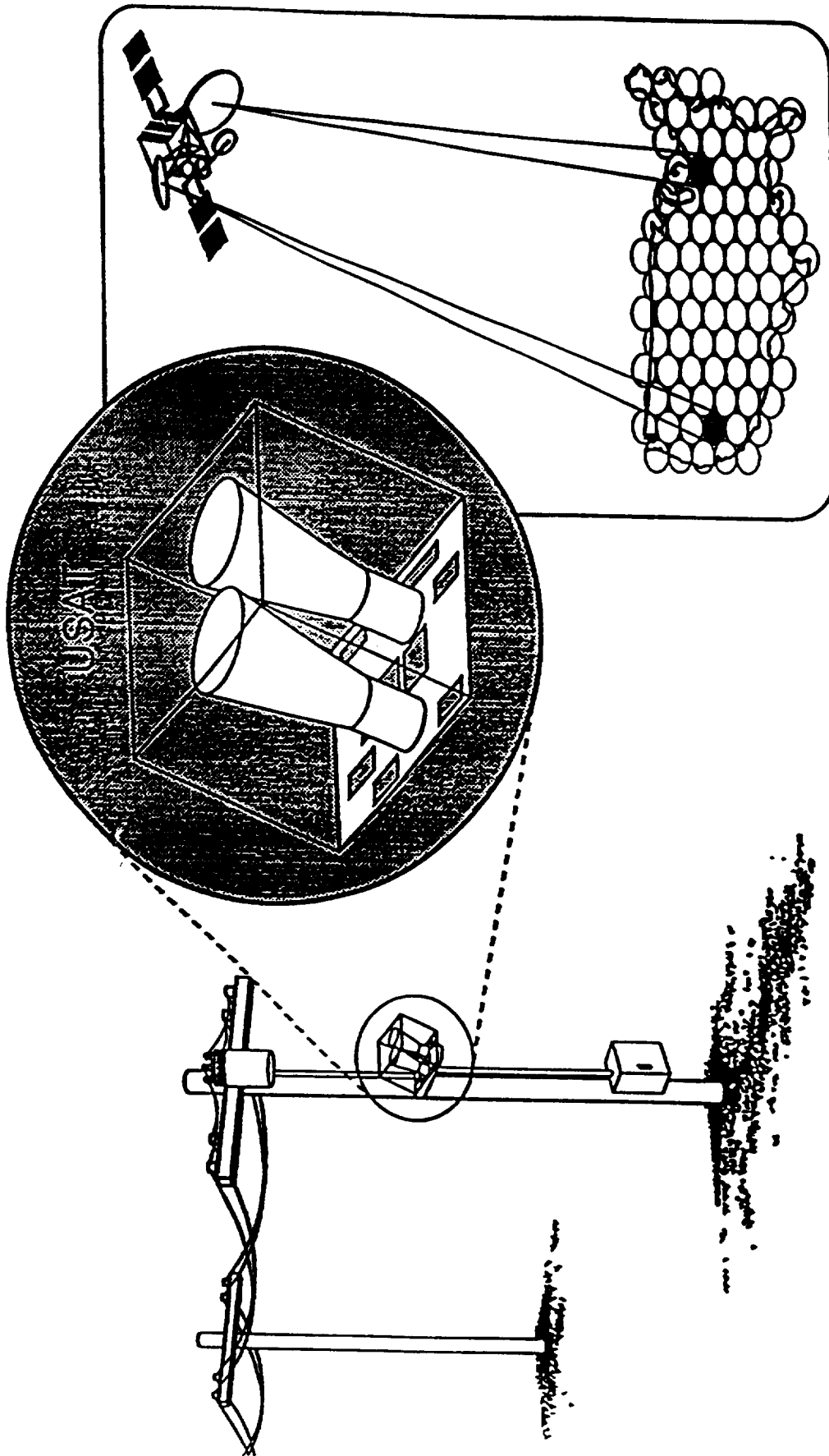
**Ship-to-Shore Connectivity Through the ACTS Satellite**

Mode 2 Operation  
Microwave Switch Matrix  
No On-board Baseband Processing



Ship-to-Shore Connectivity

# Low-Speed Data and SCADA Services

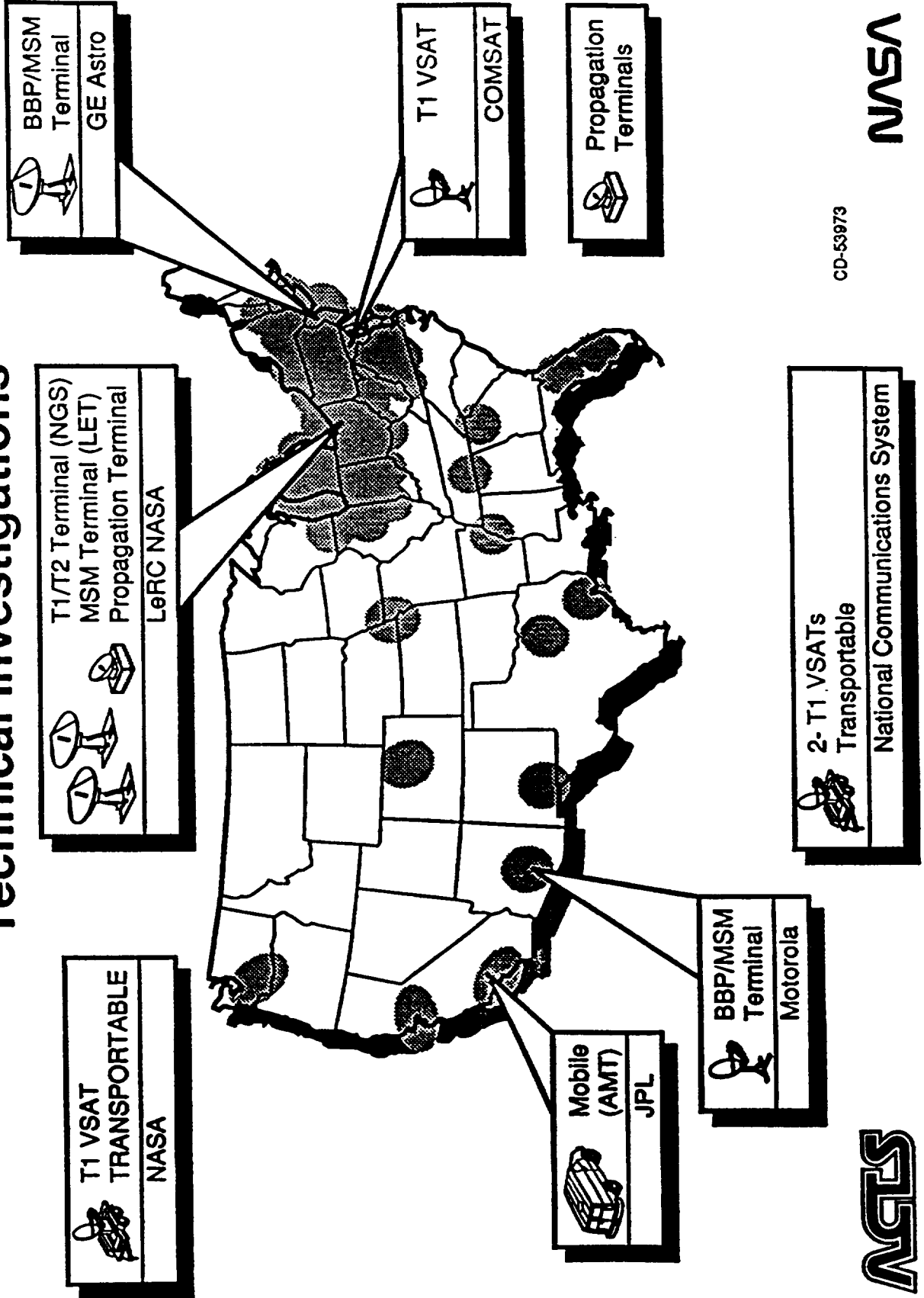


CD-64622

NASA

STEV

# Available ACTS Test Bed for Technical Investigations



CD-53973



## 20-GHz ACTS BEACON SPECTRAL ANALYSIS

D. Chakraborty and J. Gevorgiz

Jet Propulsion Laboratory  
California Institute of Technology  
Pasadena, California

### Abstract

Beat-tone components which are expected to be generated in the 20-GHz Advanced Communications Technology Satellite (ACTS) beacon transmitter when modulated by a Phase Shift Keying (PSK) telemetry channel and a ranging tone simultaneously have been analyzed using a computer simulation via a signal processing work system. Baseband signal spectra have been plotted for all combinations of telemetry and ranging formats. Locations and powers of the unwanted components have been tabulated within  $\pm 100$  kHz relative to the beacon frequency location and the spectral component power recorded down to about 20 dB relative to the beacon power.

### 1. Introduction

The Advanced Communications Technology Satellite (ACTS) will have two noncoherent beacons: one in the uplink frequency (27.5-GHz) bands and the other in the downlink frequency (20-GHz) bands. These two beacons will be used for signal fade and radiometric measurements. The salient characteristics of these two beacons are shown in Table 1 [1], where most of these characteristics have been verified experimentally [2].

The 20-GHz beacon will be derived from a phase modulator where the residual carrier power will act as the beacon source, and the sideband power will carry telemetry data and ranging information. The telemetry and ranging signal multiplexing process is shown in Figure 1. The two 20-GHz beacons can be transmitted simultaneously or in the vertical (V) or horizontal (H) polarization modes; normally the V-Pol mode will be used but provisions are made to transmit in both polarizations. The 20-GHz beacon transmitter block diagram is shown in Figure 2 [2]. The input to the phase modulator is composed of multiplexed Phase Shift Keying (PSK) telemetry data and a square-wave ranging signal; the output will contain sidebands as well as beat tones [3]. These beat frequencies will appear close to the beacon.

In a recent simulation study [4], significant spectral products close to the ACTS downlink beacon frequency were observed. These unwanted products may give rise to false lock scenario in ACTS propagation receivers during wideband initial search mode or after a prolonged deep fade, unless an appropriate software control algorithm is provided for the selection of the maximum signal component in the presence of adjacent, unwanted spikes.

The purpose of this paper is to analyze and calculate the locations and magnitudes of these unwanted products so that an appropriate software control algorithm can be developed for incorporation with the ACTS propagation receive terminals to avoid false locks.



There are five cases of multiplexed modulating signals, as shown in Table 2, where PSK telemetry (TLM) data are assumed to be present (1024 bits/sec (bps) max).

We will first discuss the basic theory of beat-frequency generation, manually solve a simple case to demonstrate the presence of these beat-frequency spikes, and compare the results when using a computer simulation model before simulating the cases described in Table 2.

## 2. Basic Theory

To illustrate the case, let us first consider a carrier being frequency- or phase-modulated by two tones not harmonically related [3]. The instantaneous angular frequency of a modulated carrier can be written as

$$\omega_1(t) = \omega_c + \Delta\omega_1 \cos(\omega_1 t) + \Delta\omega_2 \cos(\omega_2 t) \quad (1)$$

where

$\omega_c = 2\pi f_c$  - carrier angular frequency

$\Delta\omega_1$  - maximum frequency deviation due to first modulating tone

$\omega_1 = 2\pi f_1$  - angular frequency of first modulating signal

$\Delta\omega_2$  - maximum frequency deviation due to second modulating tone

$\omega_2 = 2\pi f_2$  - angular frequency of the second modulating tone

$\beta_1 = (\Delta\omega_1/\omega_1)$  - modulation index due to first modulating signal

$\beta_2 = (\Delta\omega_2/\omega_2)$  - modulation index due to second modulating signal

From quasi-stationary approximation, we know that instantaneous angular frequency

$$\omega_1 = \frac{d}{dt} (\text{phase}) \text{ or } \text{phase} = \int \omega_1 dt$$

and hence phase and frequency modulation analysis differs only by a mathematical transformation.

The generalized single-tone-modulated FM signal can be written as

$$e(t) = A_c \sum_{k=-\infty}^{\infty} J_k(\beta) \sin(\omega_c + k\omega_1)t \quad (2)$$

where

$A_c$  - unmodulated carrier amplitude

$J_k(\beta)$  - Bessel function of first kind, order  $k$ , and argument  $\beta$   
(modulation index)

$$k = 0, \pm 1, \pm 2, \pm 3, \dots$$

Therefore,

$$\text{Modulated carrier power} = \left[ A_c J_0(\beta) \right]^2$$

$$\text{Carrier power relative to unmodulated carrier power} = \frac{1}{\left[ J_0(\beta) \right]^2}$$

Similarly,

$$\text{Relative power due to first sideband} = \frac{1}{\left[ J_1(\beta) \right]^2}$$

$$\text{Relative power due to second sideband} = \frac{1}{\left[ J_2(\beta) \right]^2}$$

and so on.

The two-tone, non-harmonically related, modulated signal becomes

$$e(t) = A_c \exp j(\omega_c t + \beta_1 \sin \omega_1 t + \beta_2 \sin \omega_2 t)$$

$$= A_c \left[ \sum_{n=-\infty}^{\infty} J_n(\beta_1) \exp(jn\omega_1 t) \right] \times \left[ \sum_{m=-\infty}^{\infty} J_m(\beta_2) \exp(jm\omega_2 t) \right] \exp(j\omega_c t) \quad (3)$$

In a similar way, it can be shown that when the carrier is modulated by non-harmonically related  $N$ -tone,  $1, 2, \dots, N$ , with angular frequencies  $\omega_1, \omega_2, \dots, \omega_N$  and modulation indices  $\beta_1, \beta_2, \dots, \beta_N$ , the instantaneous angular frequency becomes

$$\omega_i(t) = \omega_c + \Delta\omega_1 \cos \omega_1 t + \Delta\omega_2 \cos \omega_2 t + \dots + \Delta\omega_N \cos \omega_N t \quad (4)$$

where

$$\beta_1 = (\Delta\omega_1/\omega_1), \beta_2 = (\Delta\omega_2/\omega_2), \dots, \beta_N = (\Delta\omega_N/\omega_N).$$

The modulated signal becomes

$$e(t) = A_c \left[ \sum_{n_1=-\infty}^{\infty} J_{n_1}(\beta_1) \exp(jn_1\omega_1 t) \right] \times \left[ \sum_{n_2=-\infty}^{\infty} J_{n_2}(\beta_2) \exp(jn_2\omega_2 t) \right] \dots \times \left[ \sum_{n_N=-\infty}^{\infty} J_{n_N}(\beta_N) \exp(jn_N\omega_N t) \right] \exp(\omega_c t) \quad (5)$$

As an illustration, we will use Equation (3) to manually calculate the beacon spectral components as applicable to Case 2 discussed in Table 2, assuming a cw tone containing the PSK telemetry channel power and a ranging cw tone at 27.7 kHz. Table 3 presents the components that are produced at the output of the phase modulator for this special case.

It should be noted that with two-tone modulation, power of the spectral components is reduced when compared to a single-tone modulation case with the same modulation index. This is due to the fact that the power of each component is determined by the product of two Bessel functions. For example, with a single-tone modulation index of 1.1,  $J_0(1.1) = 0.7196$ , resulting in a modulated carrier power of -2.8 dB relative to the unmodulated carrier power. With two-tone modulation, the modulation index should be chosen such that the modulated carrier power (beacon power) is the same as in the case of single-tone modulation. This can be achieved by choosing  $\beta_1 = \beta_2 = 0.79$  and hence  $J_0(\beta_1) = J_0(\beta_2) = 0.85$ , resulting in a carrier (beacon power) -2.8 dB below unmodulated carrier power, and the first sideband becomes  $[J_1(\beta_1) J_0(\beta_2)]^2 = [0.3650 \times 0.8500]^2 = -10.2$  dB relative to the unmodulated carrier power.

We will now calculate the beacon spectra for the simplified Case 2 with the following assumptions:

Beacon center frequency reference	0
Relative location ( $f_1$ ) of ranging tone with respect to the beacon	27.7 kHz
Relative location ( $f_2$ ) of PSK telemetry channel center frequency with respect to the beacon	64 kHz
Equal modulation indices ( $\beta_1 = \beta_2$ )	0.79
Analysis bandwidth	$\pm 100$ kHz
PSK subcarrier simulated by a cw tone	

The calculated spectral components for the above parameters are shown in Table 4. Furthermore, Table 4 also illustrates the results obtained using the communication system simulator [5], for validating the simulator model.

The last two columns in Table 4 show the comparison of the exact calculations and computer simulation results of the trial solution under consideration. The Fast Fourier Transform (FFT) process is used in the simulation with finite sampling for the spectral analysis. As a result, FFT points do not always fall on the spectral peaks, and from Table 4, it is also noted that the exact values and the computer simulation results are very close.

In summary, the simulation method yields satisfactory results. All the cases mentioned in Table 2 will now be examined using the computer simulation via a Signal Processing Worksystem (SPW) [5].

### 3. Computer Simulation Method and Results

The spectral analysis for the ACTS signal formats of Table 2 is performed using the SPW. The SPW is used to model a signal synthesizer that generates signals with specified parameters and modulation formats. Without any loss of generality, the simulation and modeling of the signal synthesizer is performed at baseband since this requires a lower sampling frequency compared to the simulation at the beacon center frequency. Figure 3 illustrates the block diagram of the implemented signal synthesizer. It consists of two major blocks for generating ranging tone and a data component. In Figure 3, the ranging or the placeholder tone is generated using two function generators that synthesize the ranging center frequency and the ranging subcarrier frequency. The data component is synthesized using a function generator for the data center frequency and a random data generator for synthesizing the NRZ data. The parameters for the function and data generators are summarized in the parameter table provided in Figure 3. The ranging and the data signal components are then combined to yield

$$\beta_1 R(t) \sin(\omega_1 t) + \beta_2 S_d(t) \sin(\omega_2 t)$$

where

$R(t) \equiv$  ranging signal

$S_d(t) \equiv$  NRZ random data sequence

$\omega_1 \equiv$  ranging signal center frequency

$\omega_2 \equiv$  data component center frequency

$\beta_1 \equiv$  ranging modulation index

$\beta_2 \equiv$  data component modulation index

The combined signal is then followed by the phase modulator, resulting in a complex baseband signal.

Figure 4 illustrates the functional block diagram of the system. The parameters presented in this figure correspond to Case 2 of Table 2. The implemented models using SPW are digital; therefore, the sampling frequency for the system is selected to meet the Nyquist criterion [6] for the highest frequency component in the analysis bandwidth (100 kHz). Furthermore, the simulation period is chosen so that a minimum of 100 data symbols is simulated.

The synthesizer described above is used for analyzing the spectral properties of the ACTS signal formats at a sampling frequency of 200 kHz with a simulation period of 20,000 points and an FFT length of 32,768 points. The results of the FFT analysis are presented in Figures 5, 6, 7, 8, and 9 for Cases 1, 2, 3a, 3b, and 3c, respectively. Each figure also illustrates a summary of the signal parameters and the signal characteristics. Presented in these figures also are the relative frequency and the peak power ratio of the spectral components down to about 20 dB with respect to the beacon power.

The results of the spectral analysis are directly dependent on the modulation index. In this article, a modulation index of 0.79 was used for both the ranging and the data components. The results presented here were compared to the experimental results shown in [7], for Cases 1 and 2. The comparison demonstrated a good match between the predicted simulation results and the measured experimental results.

#### **4. Conclusions**

The ACTS's downlink beacon frequency (20-GHz) spectral analysis has been carried out, and the baseband spectra have been plotted to identify locations and powers of the unwanted components relative to the location and power of the beacon.

Results obtained will help ACTS propagation receive terminal designers and experimenters know a priori the locations of these unwanted spikes so that appropriate measures can be taken to avoid a false lock while trying to track the beacon during initial search or acquisition after a prolonged deep fade.

#### **Acknowledgments**

Thanks are due to Chaim Zaks, P. Levine, and F. Davarian for many useful discussions.

#### **References**

- [1] F. M. Naderi and S. J. Campanella, "NASA's Advanced Communications Technology Satellite (ACTS)," AIAA Proceeding, paper no. 88-0797, pp. 204-224, 1988.
- [2] F. Gargione, "ACTS Spacecraft Beacon Characteristics," Proceedings of the First ACTS Propagation Workshop, November 28-29, 1989, Santa Monica, California.
- [3] P. F. Panter, Modulation Noise and Spectral Analysis, McGraw-Hill Book Co., 1965.
- [4] K. T. Lin, "Problems of the Beacon Spectra Produced by the GE Telemetry Simulator," COMSAT Labs memorandum, ACTS-NGS-90-052, July 25, 1990.
- [5] Signal Processing Worksystem Software, Comdisco Systems, Inc., Foster City, California.

- [6] A. Oppenheim and R. Schaffer, Discrete-Time Signal Processing, Prentice Hall, 1989.
- [7] F. Gargione, "ACTS Beacon Measurement Data," Proceedings of the NAPEX XV, June 1991, London, Ontario.

**Table 1. ACTS Beacon Characteristics**

Parameters	27.5-GHz Beacon	20-GHz Beacon
No. of beacons	1	2
Frequency/polarization	27.505 GHz $\pm 0.5$ MHz (V)	20.185 GHz $\pm 0.5$ MHz (V) 20.195 GHz $\pm 0.5$ MHz (H)
Function	Fade measurement	Telemetry/fade measurements
Modulation	None	Yes (FM & PCM)
Nominal RF output (dBm)	20.0	23
Operating temperature ( $^{\circ}$ C)	-10 to 55	-10 to +55
Frequency stability	$\pm 10$ PPM over 2 years at constant temperature  $\pm 1.5$ PPM over 24 hours for $-10^{\circ}$ C to $55^{\circ}$ C	
Output power stability	$\pm 1.0$ dB over 24 hours $\pm 2.09$ dB over full mission	
Phase noise	-49 dBC/Hz @ 50 Hz -80 dBC @ 3000 Hz	-51 dBC/Hz @ 50 Hz -92 dBC/Hz @ 19 kHz

**Table 2. Multiplexed Modulating Signal Configuration**

Case	Combination	Rel Frequencies* (kHz)	Ranging Tone Modulation
1	PSK TLM/placeholder	64/32	-
2	PSK TLM/ranging	64/27.777	Square wave
3a	PSK TLM/ranging	64/19	35.4 Hz (sq. wave)
3b	PSK TLM/ranging	64/19	283.4 Hz (sq. wave)
3c	PSK TLM/ranging	64/19	3968.2 Hz (sq. wave)

\*Relative to beacon frequency.

**Table 3. Spectral Components With Two-Tone**

Component	Spectral Power	Relative Power*
Carrier	$[J_0(\beta_1) J_0(\beta_2) A_c]^2$	$\frac{1}{[J_0(\beta_1) J_0(\beta_2)]^2}$
Sidebands due to $\omega_1$	$[J_n(\beta_1) J_0(\beta_2) A_c]^2$	$\frac{1}{[J_n(\beta_1) J_0(\beta_2)]^2}$
Sidebands due to $\omega_2$	$[J_m(\beta_2) J_0(\beta_1) A_c]^2$	$\frac{1}{[J_m(\beta_2) J_0(\beta_1)]^2}$
Beat frequencies at $\omega_c \pm n\omega_1 \pm m\omega_2$	$[J_n(\beta_1) J_m(\beta_2) A_c]^2$	$\frac{1}{[J_n(\beta_1) J_m(\beta_2)]^2}$

\*Relative to unmodulated carrier power  $[A_c]^2$ .

Table 4. 20-GHz Beacon Spectral Power (Trial Solution)

Components	Location (kHz)	Spectral Power (dB)		Power Relative to the Beacon (dB)	
		Relative to $[A_c]^2$		Manual Calculations	Simulation
Carrier (unmodulated)	0	$[A_c]^2$	0	—	—
Beacon (modulated)	0	$A_c^2 [J_0(B_1) J_0(B_2)]^2$	-2.8	0	0
1st S/B due $\omega_1$	$\pm 27.7$	$A_c^2 [J_1(B_1) J_0(B_2)]^2$	-10.2	-7.4	-7.3
2nd S/B due $\omega_1$	$\pm 55.4$	$A_c^2 [J_2(B_1) J_0(B_2)]^2$	-24	-21.2	-21.2
3rd S/B due $\omega_1$	$\pm 83.1$	$A_c^2 [J_3(B_1) J_0(B_2)]^2$	-41.5	-38.7	-38.8
1st S/B due $\omega_2$	$\pm 64$	$A_c^2 [J_1(B_2) J_0(B_1)]^2$	-10.2	-7.4	-7.6
<hr/>					
Beat Frequencies $0 \pm n \omega_1 \pm m \omega_2$					
<hr/>					
n=1, m=1 n=-1, m=-1	$\pm 91.7$	$A_c^2 [J_1(B_1) J_1(B_2)]^2$	-17.5	-14.7	-15.0
n=1, m=-1 n=-1, m=1	$\mp 36.3$	$A_c^2 [J_1(B_1) J_{(-1)}(B_2)]^2$	-17.5	-14.7	-14.9
n=2, m=-1	-8.6	$A_c^2 [J_2(B_1) J_{(-1)}(B_2)]^2$	-31.4	-28.6	-28.0
n=2, m=-2	-72.6	$A_c^2 [J_2(B_2) J_{(-2)}(B_2)]^2$	-45.2	-42.4	-42.2
n=-2, m=-1	8.6	$A_c^2 [J_{(-2)}(B_1) J_1(B_2)]^2$	-31.4	-28.6	-28.9
n=3, m=-1	19.1	$A_c^2 [J_3(B_1) J_{(-1)}(B_2)]^2$	-48.9	-46.1	-46.7
n=3, m=-2	-44.9	$A_c^2 [J_3(B_1) J_{(-2)}(B_2)]^2$	-62.7	-59.9	-59.7
n=-3, m=1	-19.1	$A_c^2 [J_{(-3)}(B_1) J_1(B_2)]^2$	-48.9	46.1	-46.6
n=-3, m=2	44.9	$A_c^2 [J_{(-3)}(B_1) J_2(B_2)]^2$	-62.7	-59.9	-59.1



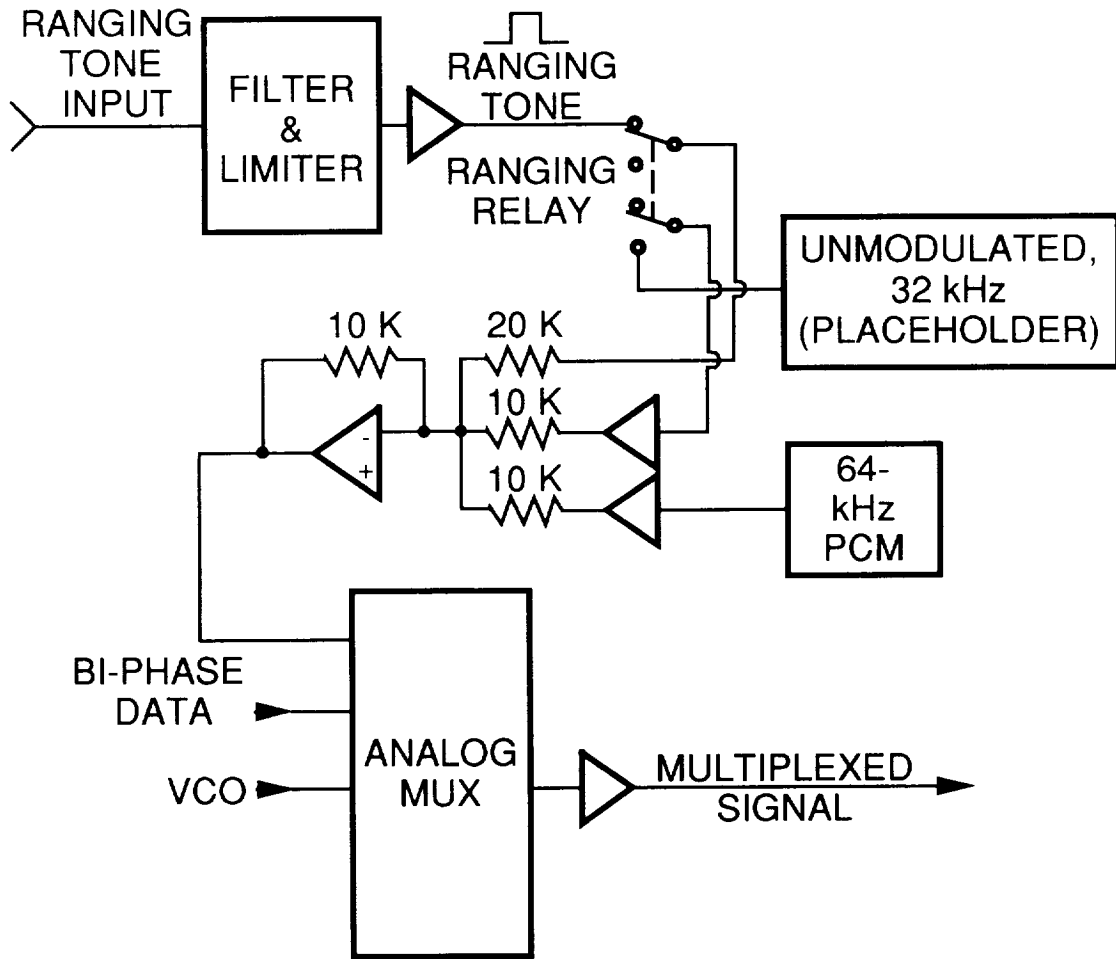


Figure 1. ACTS Telemetry Subcarrier Generation

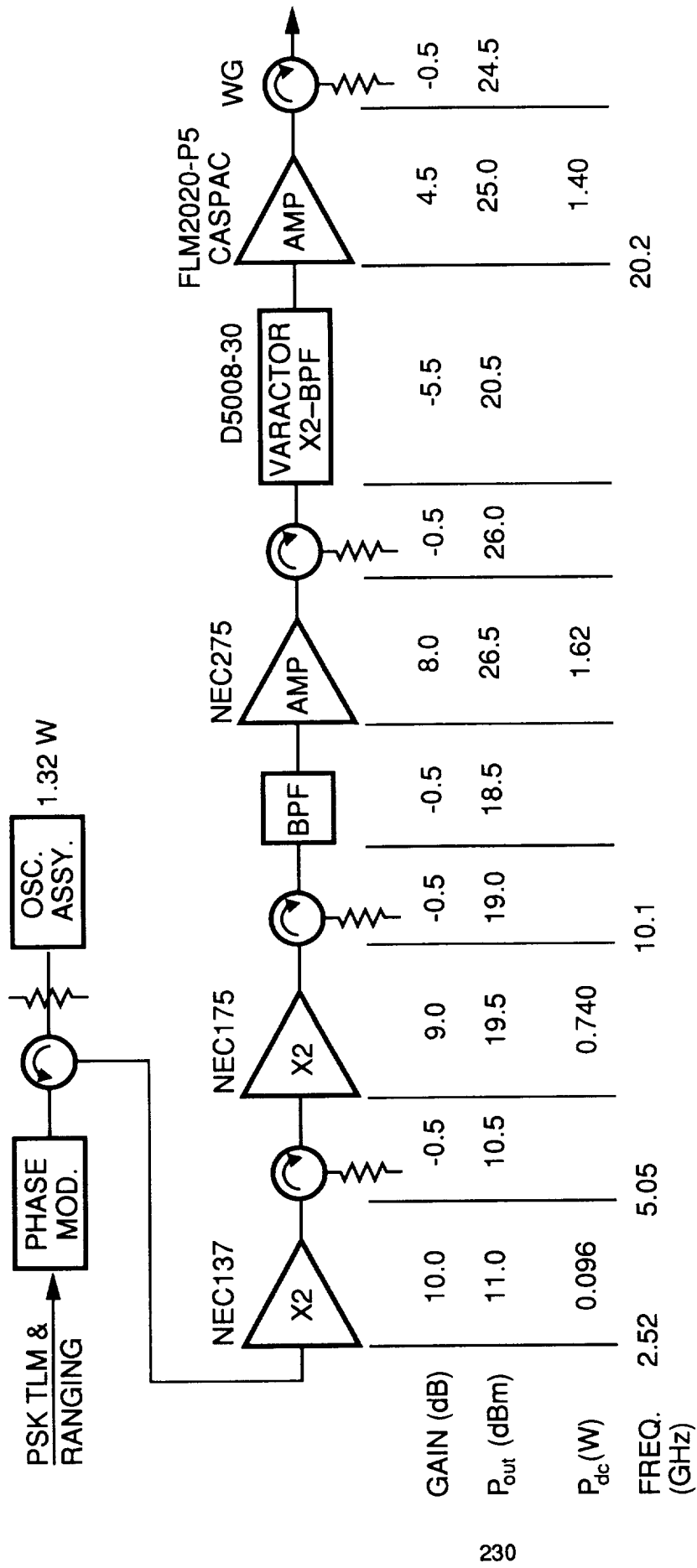


Figure 2. 20.2-GHz Ka-Band Beacon Transmitter

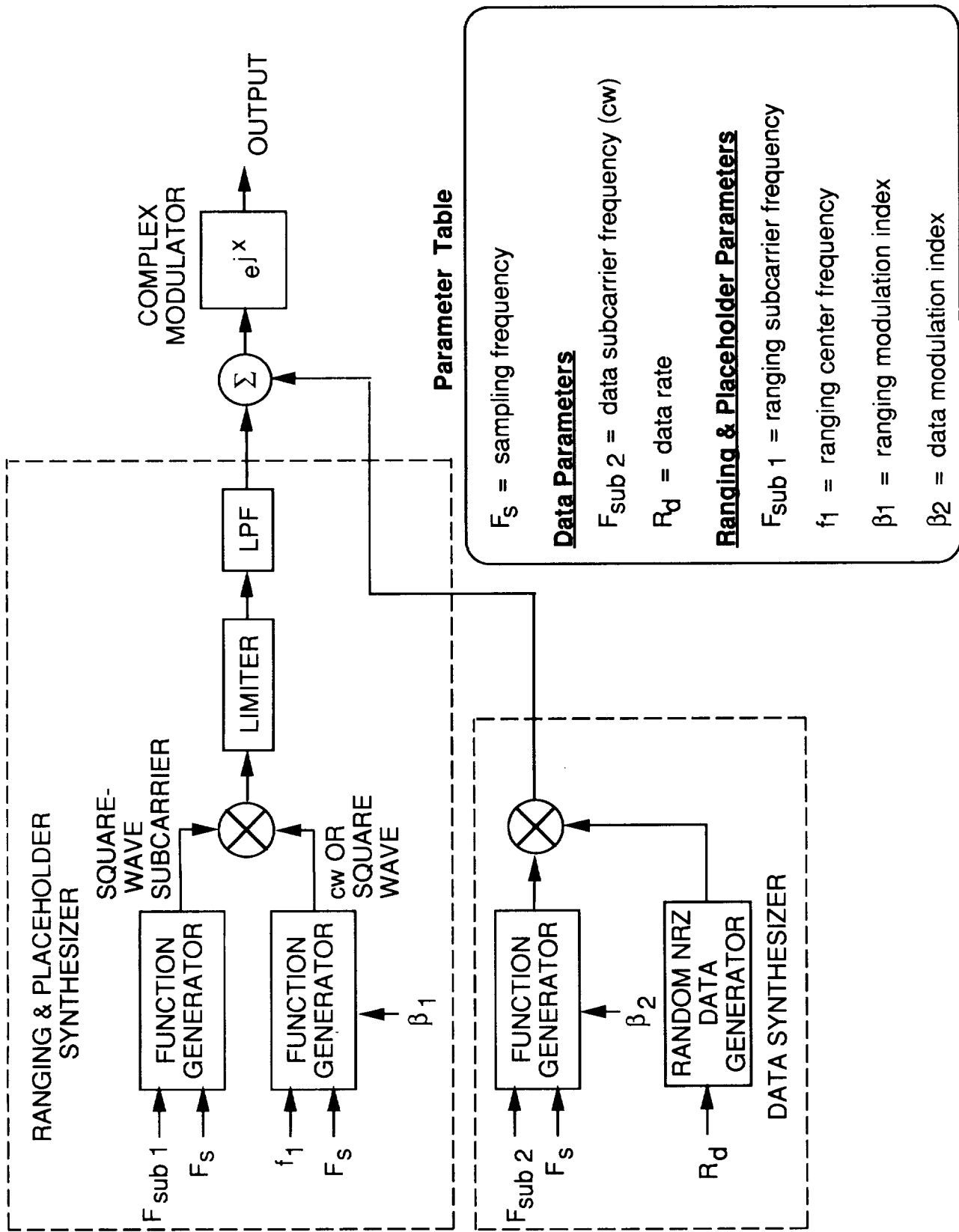
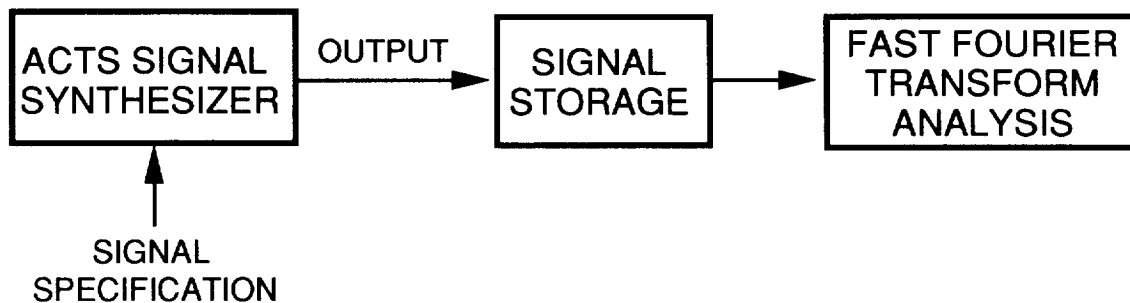


Figure 3. ACTS Experiment Signal Synthesizer at Baseband



### Parameters for Case 2

Sampling frequency = 200 kHz

$f_1 = 27.777$  kHz (square wave, no subcarrier)

Data Specification

$F_{\text{sub } 2} = 64.0$  kHz (subcarrier frequency)

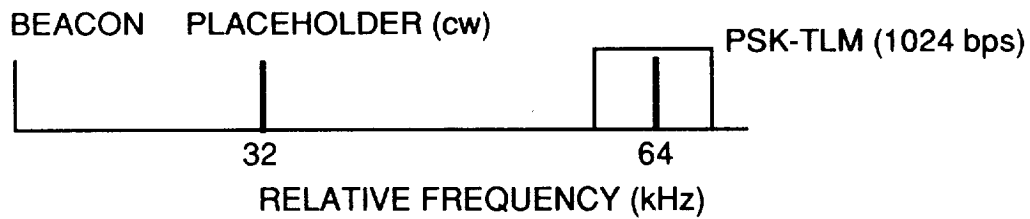
$R_d = 1024$  bps (data rate)

$\beta_1 = \beta_2 = 0.79$  (modulation index)

Simulation length = 20,000 points

FFT length = 32,768 points

Figure 4. Simulation Block Diagram



**Signal Characteristics, Case 1 of Table 2**

- $f_1 = 32 \text{ kHz}$  (cw placeholder)
- $f_2 = 64 \text{ kHz}$  (PSK carrier)
- $R_d = 1024 \text{ bps}$  (PSK data rate)
- $\beta_1 = \beta_2 = 0.79$

Relative Frequency With Respect to the Beacon (kHz)	Attenuation With Respect to the Beacon (dB)
32.00073	-7.49
64.00146	-19.9
0.0 (beacon)	0.0 (beacon)
-64.08691	-20.3
-32.00073	-7.38

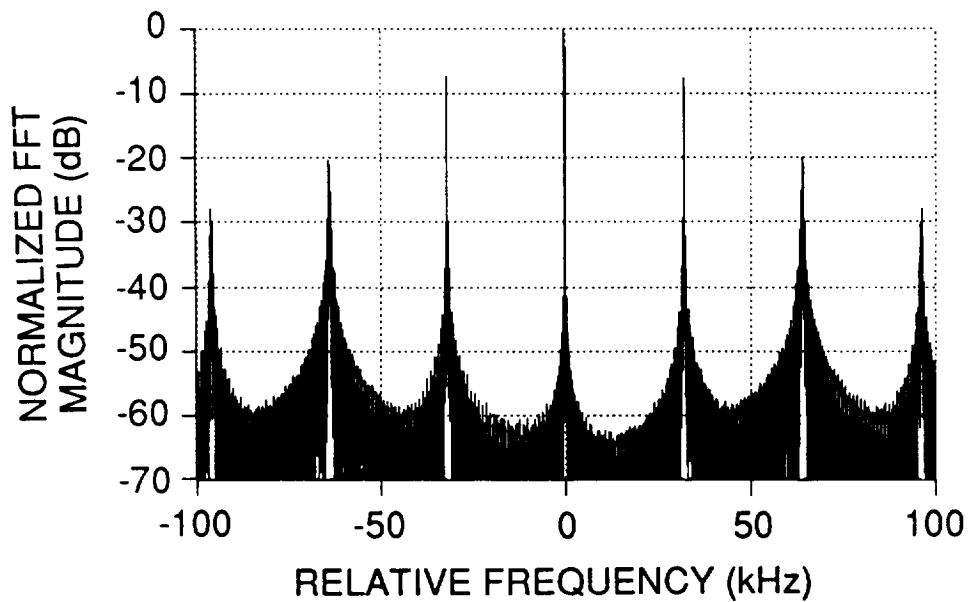
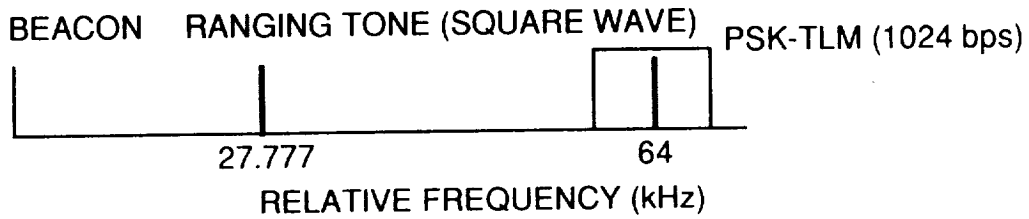


**Figure 5. Baseband Spectral Characteristics of Case 1**



**Signal Characteristics, Case 2 of Table 2**

$f_1 = 27.777$  kHz (square wave)

$f_2 = 64$  kHz (PSK carrier)

$R_d = 1024$  bps (PSK data rate)

$\beta_1 = \beta_2 = 0.79$

Relative Frequency With Respect to the Beacon (kHz)	Attenuation With Respect to the Beacon (dB)
$\pm 27.777$	-10.0
$\pm 36.13281$	-25.0
$\pm 64.08691$	-15.7
$\pm 91.86401$	-24.7
0.0 (beacon)	0.0 (beacon)

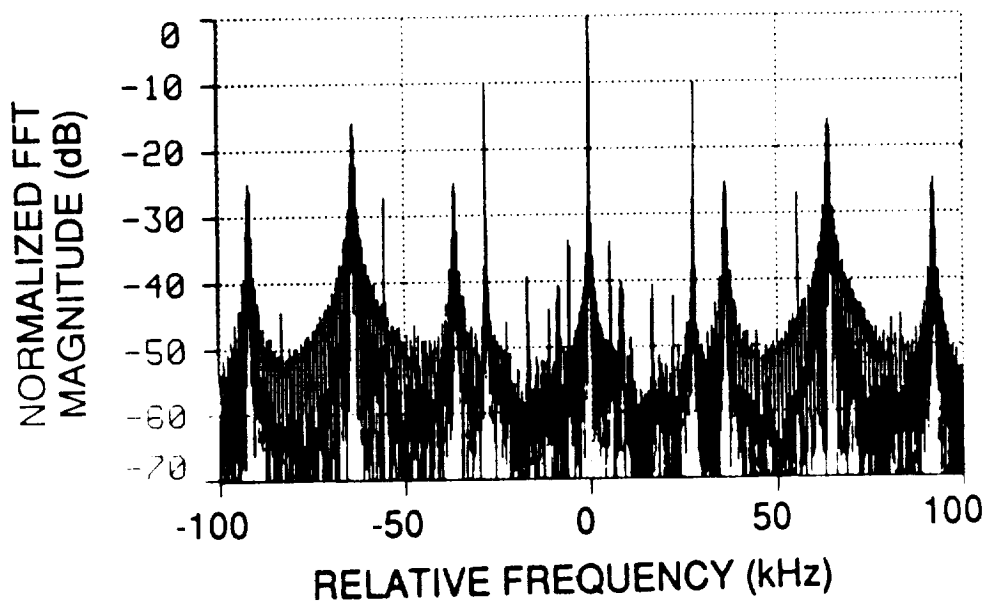
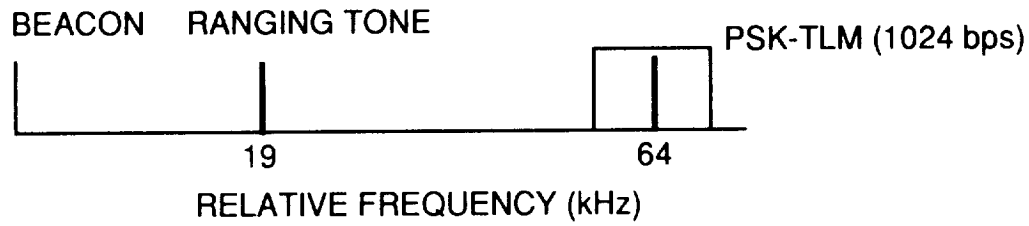


**Figure 6. Baseband Spectral Characteristics of Case 2**



**Signal Characteristics. Case 3a of Table 2**

$f_1 = 19.0$  kHz (ranging subcarrier modulated by 35.4-Hz square wave)

$f_2 = 64$  kHz (PSK carrier)

$R_d = 1024$  bps (PSK data rate)

$\beta_1 = \beta_2 = 0.79$

Relative Frequency With Respect to the Beacon (kHz)	Attenuation With Respect to the Beacon (dB)
$\pm 19.03687$	-8.33
$\pm 38.00049$	-25.5
$\pm 64.08691$	-15.73
0.0 (beacon)	0.0 (beacon)

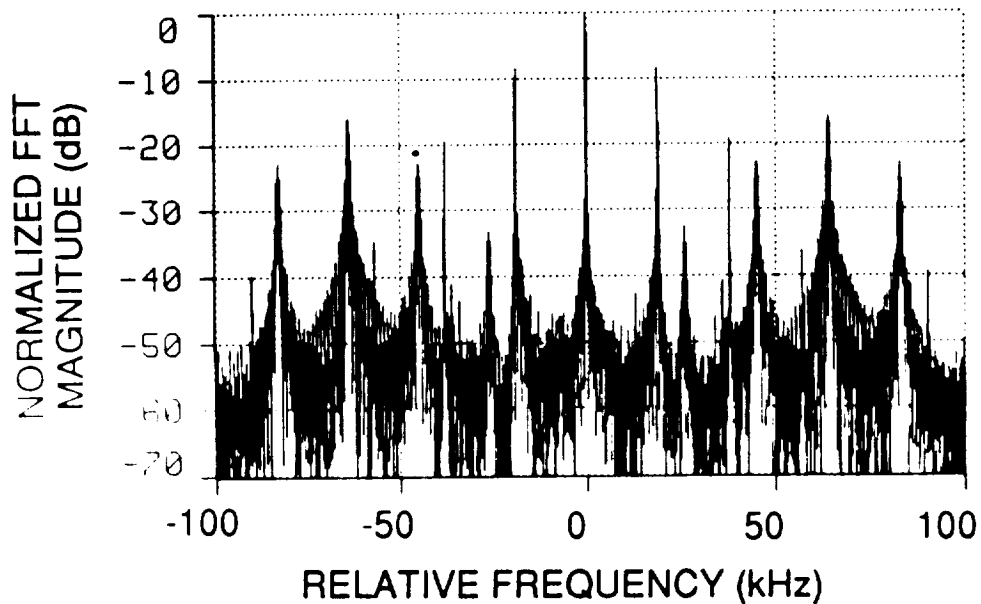
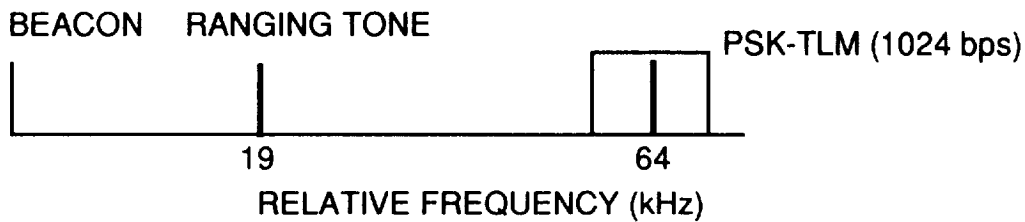


**Figure 7. Baseband Spectral Characteristics of Case 3a**



**Signal Characteristics. Case 3b of Table 2**

$f_1 = 19.0$  kHz (ranging subcarrier modulated by 283.4-Hz square wave)

$f_2 = 64$  kHz (PSK carrier)

$R_d = 1024$  bps (PSK data rate)

$\beta_1 = \beta_2 = 0.79$

Relative Frequency With Respect to the Beacon (kHz)	Attenuation With Respect to the Beacon (dB)
$\pm 18.71948$	-7.39
$\pm 19.28101$	-8.90
$\pm 38.00049$	-15.9
$\pm 64.08691$	-17.9
0.0 (beacon)	0.0 (beacon)

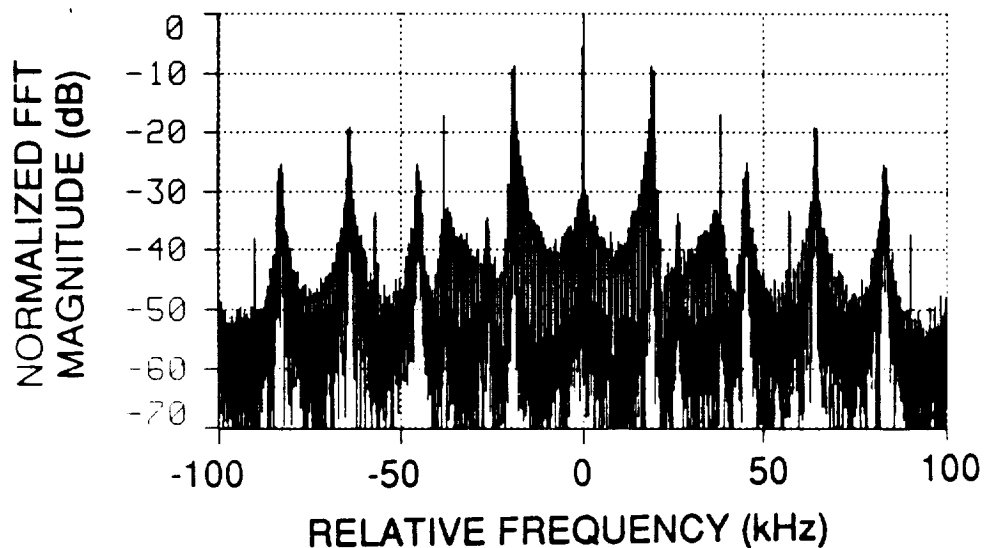
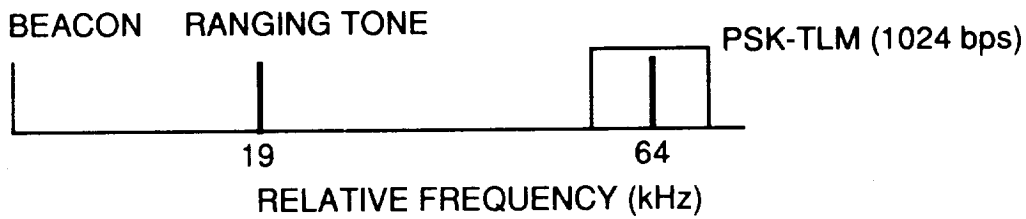


**Figure 8. Baseband Spectral Characteristics of Case 3b**





**Signal Characteristics, Case 3c of Table 2**

$f_1 = 19.0$  kHz (ranging subcarrier modulated by 3968-Hz square wave)

$f_2 = 64$  kHz (PSK carrier)

$R_d = 1024$  bps (PSK data rate)

$\beta_1 = \beta_2 = 0.79$

Relative Frequency With Respect to the Beacon (kHz)	Attenuation With Respect to the Beacon (dB)
$\pm 7.09229$	-18.6
$\pm 15.03296$	-7.6
$\pm 64.0869$	-15.8
0.0 (beacon)	0.0 (beacon)

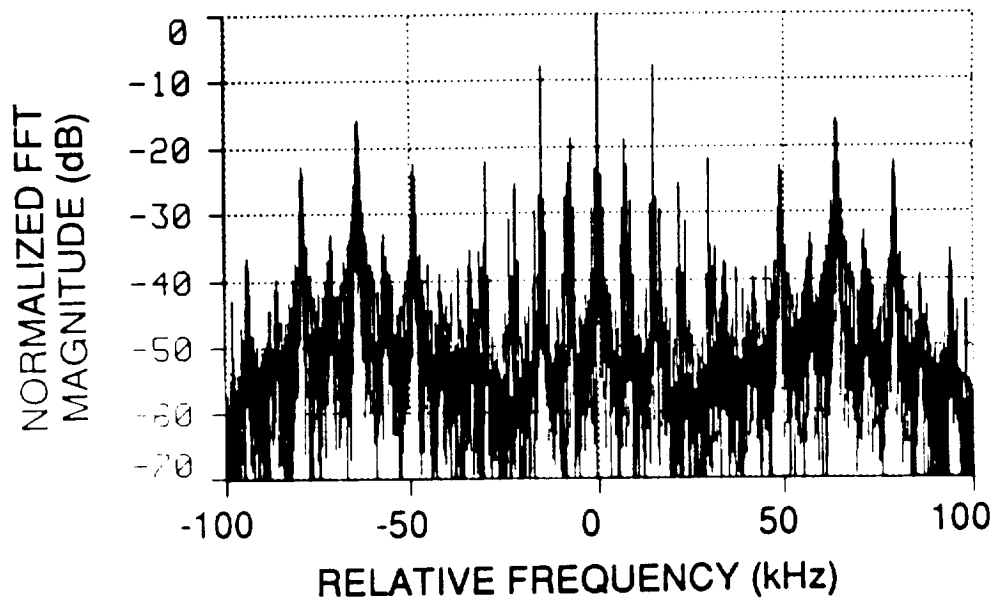


**Figure 9. Baseband Spectral Characteristics of Case 3c**



---

**ACTS Beacons Measurements Data**

**Presented by**

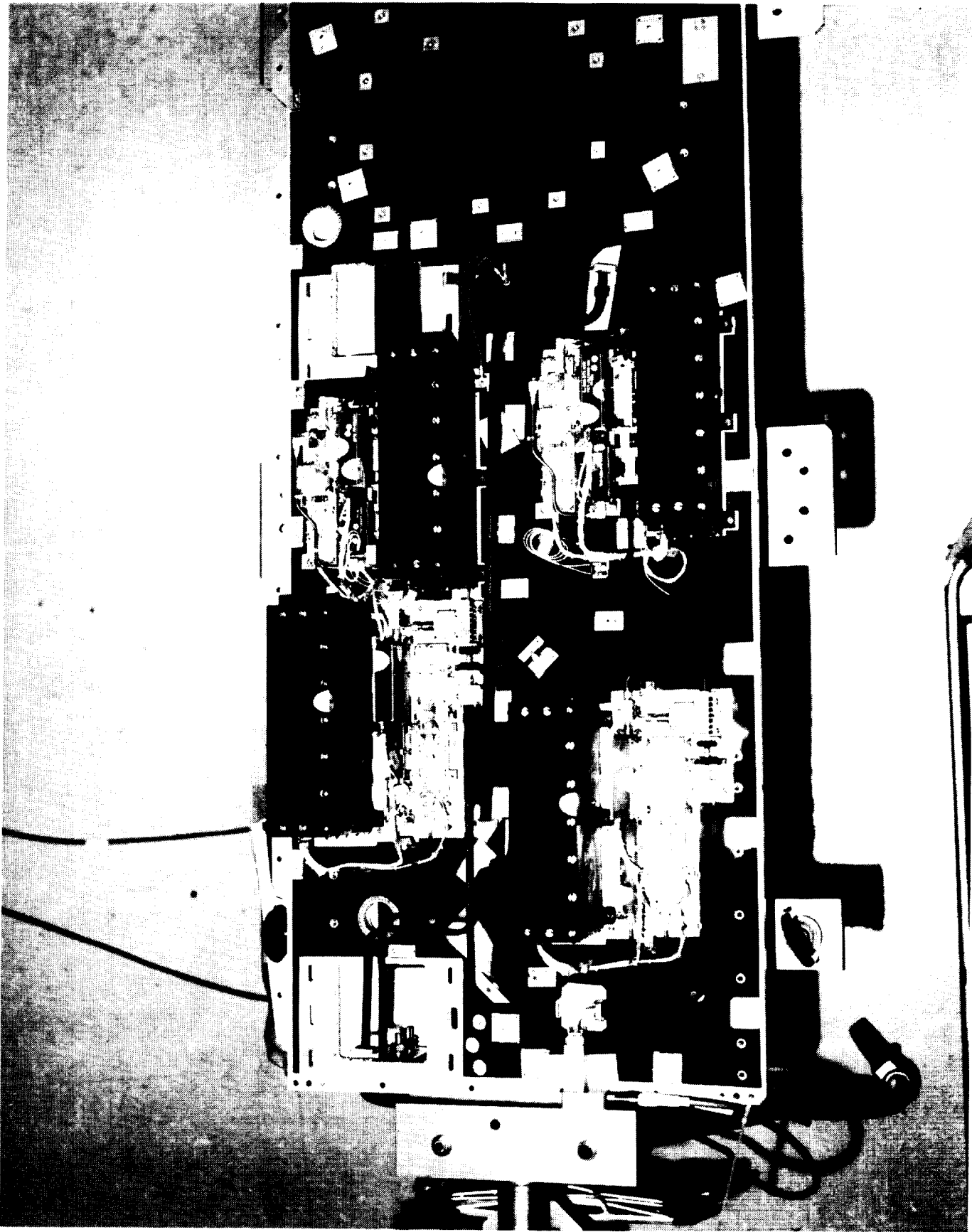
**F. Gargione**

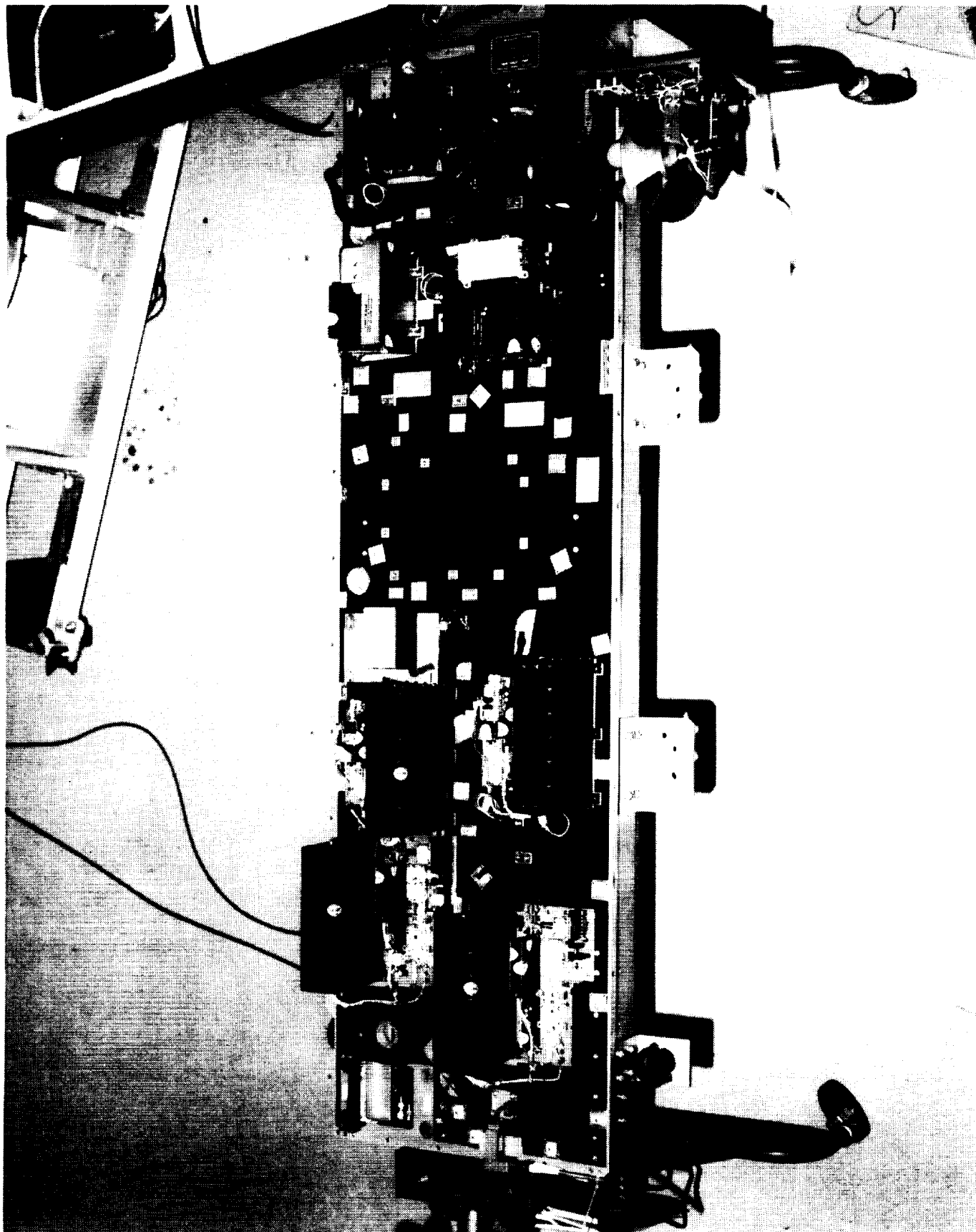
**Astro-Space Division  
General Electric Company  
Princeton, New Jersey**

**at the**

**ACTS Propagation Studies Miniworkshop  
The Sheraton Armouries Hotel  
London, Ontario**

**June 29, 1991**







# ***ACTS Beacons Measurements Data***

---

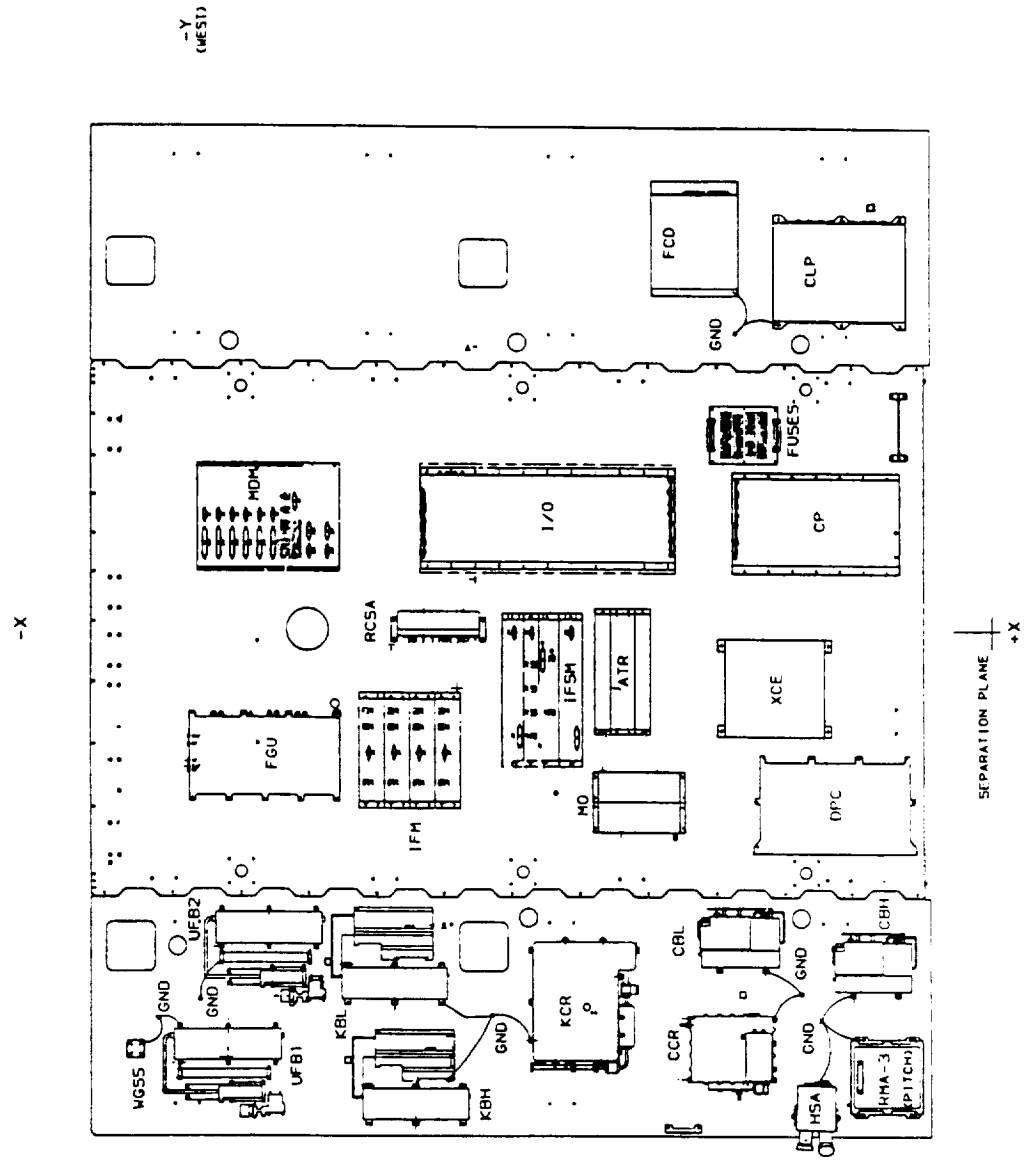
## **Overview**

- **Panel Configuration**
- **Frequency Stability Data**
- **Power Stability Data**
- **Spectral Response**
- **Conclusion**



# ACTS Beacons Measurements Data

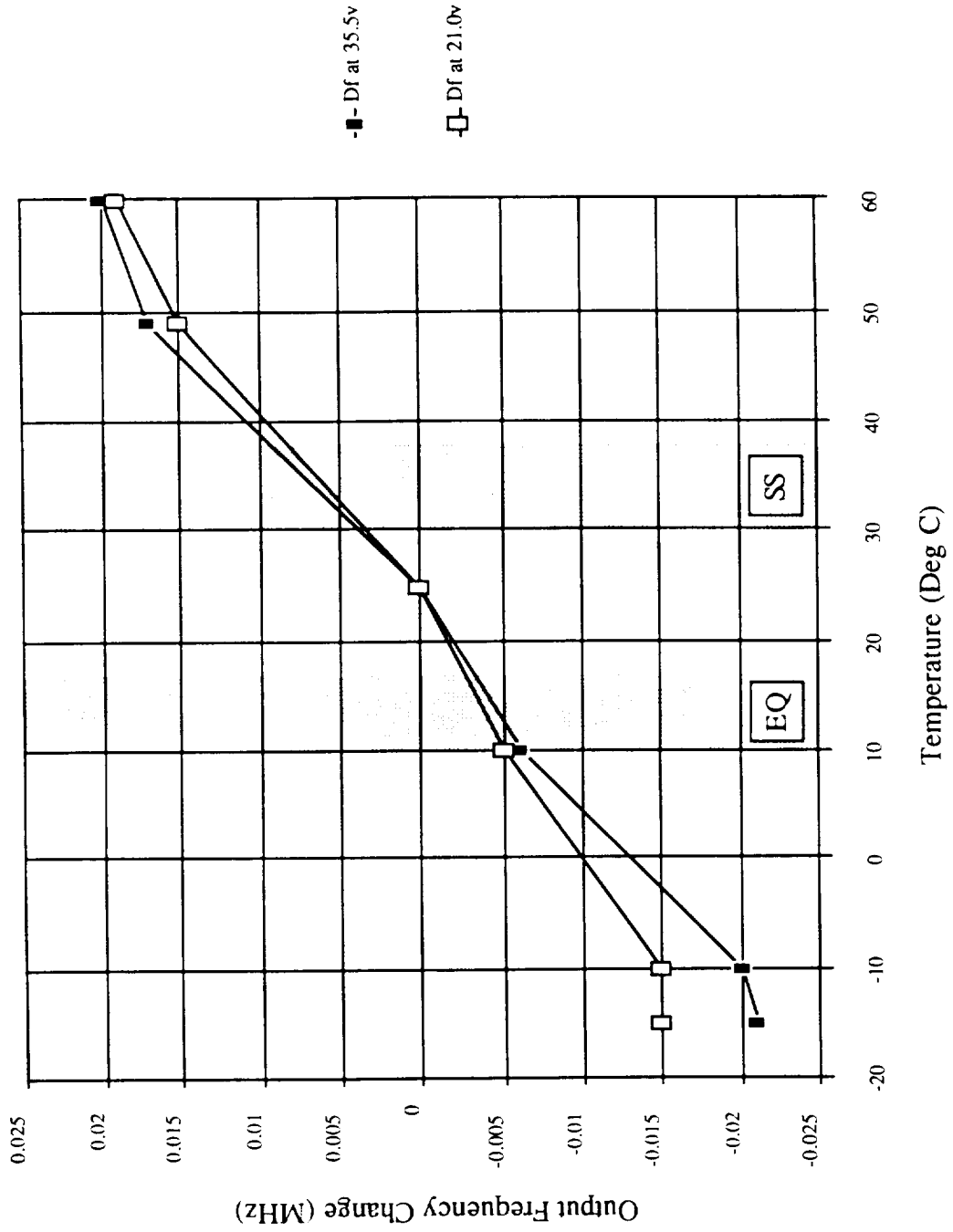
## North Equipment Panels - Component Layout





# ACTS Beacons Measurements Data

## Frequency Change with Voltage and Temperature - KBH

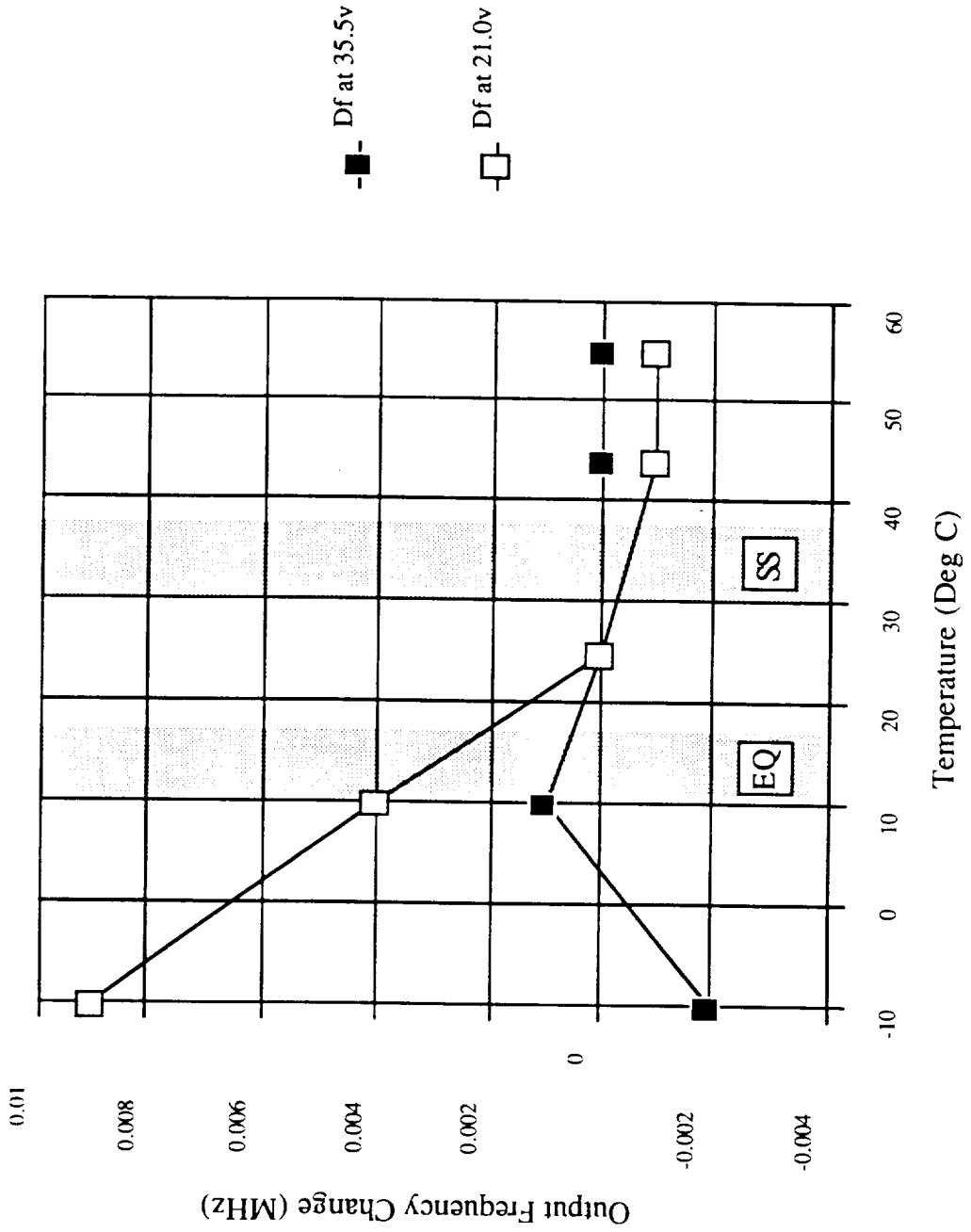


Bands show diurnal variations during Equinox and Summer Solstice



# ACTS Beacons Measurements Data

## Frequency Change with Voltage and Temperature - KBL



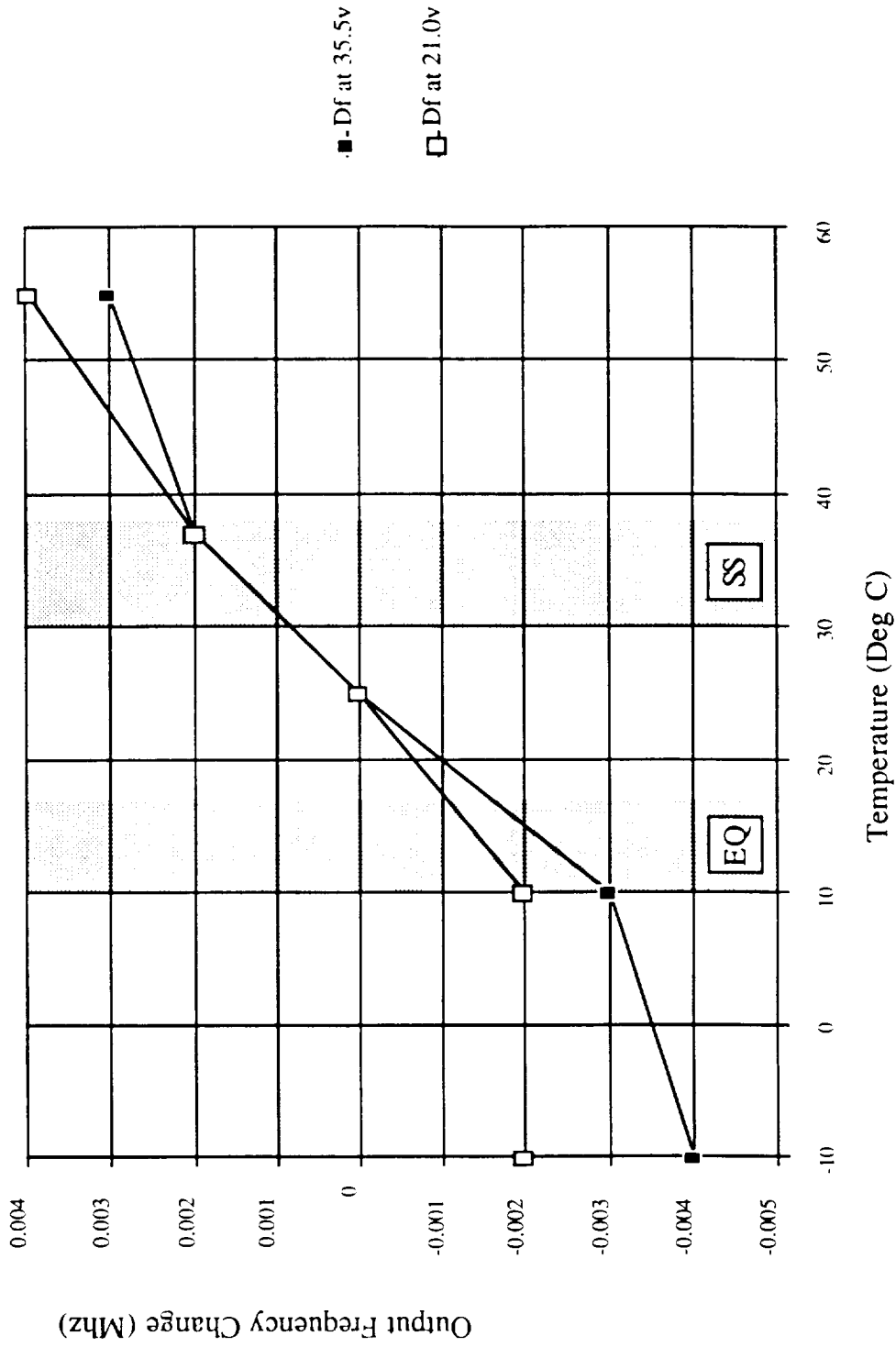
Bands show diurnal variations during Equinox and Summer Solstice





# ACTS Beacons Measurements Data

## Frequency Change with Voltage and Temperature - UFB

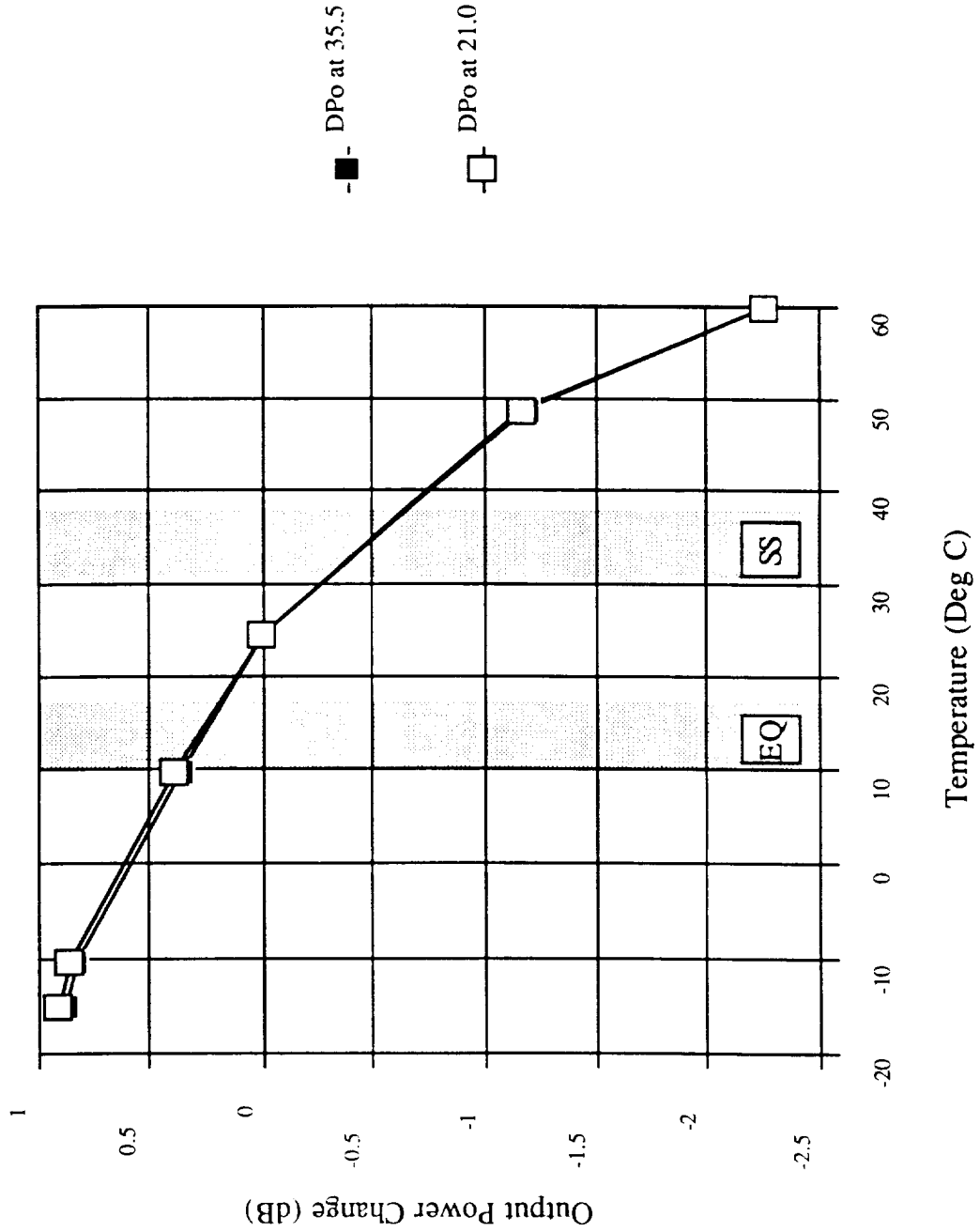


Bands show diurnal variations during Equinox and Summer Solstice



# ACTS Beacons Measurements Data

## Output Power Change with Voltage and Temperature - KBH

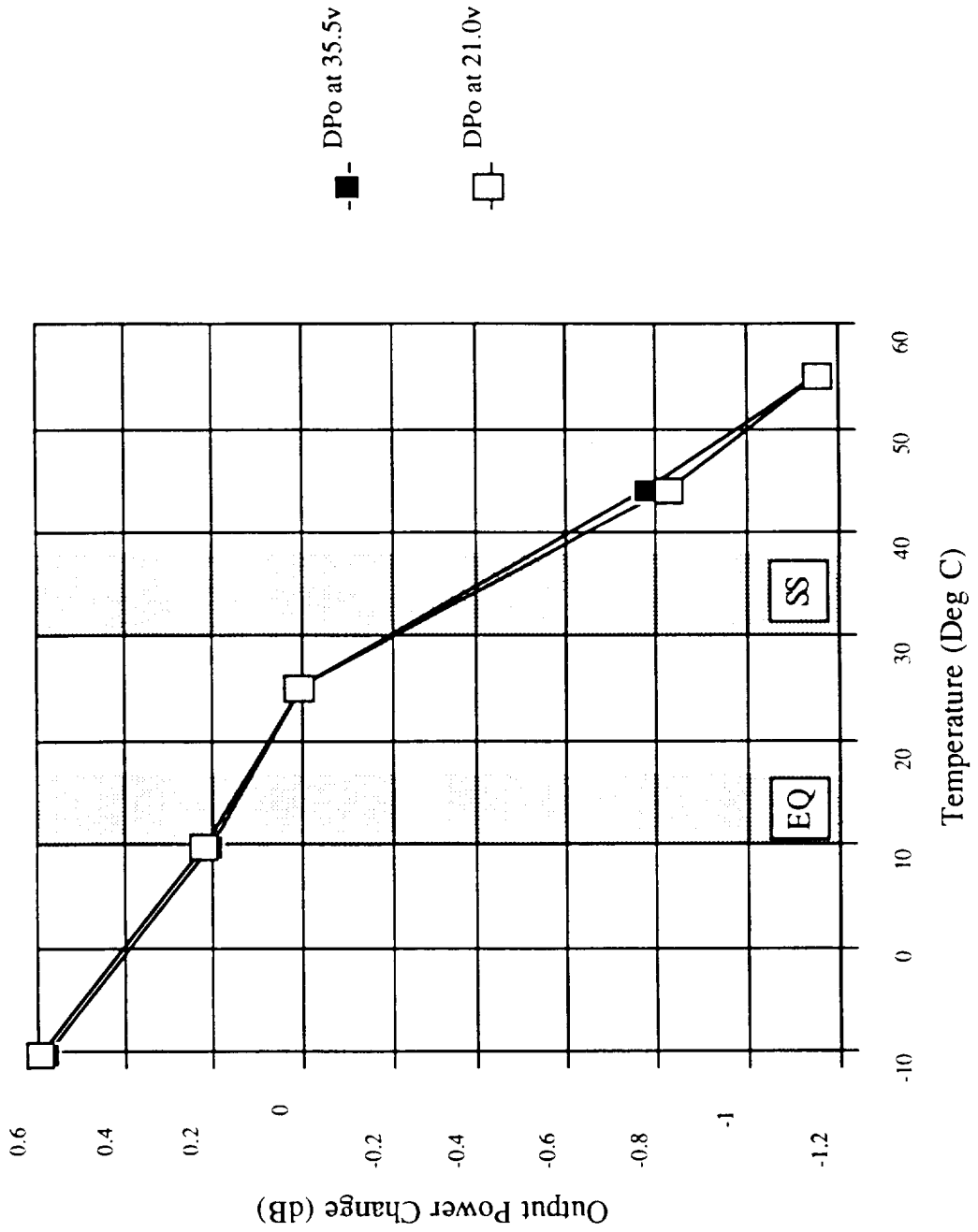


Bands show diurnal variations during Equinox and Summer Solstice



# ACTS Beacons Measurements Data

## Output Power Change with Voltage and Temperature - KBL

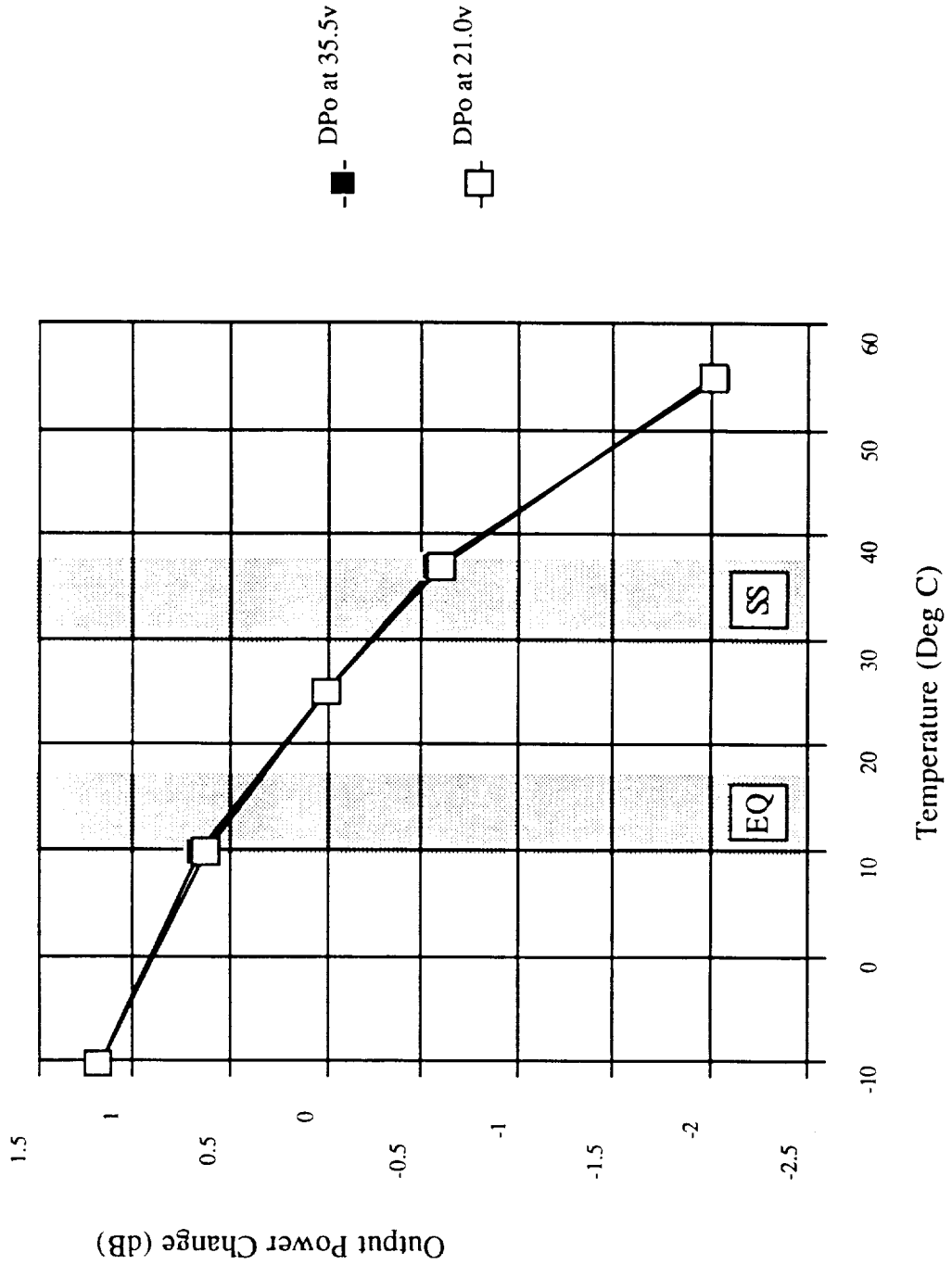


Bands show diurnal variations during Equinox and Summer Solstice



# ACTS Beacons Measurements Data

## Output Power Change with Voltage and Temperature - UFB

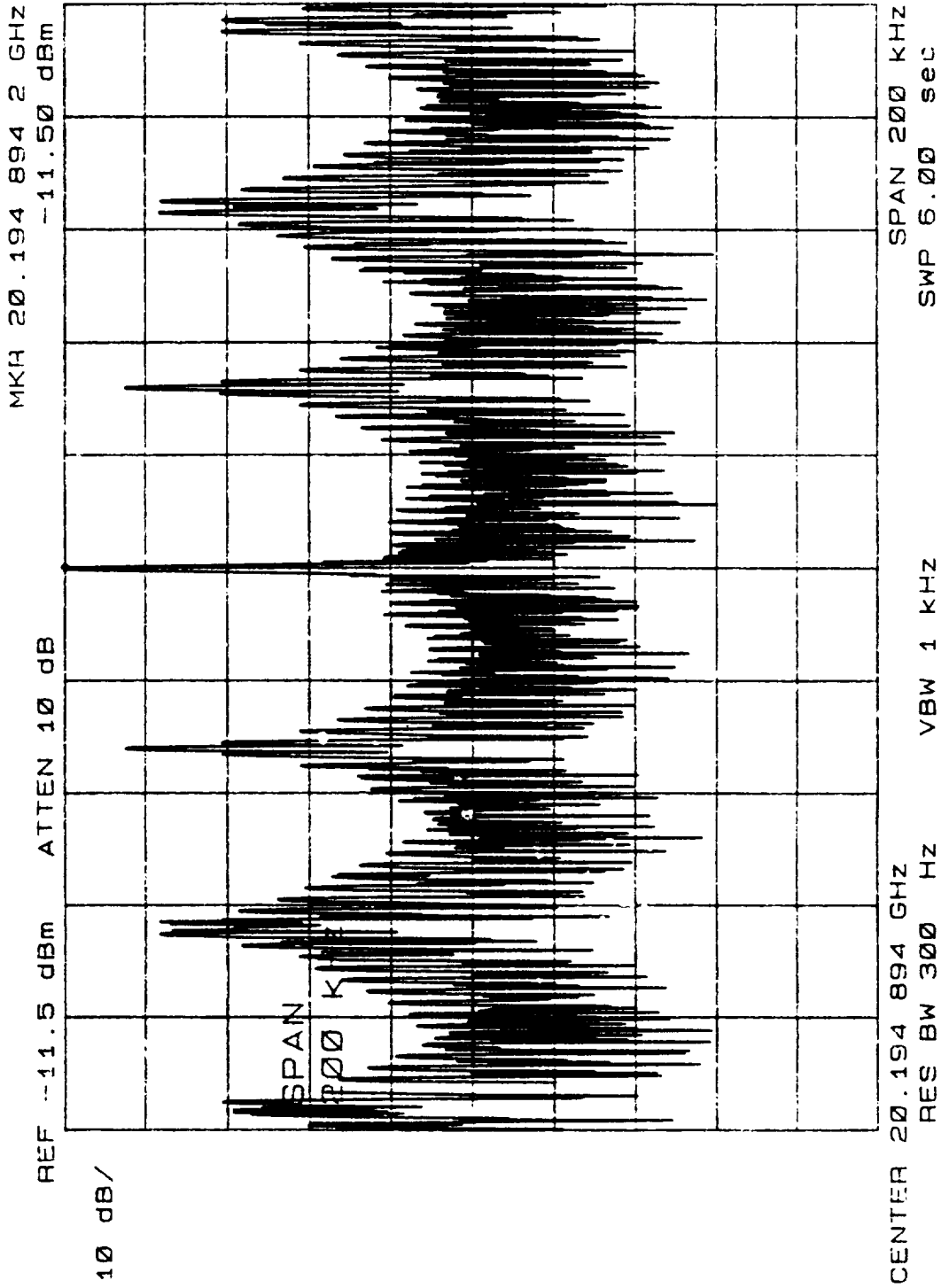


Bands show diurnal variations during equinox and Summer Solstice



# ACTS Beacons Measurements Data

## Spectral Response - KBH, RTM 1, PCM Operational, 200 kHz Span





# ACTS Beacons Measurements Data

## Spectral Response - KBH, RTM 1, PCM Operational, 20 kHz Span

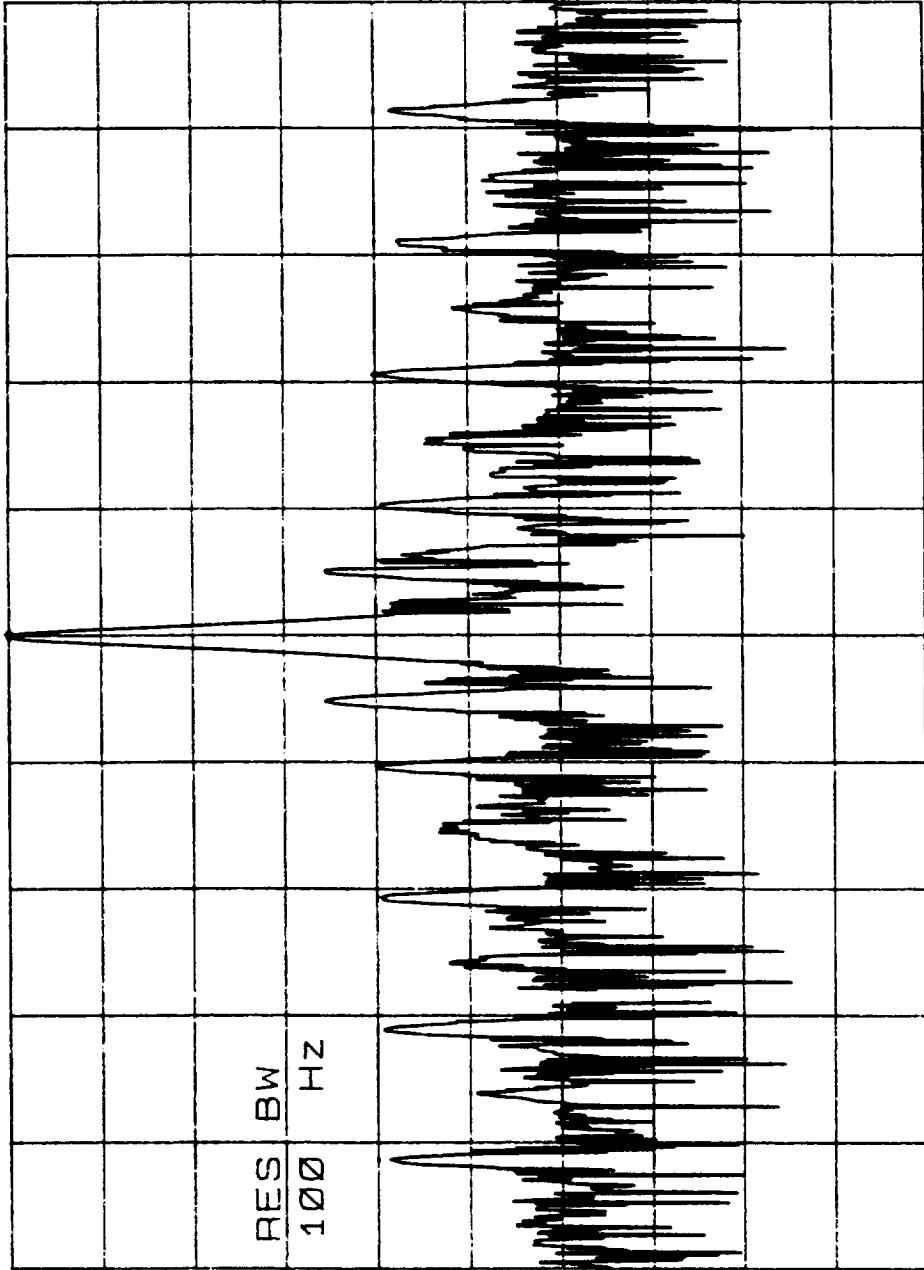
MKR 20.194 892 63 GHz

-11.50 dBm

REF -11.5 dBm ATTEN 10 dB

10 dB/

RES BW  
100 HZ



CENTER 20.194 892 6 GHz  
RES BW 100 HZ

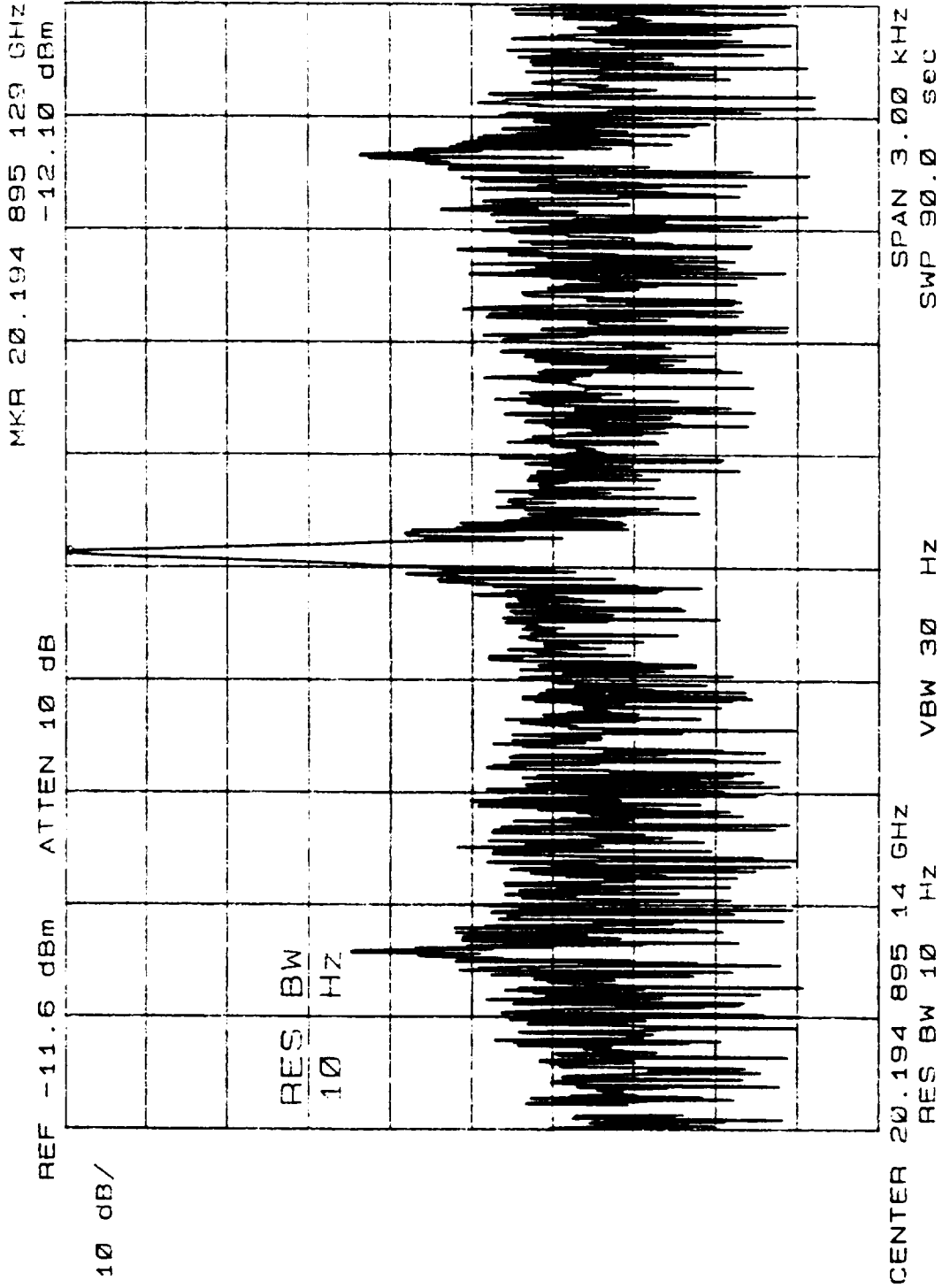
VBW 300 HZ

SPAN 20.0 KHZ  
SWP 6.00 sec



# ACTS Beacons Measurements Data

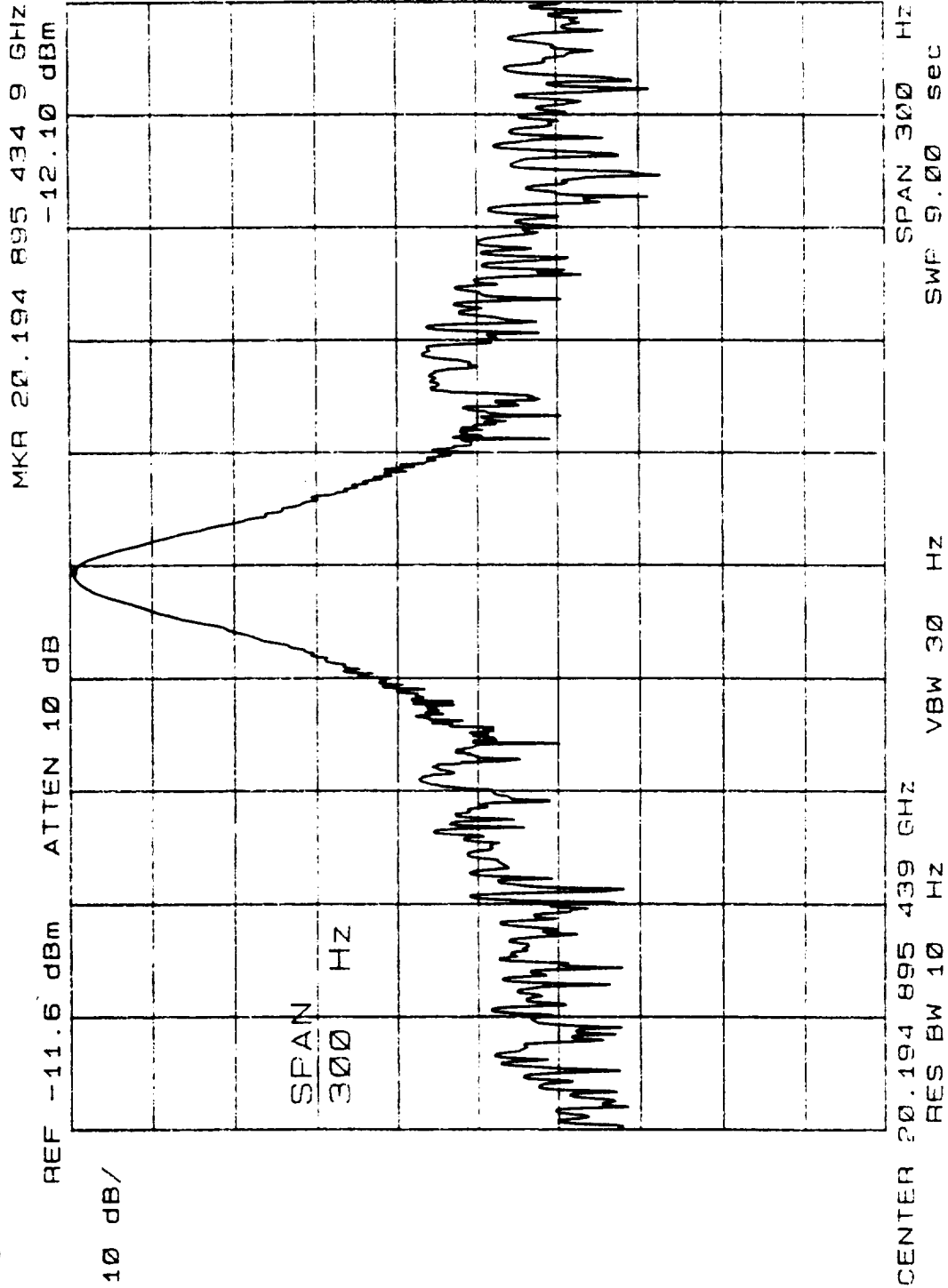
## Spectral Response - KBH, RTM 1, PCM Operational, 3 kHz Span





# ACTS Beacons Measurements Data

## Spectral Response - KBH, RTM 1, PCM Operational, 300 kHz Span



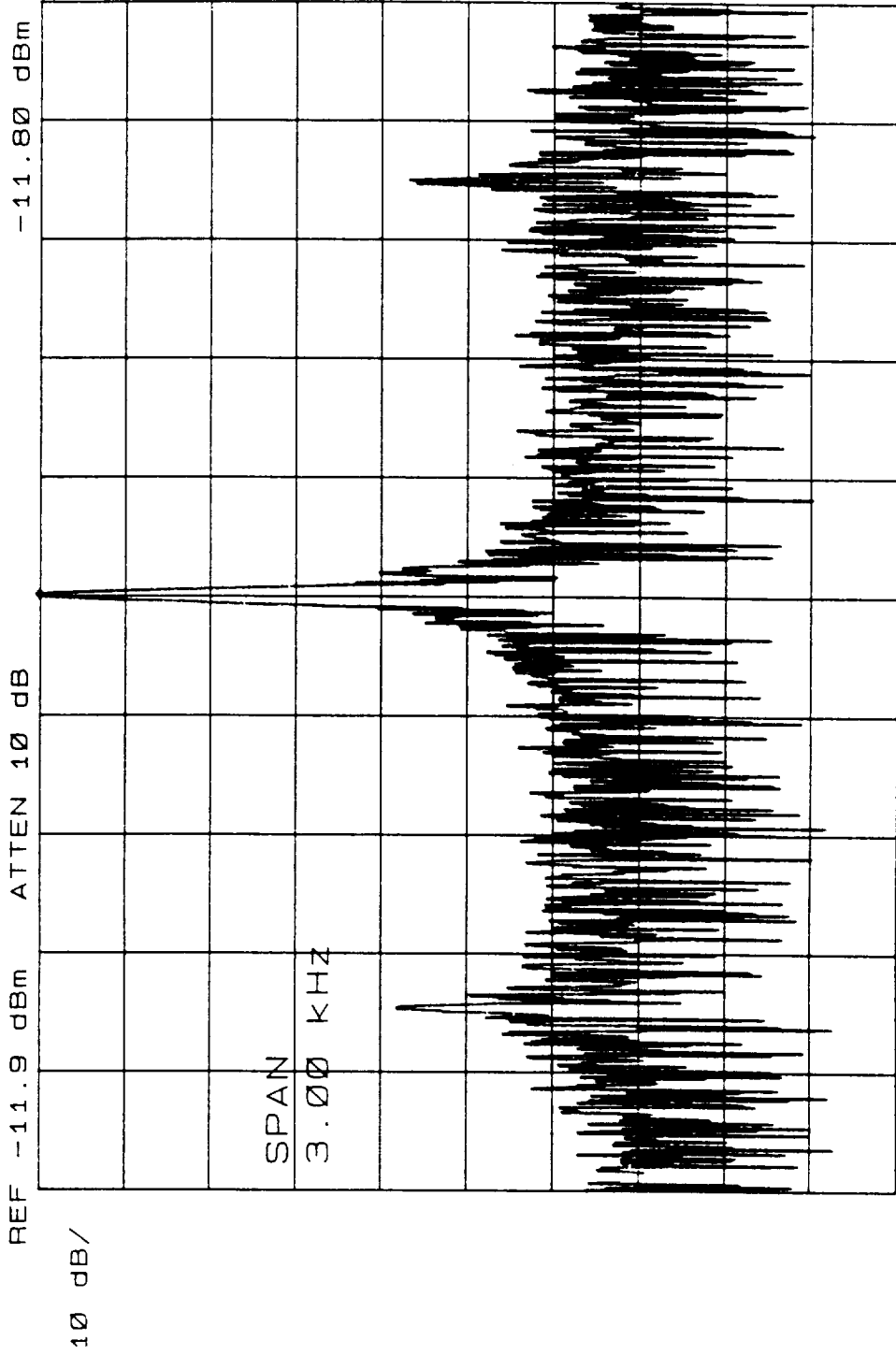




# ACTS Beacons Measurements Data

## Spectral Response - KBL, RTM 2, PCM Operational, 3 kHz Span

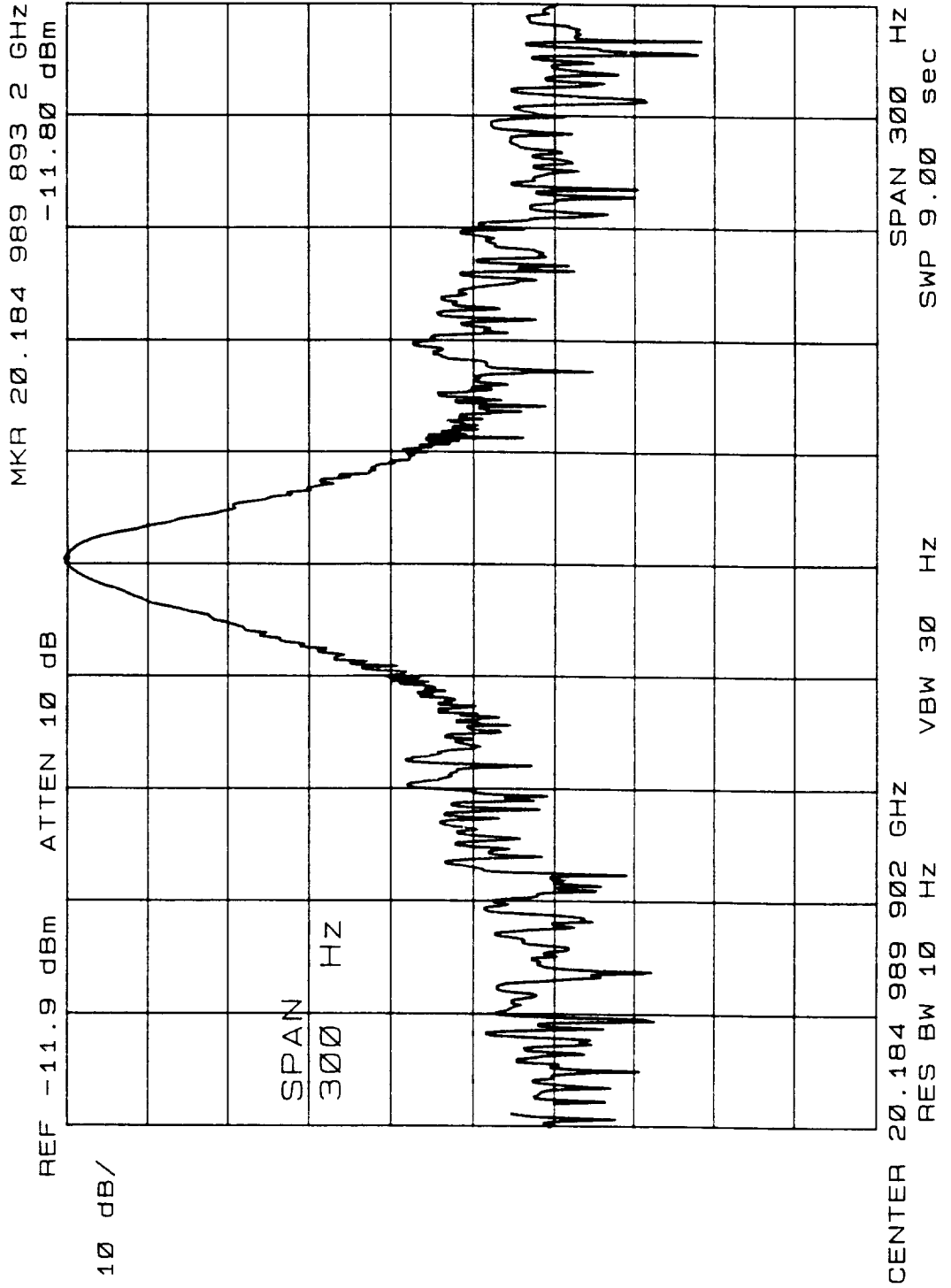
MKR 20.184 990 032 GHz  
-11.80 dBm





# ACTS Beacons Measurements Data

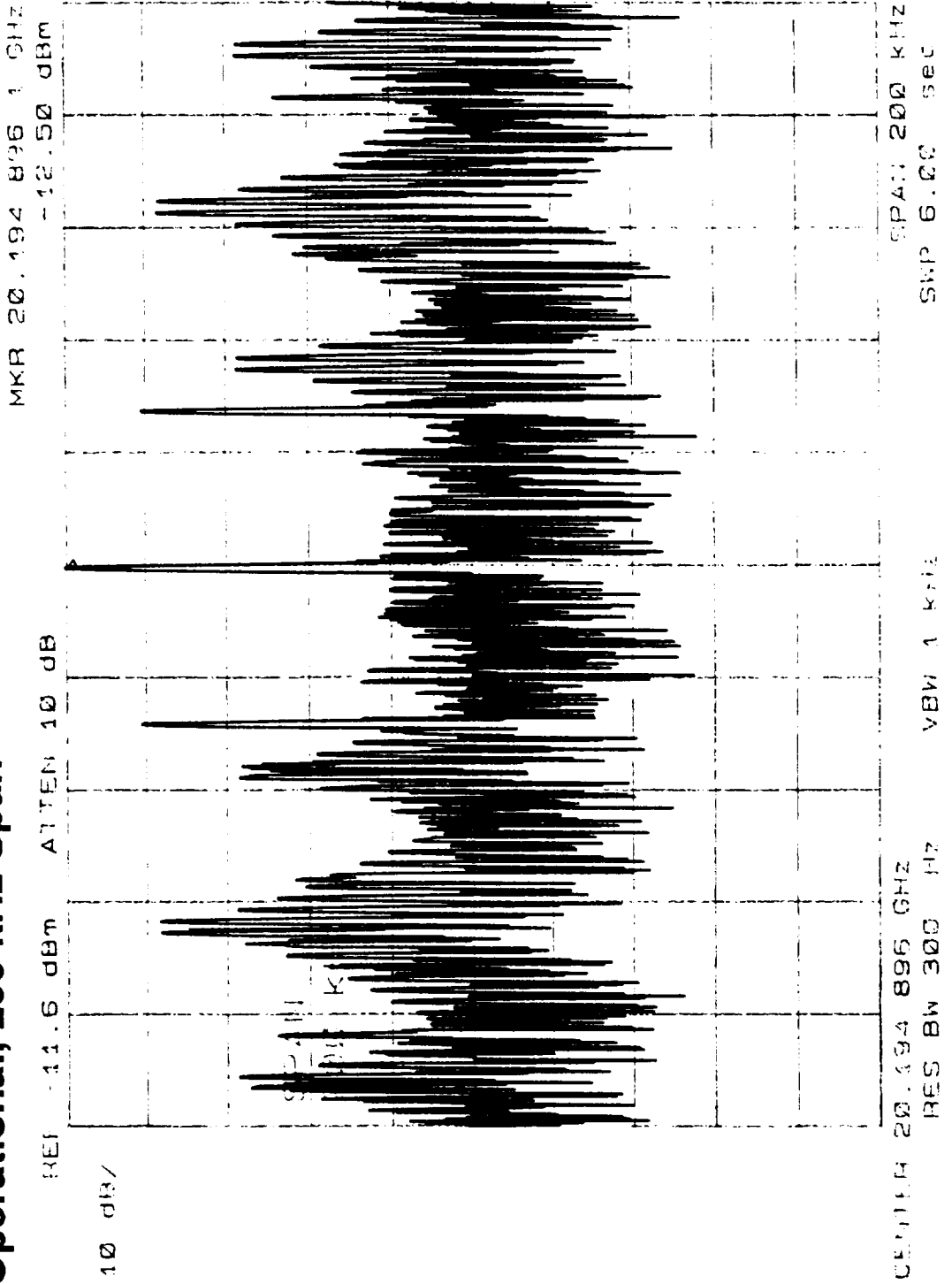
## Spectral Response - KBL, RTM 2, PCM Operational, 300 Hz Span





# ACTS Beacons Measurements Data

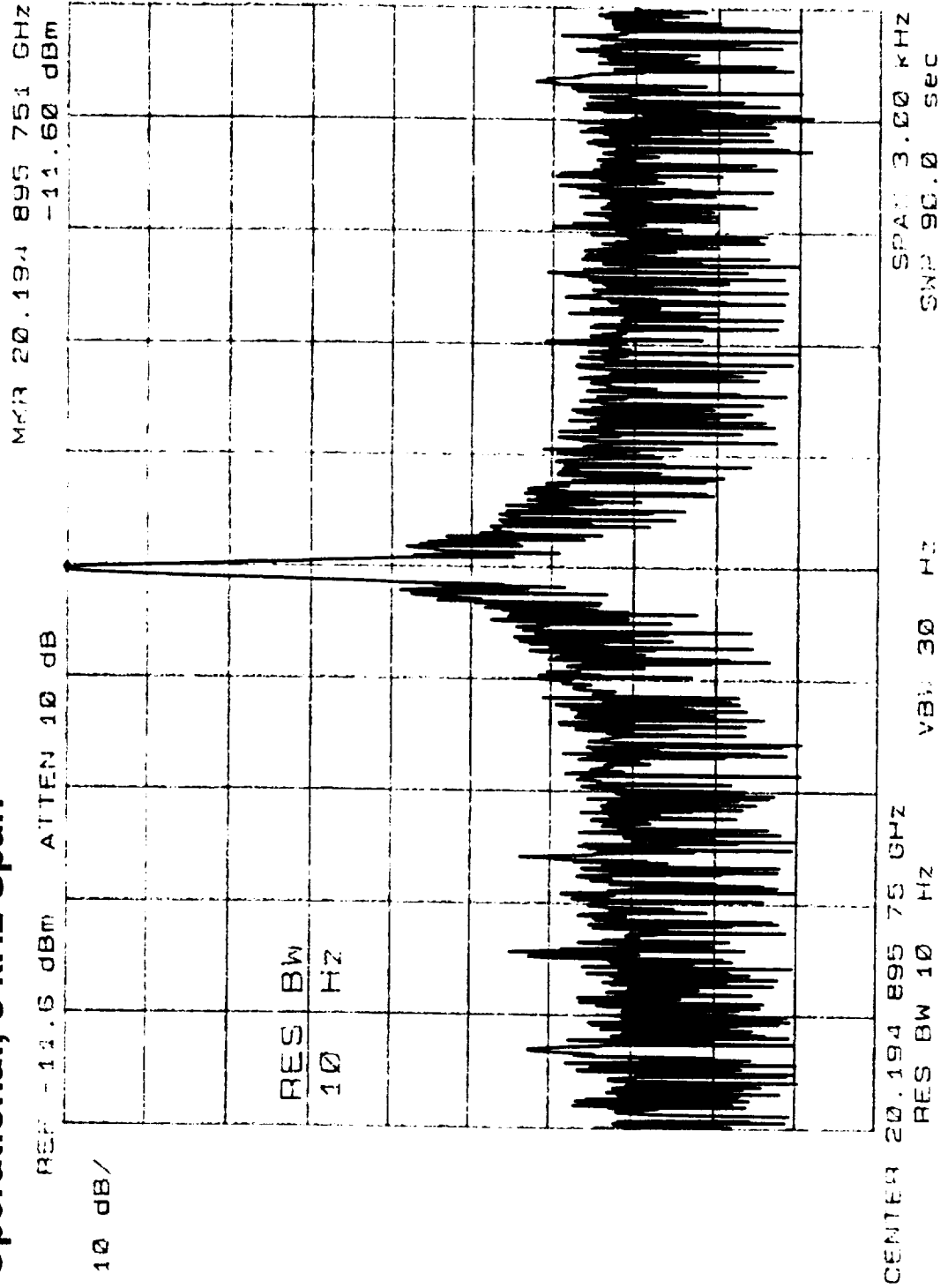
## Spectral Response - KBH, RTM 1, Simultaneous Ranging (27.7 kHz)/PCM Operational, 200 kHz Span





# ACTS Beacons Measurements Data

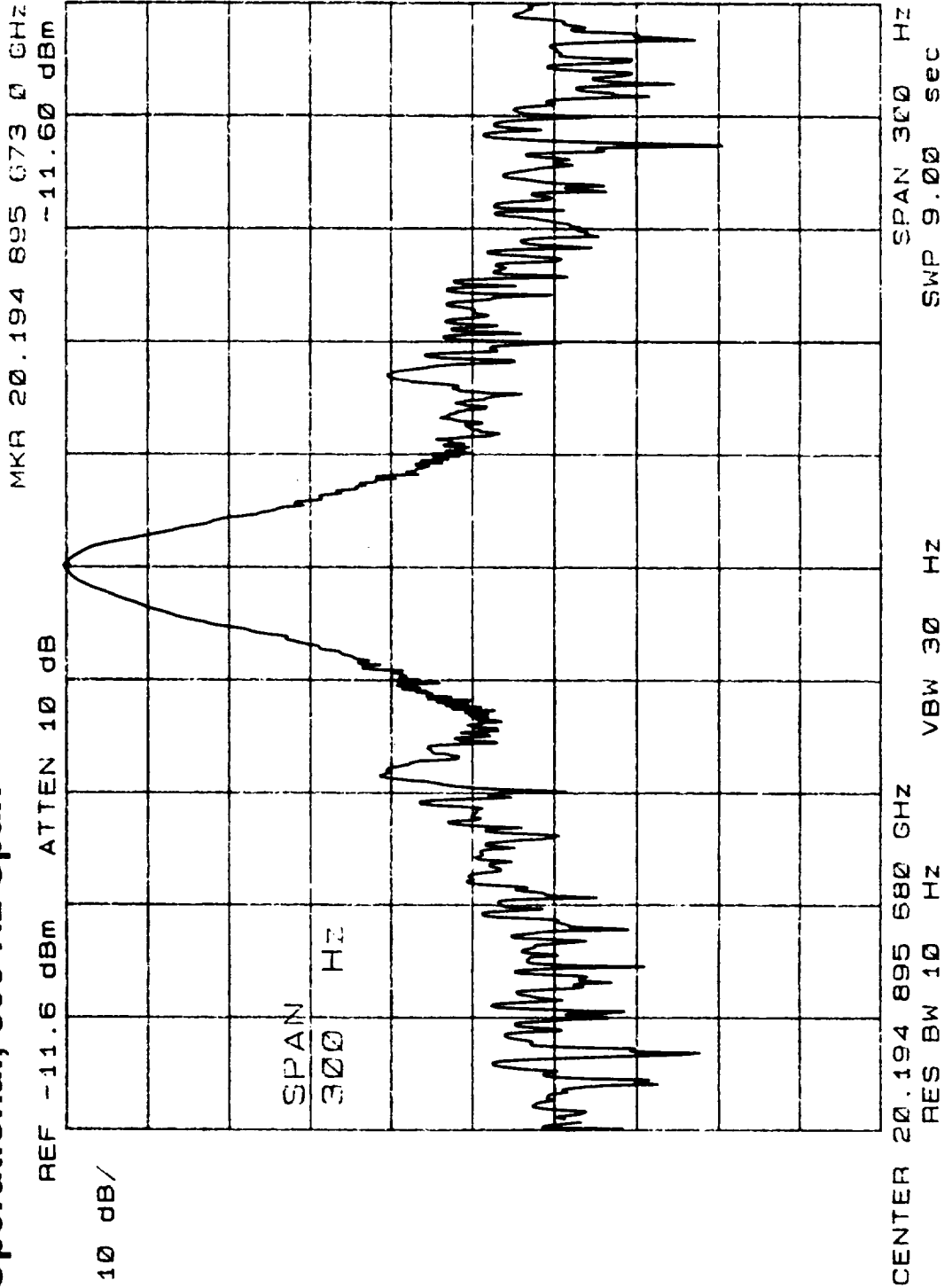
## Spectral Response - KBH, RTM 1, Simultaneous Ranging (27.7 kHz)/PCM Operational, 3 kHz Span





# ACTS Beacons Measurements Data

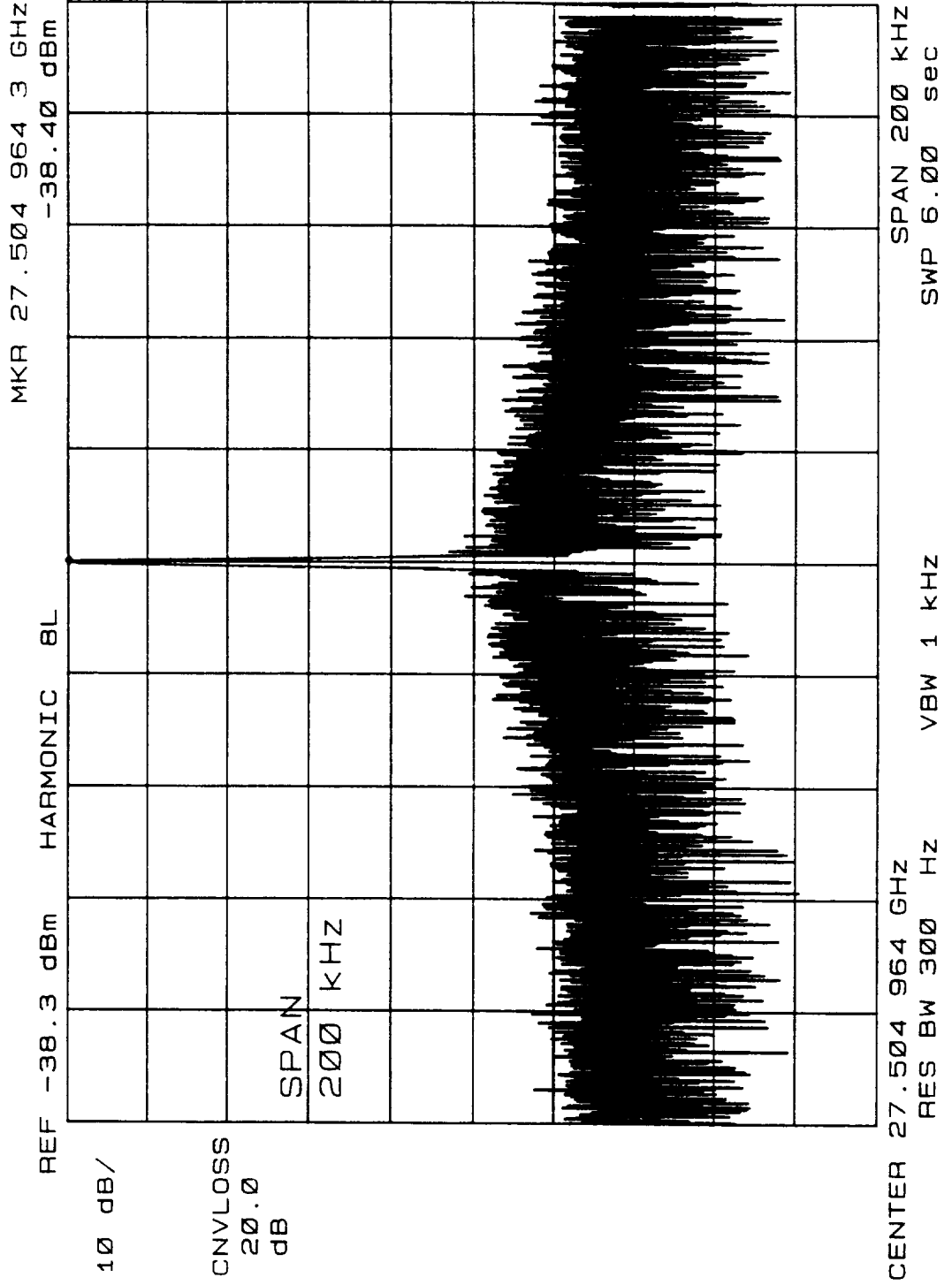
## Spectral Response - KBH, RTM 1, Simultaneous Ranging (27.7 kHz)/PCM Operational, 300 Hz Span





# ACTS Beacons Measurements Data

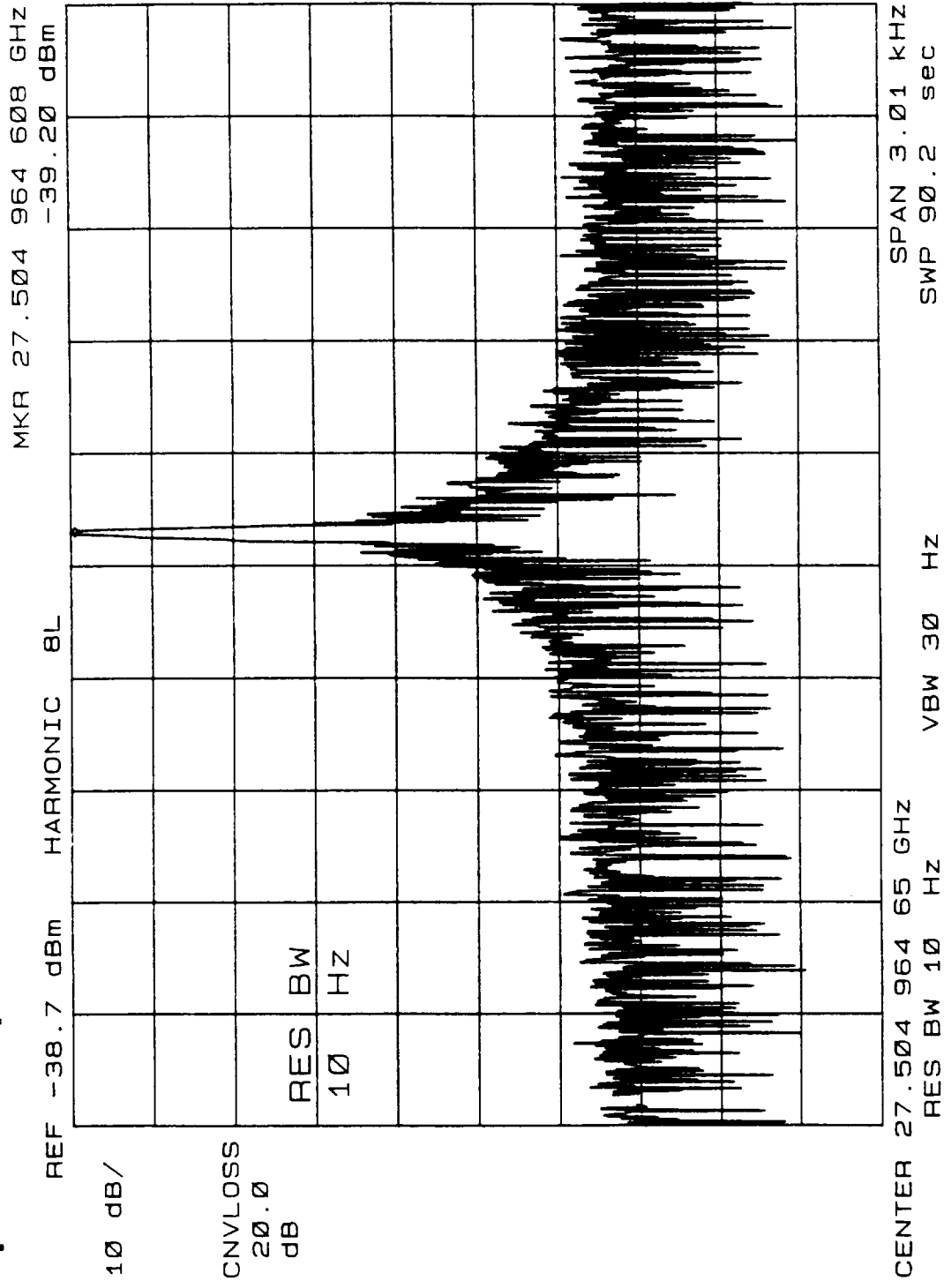
## Spectral Response - UFB 1, 200 kHz Span





# ACTS Beacons Measurements Data

## Spectral Response - UFB 1, 3.01 kHz Span





## ***ACTS Beacons Measurements Data***

---

### **Conclusions**

- **Fade measurements at the uplink frequency are undisturbed by modulation, but available for the vertical polarization only.**
- **Fade measurements at the downlink frequency are practically unaffected by the beacon modulation in the operational telemetry modes or by the contents of the telemetry data.**
- **The demonstrated short term stability of the beacons permits the use of simpler receivers with easy signal recovery after even the deepest fades.**



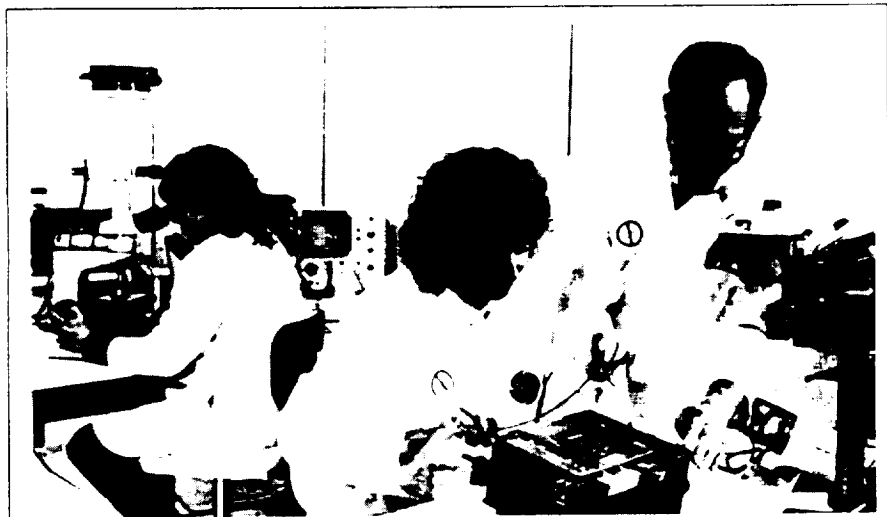
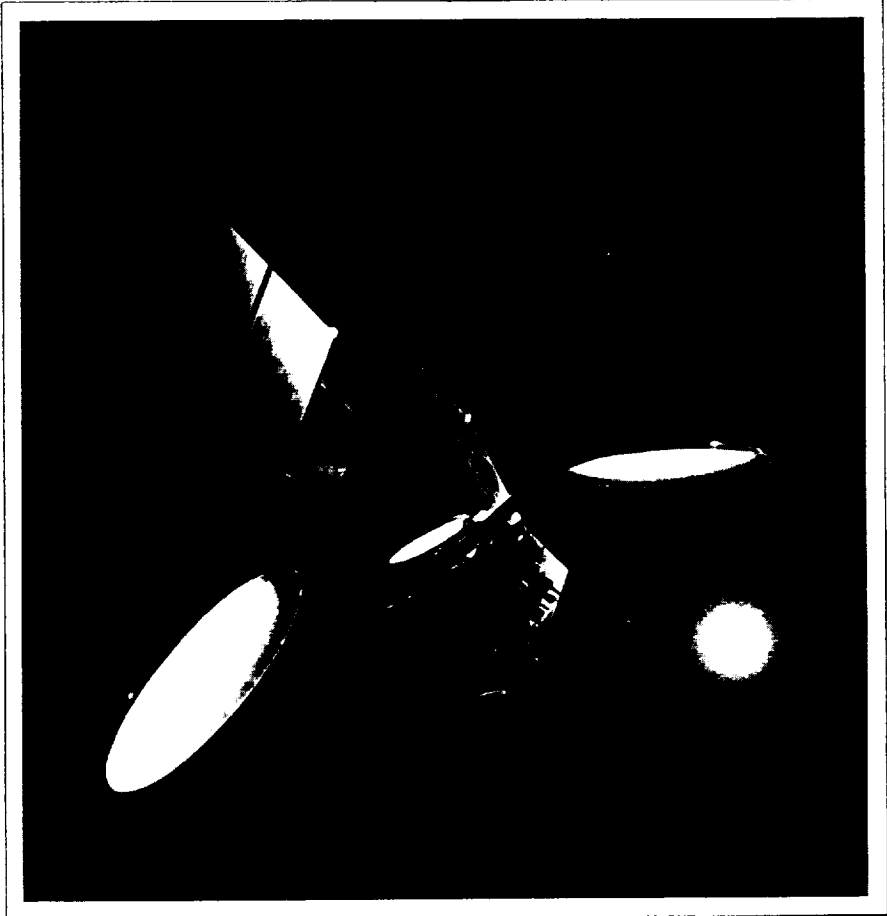
## **ACTS**

One of the most significant communications satellite programs for the future of the industry is the Advanced Communications Technology Satellite (ACTS).

For up to four years, beginning in 1992, ACTS will operate as an orbiting testbed of future communications technologies. ACTS is pioneering such technologies as multiple, hopping spot beams; high-speed, digital on-board baseband processing and switching; and adaptive rain-fade compensation techniques. ACTS will also open up a new portion of the RF spectrum for U.S. communications satellite use, since its uplink and downlink frequencies are at Ka-band.

GE Astro Space, under contract to NASA Lewis Research Center, is providing the ACTS satellite. An extension of our well-proven Satcom bus, the ACTS design incorporates the reliability and performance necessary for such an experimental mission. Development of the ACTS payload has been tailored to the mission objective of creating a mature, space-qualified base of technology from which industry can draw new communications capability. The antenna, switching, and other technologies incorporated in ACTS have been selected to support the product and technology development activities of a broad consortium of private industry, government agencies and university users.

The 1992 launch and subsequent operation of ACTS will provide the United States with the prototype for the next generation of commercial communications satellites.



*Assembly of the ACTS Ka band receiver*

# ACTS

## Specifications

Customer	NASA Lewis Research Center
Type	3-Axis Stabilized Communications Technology Satellite
Application	Testbed of New Technology Applications Available to U.S. Experimenters Free of Charge
Launch Vehicle	STS/TOS
Orbit Position	Geosynchronous, Equatorial, 100° West
Design Life	4 Years

## Communications Payload

Frequency	3 Ka-Band Channels
Bandwidth	900 MHz Each Channel, 2.7 GHz Total
RF Power	46 Watts/Channel
Redundancy	1 Standby Channel (4 For 3 Redundancy)
Coverage	Two Contiguous Sectors in Northeastern U.S. Plus Sixteen Isolated Spot Beams Covering Selected U.S. Locations. Also Full Visible Earth Coverage Via Mechanically-Steerable Spot Beam
Receive Antenna	2.2m Dish and 1m Steerable
Transmit Antenna	3.3m Dish and 1m Steerable
EIRP	Isolated Spot Beams: 60 dBW Contiguous Sectors: 59 dBW Steerable Beam: 53 dBW
Receiver Noise Figure	3.4 dB (HEMT Front-End)
On-Board Switching	High Speed Programmable 3 x 3 Switch Matrix to Provide Three Input and Three Output High Burst Rate (HBR) Channels with 900 MHz Bandwidth. Baseband Processor Provides Demodulation, Storage and Remodulation of Low Burst Rate (LBR) Data. Two 110 Mbps TDMA/DAMA Data Streams Assignable in Increments of 64 Kbits.
Fade Beacons	Stable Signals Radiated from Satellite in the Uplink (30 GHz) and Downlink (20 GHz) Frequency Bands to Permit Link Fade Measurements
Fade Compensation, HBR	Power Control on Uplink as Indicated by Monitoring Fade Beacon at Uplink Frequency. 18 dB Design Margin on Uplink and 8 dB Margin on Downlink
Fade Compensation, LBR	Combination of Convolutional Coding, Data Rate Reduction and Transmitter Margin. 15 dB Design Margin on Uplink and 6 dB Margin on Downlink

## Electrical Power Distribution

Solar Array Output	1418 Watts (4 Years)
Battery System	2 NiCd Batteries of 19 AH Each. No Payload Operation During Eclipse
Power Bus	35.5 (±0.5) Volts with Full Array Illumination

## Propulsion and Orbit Control

Design	Blowdown Hydrazine System with Redundant Thrusters and Four Tanks
Propellant	550 lbs
Thrusters	16 (0.2, 0.5, and 1.0 lbf)
Stationkeeping	±0.05°

## Structure and Thermal

Structure	Length: 80"; Width: 84"; Depth: 75"
Solar Array	With Yoke, 46.9' Tip-to-Tip
Antenna Assembly	Height: 116" Above Antenna Panel; Width: 29.9' Deployed
Thermal Control	Passive Temperature Control: Blankets and OSR; Active Temperature Control: Solid State Controllers and Heaters

## Attitude Control

Transfer Orbit Control	Autonomous Nutation Control During Spin. Initial Pointing Provided by TOS stage
On-Orbit Control	3-Axis Stabilized via Earth and Sun Sensor and Momentum Wheel. Autotrack Ref. Used During Communications Experiment Periods
Pointing Accuracy	0.025° Pitch and Roll, 0.15° Yaw Using Autotrack. 0.1° Pitch and Roll, 0.25° Yaw Using Earth Sensor.
Offset Pointing Control	±6° Pitch, ±2° Roll

## Command, Ranging and Telemetry

Command Frequency	Ka-Band: C-Band Backup and Transfer Orbit
Command Rate	100 pps FSK for Bus Functions 5000 pps SGLS for Payload
Command Capacity	379 Low Rate Discretes; 3 Serial Low Rate Data Streams; 256 High Rate Discretes; 3 Serial High Rate Data Streams
Telemetry Frequency	Ka-Band; C-Band Backup and Transfer Orbit
Telemetry Format	8 Bits/Word; 256 Words/Minor Frame; 25 Minor Frames/Major Frame; 1024 bps
Telemetry Capacity	312 Bilevel Words; 364 Analog Words; 6 Serial Words; Dwell Capability on Any Analog, Bilevel or Serial Word
Tracking Frequency	Ka-Band; C-Band Backup and Transfer Orbit
Tracking Tones	4, from 35.4 Hz to 27.777 kHz



GE Astro Space

P.O. Box 800  
Princeton, NJ 08543-0800 USA

# ACTS PROTOTYPE PROPAGATION TERMINAL UPDATE

Warren Stutzman

Virginia Polytechnic Institute & State University  
Satellite Communications Group  
Bradley Department of Electrical Engineering  
Blacksburg, Virginia 24061-0111

**Abstract** - Virginia Tech is designing and constructing a prototype ACTS propagation terminal. The design phase is complete and construction will begin soon. This paper reports on the specifics of the terminal design.

The terminals will use a single antenna with frequency separation followed by separate 20 GHz and 27.5 GHz receivers. Co-polarized attenuation and scintillations at these frequencies are to be measured. There are provisions for a field change from 20V to 20H reception if the spacecraft transmission frequency changes in the 20 GHz band. Radiometers are included to remove baseline fluctuations.

## 1. Introduction

The 20/30 GHz satellite communications band offers the possibility of very small aperture terminal (VSAT) use. However, systems must be designed carefully to mitigate the impact of rain and scintillation effects on communications. The Advanced Communication Technology Satellite (ACTS) offers a platform to perform experimental studies for accurate investigation of propagation effects on 20/30 GHz satellite communications. The ACTS systems has, in addition to sophisticated 20/30 GHz communications packages, 20/30 GHz propagation signals.

NASA intends to support eight propagation experiments across the U.S. A common hardware and software set that is properly designed and constructed will increase performance and reduce cost. Virginia Tech is charged with the development of the prototype of the ACTS Propagation Terminals (APT). This paper reports on the prototype APT development program.

The OLYMPUS experiment at Virginia Tech offered an excellent test bed for many of the systems to be used in the APT. The OLYMPUS experiment program has receivers at all three beacon frequencies (12.5, 20, and 30 GHz) and a second 20 GHz diversity terminal spaced from 25 to 50 m away from the fixed 20 GHz receiver. Each receiving terminal has a radiometer used to set the absolute beacon level which is subject to spacecraft-induced fluctuations. The total power type radiometer shares the antenna and RF section with the beacon channel.

## 2. Terminal Overview

The simple combined total power radiometer and beacon receiver proved to be extremely accurate in the OLYMPUS program. The ACTS RF system differs from that used in OLYMPUS. A complete RF downconverter block replaces discrete components. This should shorten the development phase and greatly reduce time of construction of subsequent production terminals. The IF (Intermediate Frequency) and DACS (Data Acquisition and Control System) subsystems are very similar to those used in the OLYMPUS project. The ACTS digital receiver is totally different from the analog FLL receiver used in OLYMPUS, which required a long time to develop and is rather complex.

The features of the APT are summarized in Table 1. The prototype design was guided by the subsequent production phase. Cost and reliability considerations for future production terminals weighed heavily on many decisions.

The APT consists of several systems for beacon and radiometric measurements at 20 GHz and 27.5 GHz. The block diagram of the receive terminal is shown in Figure 1.

A single conversion RF system was selected giving direct downconversion from the beacon frequencies to the 70 MHz IF. A second conversion at IF to 10.7 MHz follows which is the input frequency to the digital receiver. This design avoids an RF filter (with its loss and cost). This is the case because radiometer images are only 140 MHz apart (at RF) so they are seeing about the same scene (water vapor effects are not much different 140 MHz apart). If a double conversion receiver with about a 1 GHz IF were used, there would be 2 GHz separation at RF for the radiometer and its image. Also, the proposed design has the benefit of doubling the noise in the radiometer. The power budgets for both systems are summarized in Table 2. The operation of each system and its role in the measurements are briefly described in the next section.

## 3. APT SUBSYSTEMS

### 3.1 The RF System

The RF system is shown in Figure 2. The signals at both frequencies are received by an offset parabolic reflector antenna equipped with a dual polarized feed. The primary spacecraft operating mode is 20.195 and 27.505 GHz, both vertically polarized. As a secondary mode 20.185 GHz would be the 20 GHz signal. This is horizontally polarized. To change the receiver over to operate in this mode two pieces of waveguide hardware would be added as indicated schematically in Figure 2. Vertically polarized signals are separated in the diplexer. Each signal (20 and 27.5) then passes through a waveguide switch, a directional coupler, and a downconverter block. The waveguide switch allows for the injection of a calibration signal in the beacon path, the directional coupler facilitates the injection of excess noise for the purpose of

## Table 1. Prototype Terminal Features

### RF

1.2 meter offset reflector  
LNAs - included  
Calibration methods:  
    Port available for direct RF injection  
    Remotely controllable IF attenuator

### Radiometer

Type: Total power  
Bandwidth: 30 MHz (image adds another 30 MHz)  
Detectable temperature:  $\pm 1\text{K}$   
Calibration methods: noise diode and ambient load

### LOs

First LO type: Crystal controlled multiplier chain  
Provisions for changing between 20V and 20H frequencies:  
    second LO crystal

### IF

Input frequency: 70 MHz (beacon and radiometer)  
Output frequency: 10.7 MHz (beacon)

### Digital Receiver

Input: 10.7 MHz  
A/D precision: 10 bit  
Output: Beacon power in dB/100s  
    Occasional spectra  
Frequency drift tracking:  $\pm 140\text{ kHz}$   
Bandwidth: 15 Hz or narrower pending S/C information  
Resolution: 0.1 dB, 0.5 Hz  
Accuracy: 0.1 dB, 0.25 Hz  
Range of C/N in 15 Hz for satisfactory operation:  
    38 dB to 3 dB  
Reacquire time from deep (short) fades: under 5 s  
Acquisition time from cold start in clear air: under 1 s

### Data Collection

PC/AT based  
Sample rate: 2 Hz  
Data storage: 150 Mb tape (2.6 Mb/day of data)  
Weather ports: pressure, humidity, wind speed, wind  
    direction, two rain gauges  
Modem: 2400 baud  
No downtime to store data to tape  
WWV-based clock system  
System monitors: power failure, receiver lock, PLO, outside  
    temperature, RF encl. temperature, IF encl. temperature,  
    spare

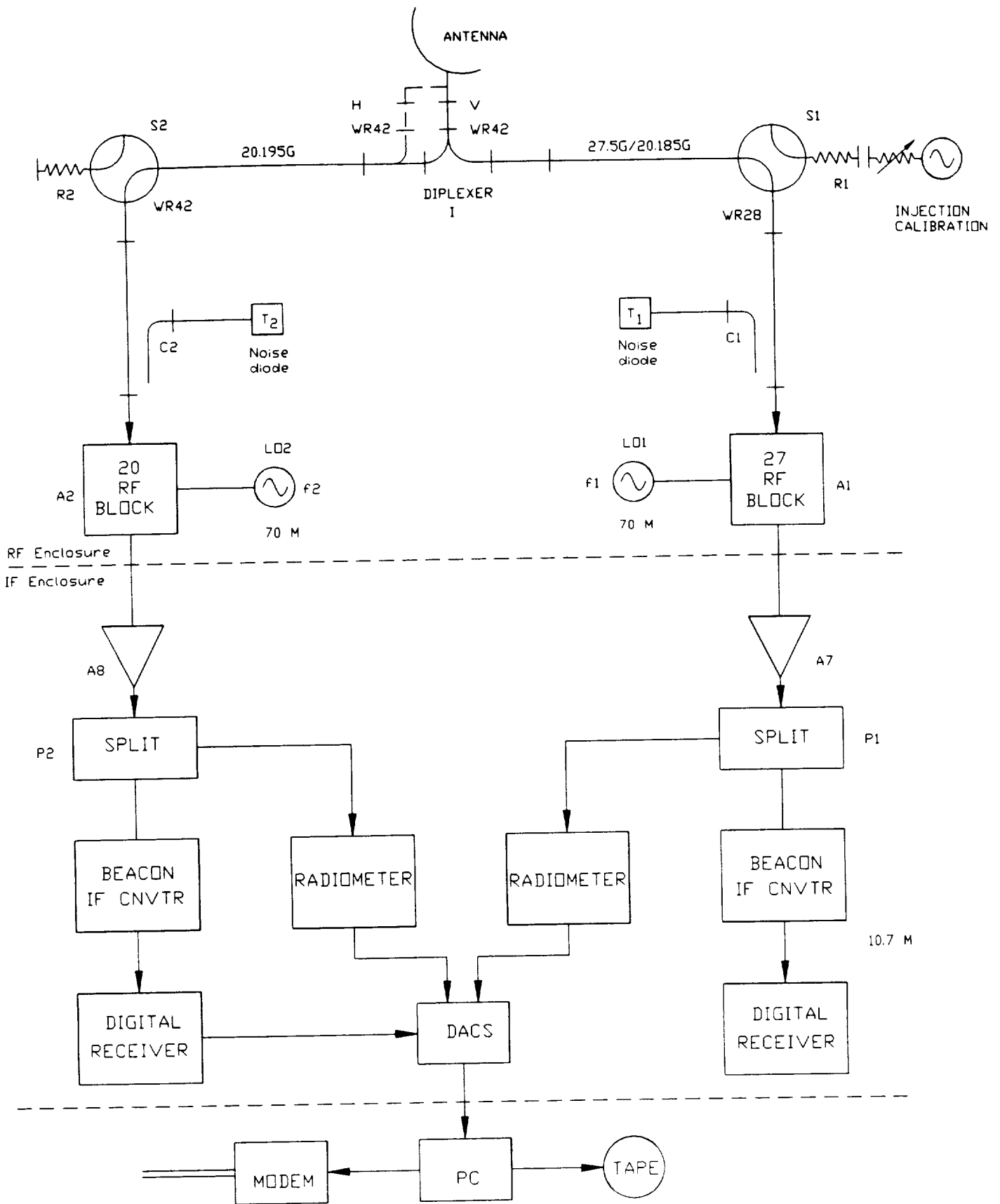


Figure 1. Block diagram of the APT.

Table 2. Power Budget Summary

Frequency	20.2 GHz	27.5 GHz
EIRP toward Blacksburg (* including modulation loss)	17.5 dBW*	16.5 dBW
Path loss	212.1 dB	214.7 dB
Clear sky loss	0.9 dB	0.7 dB
Antenna gain (1.22 m)	46.4 dB	49.0 dB
Losses	1.6 dB	1.9 dB
Converter gain	21.0 dB	21.0 dB
Converter NF	7.0 dB	7.0 dB
C/N in 15 Hz	34.5 dB	33.5 dB

radiometric calibration, and the downconverter block changes the RF signal to an IF frequency of 70 MHz. The signals are passed to the IF system for further processing.

Analysis of spurious frequencies was performed and no problems were revealed.

Note that an RF Downconverter Block is used. Although slightly more expensive in terms of parts cost over the original discrete component unit, this approach offers several advantages. The block contains low-noise amplification, thus reducing the noise temperature. The unit is very compact, reducing space problems.

The RF enclosure should house all temperature critical components, thus necessitating only one closely temperature controlled box. The configuration is such that the RF box output is a coax cable carrying 10.7 MHz and rear entry waveguide pads for RF injection calibration. This permits rotation of the entire RF box in the feed yoke to polarization align the feed. The diplexer is being constructed in-house.

### 3.2 The IF System

In the IF enclosure the 70 MHz IF signal from the output of the RF system is first amplified and then split into two portions, one portion going to the radiometer and the other to a mixer. The mixer downconverts the 70 MHz to a 10.7 MHz signal which is subsequently filtered, amplified and sent to the digital receiver.

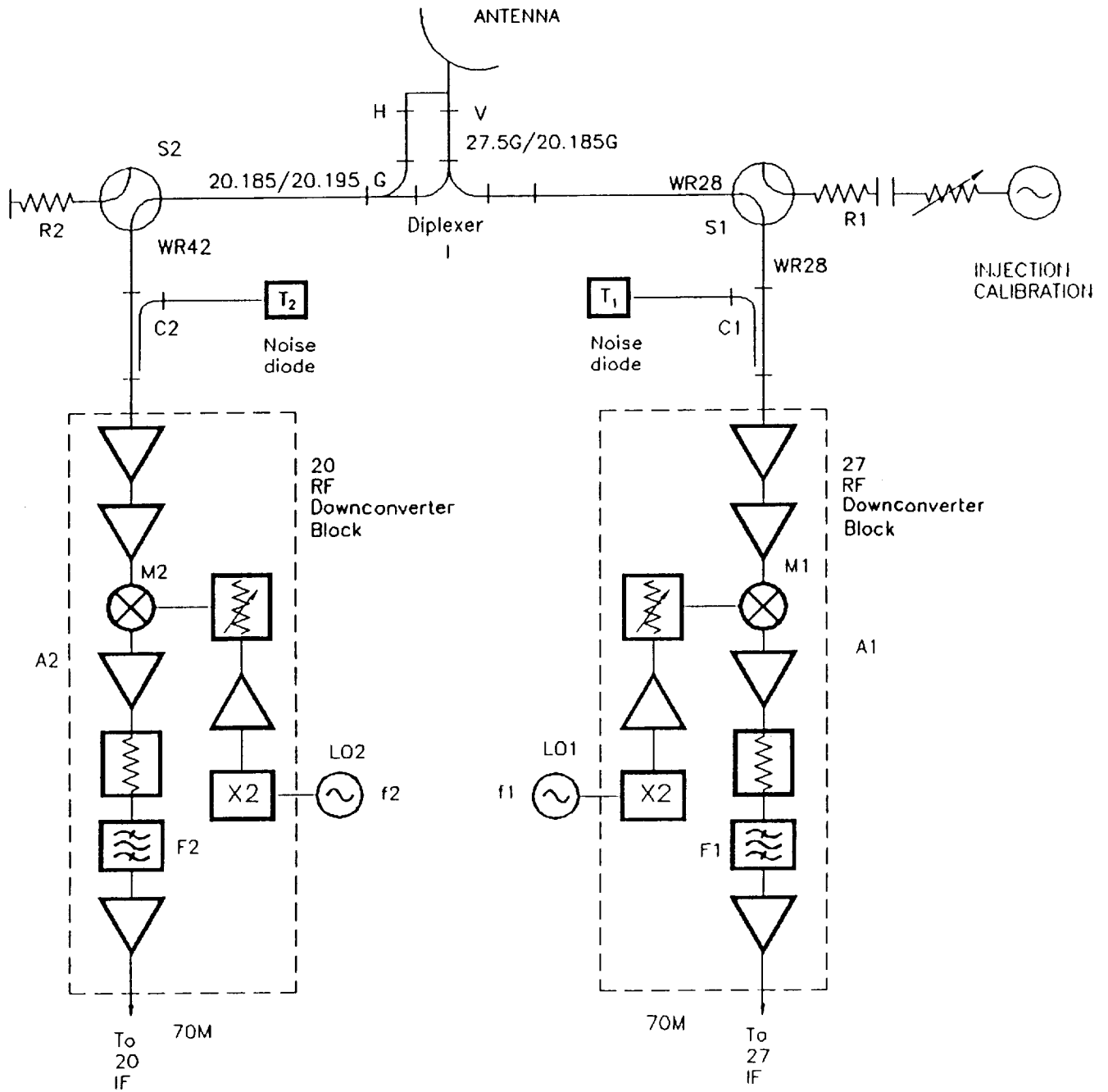


Figure 2. RF system block diagram.



### 3.3 The Radiometers

The radiometers are of total power type. They monitor the sky noise in a 30 MHz bandwidth. The radiometer consists of an attenuator for level adjustment, a bandpass filter to limit the noise bandwidth, a two-stage amplifier, a square-law detector to convert the noise into a DC signal, a DC amplifier, and a voltage to frequency converter. Automatic calibration of radiometer is achieved by injection of excess noise by means of noise diode which is housed in the RF enclosure.

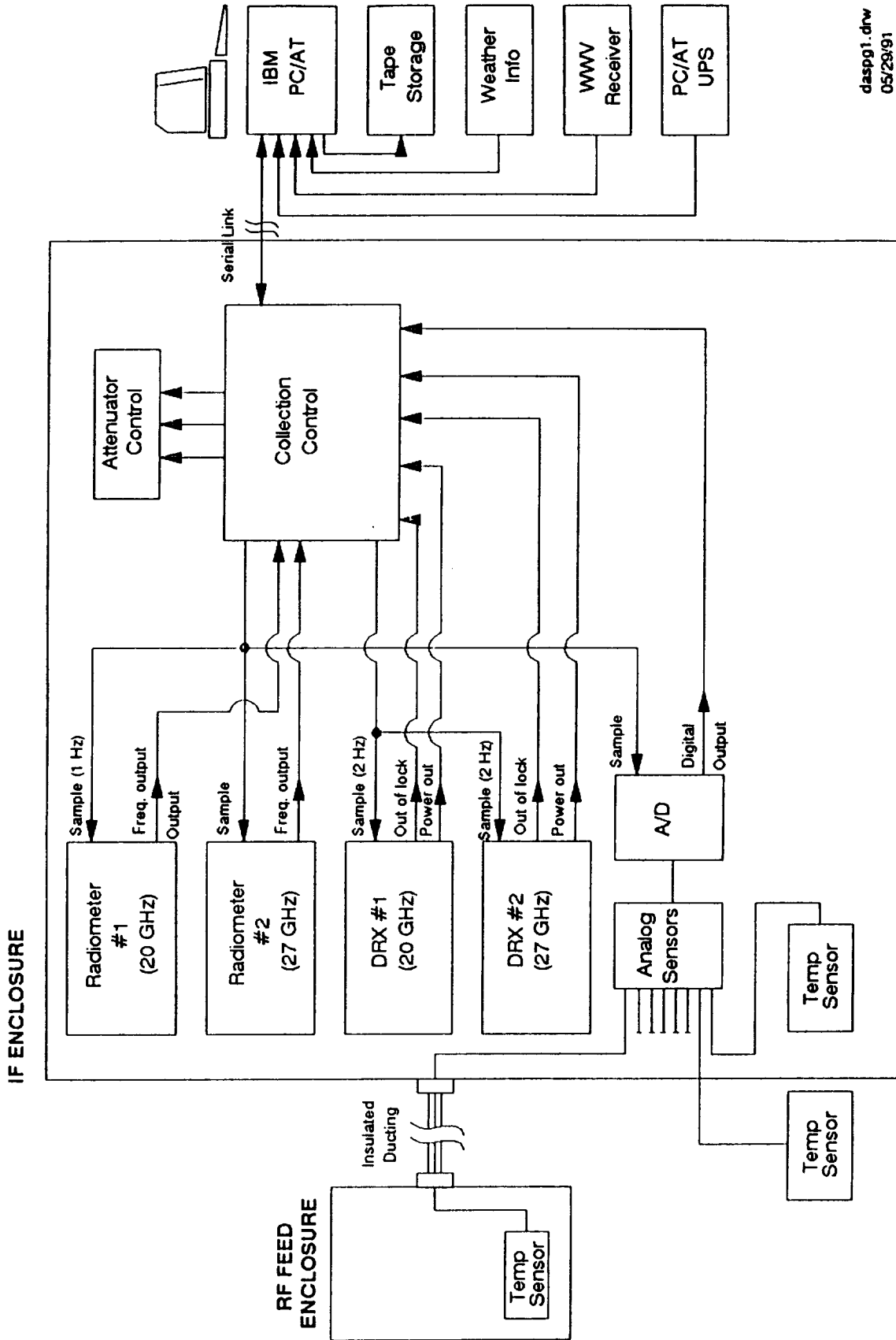
### 3.4 The Digital Receiver

Final processing occurs in the digital receiver. A digital receiver was chosen for several reasons. First, the ACTS signal spectrum at 20 GHz contains many unwanted components. Analog receiver design and operation to ensure no false signal lockups would be complicated. A "smart" digital receiver is better suited for this environment. Replication of the receiver for production units will be easier with a board and plug-in processing chip design approach. Recent chip developments make a digital receiver within reach. Finally, this development program is appropriate to the university research environment and adds to the technology development theme.

### 3.5 Data Acquisition and Control System

The Data Acquisition and Control System (DACS) shown in Figure 3 consists of three major components: the data acquisition and control hardware, the personal computer (PC) hardware and the PC software. The data acquisition and control hardware is located in the IF chassis and is used to collect data from the beacon receivers (2), the radiometers (2), environmental instruments and system temperature sensors. This hardware also controls the calibration of the radiometer channels and is responsible for transmitting all collected data to the PC via a fiber-optic service link.

The PC hardware receives all data transmitted from the DACS through a serial port and logs the data to the disk. The data are collected and displayed using a modified version of the software developed under the OLYMPUS effort.



daspg1.drw  
05/28/91

Figure 3. The Data Acquisition and Control System (DACS).

C-4

TECHNICAL REPORT STANDARD TITLE PAGE

1. Report No. 91-31	2. Government Accession No.	3. Recipient's Catalog No.	
4. Title and Subtitle Proceedings of the Fifteenth NASA Propagation Experimenters Meeting (NAPEX XV) and the Advanced Communications Technology Satellite (ACTS) Propagation Studies Miniworkshop		5. Report Date July 1, 1991	
		6. Performing Organization Code	
7. Author(s) Faramaz Davarian		8. Performing Organization Report No.	
9. Performing Organization Name and Address JET PROPULSION LABORATORY California Institute of Technology 4800 Oak Grove Drive Pasadena, California 91109		10. Work Unit No.	
		11. Contract or Grant No. NAS7-918	
		13. Type of Report and Period Covered JPL Publication	
12. Sponsoring Agency Name and Address NATIONAL AERONAUTICS AND SPACE ADMINISTRATION Washington, D.C. 20546		14. Sponsoring Agency Code RE4 BP-643-10-03-04-00	
15. Supplementary Notes			
<p>16. Abstract</p> <p>The NASA Propagation Experimenters Meeting (NAPEX), supported by the NASA Propagation Program, is convened annually to discuss studies made on radio wave propagation by investigators from domestic and international organizations. NAPEX XV was held on June 28, 1991, in the Sheraton Armouries Hotel, London, Ontario, Canada. Participants included representatives from Canada, Japan, Germany, the Netherlands, and the United States, including researchers from universities, government agencies, and private industries. The meeting was organized into three technical sessions. The first session was dedicated to Olympus and ACTS studies and experiments, the second session was focused on the propagation studies and measurements, and the third session covered computer-based propagation model development. In total, sixteen technical papers and some informal contributions were presented.</p> <p>Following NAPEX XV, the Advanced Communications Technology Satellite (ACTS) Miniworkshop was held on June 29, 1991, to review ACTS propagation activities, with emphasis on ACTS hardware development and experiment planning. Five technical papers were presented by contributors from government agencies, private industry, and university research establishments.</p>			
17. Key Words (Selected by Author(s))		18. Distribution Statement  Unclassified; unlimited	
19. Security Classif. (of this report) Unclassified	20. Security Classif. (of this page) Unclassified	21. No. of Pages 278	22. Price

